Dissertation

Heavy residues and pyrolysis oils as feedstocks in the FCC process for a more sustainable production of olefins and high-octane gasoline

carried out for the purpose of obtaining the degree of Doctor technicae (Dr. techn.), submitted at TU Wien, Faculty of Mechanical and Industrial Engineering, by

Dipl.-Ing. Marco BÜCHELE

Mat.Nr.: 01269804

under the supervision of

Univ.Prof. Dipl.-Ing. Dr.techn. Hermann Hofbauer

Ass.Prof. Dipl.-Ing. Dr.techn. Alexander Reichhold

Institute of Chemical, Environmental and Bioscience Engineering

Vienna, August 2022

reviewed by

Ao. Univ. Prof. Dr. Simone Knaus

Institute of Applied Synthetic Chemistry, TU Wien

Getreidemarkt 9, 1060 Wien, Austria

Prof. Dr. Reinhard Rauch

Engler-Bunte Institute, Fuel Technology, KIT

Engler-Bunte-Ring 1, 76131 Karlsruhe, Germany

This work was supported by the European Union´s Horizon 2020 research and innovation program within the framework of the project Waste2Road under the grant number 818120.

I confirm, that going to press of this thesis needs the confirmation of the examination committee.

Affidavit

I declare in lieu of oath, that I wrote this thesis and performed the associated research myself, using only literature cited in this volume. If text passages from sources are used literally, they are marked as such.

I confirm that this work is original and has not been submitted elsewhere for any examination, nor is it currently under consideration for a thesis elsewhere.

I acknowledge that the submitted work will be checked electronically-technically using suitable and state-of-the-art means (plagiarism detection software). On the one hand, this ensures that the submitted work was prepared according to the high-quality standards within the applicable rules to ensure good scientific practice "Code of Conduct" at the TU Wien. On the other hand, a comparison with other student theses avoids violations of my personal copyright.

Vienna, 21.08.2022

Signature

Danksagung

Zuallererst möchte ich mich hiermit bei meinem Betreuer und Doktorvater Professor Alexander Reichhold bedanken, der es mir ermöglichte Vollzeit in der Arbeitsgruppe tätig zu sein und gleichzeitig meine Doktorarbeit zu schreiben. Ganz besonders sei hier die flache Hierarchie, die Hilfsbereitschaft bei Fragen und Problemen und das überaus angenehme Arbeitsklima erwähnt, bei dem neben dem Fachlichen auch das Menschliche nie zu kurz kam. Danke Alex für die schönen gemeinsamen Jahre in der Arbeitsgruppe.

Weiters bedanke ich mich bei Herrn Professor Hermann Hofbauer, der mir in einer Vielzahl an Lehrveranstaltungen, die theoretischen Grundlagen vermittelte, um meine Doktorarbeit überhaupt starten zu können. Danke Hermann, dass du dich bereiterklärt hast meine Dissertation zu betreuen und mir in meiner Zeit an der TU Wien so viel beigebracht hast.

Meinen Dissertantenkollegen Matthias Swoboda, Helene Lutz und Florian Knaus danke ich für die großartige Zusammenarbeit. Egal was uns die Projektpartner an exotischen Einsatzstoffen geliefert haben, meistens haben wir trotzdem eine Lösung gefunden. Danke für die vielen gemeinsamen Arbeitsstunden, wo nicht nur hart gearbeitet wurde, sondern auch der Spaß immer Platz hatte. Ich bin immer gern in die Arbeit gekommen und das ist zu einem Großteil euer Verdienst. Dank sei auch hier den Diplomanden ausgesprochen, die während meiner Zeit in der Arbeitsgruppe tätig waren: Alina Buchner, Sabine Zauner, Stefan Skrivanek, Stefan Jankovic, Bernd Weber, Jan Sauer und Bernhard Pawlek.

Die wichtigsten Personen, ohne die meine erfolgreiche Studienlaufbahn nicht möglich gewesen wäre, und die mich von klein auf immer und bedingungslos unterstützt haben, sind meine Großeltern Egon und Lieselotte Büchele. Ich danke euch von ganzem Herzen, dass ihr immer für mich da wart und mich zu dem gemacht habt, der ich heute bin. Der Doktortitel gehört zu großen Teilen nicht nur mir sondern auch euch.

Zusätzlich noch ein großes Danke an meine gesamte Familie und eine Vielzahl an Freunden, die zu zahlreich sind, um sie alle einzeln zu nennen. Egal ob in der Schulzeit, der Studienzeit oder der Freizeit. Ich habe viel von euch gelernt, vor allem auch im zwischenmenschlichen Sinne.

Abschließend möchte ich noch meiner Partnerin Lena meinen Dank ausrichten. Vielen Dank für deine Unterstützung in allen Lebenslagen und deine Motivation, wenn es darum ging, dass ich an meiner Arbeit schreibe.

Abstract

The goal of this work was the (co)-feeding of alternative feedstocks in a fluid catalytic cracking pilot plant. The overall objective was to determine the feedstocks influence on the product spectrum to estimate their suitability for the FCC process. The first emphasis was on the hydrocarbon gases as they contain high-value products like olefins that are utilized in the polymer industry. The second emphasis was on the production of gasoline as the FCC process is the main provider of high-octane gasoline in a refinery. The experiments were benchmarked to runs with pure vacuum gas oil, the fossil-based state of the art feedstock for FCC units.

In the first experimental section experiments were conducted using only vacuum gas oil and variations of catalysts. The goal was to quantify the catalysts influence on product spectra and compare them with the manufacturer's specifications. Furthermore, the pilot plant's ability to act as a FCC catalyst test rig was demonstrated. Secondly, effects of fluidization gas variations were researched in a separate campaign. This was done to determine the possible change in catalyst to oil ratio and consequently, the product spectra when introducing higher fluidization gas rates into the riser for heavy residual feeding. The results showed a high shift in product spectra which underlined the importance of conducting benchmark experiments at the exact same fluidization settings as the co-feeding experiments. Otherwise, the effects of the alternative feedstocks on the FCC products could not be clearly inferred.

Heavy residual feedstocks were utilized in the past to create comparably low-value products like bunker fuels or heavy fuel oils. This practice is being phased out as the demand for such fuels steadily decreases due to stricter environmental regulations and lower demand. Consequently, other exploitation methods must be found to convert residual feedstocks into high-value products. The FCC unit's versatility enables it to process a wide variety of feedstocks so that first heavy feedstock units were constructed to the 1960s and existing units were modified. In two experimental campaigns co-feeding runs with atmospheric residue and deasphalted oil were conducted. Even though those feedstocks are state-of-the-art detailed research regarding product shifts when using such heavy residuals compared to vacuum gas oils is still scarce. Especially when it comes to the hydrocarbon gas quality whose importance keeps on increasing.

The deasphalted oil campaign showed great processability when compared to heavy VGO with a substitution rate up to 100 w%. It was concluded that deasphalted oil stemming from vacuum residue is a rather perfect feedstock for residual FCC. The atmospheric residue campaign was conducted with emphasis on the hydrocarbon gas lump quality and especially the generation of carbonyl sulfide (COS) which enriches in the propylene stream and impairs product quality as it acts as a catalyst poison for downstream polymer production. It was shown that co-feeding up to 5 w% atmospheric residue did not result in significant increase in COS and therefore co-feeding up to that rate could easily be achieved for a standard FCC unit without significant product impairment.

The last center piece of this work is the utilization of pyrolysis oils as co-feeding feedstocks. Fast pyrolysis liquids are a rather new refinery feedstock with high potential as plastic wastes can be used as source material enabling a circular plastics economy via chemical recycling. Additionally, biogenic feedstocks like wood wastes can be utilized. In 2 experimental campaigns co-feeding experiments with plastic oils and wood oils were conducted. The plastic oil proved to be a promising refinery feedstock to a substitution rate up to 40 w%. Satisfying product spectra were obtained with an increasing gasoline fraction. The wood oils proved to be more challenging as constituents originating from the wood source complicate feeding into the plant because of pipe clogging and fouling. Additionally, unwanted oxygen and water content is high. Therefore, hydrogenation was conducted to improve feedstock quality and 2 different quality types were produced. Stabilized pyrolysis oil (SPO) underwent one treatment step whereas stabilized and deoxygenated oil (SDPO) underwent two. SPO proved to be feedable up to 10 w% and increased the olefin and hydrocarbon gas fraction. SDPO was fed in the same amounts and increased gasoline production. Both were compared with standard feed. Lastly, the gasoline quality was analyzed and no significant quality drop was observed.

Kurzfassung

Das Thema dieser Arbeit ist das Co-Feeding von alternativen Einsatzstoffen in einer Fluid Catalytic Cracking Pilotanlage. Das Ziel ist die Bestimmung deren Einflusses auf das Produktspektrum, um deren Eignung zu beurteilen. Hauptschwerpunkte waren die Kohlenwasserstoffgase sowie das Benzin. Ersteres beinhaltet hochwertige Produkte (Olefine) für die Kunststoffherstellung. Zweiteres ist bedeutend, da der FCC-Prozess der Hauptproduzent von hoch-oktanigem Benzin in einer Raffinerie ist. Die Versuche wurden jeweils mit dem Stand der Technik, Vakuumgasöl als Einsatzstoff, verglichen.

Im ersten Bereich des Ergebnisteiles wurden Experimente mit Vakuumgasöl und verschiedenen Katalysatoren durchgeführt. Dabei sollten die Einflüsse der Katalysatoren auf das Produktspektrum untersucht und mit den Spezifikationen der Hersteller verglichen werden. In einer zweiten Versuchsreihe wurde die Menge an Fluidisierungsgas im Riser variiert, so dass sich die Umlaufrate und das Katalysator zu Öl-Verhältnis änderten. Dies führte zu signifikanten Änderungen in den FCC Produktverteilungen, was die Bedeutung von Vergleichsversuchen unter den exakt gleichen Bedingungen wie den Beimischungsversuchen untermauerte. Erst dadurch ist die Bestimmung des Einflusses eines Feedwechsels eindeutig möglich (Veränderung von nur einer Variable) und die Eignung von Einsatzstoffen für den FCC Prozess zu determinieren.

In der Vergangenheit wurden schwere Rückstände hauptsächlich dazu verwendet, um Produkte mit geringer Wertschöpfung wie Heizöl oder Bunkeröl herzustellen. Mittlerweile findet jedoch in der Branche ein Wandel statt, da die Nachfrage nach diesen Produkten auf Grund von regulatorischen Vorgaben kontinuierlich abnimmt. Daher wird versucht andere Verwendungsmöglichkeiten für diese Rückstände zu finden, um Produkte mit höherer Wertschöpfung zu generieren. Prädestiniert hierfür ist der FCC Prozess auf Grund seiner Vielseitigkeit bezüglich Produkte aber auch der möglichen Einsatzstoffe. In zwei Versuchsreihen wurden hierbei Beimischungen mit Vakuumgasöl (Atmosphärischer Rückstand und Entasphaltiertes Öl) getestet. Auch wenn diese Einsatzstoffe bereits Stand der Technik sind, so sind noch einige Fragen bezüglich deren Einflüsse auf die gasförmigen Produkte und dabei auf die Olefine in der Forschung nicht komplett beantwortet.

Entasphaltiertes Öl aus dem Rückstand der Vakuumdestillation zeigte eine vollständige Substituierbarkeit mit VGO in der Versuchsreihe, wobei eine Verschiebung in Richtung der schwereren Produktfraktionen beobachtet wurde. Die Versuchsreihe mit atmosphärischem Rückstand wurde durchgeführt, um die Änderung von Carbonylsulfid (COS) in der Gasfraktion zu untersuchen. Es konnte gezeigt werden, dass bis zu einer Beimischung von 5 m% Rückstand kein signifikanter Anstieg an COS beobachtet wurde, so dass keine Verschlechterung der Produktqualität auftrat. Dies ist von Bedeutung, da sich COS bei der Fraktionierung im Propylenstrom anreichert und als Katalysatorgift in der Kunststoffherstellung agiert. Die Möglichkeit des COS-Zuwachses wurde untersucht, da der atmosphärische Rückstand im Gegensatz zum verwendeten VGO nicht hydriert wurde.

Der zweite Hauptfokus dieser Arbeit lag neben dem Einsatz von Rückstandsfraktionen auf dem Co-feeding von Pyrolyseölen. Dieser neue Feed kann aus Kunststoffabfällen gewonnen werden und so dazu beitragen über chemisches Recycling einen signifikanten Beitrag in Richtung Kreislaufwirtschaft zu leisten. Dieser Einsatzstoff zeigte in einer Versuchsreihe mit Beimischungen bis zu 40 m% gute Prozessierbarkeit und eine erhöhte Neigung zu Benzinbildung. In einer zweiten Versuchsreihe wurden Pyrolyseöle aus sauberen Holzabfällen hergestellt. Anschließend wurde dieses Pyrolyseöl hydriert, um den Sauerstoffgehalt, den Wassergehalt sowie die Verkokungsneigung zu verringern. Dabei wurden 2 Batches hergestellt: ein einfachhydriertes Pyrolseöl (stabilized pyrolysis oil/SPO) und ein zweifaches hydriertes (stabilized and deoxygenated pyrolysis oil/SDPO). Die Beimischung von SPO führte zu einer Erhöhung der Gasfraktion, während SDPO zu höheren Benzinausbeuten führte. Die maximalen Beimischungsmengen beliefen sich auf 10 m%. Zusätzlich wurde eine qualitative Analyse des Benzins durchgeführt, bei der keine signifikanten Qualitätsverluste im Vergleich zu Benzin aus reinem VGO gemessen werden konnten.

Table of contents

Funding acknowledgment

Project: Waste2Road

This project has received funding from the European Union's Horizon 2020 research and innovation programme under grant agreement No. 818120.

Abbreviations

$(C_6H_{10}O_5)_n$	Cellulose
$(C_5H_8O_4)_n$	Hemicellulose
(n)-paraffin	(unbranched) alkane
α-olefin	1-Alkene
α/β-scission	Cleavage of C-C bonds between first and second (α) or second and third (β) C-atom
µm	Micrometre
ABS	Acrylonitrile butadiene styrene
Al	Aluminium
Al_2O_3	Aluminium oxide
ASTM	American Society for Testing and Materials
BASF	Badische Anilin- und Sodafabrik
BTG	Biomass Technology Group
BTX	Benzol, Toluol, Xylol
CCR	Conradson carbon residue
CFB	Circulating fluidized bed
CeO_2	Cerium oxide
CHP	Combined heat and power
CH_4	Methane
Cl	Chloride
C_n	Alkane/Alkene/Alkine with n numbers of carbon atoms
CO	Carbon monoxide
CO_2	Carbon dioxide
COS	Carbonylsulfide
COVID	Coronavirus disease
Co.	Company
CRA	Catalytic Research Associates
DAO	Deasphalted oil
DMDS	Dimethyl disulphide
E-cat	Equilibrium catalyst
EIA	US Energy Information Administration
FCC	Fluid catalytic cracking
HDO	Hydrodeoxygenated oils
Hg	Mercury
HOC	Heavy oil cracker
HS-FCC	High severity fluid catalytic cracking
H^-	Hydride ion
H_2	Hydrogen
H_2S	Hydrogen sulfide
IG Farben	Interessensgemeinschaft Farbenindustrie AG
KIT	Karlsruhe institute of technology
La_2O_3	Lanthanum oxide
LCO	Light cycle oil
LHV	Lower heating value
LPG	Liquefied petroleum gas
LOD	Limit of detection
MAT	Micro activity tests
mm	Millimetre
MMb/d	Metric million-ton barrel per day
MON	Motor octane number
MSRC	Multi-stage reaction catalysts
Na	Sodium
naphthene	Cyclo-alkane
NaY zeolite	Zeolite Y (corresponding to Faujasite) with sodium as counterion
NiMo	Nickel molybdenum

NO_x	Mixture of nitric and nitrogen oxide
N_2	Nitrogen
OECD	Organisation for Economic Co-operation and Development
olefin	Trivial name for alkene
OMV	Österreichischer Mineralölverband
O_2	Oxygen
PCLA	powdered catalyst Louisiana
PDU	Process Development Unit
PE	Polyethylene
PET	Polyethylene terephthalate
PO	Pyrolysis oil
PP	Polypropylene
PS	Polystyrene
PVC	Polyvinylchloride
P_2O_5	Phosphor pentoxide
RCR	Rotating cone reactor
RE_2O_3	Rare earth oxide
RFCC	Resid fluid catalytic cracking
RON	Research octane number
RTP	Rapid thermal processing
SDPO	Stabilized and deoxygenated pyrolysis oil
Si	Silicon
SiO_2	Silicon oxide
SOx	Sulfur oxide
SPO	Stabilized pyrolysis oil
TFY	Total fuel yield
UCS	Unit cell size
UOP	Universal oil products
USY zeolite	Ultrastable Zeolite Y
VGO	Vacuum gas oil
VTT	Technical Research Centre of Finland
ZSM-5	Zeolite socony mobil with framework type MFI 5

Formula symbols

R	Organic molecule part
H	Hydrogen atom
C	Carbon atom
H^+	Proton
H^-	Hydride ion
C_nH_{2n}	Olefin
C_mH_{2m}	Naphthene
C_nH_{2n+2}	Paraffin
C_mH_{2m-6}	Aromatic
C_nH_{2n-2}	Polycyclic olefin
EHI	Effective hydrogen index [-]
h	Hydrogen fraction [-]
o	Oxygen fraction [-]
n	Nitrogen fraction [-]
s	Sulfur fraction [-]
c	Carbon fraction [-]
u_L	linear gas velocity [m/s]
$\dot{V}_{Regenerator,\ Norm}$	Volume flow in regenerator under norm conditions [m³/s]
T	Temperature [K]
T_{Norm}	Temperature under norm conditions [K]
$d_{Regenerator}$	Diameter of regenerator [m]
$d_{Return\ flow\ tube}$	Diameter of return flow tube [m]
u_{mf}	minimum fluidization velocity [m/s]
η	dynamic viscosity [Pa·s]
ρ_g	Gas density [kg/m³]
d_{SV}	Sauter diameter [µm]
Ar	Archimedes-number [-]
ρ_p	particle density [kg/m³]
g	gravitational acceleration [m/s²]
$\overline{T}_{Riser}$	Mean riser-Temperature [K]
$T_{Riser,\ in}$	Inlet riser-Temperature [K]
$T_{Riser,\ out}$	Outlet riser-Temperature [K]
$\dot{m}_{catalyst}$	catalyst circulation rate [kg/h]
$A_{Regenerator}$	Regenerator area [m²]
$\Delta p_{Regenerator}$	Pressure loss in Regenerator [mbar]
Δt_u	measuring interval for circulation rate [h]
C/O	Catalyst to Oil-ratio [-]
$\dot{m}_{feed}$	feeding rate [kg/h]
$\dot{m}_{hydrocarbon\ gas}$	rate of hydrocarbon gas generation [kg/h]
$\dot{m}_{gasoline}$	rate of gasoline generation [kg/h]

List of tables

List of figures

1. Introduction

1.1 The possible role of Fluid Catalytic Cracking in a low carbon economy

The world population is growing and with it our demand for energy. It is estimated that from now to 2030 the population will grow to 8.5 billion people and in 2050 even 9.7 billion people might inhabit the planet [1]. This continuing surge in population together with economic growth will inevitably lead to higher primary energy consumption worldwide according to the reference case scenario of the International Energy Outlook 2021. This scenario assumes current energy legislation and technology development as well as a mediocre oil price [2]. In figure 1 on the left chart the forecasted amount of world primary energy consumption is depicted. The numbers are estimated to grow approximately 50% when comparing 2020 to 2050 reaching a value of around 935 EJ. This growth will mainly be driven by non-OECD countries especially in Asia [2]. In the right chart of figure 1 a comparison is made between 1971 and 2019 regarding the difference in sources for primary energy supply. The proportion of coal did not change significantly and remained just below 27 % whereas the decline in oil share was mostly leveled out by natural gas. Leaving out nuclear power since it is often not considered sustainable the proportional growth of renewable energy supply was only miniscule [3]. For the future the reference case from the EIA even predicts that natural gas and oil production will grow further and that their growth is driven by the booming Asian economy [2].

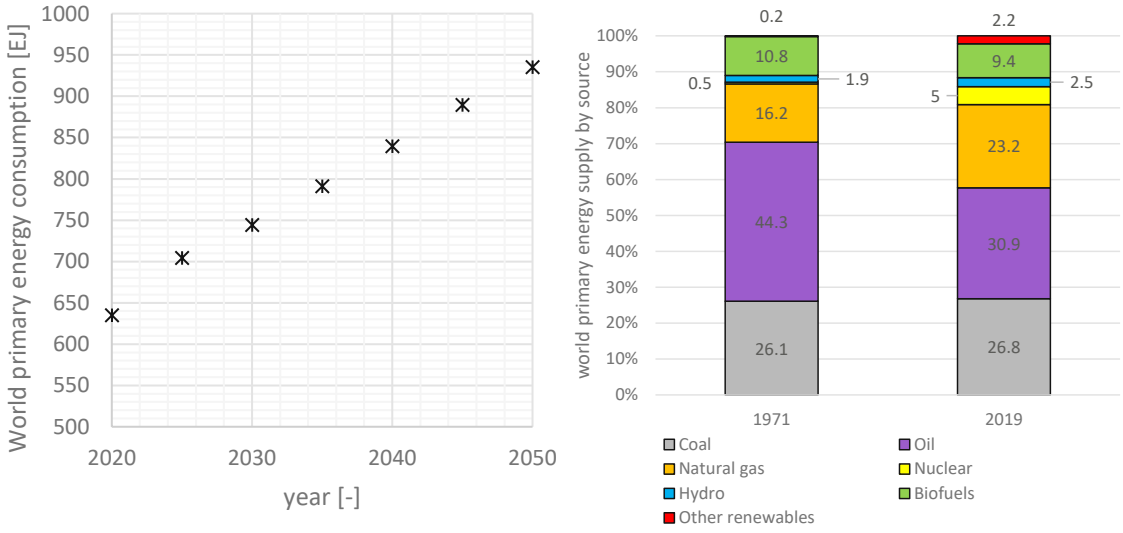

figure 1: left: world primary energy consumption projection [drawn with data from [2]]; right: world primary energy supply comparison by source between 1971 and 2019 [drawn with data from [3]*]*

This development is in stark contrast to the 2015 Paris climate agreement where the international community committed to keep global warming below 1.5 °C by reducing CO_2 net emissions [4]. As a consequence the European Union created plans for a pathway to fulfill this goal by becoming a net zero CO_2 emissions economy by 2050 [5]. This pathway is further substantiated by the “Fit for 55” proposal of the European commission published in 2021. There, the legal tools are described to reduce the European Union’s net greenhouse gas emissions by a minimum of 55% until 2030 compared to 1990 levels. Suggestions in this proposal consist of lowering the cap of emission trading certificates, heighten energy efficiency targets and to increase the energy provided by green or renewable sources, to name a few [6]. However, this development is not only exclusively a European topic. In the USA the “Build back better” initiative by the Biden Administration as well as Chinas pledge to become carbon neutral until 2060 will lead to a reckoning for global emissions [7].

One industry that will have to face the harshest consequences of current developments will be the refinery sector. Already since the beginning of the COVID 19 pandemic in 2020 around 3 million barrel per day refinery capacity has been filed for closure and a further 1.5 million are expected to do so until 2025 [7].

In the past the proliferation of world population and increasing access to automobile and aviation transport was one of the main drivers of oil industry growth with the second being the petrochemical sector [8]. But in the upcoming decade growth of fossil crude-derived fuels will diminish until at around 2035 demand will start to decrease or top-off [7] [8] [9]. Mostly unscratched from these developments will be the petrochemical sector with an estimated growth per year of around 4.3 million barrel per day until 2045 [9]. In figure 2 a forecast is depicted in which the changes of oil fraction demand depending on industry are visualized.

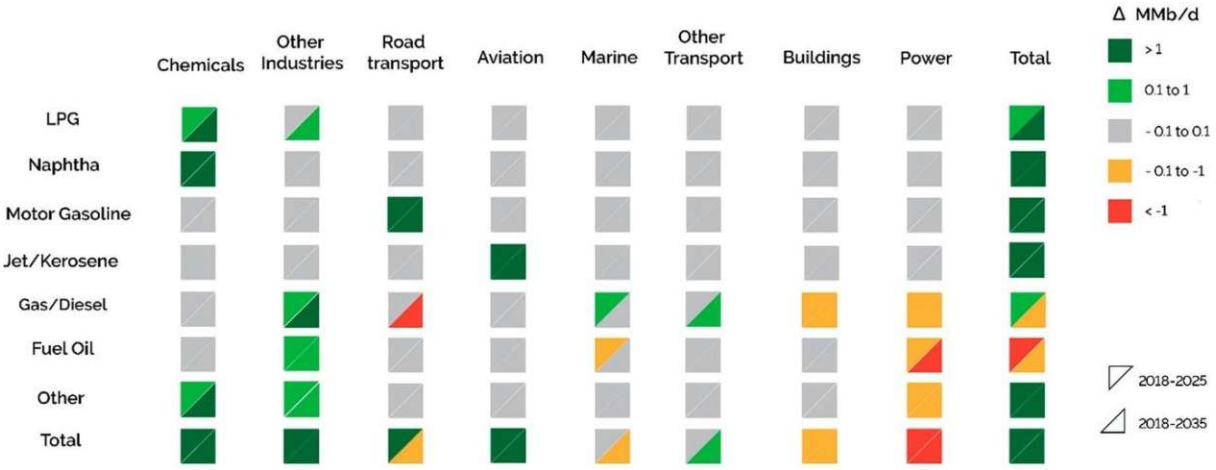

figure 2: incremental changes of oil fraction demand until 2025 and 2035 depending on sector (reprinted with permission under CC BY license from [8], created with data from [10] *)*

The combination of future market demand and environmental legislation leads to the conclusion that refinery operators must adapt to the changing circumstances to ensure long-term profitability with the petrochemical sector offering most promising opportunities [8]. Nowadays high-value building blocks for the petrochemical sector are light olefins (C_2-C_4) as well as BTX (benzol, toluol, xylol). These high-value intermediates are currently most supplied via steam cracking or fluid catalytic cracking (olefins) and catalytic reforming (BTX) [11].

Out of these processes the fluid catalytic cracking (FCC) process is especially of interest since it produces the bulk of high-octane gasoline and a high proportion of olefins, mainly propylene [12]. FCC offers a wide variety of possible products but also high versatility regarding feedstocks, making it the ideal candidate to address shifts in product distribution. The main focuses can hereby be laid on surging demand for clean fuels in the future which could be satisfied using alternative and/or biogenic feedstocks [12]. Secondly, an emphasis can also be on the generation of petrochemical products utilizing heavy residues while demand for heavy fuels like bunker oil declines [13].

1.2 The aim of this thesis

This dissertation's main aim is the feeding and co-feeding of heavy oil fractions and pyrolysis oils from sustainable sources in the fluid catalytic cracking process. Investigations include the generation of these alternative feedstocks, their characterization and their influence on product quantity and quality.

The following objectives make up this work:

- A **literature review** to describe the history and state-of-the-art FCC technology including alternative feedstock production and catalysts
- The **material and method section** describes the process and analytical methods with a focus on the utilized pilot plant and feedstocks
- The **experimental section** investigates the pilot scale FCC experiments and can be divided in three main topics
    - Experimental campaigns researching the influence of catalyst and fluidization rate changes
    - Processability and co-feeding of heavy residual feedstocks (atmospheric residue and deasphalted oil)
    - Processability and co-feeding of plastic and wood waste derived pyrolysis liquids

2. State of the art research and technology of Fluid Catalytic Cracking

2.1 Historical development of the cracking process

2.1.1 The rising need in fuels and the first cracking processes

Before 1900 there was little need for naphtha products and the demand was significantly lower than the supply. This changed dramatically with the commercial success of the internal combustion engine via automobiles. Up to 1910 the natural occurring low-boiling factions in crude oil obtained via distillation (straight run) were sufficient to satisfy the rising demand for fuel. However, afterwards this was not the case anymore so refiners had to come up with solutions [14] [15] [16].

One such solution was the so called Burton process, developed by William M. Burton and colleagues in 1913 under the funding of Standard Oil Company [14] [17]. This was the first commercially established thermal cracking process although thermal cracking itself had already been known for more than 30 years but never commercially utilized. The process worked at 5 bar and temperatures between 370 and 450 °C, which was below the critical temperature of 450°C where steel grades back then started losing their mechanical properties [14] [15] [16].

In 1915 the first major step in the long history of catalytic cracking processes was taken by Almer M. McAfee. He showed that heating petroleum oils in the presence of anhydrous aluminum chloride ($AlCl_3$), which acted as a catalyst, leads to high-quality gasoline as a product. This catalyst was deactivated over time by coke deposits and could be regenerated later in a separate process [18]. However, the high cost of producing anhydrous aluminum chloride acted as a hurdle for the process' commercial success even though McAfee's employer, Gulf Oil Corporation, spent considerable resources making the process more feasible [15] [17] [19].

2.1.2 The Houdry process

In the 1920's the octane engine was developed which led to the understanding of the direct link between gasoline composition and engine performance. In 1922 french engineer and automobile racer, Eugene Jules Houdry collaborated with the pharmacist E. A. Prudhomme after he had heard about high-performance gasoline Prudhomme had generated out of lignite (brown coal). They tried to commercialize this lignite to gasoline process with support by the French government by building a demonstration plant. This process was using a solid porous clay catalyst to produce high-octane gasoline in better quality than thermal cracking processes achieved. However, the results obtained by the demonstration plant where disappointing and the process could not compete economically. Despite this setback Houdry was convinced by the potential of catalysis in petroleum engineering after he found out that the catalysts activity was restorable via combustion of the accumulated coke. In the year 1930 he moved to the USA and commercialized the so called Houdry-process together with Socony-vacuum oil Co. and Sun Oil Co. [16][17][20][21].

In 1938 three plants utilizing the Houdry process were in operation with a total capacity of 20000 barrels per day [22]. These plants were operated in a semi-batch manner. The fixed bed reactors that were filled with a catalyst, an aluminosilicate, were alternately operated in an operation and a regeneration mode. In the operation mode the reactants flowed through fixed beds of catalyst with operation times between 30 to 135 minutes when gas oils were cracked. The generated products consisted of up to 50 w% high-octane gasoline. After operation the catalyst needed to be regenerated since secondary products, namely coke, deposited on it. This deposited coke is burned off via air injection into the reactor. Parallel operation of 2 to 3 vessels lead to a semi-continuous cyclic production where one unit is in production mode while the others are in stripping and/or regeneration mode which was also the processes greatest disadvantage [16][20][22].

For a more detailed description see [20][22]. A schematic of a crack unit used in the Houdry process is depicted in figure 3.

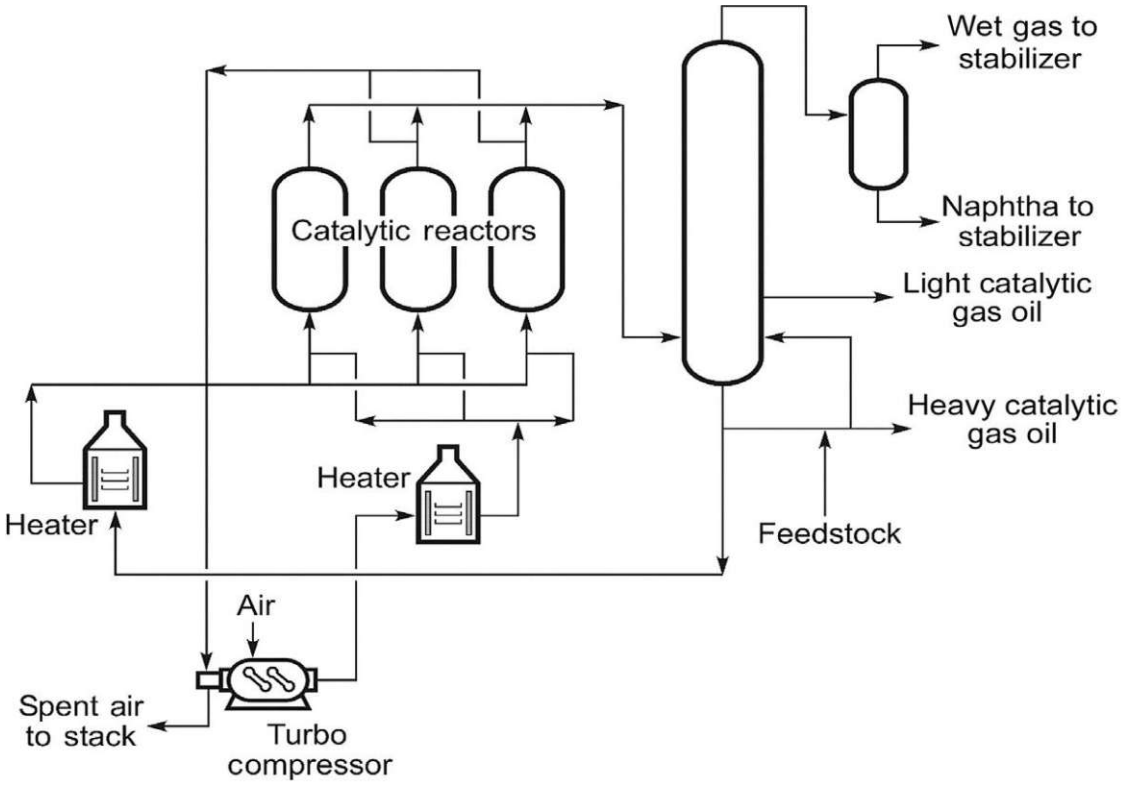

figure 3: schematic of a cracking unit for the Houdry process (Reprinted with permission from Elsevier: [23]*)*

2.1.3 Development of the first commercial Fluid Catalytic Cracking unit

Also in 1938 Standard Oil of New Jersey tried to acquire a license to the Houdry process from Sun Oil Co. (the license holder at that time) but backed down on this due to the high price of 50 million dollars xx[21][24]. As a consequence, a research group called Catalytic Research Associates (CRA) was formed to develop a superior catalytic cracking process which would make licensing the Houdry process obsolete. This group consisted originally of 4 companies but later several additional companies joined whereas German company IG Farben had to leave the group in 1940 due to the second world war. The formation of CRA was, in hindsight, a wise decision since the development of said process costed only 15 million $ in the endxx [21]. The war also fueled the research additionally since there was a high demand for aviation gasoline, butadiene for rubber production and other war materials. Especially the aviation gasoline via catalytic cracking was deemed essential since it gave the alliance planes a boost in engine power [16][21][24][25].

The consortium decided to step away from using catalyst pellets and to use powdered catalysts instead that were easier transportable. This was necessary since a continuous operation seemed only feasible if cracking and regeneration were conducted in separate reactors (unlike in the Houdry process). The first tests then were carried out in a so-called pipe coil reactor where catalyst circulation was achieved using mechanical screw pumps. However, plugging and wearing lead to unsatisfactory outcomes [24] [26].

As a result, after corresponding with researchers from the Massachusetts Institute of Technology air injectors were tested in a pilot plant to transport the catalyst and to overcome the pressure drop. This proved successful and more experiments were conducted which provided valuable design data. Eventually, the world's first commercial fluid catalytic cracker went on stream in 1942 at Standard Oils refinery in Baton rouge, Louisiana. It was named PCLA I (PCLA = powdered catalyst Louisiana) and typical actual feeding rates of around 15000 barrels per day were achieved. A flow plan of the unit is depicted in figure 4 [24][26].

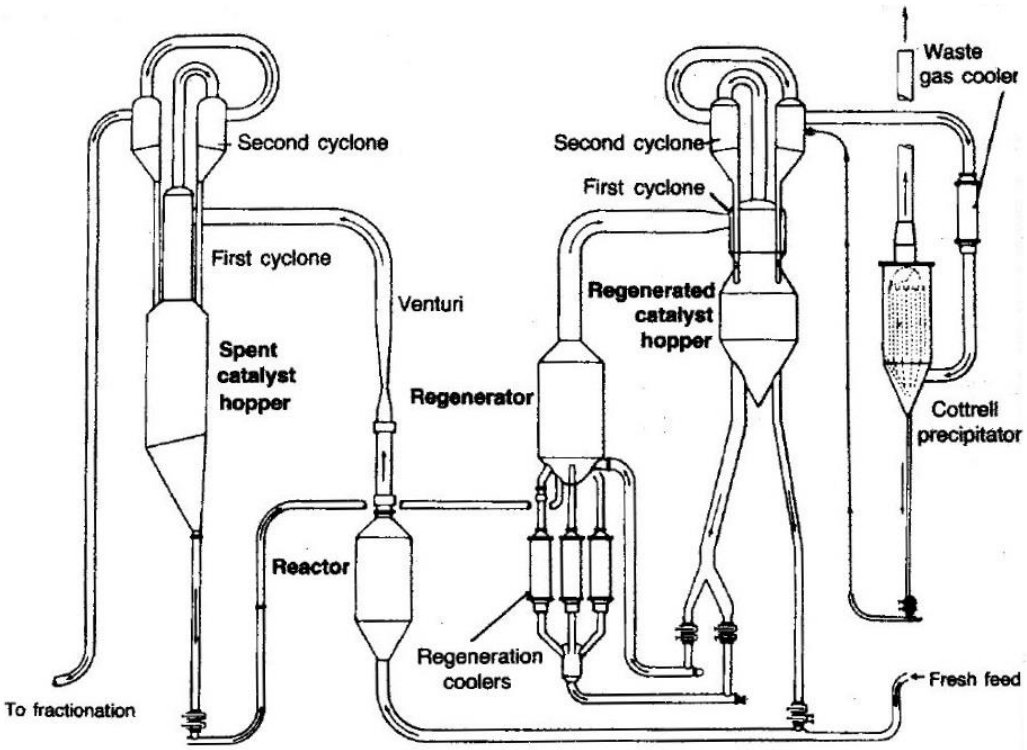

figure 4: schematic of first commercial Fluid catalytic cracking plant in 1942 (PCLA I) [24]

The feed was preheated in multiple heat exchangers and fed as vapor together with steam into the reactor. On the way it was mixed with a stream of catalyst in a catalyst to oil ratio of around 4. The cracking occurred in the cylindrical reactor at around 480 – 495 °C (900 – 925 °F). The cracking products were separated from the catalyst via cyclones and left the plant to get fractionated. Around 99.9 w% of the catalyst was removed by the cyclones. The rest was scrubbed in the fractionator in a heavy cut at the bottom. Residues of cracking gases in the catalysts were stripped via steam. The flow of catalyst to the regenerator was controlled via slide valves and the regeneration took place at roughly 565 °C (1050 °F). The generator temperature was thereby controlled via recycling of regenerated catalyst and sending it through regeneration coolers. These recycling rates were also regulated via slide valves. Therefore, the plant was designed as a circulating fluidized bed. Through this design high shares of fuels were achieved with naphtha making up around 43 vol% and fuel oil around 40 vol% of products. This first commercial FCC plant was successfully in operation for more than 20 years until it shut down in 1963 [24] [26] [27].

2.1.4 First improvements

Even before PCLA I went online the improved Model II was already under construction. Unlike its predecessor it was designed with a bottom, down flow withdrawal for the catalyst at both riser and regenerator (unlike the top withdrawal of model I). This change was possible since operation was conducted at lower superficial velocities which led to the formation of bubbling fluid beds in the reactor and regenerator. This new design had several advantages. It used comparably less steel but also consisted of larger vessels where the cyclones were internalized. It had a greater capacity of regeneration, in other words burning of coke, which enabled higher conversion rates. A better management of circulation and therefore catalyst handling was possible. Lastly, it had a great surplus in energy balance which made feed pre-evaporation obsolete so that liquid feed could be injected. This design was used to construct PCLA II and III next to PCLA I in the refinery in Baton Rouge (now being part of ExxonMobil) and improved versions of these two units are still in operation to this day [24] [26] [28] [29].

Shortly after, still in the 1940s, significant improvements in the air compressor equipment and their utilization were made which enabled higher operating pressures. This led to new plant configurations and designs especially for the regenerator but also for catalyst stripping sections. Furthermore, unit heights could be reduced while still increasing their capacity. At the end of the war around 34 FCC units were operational and refiners switched from generating mainly high octane “base stock” for aviation gasoline to lower quality ordinary gasoline which automobiles used [16] [21] [27] [28].

2.1.5 Breakthrough in catalyst technology

The advancements in FCC design can be divided in 2 major sections: the early days when synthetic clay catalysts were used and the zeolite catalyst era. The synthetic amorphous catalysts were temperature sensitive which limited regenerator temperatures to a maximum of around 590 °C (1100 °F). To comply with this limitation advanced water spraying systems were installed throughout the dilute section of the regenerator and in flue gas lines. This was even more important to prevent so called runaway afterburning. The low temperatures lead to significant amounts of CO in the flue gas which could be ignited at hot spots leading to temperatures up to almost 1000 °C (1800 °F). Additionally, long residence times of catalyst were necessary due to low regenerator temperatures and the catalysts low activity. For the reactor section the low activity of the acid-treated natural clay catalysts also resulted in high recycling rates and low reactor bed heights. This changed dramatically with the introduction of a new catalyst type that provided enhanced activity and stability [27] [30].

In the mid-1960s with Mobil Oils’ invention of zeolite catalysts some drastic design changes occurred. One major change which is still in use today is the invention of riser cracking which was originally invented in 1956 by Shell but really started to take off in the 1960s and the elimination of dense-bed cracking. This was enabled by the catalyst’s drastically higher activities (around a factor of 1000) compared to clay catalysts. Consequently, the recycling operation mode was abolished, and a single pass operation mode was chosen with higher feedinput. In the 70s with further advancement in catalyst technology many improvements like complete CO combustion were introduced which were made possible by catalysts that withstood heightened regenerator temperatures due to their higher thermal stability. Also findings regarding the impairment of catalyst activity and selectivity through coke led to the reduction of carbon on regenerated catalyst particles below 0.1 w% [16][27] [28] [30] [31].

2.1.6 Heavier feedstocks

In 1961 the first heavy oil cracking unit was introduced by Kellogg in the Philipps Borger refinery in Texas under the name Heavy oil cracker (HOC) which processed atmospheric residues. After spikes in oil prices during the oil shocks in the 1970s the petroleum refining industry needed to explore new heavier crudes to be less dependent on light crudes from the middle east. Additionally, a rising demand in light distillates fostered advancements in the cracking of heavy oils. These modified process chains contained either feed pretreatment or resid catalytic cracking or sometimes even both [16][32] [33].

One advancement was the development of catalysts designed for the cracking of heavy crudes which were less prone to metal passivation since resids tend to contain more heavy metals in comparison to lighter FCC feedstocks. Especially vanadium and nickel proved to pose problems since they deactivated common FCC catalysts rather quickly [16].

Furthermore, an increased coke production occurred when processing heavy feedstocks. As a result two stage regeneration was invented in the 1980s. Hereby, the coke was only partially (around 70 w%) burned off in partial burn mode in the first stage. The second stage was run in full combustion mode to reduce the remaining coke to acceptable levels. Often additional cooling was required [16] [28].

2.1.7 FCC as a feedstock provider for the petrochemical industry

A rather recent development in the long history of FCC processes is the promotion of FCC as a feedstock provider for petrochemicals. Invented in 1965 by Argauer and Landolt [34] the introduction of ZSM-5 zeolite as a catalyst additive by Mobil Oil helped shift the product yield towards LPG and olefins. This introduction was fostered by the banning of leaded gasoline which made alternatives of octane enhancement necessary. Furthermore, higher reactor temperatures and higher catalyst to oil ratios were implemented in so called high severity fluid catalytic cracking (HS-FCC) to optimize high propylene yields under high conversion. This evolution was boosted by skyrocketing olefin, especially propylene, prices since the mid-1990s [16] [35] [36] [37] [38].

2.2 FCC state of the art unit configurations

Since the introduction of the first commercially applied cracking process unit in 1936 by Houdry [22] major developments and breakthroughs have happened which were described in the previous chapter. These advances occurred not only in catalyst development but also in reactor designs which changed considerably. This design evolution spanned from fixed beds to moving beds to fluidized beds operation modes. The first, fixed bed operation, plays currently no longer any significant role in commercial operation due to its capacity limitations originating from high catalyst deactivation rates as well as short cycle lengths. Furthermore, no real steady state operation was possible and strict limitations of feeding only low-boiling feedstocks due to a need for complete evaporation were severe disadvantages [39] [40].

To overcome the limitations of fixed bed processes moving bed designs were introduced. In moving bed processes the catalyst pellets flowed downwards via gravity through the reactor and subsequently the kiln. From there the catalyst is then transported via bucket elevators or pneumatic lifts back to the plant top. Examples of such processes are the Airlift Thermofor Catalytic Cracking process, the Houdryflow catalytic cracking process or the Houdresid catalytic cracking process. This work, however, will focus on fluidized bed systems due to their overall dominance as the state of the art catalytic cracking process [39] [40].

Fluidized solid operations helped catalytic cracking gain its breakthrough. Together with the introduction of zeolite-based powdered catalysts larger units with higher conversion were built. After the first fluid catalytic cracking plant was built in 1942 numeral unit configurations were developed and built. In this section a general process description is given and some of the currently employed state-of-the-art FCC process units are described [39] [40].

In fluid catalytic cracking the reaction zone is designed as an entrained flow reactor where the catalyst circulates continuously between reactor and regenerator section. Thereby, transferring (almost) all of the heat originating from coke combustion to the reactor and oil feed. In figure 5 a process flow diagram shows a common FCC unit configuration with its corresponding fractionation column and its product streams [39] [40].

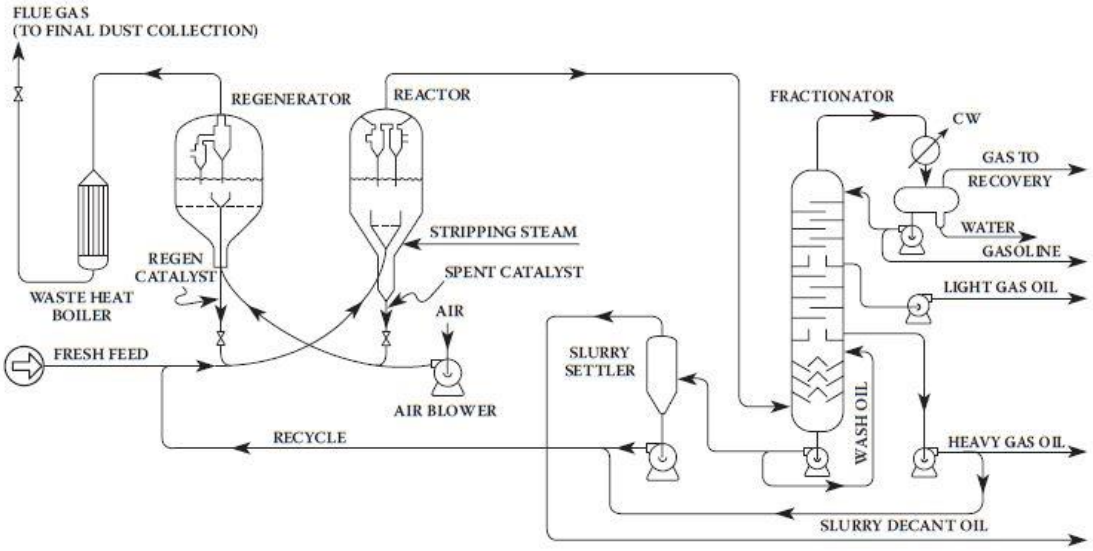

figure 5: FCC unit configuration with fractionation, recycling and product streams [41]

Preheated fresh feed is introduced into the FCC unit together with recycled feedstock which is comprised of a heavy product section and therefore not as keen to cracking reactions as the fresh feedstock. Nonetheless, to some degree further conversion of the recycle feedstock is possible. Combined or separate feeding of those two components varies between different plant designs [40].

In the first part of the reactor which is made up of a long vertical pipe, a so called “riser”, the hot catalyst and the feedstock get in contact (which evaporates part of the feedstock) and then they flow co-current from bottom to top. The initial transport of the catalyst is enabled via steam which acts as a lift gas. While the catalyst/feedstock mixture flows upwards at high flow rates (10-20 m/s superficial gas velocity) the cracking reactions occur. Lighter products are generated resulting in a continuous increase of the vapor phase volume. At the riser top the mixture enters the second part of the reactor section which is separation [40].

In a first separation step the catalyst and vapor phase are separated via cyclones thereby preventing any unwanted catalytic overcracking. Further thermal cracking, however, might still occur until the vapor phase is cooled down. The second separation step is the stripping of heavier product remains off the catalyst particles by using a stripping agent (steam). Although, most of the cracking reactions occur in the riser, a minor portion is still taking place in the separation part of the reactor which can still be significant. This goes especially for units operating at elevated temperatures to promote LPG production [40].

The product gas is leaving the reactor top and is disaggregated in a fractionation column. Here, not only the FCC products are obtained which are then further refined downstream in conversion or purifying units but also the recycle oil which is fed back to the fresh feed stream [40]. For a more detailed description of the FCC products refer to chapter 2.5.

The spent catalyst leaving the reactor section must be regenerated by burning off the coke deposited on the catalyst’s surface and in the catalyst’s pores. This is accomplished in the regenerator using air as fluidization gas. Through variation of the amount of airflow the coke burn-off as well as the catalyst temperature is set. The residual coke on the regenerated catalyst is hereby in the range of 0.01 – 0.4 w%. The combustion heat is then transferred from the regenerated catalyst to the feedstock enabling the cracking. A general term to describe the catalyst coke dependence on the coke yield and catalyst to oil ratio is the so called delta coke which is described in equation (1) [40]:

$$Delta\ coke = \frac{coke\ yield}{catalyst\ to\ oil\ ratio} \quad (1)$$

The reactor and regenerator can be assembled in two different configurations which are illustrated in figure 6. In the stacked design (left) the reactor and regenerator are positioned above each other in a single vessel. Examples for such stacked units are the orthoflow model B and the first HOC model from M. W. Kellogg Co. (now Kellog Brown & Root). In the side-by-side design the reactor and regenerator are separated into two vessels which are connected via pipe systems for catalyst transport. This design is more commonly used and employed in a variety of designs by Universal Oil Products (UOP), Shell, ExxonMobile and others [42][28]. For further design descriptions refer to complementary literature by Murcia [28] or Gary et al [41].

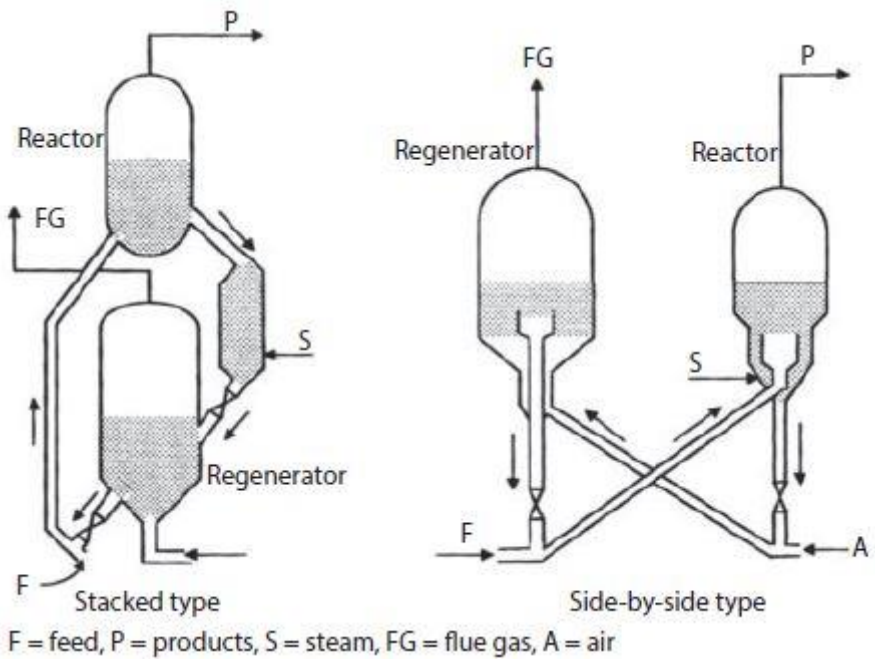

figure 6: reactor and regenerator configuration types - left: stacked design - right: side-by-side design (Reprinted with permission from John Wiley and Sons [42]*)*

2.3 Resid Fluid Catalytic Cracking (RFCC)

Heavy feedstocks often contain higher aromatics compared to conventional light crudes that are made up of more paraffinic structures. This structural difference leads to higher yields of non-valuable products when resid is fed. Additionally, the metal content (especially nickel and vanadium) as well as the high conradson carbon content (CCR) of such feeds rises challenges for processing residues. Habib et al [43] demonstrated that heavy metals increase the hydrogen and dry gas yield while decreasing LPG and gasoline. The heavy metals also poison the catalyst which makes a higher catalyst make up rate necessary therefore increasing the costs of operation. Lastly, the conversion often drops inevitably when feeding residues which makes RFCC only profitable for feedstocks with low metal content and low CCR. As a rough estimate, around 40 w% of CCR is later converted into coke inside the FCC unit, however metals can increase this yield even further up to 50 w% [44]. This significantly higher coke generation inside the unit increases temperatures in the regenerator if the severity of the FCC operation is unchanged. As a consequence, catalyst coolers are often necessary. Increasing the catalyst to oil ratio can help address rising coke yields by reducing delta coke. In that case, the amount of coke per mass of catalyst is reduced providing higher catalyst activity. [40] [44].

The effect of metal poisoning of the catalyst can be limited by a certain degree via usage of feed additives. For metal passivation antimony has been used successfully since 1976 against nickel. When injecting the fresh feed antimony is added after feed preheat to prevent any thermal decomposition. There, it is often introduced via light cycle oil or slurry oil recycling. The antimony reacts in the hot fresh feed with the nickel via alloy formation. The dosage of antimony depends hereby on the amount of nickel in the feedstock. High overall retention rates of more than 90 % of antimony can be achieved when the bottoms of the FCC products are recycled. As a downside its hazardous properties must be mentioned as well as the possibility of poisoning CO promoters in the catalyst [45].

The Heavy oil cracker (HOC) of M.W. Kellogg Co. is an adaptation of the standard FCC process which can process residues with increased amount of metal contaminants and asphaltenes. It was the first process specifically designed for residual cracking with its initial design being launched in 1961. Even without pretreatment the HOC process can convert feedstocks that contain around 5 – 30 ppm nickel and with Conradson carbon residue values of around 5 – 10 w% [23]. With pre-hydrodesulfurization feedstocks with metal and coke contents above these values are processible and production of high quality olefin derivatives and naphtha/diesel fuel blends is even possible. The first HOC units were designed in side by side configuration while the newest ones employ a stacked design [23] [46]. An illustration of the reactor/regenerator section of a HOC process unit is depicted in *figure 7*.

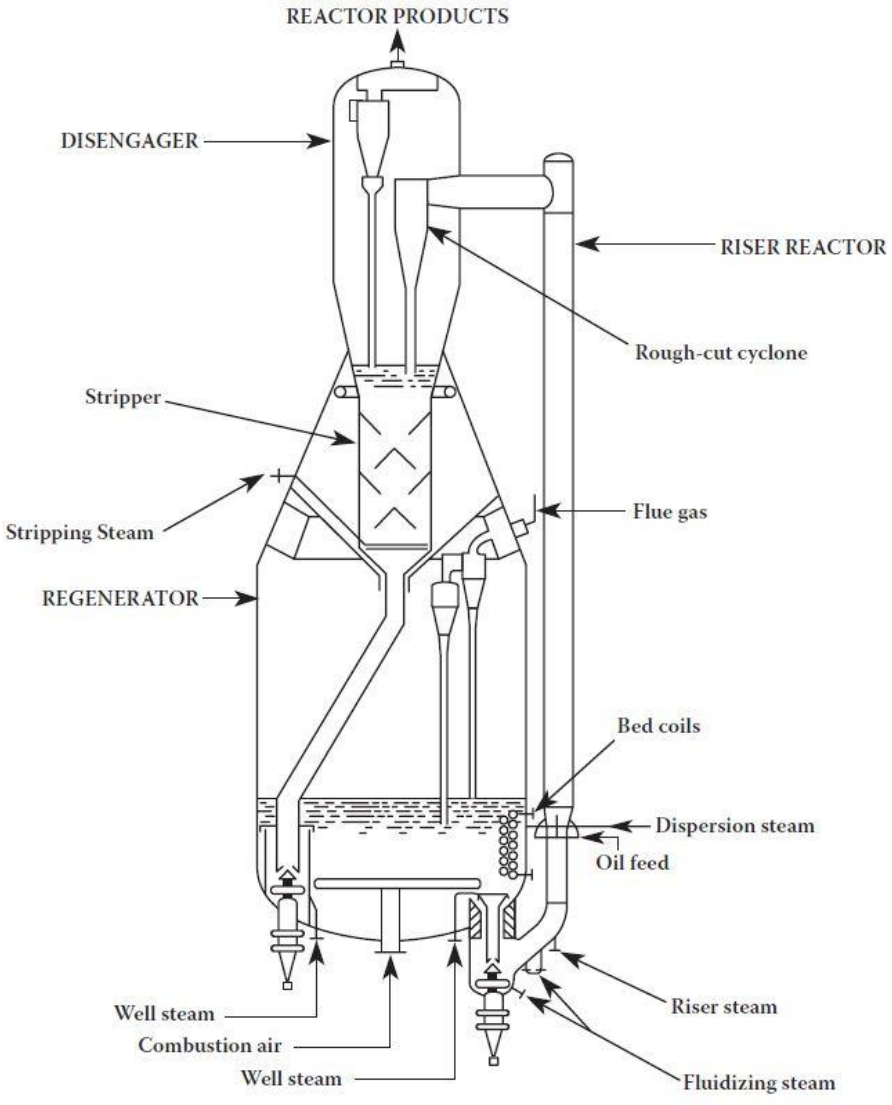

figure 7: residue fluid catalytic cracking unit (HOC process) by M.W. Kellogg [41]

The general mode of operation is the same as for standard FCC processes with a few adjustments. The reactor is an external vertical riser with low contact times, which is fluidized by steam in amounts which are significantly higher than for gasoil units. This enables a more complete vaporization of any volatile compounds. At the riser end a closed cyclone system is located where the hydrocarbons are removed from the catalyst in a two-stage stripper to reduce catalyst circulation coke. The coke is burned off in the regenerator bed at around 730 °C. This temperature is maintained via steam coils in the bed or external coolers which convey excess heat for e.g. feedstock preheating. This heat release from burning coke and asphaltenes is significantly greater than for conventional plants. To further minimize the excess heat the recycling of slurry oil and cycle oils is reduced or even eliminated. The high metal levels often necessitate a high amount of catalyst make-up which is regulated by plug valves. The catalysts specialized for treating heavy oils consist of a high amount of zeolite and have pore structures which minimizes the trapping of larger molecules [23] [46].

Later on specialized plants for residual catalytic cracking were developed by Kellogg's competitors. The RCC (resid catalytic cracking) process was invented by UOP with the first plant being erected in the 1970s. Stone and Webster in collaboration with Total Petroleum as well as Shell followed in the 1980s with their respective designs [46]. For detailed information regarding different heavy residue plant configurations refer to complementary literature such as [23] [46] [41].

2.4 The refinery and the FCC units integration in it

Generally, all types of hydrocarbon feedstocks can be fed into an FCC unit which is one of its main advantages. The atmospheric and vacuum distillation are a major provider of feedstock for the Fluid Catalytic Cracking unit. Henceforth, those upstream fractionation processes are shortly summarized in the following:

2.4.1 Desalting

The crude oil that is recovered from a reservoir is usually contaminated with different compounds like water, gases and solids/impurities. Those compounds are separated from the oil in vessels via gravimetric separation. An additional dewatering and desalinating step is often attached where rests of water-soluble salts and solids are removed via water washing. The water is mixed with the crude oil to create fine droplets. The water-oil mixture is then heated to reduce viscosity and the 2 phases are separated from each other in settling tanks. This can be achieved by adding chemicals for demulsifying or by applying an electrostatic field to make the droplets conjoin and form a water phase. The removal of said salts and impurities is crucial for the refinery since corrosion, pipe clogging or catalyst poisoning could occur otherwise in later processes [47] [48].

2.4.2 Atmospheric distillation

After this purification step the oil is put under pressure and preheated via heat exchangers and furnaces to the desired temperature. A determined portion of feedstock hereby evaporates already in the pipe and this vapor stream then enters the flash zone of the fractionation column of the atmospheric distillation. In the flash zone steam, which acts as a stripping medium is mixed with the feed. The liquid fraction of the oil leaves the column at the plant bottom. This atmospheric residue is then pumped to other refining and/or fractionation units. The vapor fraction flows upwards the column and gets in contact with the colder reflux flowing down from the column. From bottom to top the temperature in the column decreases thereby fractionating the oil parts depending on their boiling temperatures. The products in the desired boiling ranges are drawn from the side of the column. These fractions are equilibrium mixtures that also still contain lower boiling compounds that are stripped and reintegrated into the distillation column. The gained primary fractions through this process are listed in table 1 [47][48].

2.4.3 Vacuum distillation

The atmospheric residue that was obtained in the atmospheric distillation is often further fractionated in a vacuum distillation column. This distillation is usually conducted under pressures of around 25 - 40 mm Hg or 30 - 50 mbar absolute. Through the integration of steam the partial pressure of the hydrocarbons can be reduced even further to encourage vapor formation[48]. This reduced pressure is necessary to decrease the boiling temperatures of the remaining fractions since a heating above 350 °C would lead to cracking of the residue. This would lead to coke forming which could deposit in the distillation column. The fractionation principle is the same as with atmospheric distillation. The products of vacuum distillation are also listed in table 1 [47] [49].

table 1: products of crude distillation as described by [50]

Atmospheric distillation
Dry Gas ($C_1 – C_2$)
Liquid Petroleum Gas (LPG)
Light straight run naphtha (LSR)
Heavy straight run naphtha (HSR)
Light gas oil
Atmospheric gas oil
Vacuum distillation
Vacuum gas oil (VGO)
Vacuum Residue

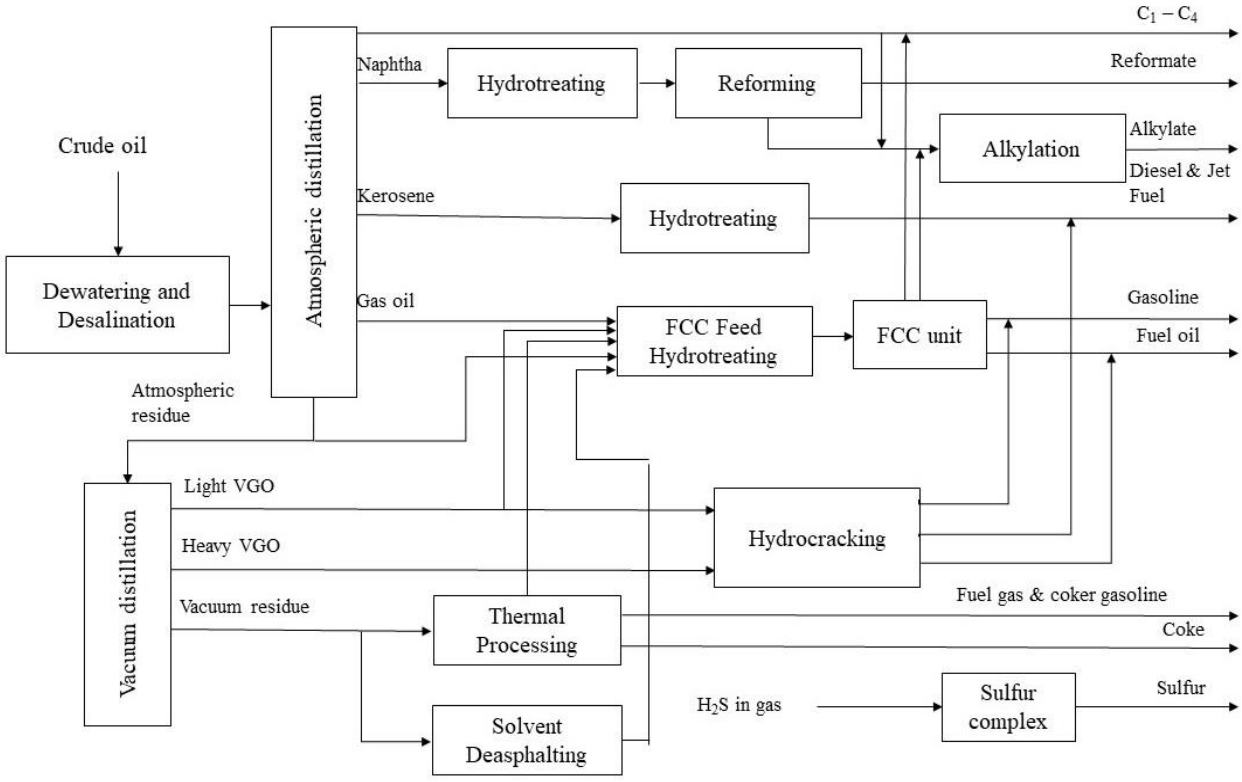

figure 8: schematic of a typical refinery with the Fluid catalytic cracking unit at its center (redrawn and adapted from Spight [47] *and Fahima et al. [49])*

Conventional feedstocks for an FCC unit are derived from:

- Atmospheric distillation (atmospheric gas oil and residue)
- Vacuum distillation (vacuum gas oil)
- Solvent deasphalting (deasphalted oil)
- Thermal processing units like visbreaking or delayed coker

These feeds can be partially or fully hydrogenated beforehand to reduce sulfur content in the FCC products. But there are also plants were unhydrotreated feeds are utilized [47] [51]. Solvent deasphalting is described in detail in a later section. The same goes for unconventional feedstocks like pyrolysis oils.

The position of an FCC unit in a typical refinery and the upstream conversion and fractionation processes that provide it with feedstocks are illustrated in figure 8. High-octane gasoline, which can be directly used for blending or further refined in alkylation, as well as olefinic gases (especially C_3 and C_4) are nowadays considered the main products of the FCC process [25] [38].

2.5 Products from the FCC process

The basic goal of an FCC unit is to increase or maximize the overall profitability of the refinery. It does so by mainly converting heavy fuel oils and gas oils in high-octane gasoline and LPG (mainly olefins) but also diesel blending component to some extent. In operation the goal was in the past to fulfill the minimum octane requirements while maximizing the gasoline yield.[52]. The main products from an FCC unit are listed in the following:

- Dry Gas: Dry gas is a low-valuable and often non-wanted product that is often tried to be minimized. Usually it consists of C_1 and C_2 hydrocarbon gases. However, sometimes it also contains inert gases (e.g. N_2, CO_2, CO, O_2), C_3+ compounds and H_2S. Once acid gases like hydrogen sulfide are removed via amine-washing the dry gas is normally used as a fuel gas for the refinery. If it contains a significant amount of hydrogen some refineries separate it from the rest of the dry gas stream in membrane separation, pressure-swing adsorption or other processes to later use it for hydrotreating. The generation of dry gas is fostered by metal contamination of the feed, thermal cracking reactions, too high residence times of already cracked products in the riser and an insufficient atomization of feed in the riser entrance [52] [53].

- LPG (liquefied petroleum gas): The LPG fraction consists mainly of C_3 and C_4 hydrocarbon compounds that can be separated in a splitter for further valorization. Around 70 % of the C_3 share is propylene which is a petrochemical feedstock used mainly for polymer production. Alternatively, it can be processed in alkylation to generate gasoline. The C_4 compounds of which butenes make up around 85 % (n- and iso-butene) can also be processed further after separation in the splitter. Again, upgrading via alkylation is a viable option but also direct blending into gasoline is possible. However, before utilizing these gaseous compounds purification steps are required. These steps are extraction via caustic soda and alkanolamine which remove hydrogen sulfide H_2S and mercaptanes. The LPG production can be promoted by increasing the reactor temperature beyond the overcracking points from gasoline and LCO and by increasing the cat to oil ratio. Additionally, a second injection point of feed into the riser can further heighten the mixing zone temperature which also leads to higher LPG yields [42] [52] [53].

- Gasoline: The high-octane gasoline was historically the most desired product of an FCC unit. The gasoline from catalytic cracking is defined by a comparably low motor octane number (MON) but a rather high research octane number (RON). To fulfill the requirements imposed by norms the FCC gasoline is blended with other streams like reformate. Improvement of the octane number can be achieved via higher cracking temperatures and selection of a catalyst that is specialized on gasoline production (smaller unit cell sizes, lower rare earth content, higher matrix activity). Sulfur is another key parameter for gasoline since it is strictly regulated. The sulfur in gasoline mainly originates from the FCC gasoline which itself is mostly influenced by the feed sulfur content. As a countermeasure hydrogenation is often applied (either for the feedstock or the gasoline) [52] [53] [42].

- LCO (light cycle oil): LCO is a blending component for diesel and fuel oils. It gets its name from its recirculation back into the plant which is often conducted due to its high aromatics content (50 – 75 w%). This also leads to a poor cetane index of around 15-25 which makes it a low quality blend. The high aromatics content (mostly two-ring and three-ring napthene components) also lead to a high density at 15 °C of 940 – 980 kg/m³. However, it can be utilized as a blending stock for diluting heavy oils and it can also be upgraded via hydrogen treatment. The LCO yield can be increased by lower reactor temperatures and lower cat to oil ratios [42] [52] [53].

- Residual oil/Slurry/Decanted Oil: The residual oil is the heaviest FCC product and has even higher aromatic contents and therefore also densities than LCO (density at 15 °C around 1050 – 1100 kg/m³). It is often used for fuel oil blending or for coke production. Decanted oil is the lowest valued product and its production is preferably minimized as much as possible. The quality of the slurry depends heavily on the utilized feedstock. Generally speaking, sulfur and ash content as well as aromatic content are the three most important parameters that must be considered. The ash content which is largely made up by catalyst particles is strongly influenced by the performance of the gas/solids separation of the cyclones. Part of this product is often recycled into the plant for a second time [40] [42] [52] [53].

- Coke: The coke is structurally and chemically not well defined. It originates from a minimum of four sources: catalytic coke, contaminant coke, feed residue coke and catalyst circulation coke. The catalytic coke is the one that is formed in secondary reactions during cracking. Contaminant coke is formed by catalytic reactions that are fueled by metals (nickel, vanadium). Also the catalyst deactivation by organic nitrogen plays a role. The feed residue coke is a heavy residue part of the feed which can be described using the conradson carbon or micro tube carbon test. During the cracking reactions it deposits without further reaction on the catalyst. The catalyst circulation coke is made up of hydrocarbons that are carried over from the reactor section and are not thoroughly stripped out of the catalyst pores. As a consequence, it is rather rich in hydrogen and directly reduces conversion [43] [52] [53].

2.6 Process operation parameters

2.6.1 Feedstock quality

The feedstock quality is considered by some as the process variable with the greatest influence on product quality and yields as well as operating conditions [51]. It naturally depends on the origin of feedstock as the FCC process' variability is one of its greatest features enabling it to process materials from a wide variety of sources.

Originally, FCC units were designed to process gas oils, however, newer units and step-wise modifications of older units made it possible to convert more complex feedstocks and residue containing blends. As a rough estimate of the feedstock quality molecular weight, feedstock boiling range or average boiling point are often considered suitable. In general experience, higher values of these three parameters lead to higher yields of coke and naphtha. However, for more accurate yield estimates such parameters are considered insufficient and more detailed description of the feedstock are necessary [23].

The levels of contaminants are significant parameters that greatly affect process performance. These contaminants are found in higher levels in viscous feedstocks and must be removed or minimized to enable a stable plant operation and adequate catalyst activity [23]. In table 2 contaminants and their negative impacts on the catalyst are listed:

table 2: feedstock contaminants and their effect on the catalyst (adapted from [23]*)*

contaminants	effect on catalyst
particulate matter	deactivation of active sites
	pore plugging
coke precursors	formation of coke
	catalyst fouling
	deactivation of active sites
	pore plugging
nitrogen	adsorption of basic nitrogen
	destruction of active sites
sulfur	catalyst fouling
	deactivation of active sites
metals	fouling of active sites
	fouling of pores

The adverse effects of particulate matter on the catalyst are of simple nature since they can just mechanically plug the catalyst pores or deactivate active sites by depositing on them. As a countermeasure FCC feedstocks should generally have a low solids content which can be ensured via a guard bed or by filtering via e.g. clay [23].

Similarly, the coke precursors which are measured via CCR lead to the same problems by depositing on the catalyst, plugging the pores, and forming additional coke during cracking. As a consequence temperature in the regenerator rises and adaptations like catalyst cooling must be applied when the temperatures rise above optimum operating levels for the catalyst [23].

Heavier feedstocks typically contain higher amounts of nitrogen and sulfur, which can later be found in waste streams, flue gas and products where limit values must be fulfilled. Furthermore, catalysts are sensitive to both sulfur and nitrogen since they act as catalyst poisons by irreversibly damaging the catalyst. Especially, the basic structure of nitrogen in hydrocarbon feeds reduces the activity of the acid sites [23].

The metals induce two different negative effects. The first being the acceleration of dehydrogenation reactions when deposited on the catalyst. Those metal-catalyzed reactions generate higher hydrogen and light gas as well as coke yields. Secondly, metals deposit on the active sites thereby causing a declining activity [23].

2.6.2 Feedstock preheating

The preheating temperature of fresh feedstock is an independent variable that has a direct effect on FCC operation. When increasing the preheat temperature less heat needs to be supplied by the regenerated catalyst to ensure feed evaporation. If no change is made regarding the heat supplied from the regenerator an increase in reactor temperature is inevitable [40].

2.6.3 Ratio of recycled and fresh feed

While the overall maximum feedrate is limited by the plants design capacity, the ratio of recycled and fresh feed can be independently adjusted to optimize operation. When no feed is recycled the unit runs on a complete once-through operation mode and the conversion and corresponding yields reflect the fresh feed properties. Via recycling some of the least valuable products like (heavy) cycle or decanted oil the product spectra can be tweaked towards lighter products. However, feed reactivity changes since the recycled feedstock is more aromatic. Therefore, adjustments of other parameters like catalyst to oil ratio could be necessary [40].

2.6.4 Catalyst activity

The activity of the catalyst is dependent on 2 factors: the carbon content on the regenerated catalyst and the amount and quality of catalyst make up (catalyst refreshment rate). Generally, the carbon content after regeneration is kept to the lowest possible level to have the highest selectivity so the addition of new catalyst is the prime determent of catalyst activity in industrial operation. However, refiners do not withdraw any catalyst deliberately since some catalyst is already lost via flue gas or slurry oil. Therefore, new catalyst is only added to level out this losses during operation. If a higher activity is required fresh higher-activity catalyst is added for catalyst make up which is the more economical route. This higher activity then usually leads to more naphtha and less coke yields. Summarized, feed composition (which influences coke generation) and catalyst makeup rate are the two dominant factors that decide the performance of an equilibrium catalyst in an FCC unit [23] [40].

2.6.5 Catalyst-to-oil-ratio and catalyst circulation

The catalyst to oil ratio is highly dependent on the coke yield and the restraints in delta coke (see equation (1)). To maintain the heat which is required for feed evaporation and cracking the catalyst to oil ratio must match the coke yield, to keep the delta coke in adequate levels and maintain heat balance between regenerator and reactor section. The catalyst circulation rate is dependent on the cat-to-oil ratio (see equation (19)) and the unit feed capacity [40]. One parameter that greatly influences and in fact enables steady catalyst circulation is the pressure balance in the FCC unit. By altering the pressure balance at different plant sections it is possible to maximize catalyst circulation and to minimize the strain on wet gas compressors and blowers which could maximize plant capacity [54].

2.6.6 Reactor temperature

The reactor temperature in commercial units is in a delicate balance with various parameters like catalyst to oil ratio, feedstock quality, feed preheat or temperature of the regenerated catalyst so that the thermal balance of the whole process is maintained. So, to increase the reactor temperature higher coke yields and catalyst circulation rates are needed if feed preheat is constant. The increase in temperature itself leads to higher conversion since more severe cracking reactions occur and higher yields of LPG and naphtha are achieved. The LCO yield decreases but not on the same level as the other yields increase, therefore, higher conversion is achieved. Additionally, the catalyst to oil ratio is also increased to maintain the heat balance so a change in reactor temperature is co-dependent on several parameters and not an independent parameter by itself [23] [40].

2.6.7 Regenerator temperature

Just like the catalyst-to-oil ratio the regenerator temperature is dependent on the heat balance and therefore only changeable in a restrained operating window. However, through the regenerators design some flexibility can be implemented. Such implementations could be catalyst coolers, two-stage regeneration or increased air blower capacity [40].

2.7 Reaction mechanisms of cracking processes

In general, two types of cracking mechanisms can be distinguished: thermal and catalytic cracking. While the focus in the catalytic cracking process is on the latter, thermal cracking will also be explained shortly since it also occurs in FCC units to a lower extent due to the elevated temperatures [53] [55].

2.7.1 Thermal cracking

Thermal cracking occurs when hydrocarbons are heated above a temperature threshold which is dependent on the specific hydrocarbons. At elevated temperatures (starting from 425 °C according to Coker [42] and Sadegbeghi [56]) C-C bonds split and free radicals form which are the backbone of the thermal cracking mechanism. See equation (2) as an example when a paraffin molecule is cracked. The following thermal cracking mechanism is described according to Coker [42] and Sadegbeghi [56].

(2)

Those radicals are short-lived due to their high reactivity and perform further reactions: α - scission, β - scission and polymerization. Both scissions are named by the location where the breaking occurs where α - scission occurs one carbon atom away from the radical and β -scission two atoms away. As described by Gates et al [57] α – scission generates a methyl radical (see equation (3)) whereas β - scission creates ethylene and a new primary radical with two fewer carbon atoms (see equation (4)).

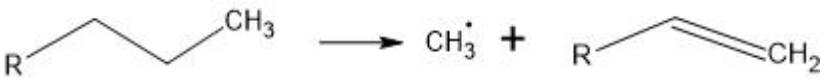

(3)

The new primary radical from β - scission can then crack and generate further ethylene and primary

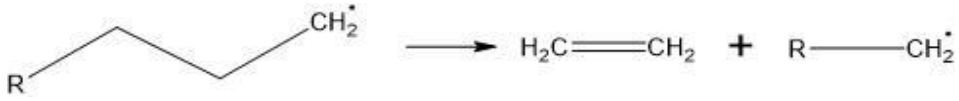

(4)

radicals. The methyl radicals from α – scission extract hydrogen from neutral hydrocarbons which leads to the formation of methane and secondary or tertiary radicals which can then crack further resulting in α-olefins and primary free radicals (see equation (5)). According to Sadegbeghi [56] α – scission occurs but is thermodynamically less favored.

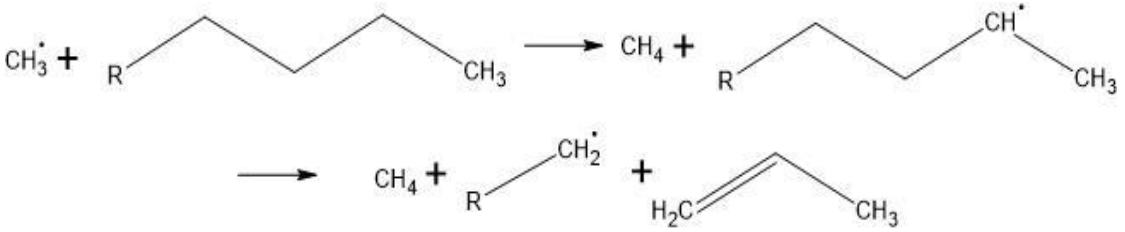

(5)

Primary radicals can also perform hydrogen extraction of paraffins (like methyl radicals) which leads to shorter-chain paraffins and secondary free radicals (see equation (6)). However, methyl radicals are less stable and therefore, hydrogen extraction is faster than for other primary radicals.

(6)

Through these reaction sequences the generation of C_1 and C_2 molecules is promoted. Only to a smaller extent other products like α-olefins are formed and to an even lesser extent branched molecules (isomerization). These olefins often react further to coke via polymerization and condensation resulting in high coke yields in thermal cracking.

2.7.2 Catalytic cracking

Catalytic cracking can be roughly grouped into primary and secondary reactions. Primary cracking occurs when the evaporated feedstock molecules undergo a first reaction, while secondary reactions are the cracking of the primary cracking products or the rearrangement of those (see figure 9). In primary cracking the feed cracks into dry gas and LPG (H_2 and C_1 to C_4) as well as gasoline and LCO. The secondary reactions are mostly caused by hydrogen transfer. Some of which are wanted like isomerization and others which generate unwanted products like coke (cyclization following polymerization) [53] [56].

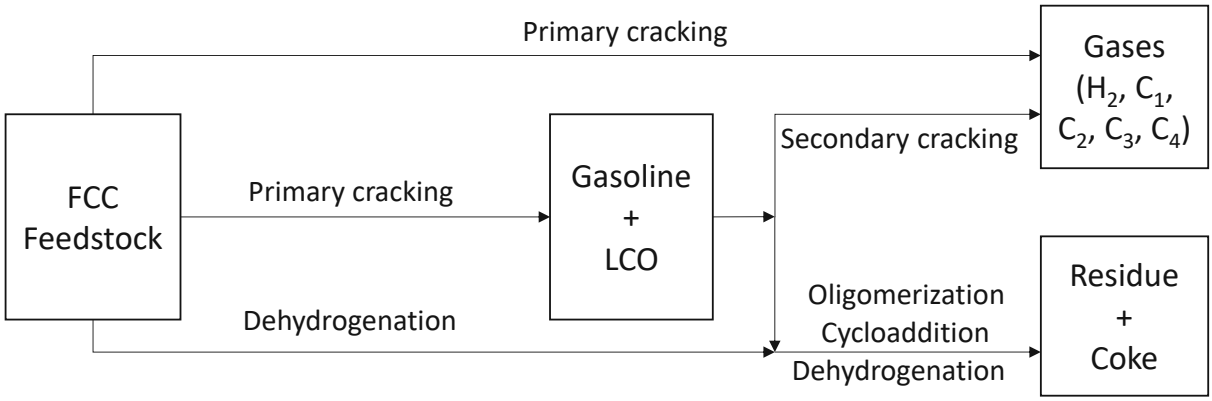

figure 9: catalytic cracking reaction network (redrawn and adapted from [53]*)*

Unlike the radical mechanism of thermal cracking, catalytic cracking follows an ionic reaction mechanism. Those ions are called carbocations and are positively charged carbohydrate molecules. A distinction can be made between carbenium ions and carbonium ions which are generated in different pathways. To form these ions catalyst acid sites are needed of which two types are present in FCC catalysts: Brønsted and Lewis acid sites (see chapter 2.8). Brønsted sites act as a proton donor while Lewis acid sites are electron pair receivers [42] [56].

Carbonium ions (e.g., CH_5^+) are formed when protons are attached directly from a Brønsted acid site to a paraffin, creating a carbon atom that is positively charged with 5 bonds. However, due to the carbonium ion's instability not many are formed for a lack of strength of the acid sites.

Therefore, further details will be excluded and focus will be laid on carbenium ions. Carbenium ions can be generated via Brønsted and Lewis acid sites. For the pathway via Brønsted acids an olefin molecule is required which is either generated via mild thermal cracking or native already in the virgin feed. There, like with carbonium ions, a proton is donated by a Brønsted acid and a carbenium ion is created (see equation (7)) [42] [53] [56].

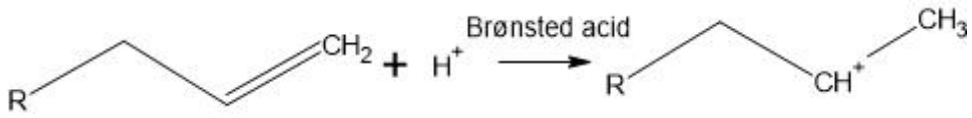

(7)

The second pathway (equation (8)) is via a lewis site where a paraffin is stripped of a hydrid ion (H^-).

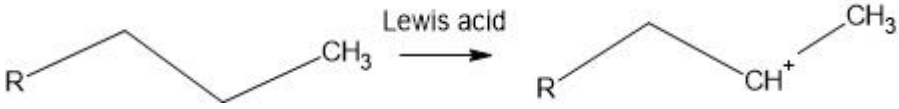

(8)

Via these pathways different carbenium ions are formed which have individual stabilities. Bernstein [58] showed that the hydrogen at the terminal carbon atoms are more difficult to abstract than the inner ones due to their difference in C-H bond energy. Referencing the work from John and Wojciechowski [59] Venuto and Habib [60] eventually concluded that the ions with the lowest stability is the methyl carbenium ion. From there on the stability increases when more carbon atoms are bonded to the positively charged carbon atom in the molecule resulting in the highest stability for tertiary carbeniumions) (see equation (9)).

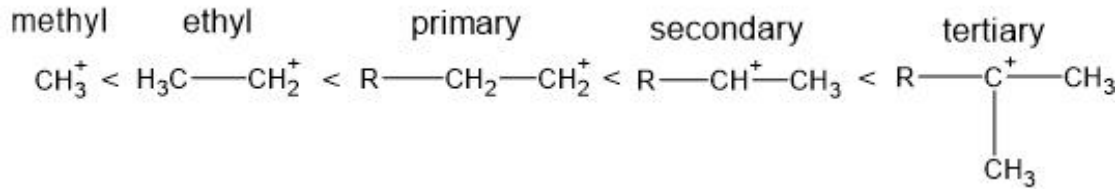

(9)

When the carbenium ion is formed different reactions can take place with the β-scission being the most prominent one in catalytic cracking. There the corresponding C-C bond is cleaved due to lower bonding energy and an olefin as well as a new shorter-chain carbenium ion is generated (equation (10)). John and Wojchiechowksi pointed out that the shortest olefin that is generated through this mechanism is propylene [59]. This chain reaction is propagated until the charge is negated which happens when either opposite ions collide (carbenium ion and hydrid ion) or when the positive charge is transported to the catalyst. The carbenium ion cracks until the former long chain molecule is broken up and only molecules with a maximum number of carbon atoms of 4 or 5 are left. These are less reactive, and the charge is passed on to a new long-chain hydrocarbon and the reaction cycle starts anew. β - scission is mono-molecular and, therefore, not equilibrium driven [42] [53] [56].

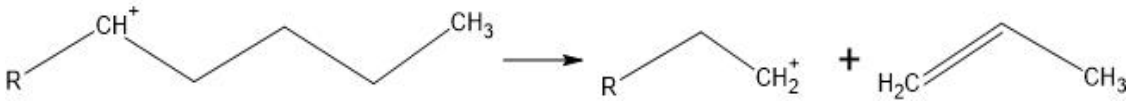

(10)

Beside the cracking of olefins to smaller olefins the following reactions also take place in β-scission:

- alkylaromatics: side-chain cracking and dealkylation eventually lead to aromatics and olefins
- ion collision: carbenium ion and hydrid ion react to paraffins

The different stabilities of carbocations promote the formation of tertiary ions that create branched molecules when cracked. This is not the case for thermal cracking which yields straight molecules due to the different reaction mechanisms. This enhanced production of branched molecules (isoparaffins and isoolefins) has several advantages [42][56]:

- higher octane number in the gasoline
- higher yields of high-value compounds in LPG (isobutane, isobutene)
- reduction of cloud point in LCO (for possible diesel blending)

Zeolites, especially rare-earth-exchanged zeolites, promote hydrogen transfer reactions via bridging two or three acid sites together in the catalyst lattice. These reactions are actually hydride ion transfer reactions where at least one reactant is an olefin which is adsorbed at an active site. As an example reactions of olefins and a naphthene are illustrated in detail (equation (11)). The naphthene acts hereby as a hydrogen donor. Through a 3 step reaction the naphthene transfers 3 hydride ions to 3 olefins leading to 3 paraffins and becoming an aromatic in the process [42][56] [53].

$$3C_nH_{2n} + C_mH_{2m} \rightarrow 3C_nH_{2n+2} + C_mH_{2m-6} \qquad (11)$$

These hydrogen transfer reactions have specific upsides and downsides. The upsides are the higher stability and yield of gasoline since the double bonds in olefins are eliminated. This is not only advantageous regarding gasoline storage but also regarding the prevention of overcracking of gasoline since olefins are reactive components. The downsides are higher aromatics in the fuels (gasoline, LCO) as well as lower light olefin yields in LPG [56].

An unwanted reaction that also leads to increased coke production due to hydrogen deficiency is dehydrogenation which generates molecular hydrogen. According to Venuto and Habib [60] dehydrogenation only occurs in the presence of metals (nickel, vanadium). Clean feedstocks and catalysts that do not contain any heavy metals do not yield any significant hydrogen levels [56].

Coking comprises of a variety of reactions which are still not understood in detail. While excessive coking is unwanted a minimum amount of coke is required for autothermal operation. Analogue to hydride transfer reactions coking reactions are bimolecular (either via carbenium ions or free radicals. Appleby et al [61] postulated that unsaturated molecules (polycyclic olefins and/or aromatics) are coke precursors that can polymerize and condense to multi-ring high molecular weight aromatics which deposit on the catalyst as coke [56]. Equation (12) illustrates in principle such a coke forming pathway [53].

$$C_mH_{2m-6}\ or\ C_nH_{2n-2} \xrightarrow{H\ loss} Coke \quad (12)$$

via alkylation, condensation, polymerization

From a thermodynamic perspective catalytic cracking is overall endothermic even though some reactions are exothermic. The major differences in thermal and catalytic cracking of different hydrocarbon compounds are summarized in table 3 (modified from Greensfelder et al. [62])

table 3: differences between thermal and catalytic cracking depending on hydrocarbon type [63]

hydrocarbons	thermal cracking	catalytic cracking
n-paraffins	major product: C_2; few branching; more α-n-olefins above C_4	major product: C_3 - C_6; intensive branching; few α-n-olefins above C_4
alkylaromatics	cracking within side chains; crack at lower rate than paraffins	cracking next to ring structures; crack at higher rates than paraffins
naphthenes	crack at lower rate than paraffins	crack at higher rates than paraffins
olefins	slow double bond position shift; little isomerization and non-selectivity for tertiary olefins; only minor hydrogen transfer	rapid double bond position shift; high isomerization and selectivity for tertiary olefins; significant hydrogen transfer
aromatics	slow formation at 500 °C	rapid formation at 500 °C

2.8 Zeolite catalysts

Modern zeolite catalysts that have overtaken the market of FCC catalysts since the 1960s offer a wide variety of advantages regarding cracking capacity and production of valuable liquid products compared to their predecessors. Modern FCC catalysts are fine powders with average pore sizes around 75 µm and consist of 4 major compounds [64]:

- Zeolite
- Matrix
- Filler
- Binder

2.8.1 Zeolite

Zeolite Y is the main component of an FCC catalyst that gives it its selectivity and catalytic activity. Zeolites have a strict lattice structure and arrange in tetrahedra where a silica or alumina atom is in the center and surrounded by 4 oxygen atoms (see figure 10). Silicon and aluminum have different oxidation states (silicon +4 and aluminum +3) which lead to different charges of the tetrahedra. The aluminum tetrahedra are -1 charged and the silicon tetrahedra are neutrally charged. When synthesizing zeolites sodium hydroxide is used which acts as a positive ion that neutralizes the negative charge of the aluminum tetrahedron. However, the so generated NaY zeolite contains high amounts of sodium which makes it hydrothermally unstable. Therefore, the sodium is often displaced with ammonia which evaporates when the zeolite is dried during production. As a result the previously mentioned Brønsted and Lewis acid sites are produced that give the zeolite its catalytic activity [64].

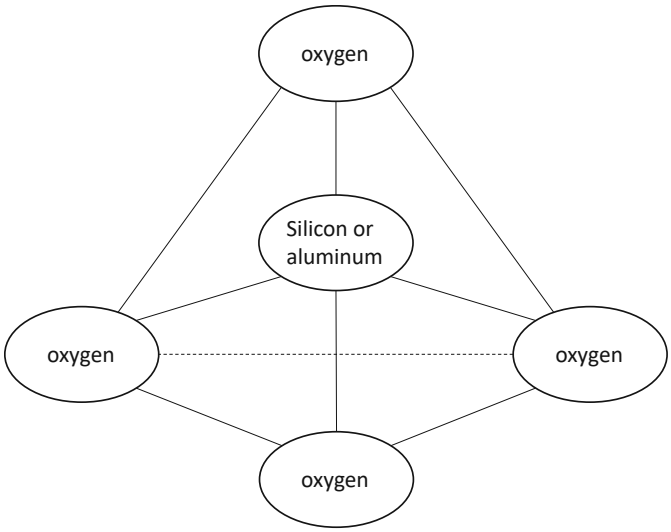

figure 10: silicon/aluminum tetrahedron of zeolites (redrawn and adapted from [64]*)*

Unit cells are the basic components of zeolite structures. Their size is defined as the distances between the repeating cells in the zeolite framework. From the unit cell size (UCS) one can conclude the amount of aluminum sites as well as the catalytic activity and, therefore, acidity of the catalyst since silicon does not possess catalytic properties. Higher amounts of aluminum lead to bigger UCS since aluminum atoms are bigger in comparison. Fresh catalyst has higher UCS and therefore high alumina in its zeolite structure. When put under harsh hydrothermal conditions (e.g. in the regenerator) it dealuminates and the UCS is decreased forming so-called equilibrium catalysts (e-cat). The sodium and rare earth content influences the final unit cell size. Due to this phenomena fresh catalyst is more reactive than equilibrium catalyst since it contains higher alumina and therefore, higher amounts of acid sites which are catalytically active [64].

Rare earth elements, mainly lanthanum and cerium stabilize aluminum atoms regarding its hydrothermal resilience. This leads to higher UCS compared to rare earth free zeolites. Consequently, zeolite activity is enhanced, and gasoline yields are higher but with lower octane numbers. This results from promoted hydrogen transfer reactions [64].

Sodium in the FCC catalyst originates either from the production process or from impurities from feedstocks. It is mostly referred to as soda (Na_2O) in the context of FCC catalysts and measured as a weight fraction. It is an unwanted compound in an e-cat since it destabilizes zeolite under hydrothermal conditions and reacts with the acid sites making the catalyst less selective, thus, reducing octane numbers. The zeolites applied in petrochemical industry are synthesized artificially and do not occur in nature (the natural corresponding zeolites are faujasites) [64].

2.8.2 Matrix

The Matrix of an FCC catalyst does not have an overall standard definition. In this thesis the definition by Sadegbeghi [64] is used where matrix is defined as all components beside zeolite where active matrix describes components that are catalytically active but are not zeolite. The matrix is based on different forms of silica and aluminum, together with kaolin clay with the latter two being catalytically inactive. Active matrix mainly constitutes of amorphous, rarely also crystalline, aluminum which contributes tremendously to the FCC catalysts performance by cracking large molecules with boiling points above 490 °C that cannot enter zeolite pores. Those pre-cracked molecules can then diffuse through the porous structure of the matrix to access the zeolite pores otherwise. Therefore, the active matrix provides acid sites for primary cracking. This importance of alumina as an active matrix component for bottom cracking is emphasized by Humphries et al [65]. Hayward et al [66] expressed that this symbiotic interaction between zeolite and matrix results in better cracking than just the sum of those individual effects. Higher boiling fractions of FCC feeds contain more contaminants like nitrogen or metals so the aluminum of the active matrix also acts as a trap for those contaminants to passivate them and deny access to the more sensitive zeolite sites [46] [64].

2.8.3 Filler and binder

A Filler reduces the catalysts activity and gives mechanical structure and physical integrity. Kaolin [$Al_2(OH)_2$, Si_2O_5] is the clay commonly used as filler. Binders are components that hold zeolite, matrix and filler together and act as a kind of glue. It also provides necessary physical properties together with the filler like proper particle size distribution, density, attrition resistance etc. [64] [67] [68].

2.8.4 Additives

Beside the basic compounds additives are additionally used to shift FCC yields in the desired direction and to inhibit the generation of pollution in the regenerator flue gas. One can distinguish between catalyst and feed additives [45].

CO promoters are a standard catalyst additive that accelerate the full combustion of coke into CO_2 to reduce the danger of flue gas afterburning in the freeboard or the cyclones and its negative side effects like local hotspots. The most common CO promoters contain platinum as an active component in concentrations of 300 – 500 ppm. It is usually added daily 2 to 3 times in an industrial FCC unit. However, CO promoters must be utilized cautiously depending on the specific needs of any FCC unit since in partial burn units addition of CO promoters can increase coke on the catalyst. This is due to a competition for oxygen between the coke combustion reactions and the CO_2 formation. Also NO_x formation can be negatively impacted [45].

Sulfur oxide emissions (SO_x) are formed in the regenerator when sulfur containing coke is combusted but these emissions are regulated. Currently the limit of SO_2 emissions in the flue gas are below 15 ppm (at 0.0% oxygen) [45]. The most economical solution beside feedstock desulfurization is often the addition of SO_x reducing additives. The additive is quite a complex powder containing magnesium oxide, vanadium oxide and cerium oxide. The latter two promoting the formation of SO_3 from SO_2 in the regenerator. The SO_3 reacts then with the magnesium oxide to form metal sulfates. These are carried into the riser together with the catalyst where they are regenerated via reaction with hydrogen or steam. As products magnesium oxide and hydrogen sulfide are generated. Again, excess oxygen is needed to enable the additives impact. Mostly between 5–10 w% of fresh catalyst make up must be dosed. Similar to SO_x additives, NO_x additives have also been employed with mixed success rates which is the reason they are not expressed here in detail. The active compounds of said NO_x additives were copper, zinc and rare earth metal catalysts [45].

ZSM-5 is a zeolite different in pore structure from zeolite Y that promotes LPG yields and enhances the gasolines octane number. This is accomplished through ZSM-5's shape selective channel structure that allows low-octane paraffins and long chain olefins to enter its pores where they react to short chain (C_3 to C_5) iso-olefins. Kokotailo et al [69] were among the first to describe ZSM-5's unique tetrahedral structure.

They showed that its framework is built from two intersecting channel systems and 10-membered ring openings which determine the channels diameter (see figure 11). Lio et al [70] concluded that the enrichment of aromatics in gasoline that occurs when using ZSM-5 is not only due to the relative decrease of olefins but also through a generation of aromatics out of these short-chain olefins. As a downside the boost in octane number goes along with a decrease in gasoline yield. This can be considered a trade-off since LPG yields increase in the same dimension. Especially propylene focused FCC make substantial use of ZSM-5 as an additive. To gain any significant change in octane at least 1 w% of catalyst must be ZSM-5 additive but typically this value is much higher [70].

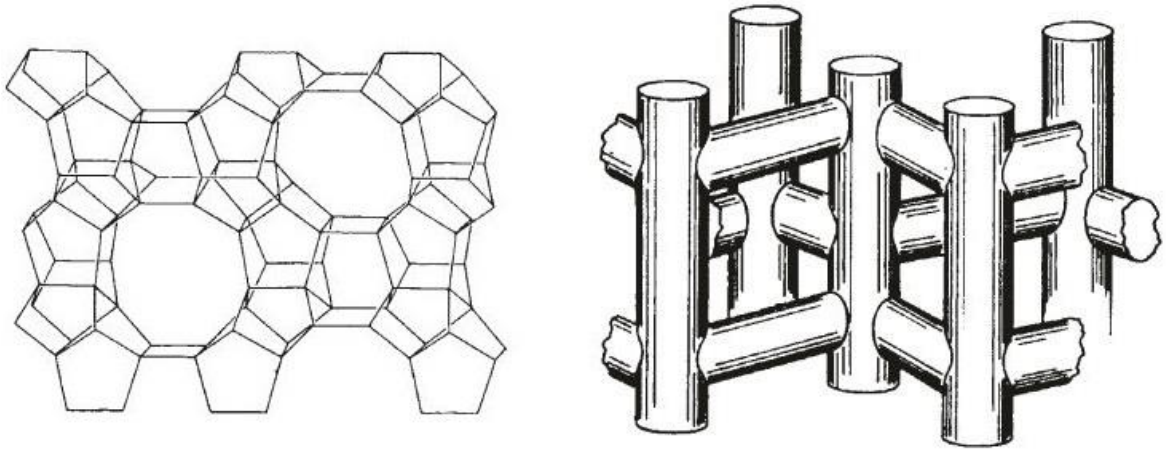

figure 11: left: 10 membered ring openings of ZSM-5 right: intersectional channel system of ZSM-5 (Reprinted with permission from Springer Nature [69]*)*

2.8.5 Resid catalysts

The burdens heavier residual feedstocks lay on FCC catalysts due to their higher contamination levels led to the development of specialized catalysts. In general, the high metal content in the residues impair the catalysts performance greatly due to metal passivation. This leads to higher hydrogen, dry gas and coke production [43]. To counter this, resid catalysts often contain metal traps (especially for nickel) based on alumina structures. There, nickel reacts to nickel aluminates which are less potent in fostering unwanted dehydrogenation reactions [45] [71]. Beck et al [67] showed that high ratios of lanthanum to cerium control the destruction of the zeolite structures caused by vanadium. This effect was most prominent when the lanthanum was precipitated onto the matrix.

In heavy residue catalysts the active matrix takes an even more important role in cracking than it does in conventional gas oil catalysts. It is important that the activities of both zeolite and matrix are balanced so that the desired fuels in the gasoline and LCO ranges are generated. Too low matrix reactivity on the one hand would result in high delta coke and gas yield. Too low zeolite activity on the other hand would lead to heavy products in the vacuum gas oil range. This balancing must also be kept in regard to deactivation. Both zeolite and active matrix must deactivate roughly at the same rate to ensure an optimum regarding selective pre-cracking and cracking at the zeolite [46] [67].

The enhanced coke production of heavy residues naturally results in a higher thermal load residue catalysts must resist. The residues feed composition with its high aromatic content also diminishes hydrogen availability. Taking into account these challenges mentioned above Mitchell et al [46] summarized the requirements for catalysts in RFCC:

- Minimize coke yield via enough matrix activity
- Catalytic bottom cracking on matrix acid sites
- High selectivity of gasoline (balance of matrix and zeolite activities)
- High metal tolerance (rare earth and alumina metal traps)
- High hydrothermal and thermal stability (e.g. via usage of USY zeolites)

BASF developed multi-stage reaction catalysts (MSRC) after they discovered that nickel unlike vanadium mostly deposits and enriches on the catalyst surface and its outer layers. Therefore, doping the whole catalyst particle with nickel traps is a material waste since the inner layers of the particles never get in contact with nickel. The MSRC concept solves this issue by combining two different catalyst structures in one particle. This is achieved by a three-stage production process where the inner layer is first generated via spray drying, which is then added to a slurry and again spray dried, thereby forming the outer layer. As a third step the catalyst particles are generated via Y zeolite crystallization and after-treatment. The zeolite hereby grows into both inner and outer layer binding them together and preventing attrition of the outer layer. It is important that the outer layer forms uniformly from all sides on the particle to ensure its metal capturing capability. Tests on commercial units showed that MSRC catalysts outperformed conventional resid catalysts regarding hydrogen and coke formation (reduction of 0.7 w%) and gasoline + LPG production (increase in 0.7 w%) [71]. In figure 12 the nickel and vanadium concentration over the particle diameters (left) as well as the alumina traps distribution in different resid catalysts (right) are illustrated [71] [72].

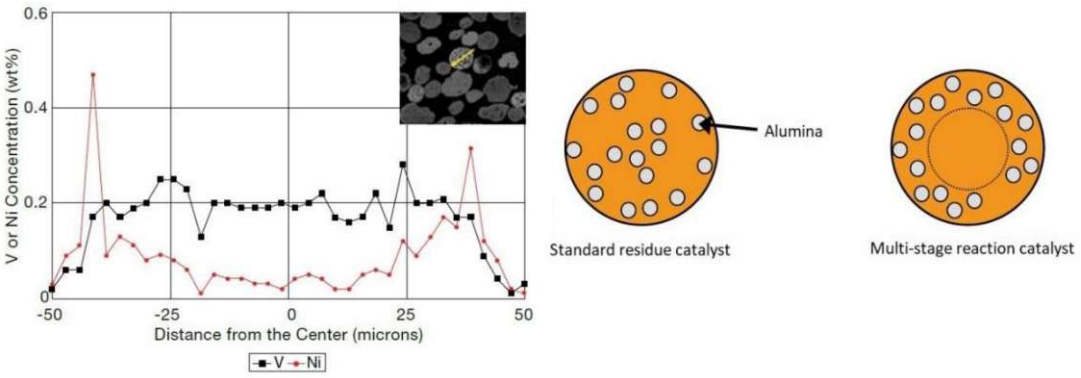

figure 12: Ni & V distribution over catalyst diameter (left) and layer model of heavy residue catalysts (adapted from [71]*)*

2.9 Deasphalted oil via solvent deasphalting

Deasphalted oil is a feedstock that is obtained via solvent deasphalting processes. In said extraction processes alkanes act as the solvent and cause polar components of the oil to precipitate. Propane is often used since it has unique properties and is normally already available at a refinery. At low temperatures (38-60 °C) it provides high solubility of paraffins where at higher temperatures (>93 °C) the solubility is almost non-existent for all hydrocarbons. These low temperatures are a big advantage since significantly less energy is consumed than in thermal processes which also make it quite cost-effective. Thus, also thermal decomposition reactions do not take place in the same amount. But also butanes (iso- and n.butane) and other alkanes up to C_6 are used as solvent when processing high viscosity feedstocks since they have higher critical temperatures [73] [74] [75] [76] [77].

As feedstock for the deasphalting process vacuum residues and, to a lower degree atmospheric residues are used. The separation principle is based on different molecular weights and densities which also enables the comparably low temperatures mentioned above. The two products that are separated are deasphalted oil and asphaltene/resins. A schematic of solvent deasphalting is illustrated in figure 13 [73] [75].

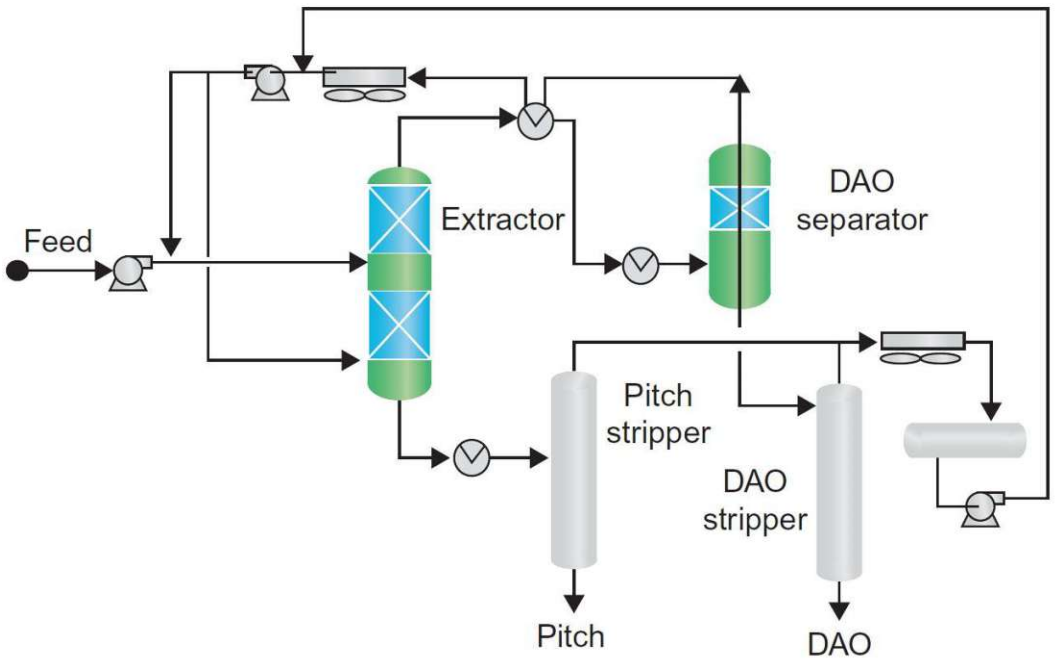

figure 13: solvent deasphalting process schematic (Reprinted with permission from Elsevier [73]*)*

A small portion of solvent is added to the heavy feedstock before entering the separation column to reduce viscosity which enables a proper mixing and cooling of the feedstock to the desired entrance temperature of the extractor. Here, the feed enters at around two thirds of the height of the multistage baffle tray column and the cooled solvent is introduced close to the bottom. The oils get extracted by the solvent and rise to the column top. The resids and asphaltenes, on the other hand, flow to the bottom. The separation is controlled by the solvent to oil ratio which is for propane 4-8 volumes per volume feed. But also temperature plays an important role for separation. Hence, a rising temperature gradient from bottom to top is maintained at all times. The DAO quality can hereby be influenced by the temperature where lower temperatures reduce the quality but increase the yield. A higher solvent to oil ratio enhances the quality regarding the Conradson carbon residue content due to a lower asphaltene content [73] [74] [75] [77].

The DAO-solvent mixture gets then separated in 2 steps: first in a kettle-like evaporator and then in a DAO flash tower. The vaporized solvent then flows back from both steps into a solvent accumulator from where it is pumped again to the feed. The DAO, now only containing a low amount of solvent, flows then into the DAO stripper where superheated steam removes any remaining solvent. This solvent/vapor mixture is then further treated and the solvent is again recycled. The purified DAO leaves the DAO stripper at the plant bottom [73] [75] [77].

The asphalt-solvent mixture is purified in the same way as the DAO-solvent mixture. First a portion of the solvent from the pressurized mixture is condensed in a flash drum and then the rest is stripped via superheated steam in a column. This solvent/vapor mixture join the ones from the DAO stripping. The asphalt (also called Pitch in figure 13) leaves the column at the bottom and is stored. Heavy metals (Ni and V) are not soluble in the solvent but remain in the asphalt which generates a relatively low content of heavy metals in DAO. This makes it a possible feedstock for the catalytic cracking process but also for hydroprocessing (desulfurization) and for the production of lubricant oils [73] [74] [75] [76] [77].

2.10 Pyrolysis

Pyrolysis is a thermochemical conversion process in which organic compounds, often biomass, are transformed into gases, liquids and chars. This occurs under absence of oxygen and through thermal decomposition of said compounds. Further process conditions are atmospheric pressures and temperatures between 300 and 600 °C. Slow pyrolysis processes are traditional suppliers of charcoal. There mostly woody biomass is heated at slow rate to 300 - 400 °C. Fast pyrolysis is conducted at higher temperatures of around 500 °C with very high heating rates. The focus in this process lies on the production of liquids, often also called biocrudes or bio-oils so conditions are chosen in which the liquid yield is maximized. However, gases and solids (chars) are always obtained by-products so a 100% conversion to liquids is not possible [78] [79]. The advantages of such a bio crude production are according to Venderbosch et al [80]:

- Independence of fuel production and consumption
- Onsite nutrient recycling via separation of minerals from fuel
- Renewable fuel production and possible secondary conversion in separate processes
- Possible refinery feedstock
- Smaller storage and lower transport requirements than for virgin biomass
- Improved transferability into reactor

The main product of fast pyrolysis can be generated in yields ranging up to 80 w% on dry feed according to Bridgewater et al [78]. Venderbosch [81], however, mentions that the usual range of liquid yields of pilot plants and laboratory units is between 60 and 70 w%. The char and gas by-products are not considered waste since they can be utilized in the process to provide thermal energy which makes fast pyrolysis basically waste-less apart from inorganic ashes [78] [81].

To boost the yield of bioliquid in pyrolysis the heating rate of the biomass must be realized in a rapid way so that the heat is transferred via convection or radiation onto the biomass surface and penetrates the particle by conduction. To achieve this the cold biomass is often mixed with an inert, preheated heat carrier like hot sand. Furthermore, the biomass is grinded into particles less than 2 mm to enable the necessary penetration depth throughout the particle. The so generated main products (liquid, gas and char) are formed in primary reactions during residence times of under 1 second. Afterwards, secondary reactions occur where the primary decomposition products further react via cracking to non-condensable gases or polymerize to char. A possible reaction pathway of wood can be found in figure 14 (derived from Venderbosch et al [80] and originally proposed by Shafizadeh et al [82]). In this figure only the carbon-containing molecules are depicted. Biomass moisture and water generated via decomposition for example also play a significant role. Therefore, it is essential to keep secondary reactions from happening which is accomplished by rapid cooling and condensation of the vapours (quenching). 90 % of the reactions in pyrolysis occur in the first 2 seconds enabling these low residence times. However, Kersten et al [83] detailed that residence times, particle sizes and pyrolysis temperature are less imperative on liquid yield than previously assumed and impact more the liquid composition. Wang et al [84] further refined these findings by showing that they apply when no or few catalytically active char (especially ash in the char) is present.

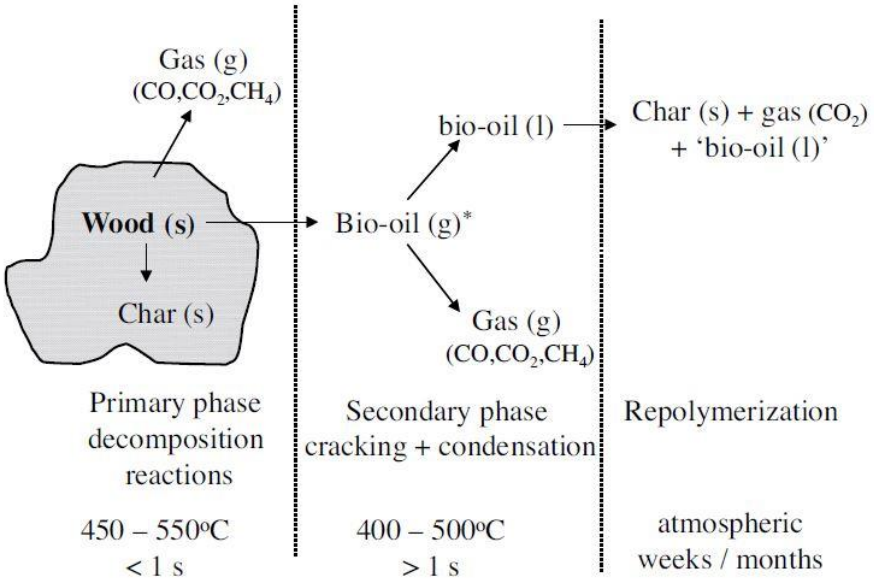

figure 14: possible reaction pathway of woody biomass (Reprinted with permission from John Wiley and Sons [80]*)*

2.10.1 Pyrolysis oils derived from biogenic waste-feedstocks

Biogenic feedstocks mostly contain three major compounds: cellulose, hemicellulose and lignin which are different in structure [85]. Cellulose is a long chain molecule build of D-glucose monomers which are linked in a 1-4 β-configuration with a rough elemental composition of $(C_6H_{10}O_5)_n$ where n accounts for the number of monomers. The average molecular weight of one cellulose polymer is around 100000 g/mol. It has a crystalline and an amorphous form which decompose at different temperatures and therefore yield different products. Hemicellulose is made up of different polysaccharides (mainly xylose but also glucose, mannose, arabinose etc.) and therefore more heterogenic than cellulose. It has a branched structure and binds to cellulose microfibrils. Its elemental composition is roughly $(C_5H_8O_4)_n$ where n is the amount of monomers. Lignin is a high complex mixture of aromatic polymers that are branched and partly substituted with methoxy groups. It has an amorphous structure and is high in molecular weight. Together, these 3 compounds form lignocellulose. Their fractions vary between 40 – 50 w% for cellulose, 20 – 40 w% for hemicellulose and 10 – 25 w% for lignin. Naturally, woody biomass contains significantly more lignin than herbaceous plants which have in contrast higher amounts of hemicellulose ranging between 35 – 50 w% [81]. Beside the 3 main components biomass also contains inorganic compounds (ashes) and extracts like oils, fats, resins, proteins, waxes, terpenes etc. [80] [81] [85].

According to Yang et al [86] these 3 main compounds degrade differently thermally (see figure 15) due to their difference in structure which also influences the pyrolysis products . However, Gupta et al [87] illustrated that independent from structure also moisture contents, contaminant levels, heating rates and inert or oxygen-rich atmosphere influence thermal decomposition.

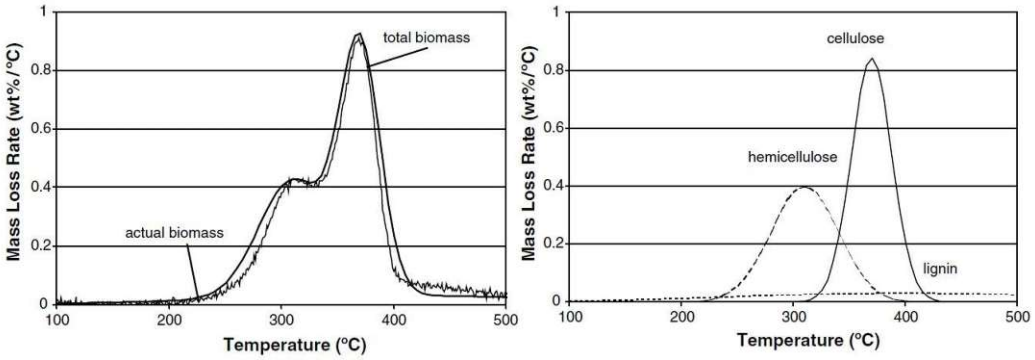

figure 15: thermogravimetrical analysis of decomposition of biomass (left) and its compounds (right) - (Reprinted with permission from John Wiley and Sons [80]*)*

Yang et al [86] illustrated that pyrolysis of biomass constitutes of 4 different phases: moisture evaporation and the degradation of cellulose, hemicellulose and lignin. The first step can be mostly outsourced out of the pyrolysis reactor via pre-drying of the biomass. Of the three main compounds hemicellulose is the first to degrade mainly in the range of 220 – 315 °C. After that cellulose decomposes roughly between 315 – 400 °C. The lignin degradation occurs continuously between 150 – 900 °C at a slow rate according to Yang et al [88]. Venderbosch [80] states slightly different values with hemicellulose degradation between 220 – 400 °C, cellulose decomposition between 320 – 420 °C and lignin degradation between 160 – 900 °C (see also figure 15). The decomposition order, however, is the same.

The gas components that are generated are mostly CO, CO_2, CH_4 and to a lesser extent H_2. The production of these compounds also varies depending on the biomass fraction. Hemicellulose accounts for higher CO_2 yields, whereas cellulose promotes CO generation. These differences can be mainly associated with different functional groups. Lignin again shows a different behavior and promotes H_2 and CH_4 production resulting from its ring structure and its added methoxy groups [88].

Pyrolysis liquid has an almost black, dark-brown color which originates from its lignin-derived compounds that are dissolved in an aqueous phase which is emulsified in an organic phase. The bio crudes water content ranges from 15 to 35 w% with the majority being derived from the original biomass making this parameter strongly dependent on the biomass source. Only about 10 w% of the water is reaction water of the pyrolysis itself. Up to around 23 w% water content the emulsion of aqueous and liquid phase is stable. Above phase separation occurs rapidly. To reduce the water content evaporation is possible albeit only under vacuum due to the polymerization that occurs at higher temperatures. As a result, the viscosity of bio crude increases and the heating value can be elevated. A typical heating value for a pyrolysis oil is 17 MJ/kg at 25 w% water [78]. The density of the bio crude is around 1200 kg/m³ depending on the water fraction. [81]

The acidity of fast pyrolysis oils is often considered a challenge. As a standard rough measurement, the pH-value is used to judge the oils corrosive properties. Especially from untreated woody biomass the pyrolysis oils pH-value is low ranging from 2-3 [89]. This originates from the degradation of hemicelluloses during production where volatile acids (acetic and formic acid) are formed that are mainly responsible for the acidity with acetic acid being the most abundant one [81]. Other fractions that determine acidity are hydroxy acids from the “sugar” fraction, phenolics and fatty as well as resin acids. Oasmaa et al [89] tested volatile carboxylic acids levels in long-term storage tests and showed that they didn’t change significantly when stored at or below room temperature for 6 months but a slight increase was observed in the first 2 months. A reduction of said acidity could be an important factor to facilitate the processing of (upgraded) pyrolysis oils in existing refinery processes and is also currently under research. Moens et al [90] concluded that stabilization of crude pyrolysis oil with methanol over a solid acid catalyst does not lead to satisfyingly low acidity due to the oils high water content that shifts the equilibrium towards the acids.

Another pathway to stabilize and reduce the acidity of the bio crude is hydrodeoxygenation where the oxygen is removed and, therefore, the acids are converted. This bio-oil hydroprocessing is deemed necessary if other applications besides burning the bio crude directly as boiler fuel are emphasized since the oils high oxygen content and high molecular weight prevent a direct usage in refinery structures [89] [90] [91].

As of 2019 the only commercially applied pyrolysis processing systems were the circulating bed and rotating cone processes [81]. Further technologies comprise of bubbling fluidized bed, ablative reactor, entrained downflow, microwave, screw/augur kiln and moving grate vacuum systems which will not be discussed in detail in this work (for further information see [80] [92]).

-Circulating Fluidized Bed (CFB)

Ensyn employs a process which was developed originally at the University of Western Ontario, Canada in the early 1980s. About the same time at the University of Waterloo a similar process (bubbling fluidized bed) was developed by constructing a bench-scale unit with low feedrates of only around 15 g/h [93]. The unit utilized hot sand for heat transfer in a fluidized bed and operated under atmospheric pressure. Several experiments were carried out at that first unit to determine the influence of temperature, residence time, feedstock, particle size with the goal of maximizing liquid yield [93] [94]. In 1984 the company Ensyn was founded by former employees of the University of Western Ontario and the process has been marketed under the label rapid thermal processing (RTP™) using a circulating fluidized bed [95]. Ensyn commercialized the process successfully via several scale-up steps and entered an alliance with Honeywell UOP (creating the joint venture evergreen technologies LLC) in 2008 which was expanded in 2014 to commercialize the co-processing of biocrude in refineries [81] [80] [96].

A process development unit (PDU) of Ensyn was sent to VTT in Finland in 1995. VTT modified the unit and after substantial improvements filed a patent in 2010 and licensed the technology to Valmet [97]. Again, the process principle is based on the CFB technology with an integrated char combustion. There they combined the fast pyrolysis with already established CHP (combined heat and power) technology to obtain an overall plant efficiency of around 90%. For more detail regarding VTTs contribution to fast pyrolysis development refer to Oasmaa et al. [81] [98].

In CFB pyrolysis processes the biomass enters the reactor via a screw where rapid mixing between biomass and a hot bed material (sand) occurs. This reaction takes place in a riser reactor, like FCC, and both char and sand leave the reactor at the plant top together with the gases. To enable this pneumatic transport of solids high rates of fluidization are necessary. Shortly after the reactor a cyclone separates the gaseous and solid compounds. The char and sand enter a combustion chamber where the char is burned off, thereby heating the sand and providing the necessary enthalpy for pyrolysis. The gases flow through an oil recovery system where the vapor is quenched and aerosols are collected and removed from the non-condensable gases [80] [92].

-rotating cone

Already in 1989 during a PhD project a first prototype of the rotating cone reactor was developed at the University of Twente [78]. This concept was further refined in subsequent projects in the 1990s to create a fully heat integrated laboratory plant (see Wagenaar et al. [99]). BTG (Biomass Technology Group) filed later a patent and developed the concept further in the years 1996 – 2006. In 2004 a first commercial unit (50t/d capacity) was purchased by Genting Bio-Oil Sdn Bhd for processing empty fruit bunch of palm oil mills. In 2007 BTG-Bioliquids was established to commercialize the technology which resulted eventually in the construction of the EMPYRO plant in 2015 (see table 4) [81].

The general working principle of the Rotating cone reactor (RCR) is very alike the CFB concept. The high mixing rates of bed material and biomass, however, are accomplished mechanically via a rotating cone. This enables operation without such high amounts of fluidization gases as CFB requires. In the RCR the char and sand drop at the edges of the cone into a fluid bed where they are transported into a fluidized bed combustor providing again the necessary heat for the pyrolysis reaction. The liquids are collected in a condenser and separated from non-condensable gases [80] [92].

For a schematic of the CFB and RCR concept see figure 16. In table 4 some current pyrolysis oil production plants with the highest capacities are listed.

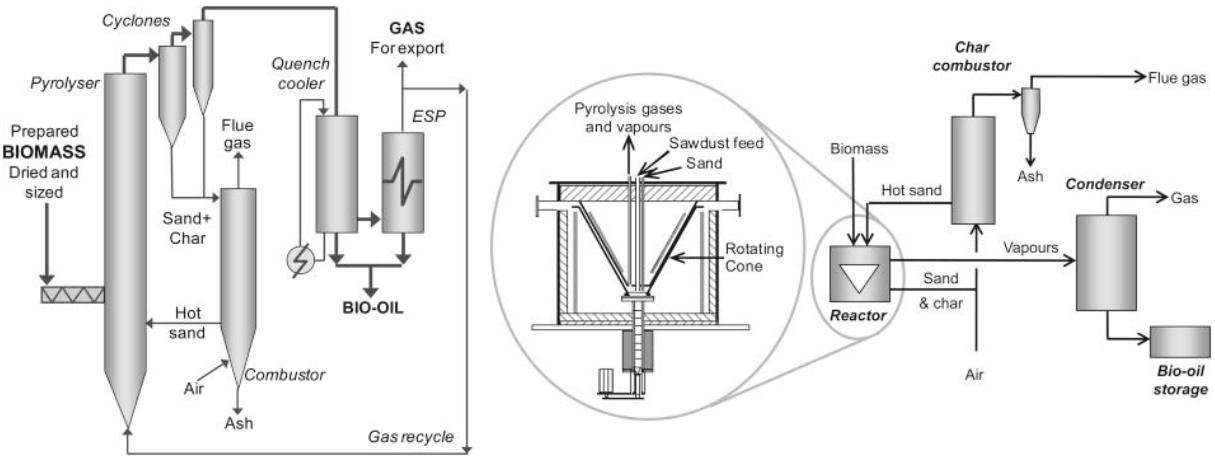

figure 16: left: CFP pyrolysis plant concept right: RCR pyrolysis plant concept (Reprinted with permission from Elsevier [92]*)*

table 4: biggest pyrolyis Oil (PO) production plants to date that use woody biomass (listed and adapted from Oasmaa et al.[98]*)*

plant	capacity	status	location	Ref.
Fortum (VTT/Valmet)	30 MW_{th}, 50000 t/a PO	online	Joensuu, Finland	[81] [98]
Ensyn	8 MW_{th}, 3.5 t/h input	online	Renfrew, Canada	[98]
Ensyn/Envergent	30 MW_{th}, 8.3 t/h PO	under construction	Cote Nord, Canada	[98] [81] [96]
EMPYRO (BTG-BTL)	15 MW_{th}, 2.7 - 3.3 t/h PO	online	Hengelo, The Netherlands	[81] [98]
GFN (BTG-BTL)	24000 t/a PO	online	Lieksa, Finland	[98] [100]
Pyrocell (BTG-BTL)	35000 - 40000 t/a input	online	Gävle, Sweden	[98] [100]

2.10.2 Pyrolysis oils derived from plastic waste-feedstocks

Beside biogenic feedstocks solid plastic wastes are predestined as a viable source for pyrolysis oils. Especially, since there is an abundance of wastes that were in the past and still are nowadays landfilled or burned due to their high caloric values. To close the tap on plastic that ends up in the environment and repurpose its waste as a resource for a circular economy attention has been shifted on chemical recycling routes. One such route employs pyrolysis as a first conversion step where the generated pyrolysis crude could then be further processed to fuels and monomers for plastic production [101] [102] [103].

One of the main advantages that pyrolysis offers in regard to waste plastic treatment is the possibility to convert mixed plastic wastes. Sorting wastes is labor intensive and therefore a significant cost factor which could be avoided. Additionally, plastic wastes that are not easily mechanically recyclable like composites, demolishing wastes or multilayer packaging are processable. Furthermore, problems originating from non-compatibility of plastic wastes (like e.g. PVC in PET recycling) that prevent mechanical recycling could be addressed [102].

The basics for pyrolysis are the same for plastic waste treatment as for using biogenic sources. The three main product fractions are gases, liquids and solids where the focus is on maximizing liquid product fraction and boosting oil quality. One factor that greatly influences yields is the type of plastic type used. Sharuddin et al [101] summarized the most common plastic types according to their moisture content, ash content, fixed carbon and volatile matter. According to Abnisa & Daud [104] high contents of volatile matter favor generation of liquids whereas higher ash contents result in the opposite (higher gas and solid yields). Judging from the numbers provided by Sharuddin plastics have a high potential to generate high liquid crude yields due to their significant volatile matter content of 90 w% and more and their low ash content. This conclusion is also supported by Islam et al [105].

The most prominent process parameters in plastic pyrolysis are temperature, reactor type, residence time, catalyst, pressure as well as type and rate of fluidization gas [101][103]. Since pyrolysis is a thermal cracking process temperature is considered to be the parameter with the greatest influence on the product spectra. For pure thermal pyrolysis, reactor temperatures between 500-550 °C were the ones yielding the highest amounts of pyrolysis crudes. These values could be reduced down to 450 °C if catalysts like zeolites were incorporated into the pyrolysis process that promote the formation of the desired liquid fraction [101].

Higher retention time in the reactor promote secondary reactions and the formation of non-condensable gases and chars. This was already described pathway wise for woody biomass [101] [103]. The influence of pressure on the product distribution is not yet thoroughly researched according to a review conducted by Al-Salem et al [103]. Lopez et al [106], however, conducted pyrolysis experiments converting waste tires under vacuum which resulted in comparably higher gas yields. Therefore, pressure below atmospheric pressure seems less favorable for plastic crude production. In one study Murata et al [107] conducted pyrolysis experiments with polyethylene under various pressures. It was found out that from 1 to 8 bar pressure the yields of non-condensable gases increased. This effect decreased from 410 to 440 °C tremendously. As a consequence temperature was described as the predominant influence parameter on product distribution. Interestingly, however, it was observed that higher pressures led to a decrease in average molecular weight of the gases.

The choice of carrier gas to create the oxygen-depleted environment for pyrolysis was found to have an influence on product distribution. Due to practicality reasons most research groups utilized easy to handle nitrogen. Even though hydrogen or propylene provided higher yields of condensable product but require additional safety measures. Helium was discarded as carrier gas because of its higher price. For further details please refer to the review by Sharuddin [101]. However, as Ragaert et al [102] pointed out, steam might still be the best choice due to its high availability and low cost in industrial complexes.

A great variety of reactor designs has been tested over the years by various research groups. Many laboratory plants utilized a batch or semi-batched design and cannot be deemed suitable for production at industrial scale due to high labor costs and the need for frequent feedstock charging. Thus, a continuous design must be chosen. For an overview of potential reactor designs complementary literature is recommended [103] [101]. Since this thesis focuses on feedstocks suitable for FCC co-feeding some selected pyrolysis processes to generate plastic crude which operate at least at pilot scale are described in the following.

-STYX Screw reactor

The STYX is a patented type of screw reactor which was developed by the KIT (Karlsruhe Institute of Technology). The pilot plant which is located in Karlsruhe has an input of 1 kg/h of mixed plastic waste. Via two feeding screws feedstock and sand which acts as a heat carrier enter the screw reactor at one side. The proportion of feed to sand is hereby around 1:4 and nitrogen acts as inert gas. The reactor itself is electrically heated and the residence time of the plastic wastes is between 15 and 25 min making it an intermediate pyrolysis process rather than a fast one. At the reactor end solids like sand and char are collected while the pyrolysis vapors exit the reactor via filter candles. Liquid products are then gathered via a multistep condensation unit and the pyrolysis gases leave the plant via a flare (see figure 17) [108] [109].

Arcus Greencycling GmbH is commercializing this process and currently building a pilot unit in Höchst, Germany with an estimated mixed plastic waste input of around 4000 t/year. Commencing of operation is planned in 2022. In this demo plant a more integrated plant design will be tested where the pyrolysis vapors will be used to generate electricity and heat for the endothermic cracking reactions [110] [111].

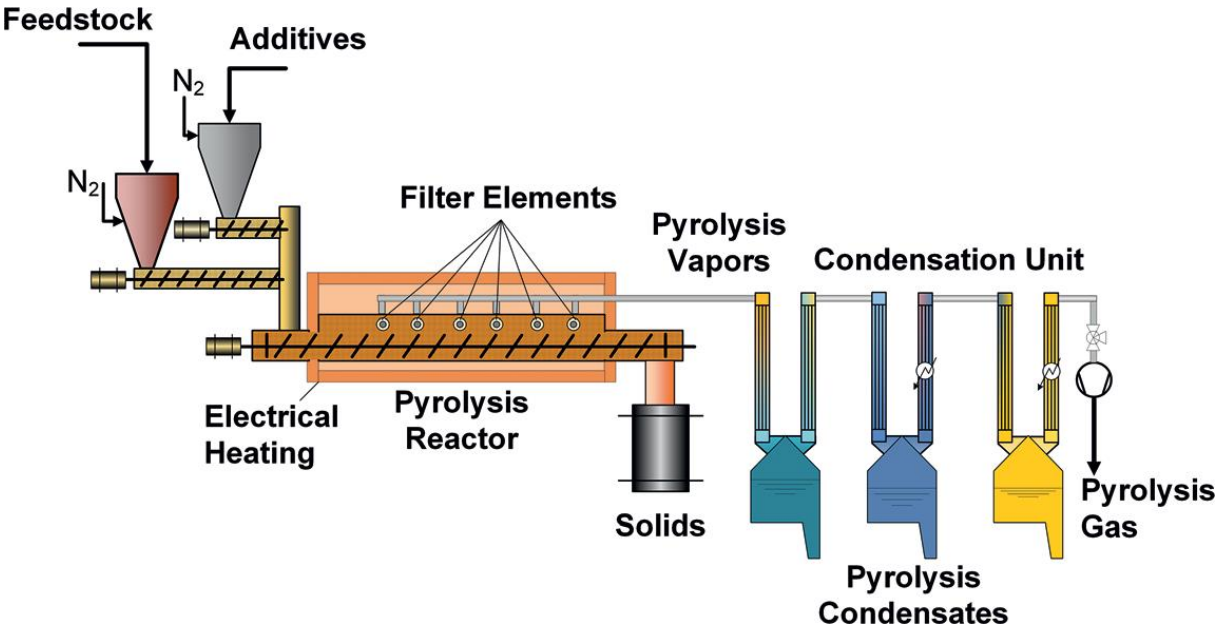

figure 17: process flow chart of STYX thermal pyrolysis plant (Reprinted under the Creative Commons CC BY license [109])

-Reoil®

OMV developed and patented the so called ReOil® process (flow chart see figure 18). Currently rather uncontaminated and presorted plastic flakes (PE, PP & PS) are introduced and melted in an extruder. Then they are mixed with a high-boiling solvent (vacuum gas oil or decanted oil/slurry oil from the FCC) and then thermally cracked in a pipe reactor under inert atmosphere. The addition of solvent hereby fosters heat conductivity. The products are then separated in fractionation columns (flashing) and part of them are recycled back into the mixer. Valuable products are light and heavy syncrude which can either be directly used or further processed in downstream units. Unwanted constituents like colorizers, stabilizers or fillers that are added to give plastics certain properties enrich in the so-called purge. The light purge fraction could then be introduced as an FCC feedstock whereas the heavy purge might be used as fuel for e.g. cement production [112] [113].

Currently a pilot plant is operational in Schwechat, Austria since 2018 with an input capacity of 100 kg/h which corresponds to around 100 l/h of liquid product. Total runtime of the plant so far accumulate to more than 13000 h. As next steps scale ups are planned in which a plant is planned to be commissioned in 2023 with a input capacity of 16000 t/year or 2 t/h [114].

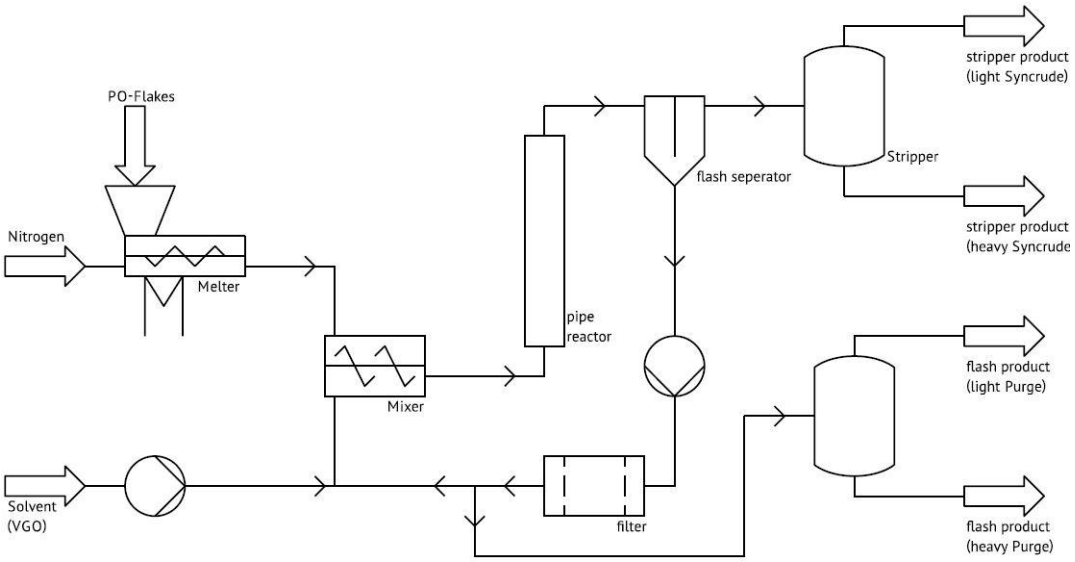

figure 18: ReOil process flow chart (adapted and reprinted with permission under Creative Commons Attribution 4.0 International License from [112])

Beside these two processes various other pyrolysis plants are currently commercialized which are not covered in this thesis. Reviews by Butler et al [115] and Qureshi et al [116] are recommended which give an overview of currently employed plant designs and their locations.

2.11 Co-feeding pyrolysis oils in the FCC process

Wood-derived Pyrolysis liquids often have considerable weaknesses like high oxygen content, immiscibility with fossil feedstocks and/or a high tendency of coking at comparably low temperatures as was mentioned in the previous chapter. To boost pyrolysis oil quality hydrotreating is often chosen to deoxygenate the feedstock. However, excessive hydrogenation is generally not deemed optimal due to a necessarily high demand on hydrogen and consequently increased operational costs. Beside oxygen content, other requirements for fuel use need to be met so that a pure biorefinery solely targeted for pyrolysis oils does not seem feasible. Therefore, the usage of already existing fossil refinery structures is recommended as a ready-to-use and convenient solution. While there are several possibilities to integrate pyrolysis oils into refineries focus will be laid on co-processing in the fluid catalytic cracking process. Other pathways like co-hydrotreating will not be described in detail [117].

Co-processing pyrolysis oils in fluid catalytic cracking units provides several advantages [117]:

- Zeolite catalysts promote deoxygenation reactions (dehydration, decarbonylation, decarboxylation) via generation of water and carbon oxides. Adjaye and Bakhshi [118] were among the first to show these capabilities of zeolites for the deoxygenation of bio-oils. Vitolo et al [119] further proved this concept by processing wood-derived pyrolysis oil using different ZSM zeolites.
- Hydrogen transfer reactions from hydrogen-richer fossil feedstock to the bio-oil occur which not only diminishes excessive coke production but also helps deoxygenating the bio-oil thereby reducing pretreating requirements.

To quantify and compare the need for these hydrogen transfer reactions the usage of the effective hydrogen index (EHI) is proposed. This Index as described by Chen [120] is formulated in equation (13):

$$EHI = \frac{h - 2 \cdot o - 3 \cdot n - 2 \cdot s}{c} \quad (13)$$

Here, mole fractions of the five main constituents (hydrogen, oxygen, nitrogen, sulfur, carbon) of a specific feedstock need to be filled in to receive the corresponding EHI. Chen [120] formulated that an EHI lower than 1 is a strong indicator for excessive coke generation. This is especially true for unhydrogenated fast pyrolysis liquids with values as low as 0.5. VGO, on the other hand, has an EHI around 1.7 [121]. Via co-feeding of VGO and (hydrotreated) pyrolysis liquids blends the hydrogen index could be kept above the critical threshold. Note that plastic-derived pyrolysis soils generally do not have these problems at such an extent due to their comparably low oxygen content.

Beside the high oxygen and low hydrogen content unhydrogenated wood-based pyrolysis oils face another challenge regarding FCC co-feeding which is coking in feeding lines already at temperatures around 60 °C. This plugging and fouling (elicited by the coking) necessitates separate cooled and/or isolated feeding lines for the pyrolysis oil. This means that to efficiently use this feedstocks changes in plant design might be necessary. It is estimated that only up to 5 w% of co-feeding can be achieved with crude wood based pyrolysis oil. Higher percentages should possibly be achievable only with hydrogenated oils. For more practical information regarding this topic refer to the whitepaper by Lammens et al [122].

The co-processing approach has already been researched in experimental studies by a variety of research groups. Castello and Rosendahl gave an overview of these studies in [117]. An adapted and partially extended version of this summary can be found in table 5. There, key parameters of said studies are summarized with emphasis on information about the pyrolysis oils, admixture rate and the yields of relevant product fractions. All pyrolysis oils were blended with vacuum gas oil. The gas fraction is defined as the sum of dry gas and LPG. Note that a wide variety of plant designs were used in these studies ranging from micro activity tests (MAT) to demonstration plants. As feedstocks raw PO/ paraffin wax and hydrodeoxygenated Oils (HDO) were used. One industrial-scale co-feeding approach with FCC has been realized in Sweden (see Pyrocell plant in previous chapter) with co-feeding rates of about 0.5 – 1 w% [123] [124].

table 5: co-processing results of VGO and pyrolysis oils with emphasis on gas, gasoline and coke yields

Type of PO	source	ratio [w%]	O [w%]	Co- FCC yields [w%]			FCC yields [w%]			Ref.
				gas	gasoline	coke	gas	gasoline	coke	
Raw PO	Pinewood chips	10 - 20	38	17.5-27.0	36-42	8-10	10-20	40-42	7-8	[125]
Raw PO	Jatropha curcas	5 - 20	32	25.2-41.1	29-35	4.2-5.5	17.3	44	5.6	[121]
Raw PO	Forest thinning	20	36.5	14	17	10	10	16	5	[126]
Raw PO	Pinewood chips	5 - 10	50.7	13.5-22.0	37-42	5.5-7.0	16-22	40	6.5-7.2	[127]
Raw PO	Pinewood chips	10	51	14.5-18.0	37.0-39.5	6.5-7.6	17.5-22.5	40-42	7.1-8.2	[128]
Raw P-wax	HDPE pellets	20	-	24	26	6.5	23	27.5	8	[129]
Raw P-wax	Raw HDPE	20	-	12-27	24-32	4.0-8.5	12-25	25-29	4.5-9.0	[130]
Raw PO	Mixed plastic waste	5-20	4.5	40.8-44.3	40.0-41.8	6.3-6.4	41.7	42.8	6.3	[131]
HDO	Jatropha curcas	5	10	30.3	32.5	4.2	17.3	44	5.6	[121]
HDO	Forest thinning	20	22	12	18	8	10	16	5	[126]
HDO	pinewood	20	21	21-28	42-47	4-7	17-32	43-48	2.5-4.0	[132]
HDO	Pinewood chips	10	27.4	14.9-19.4	41-43	6.9-7.8	17.5-22.5	40-42	7.1-8.2	[128]

3. Material and methods

3.1 Pilot plant

The pilot plant's predecessor was designed and built in 1996 by Reichhold [133]. In 2010 an evaluation of the concept was conducted by Bielansky [134] and a second bigger plant was built, which was used for this thesis' experiments. The pilot plant is located at Technische Universität Wien (Technical University of Vienna) in Vienna, Austria and is constructed as an internally circulating fluidized bed system. This design leads to a stronger thermal coupling of the riser and regenerator section but comparably uses less space compared to externally circulating fluidized models. A schematic of said FCC unit is depicted in figure 19. Some parameters under which the plant was operated in the course of writing this thesis are listed in table 6. However, note that wider ranges of operation are possible (e.g. see [135] [136])

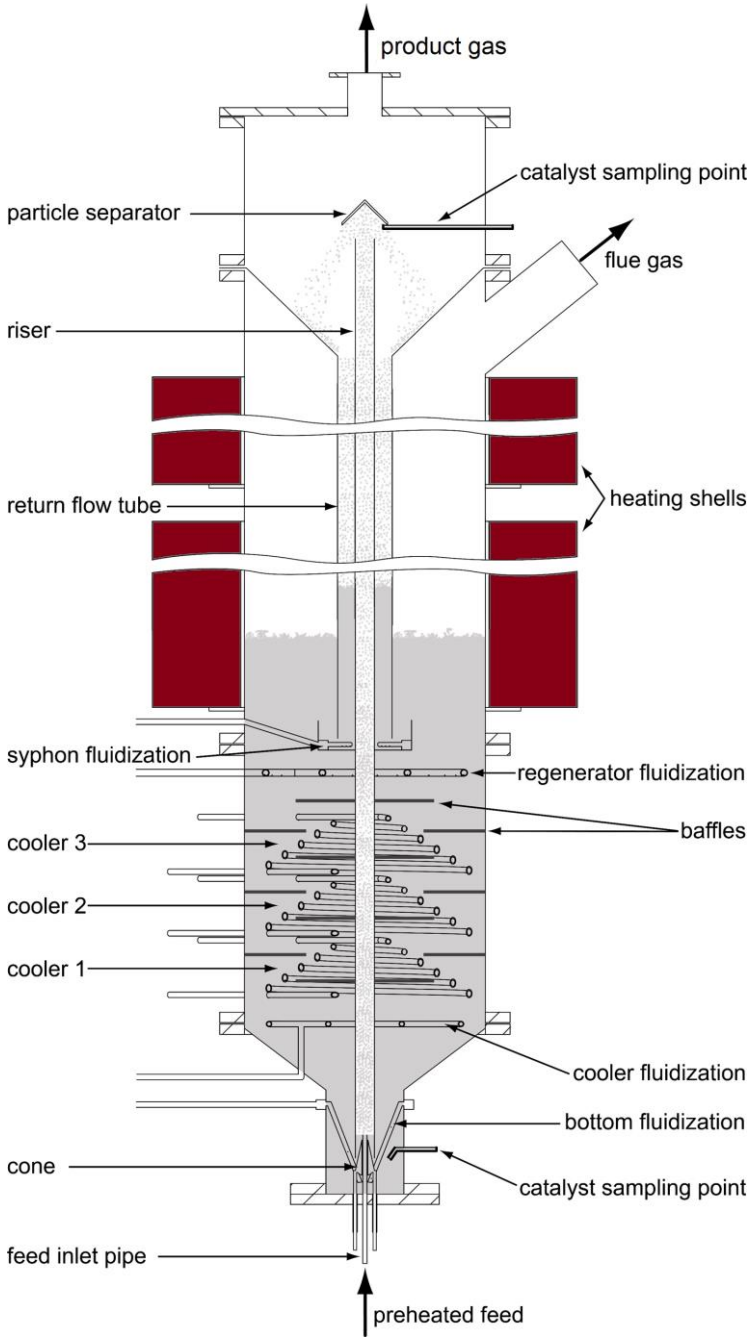

figure 19: schematic of the FCC pilot plant located at TU Wien (adapted from [134]*)*

table 6: selected parameters of the pilot plant

parameter	value	unit
total height	3.2	m
riser length	2.5	m
riser diameter	0.0215	m
regenerator diameter	0.33	m
regenerator temperature	610 - 620	°C
riser temperature	525 - 555	°C
pressure	ambient	-
residence time in riser	around 1	s
catalyst mass	50 - 70	kg
feed rate	1.5 - 2.5	kg/h
bottom fluidization (N_2)	4	Nl/min
riser fluidization (N_2)	0.1 - 5	Nl/min
syphon fluidization (N_2)	12 - 15	Nl/min
cooler fluidization (air)	10	Nl/min
regenerator fluidization (air)	25 - 33	Nl/min

The prepared preheated feedstock is transported via a gear pump into a tubular oven where it is heated close to boiling temperature (around 290 – 340 °C depending on feed). From there the preheated feed enters the riser reactor through a feed inlet pipe (see figure 19). There, the feed evaporates when it gets in contact with the hot catalyst and the cracking reactions begin. This also leads to an increase in volume and the cracking gases flow together with the catalyst upwards the reactor (hence the name riser). Additionally, fresh catalyst is sucked into the riser. The residence time in the riser is around 1 second. At the plant top the catalyst and product gas get separated mechanically via a particle separator. But also the increase in diameter which leads to slower gas velocities helps with separation. The product gas leaves the plant at the top and flows into a flare and/or a sample collection apparatus (see figure 21 and figure 23). The catalyst then falls into the return flow tube. From here it gets transported into the regenerator passing a syphon which acts as a gas barrier between reactor and regenerator section. In the regenerator the deposited coke on the particles is burned off. The coke is generated via secondary reactions during cracking and deactivates the catalyst. By burning of the coke the necessary energy for the endothermal cracking reactions is provided. Therefore, the FCC pilot unit runs in a mostly autothermal mode. The regenerated catalyst then flows down through the cooler section where it can get cooled down for the desired riser temperature. The baffles provide hereby enough interaction between catalyst and cooling loops. The bottom acts as another gas barrier and from there the regenerated catalyst is sucked in again into the riser. This catalyst circulation is also depicted schematically in figure 20).

The Cooler and regenerator sections are aeriated via pressured air (5 bar). The syphon, bottom and the riser are using nitrogen (5 bar with a purity of 5.0 = 99.999%) as fluidization gas since it is inert.

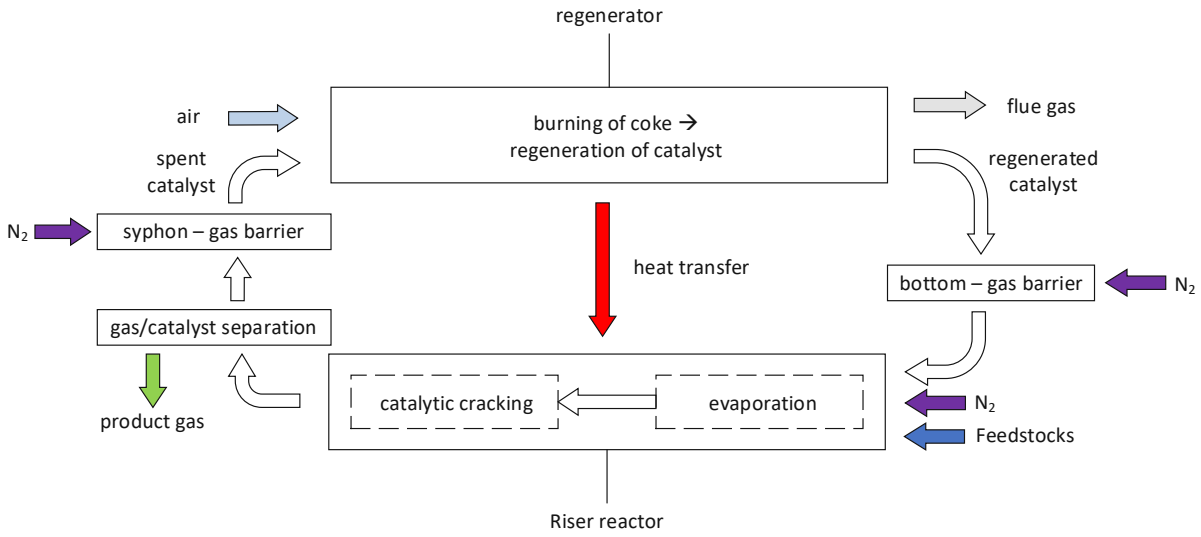

figure 20: schematic of the catalyst cycle

For more detailed information regarding the concept and the design of the pilot plant please refer to the aforementioned doctorate thesis of Reichhold [133] and Bielansky [134]. A P&ID of the whole pilot unit is illustrated in figure 21.

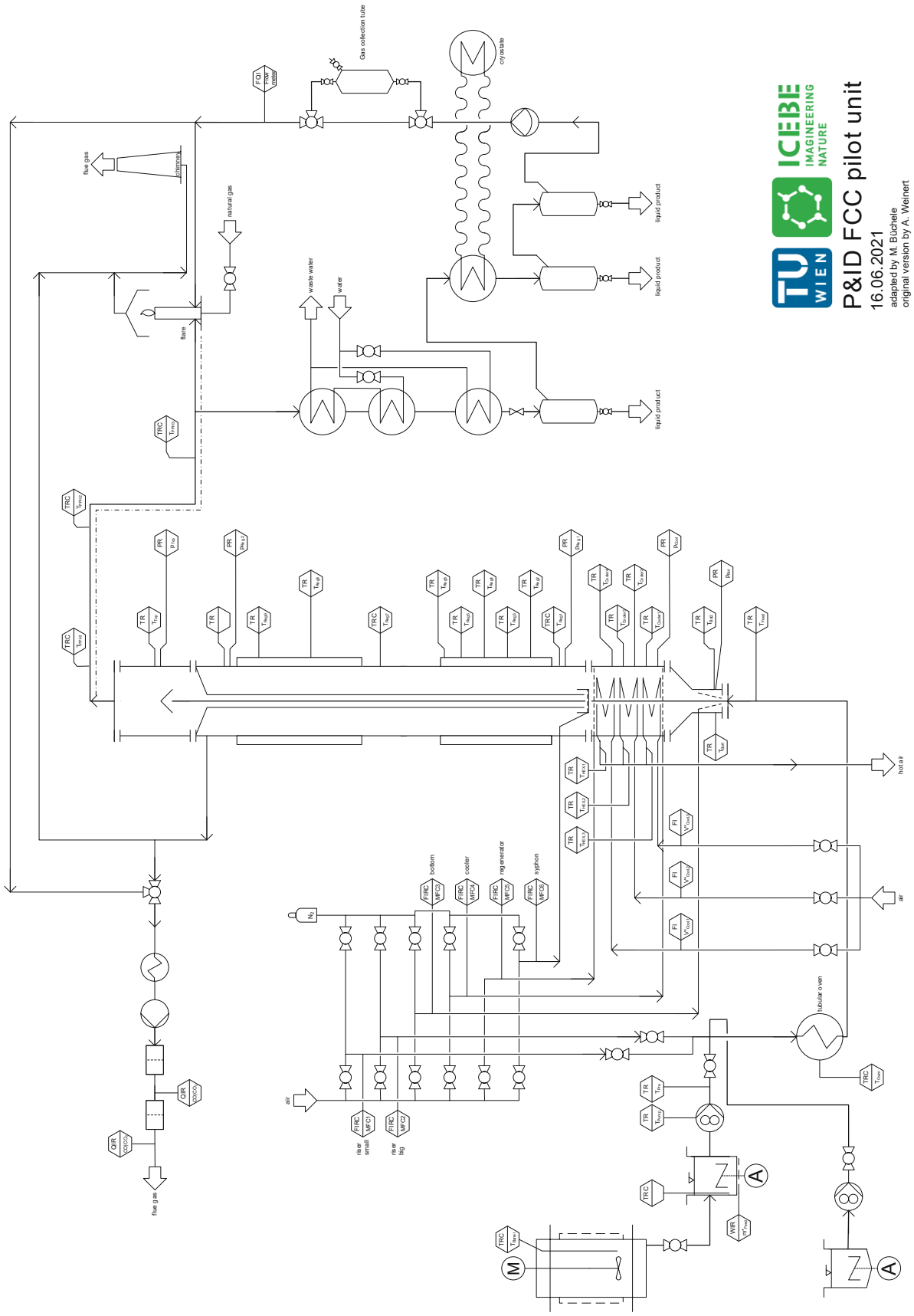

figure 21: P&ID of FCC pilot unit (adapted from [137]*)*

3.2 Fluidization conditions in the pilot plant sections

The different fluidization regimes in the pilot plant sections are summarized in table 7 together with the respective fluidization medium and their function. A german version of this summary was published by Büchele in [138]. For a more detailed description of the fluidization conditions in the FCC pilot plant refer to Bielansky [134].

table 7: fluidization regimes in plant sections

section	fluidization regime	function	medium
bottom	fluidized bed	gas barrier, even catalyst entrainment	nitrogen
syphon	fluidized bed	gas barrier, stripper, catalyst circulation	nitrogen
regenerator	fluidized bed	catalyst regeneration, heat/enthalpy supply	air
cooler	moving bed	temperature control	air
riser (reactor)	pneumatic transport	high heat and mass transfer between gas and solids	nitrogen, feed

3.3 Fluid dynamics

The minimum fluidization velocity (u_{mf}) is the velocity where a fluidized bed is formed (see figure 22). To ensure the formation of a fluidized bed all three catalysts were tested on their fluid dynamic behavior in the regenerator section. This is important since a fluidized bed ensures a comparably homogenous distribution of heat and oxygen throughout the catalyst pack which enables a more thorough burning of the coke deposits and therefore an even regeneration of catalyst.

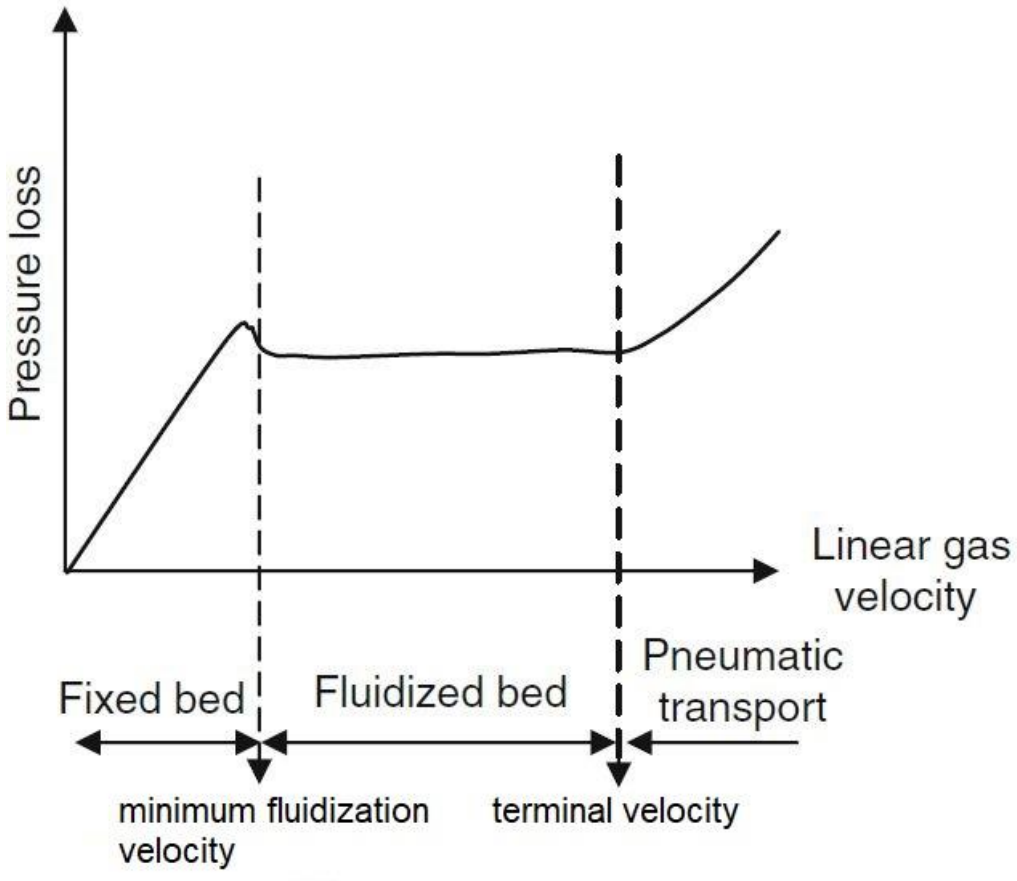

figure 22: pressure loss depending on linear gas velocity (adapted and reprinted with permission from Elsevier [54])

The testing was conducted under regenerator temperatures of around 610 °C (a standard temperature in experiments in the utilized pilot plant). There the amount of regenerator fluidization gas was changed from top to bottom to avoid agglomeration of the catalyst particles. For each fluidization setting the pressure drop in the regenerator was noted. After the minimum fluidization velocity is passed the pressure drop sinks significantly while in fluidized bed mode it stays relatively constant. The flow of fluidization gas is hereby calculated into the linear gas velocity using equation (*14*) by assuming that p · V is constant.

$$u_L = \dot{V}_{Regenerator,Norm} * \frac{T}{T_{Norm}} * \frac{1}{\left(d^2_{Regenerator} - d^2_{Return\ flow\ tube}\right) * \frac{\pi}{4}} \tag{14}$$

Via approximation and extrapolation of the data points for both fixed bed and fluidized bed two straights are calculated. The point where those two straights intersect corresponds approximately with the minimum fluidization velocity. This experimental determination of the minimum fluidization velocity was then cross-checked using the calculation devised by Wen and Yu [139] (equation (15)).

$$u_{mf} = \frac{\mu}{\rho_g \cdot d_{SV}} \cdot \left[\sqrt{33.7^2 + 0.0408 \cdot Ar} - 33.7\right] \tag{15}$$

Whereas Ar is the Archimedes number (also called Galileo number [140]) which is defined as the ratio of gravitational/floating forces in relation to the viscous forces [139][141](equation (16)):

$$Ar = \frac{\rho_g \cdot d^3_{SV} \cdot \left(\rho_p - \rho_g\right) \cdot g}{\mu^2} \tag{16}$$

To calculate the U_{mf} most accurately the Sauter mean diameter d_{SV} was used which is a particle size average. It describes a sphere with the same relation of volume to surface area than the particle [142].

3.4 Plant operation

The plant operation was conducted according to an operational manual that was developed over the years by the research group fluidized bed systems and refinery technology at TU Wien. This ensured maximum safety for staff as well as comparability between different experimental campaigns. To give an overview of the scope of a pilot plant experiment some key elements of procedure are summarized in the following. This summary is an adapted version from [138].

An experiment for a specific setting consisting of several sample collections was usually conducted in a working day (about 14 hours) and consisted of the following operations:

- Heating the plant to operating temperatures (4h)
- Start-up of measuring devices and pilot plant until it reaches stationary operation (3h)
- Plant operation at stationary point and sampling (4h)
- Shutdown of pilot plant (cleaning and regeneration) (3h)

Afterwards the plant takes around 24 hours to cool down again to room temperature. Since no manual labour is involved to achieve this it is not counted towards the plant operation. However, this cooling down phase must be taken into account when conducting maintenance after the experiment.

The feedstock that is planned to be used in the experiment was prepared beforehand. When feeds are mixable the admixtures are prepared in the right proportions in a separate vessel. If the feeds are not mixable said admixtures are realized by pumping via two pumps out of two individual vessels.

For heating-up the plant is fluidized with air to save nitrogen. Regenerator, Freeboard and the tubular oven are heated via heating modules until they reach the desired temperature. While heating-up a high circulation rate of catalyst is encouraged since a more homogenous heating is hereby achieved. As soon as the plant is hot enough the fluidization of syphon, bottom and the riser is changed to use nitrogen as medium. The successful formation of the gas barriers between the reactor and regenerator section is proved by the decline of oxygen in the regenerator section which is constantly measured. This decline is achieved since part of the nitrogen flows into the regenerator section.

At this point the feeding is commenced. To ensure enough circulation of catalyst and to prevent a runaway of the riser temperature the feeding rate is slowly increased until it reaches the desired amount. In parallel the riser fluidization is decreased to a suitable level depending on the feedstock. Then the plant is operated until a stable condition is observed. This is mostly seen after around 30 minutes of feeding at the final rate. Most attention is hereby given to the correct riser temperature and to a stable level of oxygen and carbon dioxide in the regenerator which ensures a stable heating balance. If necessary, cooling is applied since a decrease in feedrate is often not wanted because it would result in less product for sampling.

At stationary operation the samples are taken from the condensation apparatus (see next chapter). Additionally, measurements of the catalyst circulation rate are done after every sampling. After the last probe is collected plant shutdown is commenced. Hereby, the feed flow into the pilot plant is stopped and the temperatures are increased to around 700 °C. This is done to burn any remaining coke and feed deposits. After the cooling down period a plant check-up and maintenance is conducted.

3.5 Sample collection

A sample collection is conducted continuously in a 15-minute window where a valve to the condensation and collection apparatus is opened and a membrane pump is turned on. Afterwards said valve is closed again and the pump is turned off. During sampling a part of the hot product gas bypasses the torch and enters a multi stage cooling section. First the gas temperature is reduced in water cooled double wall heat exchangers. After that the gas enters the water cooled condensation apparatus where the first part of the liquid fraction condenses. From there the gas enters a second condensation apparatus which is cooled further down using -25 °C cold ethanol as a cooling medium. Here, the second part of the liquids are collected. Lastly, in a third condensation apparatus rests of liquids are mechanically separated from the gaseous fraction via a porous frit. These 3 parts make up the liquid fraction. The product gas then passes a gas washing bottle and a filter that protect the membrane pump from any remaining droplets of liquid. The gaseous fraction flows then through a gas collection tube, where a sample is taken. Lastly, a gas meter measures the volume flow of product gas and the gas then enters the torch via a second line. The carbon oxides are measured after the 15-minute window when the gas collection tube is bypassed and a valve to the gas analyzer is opened. A schematic of the sample collection apparatus is depicted in figure 23.

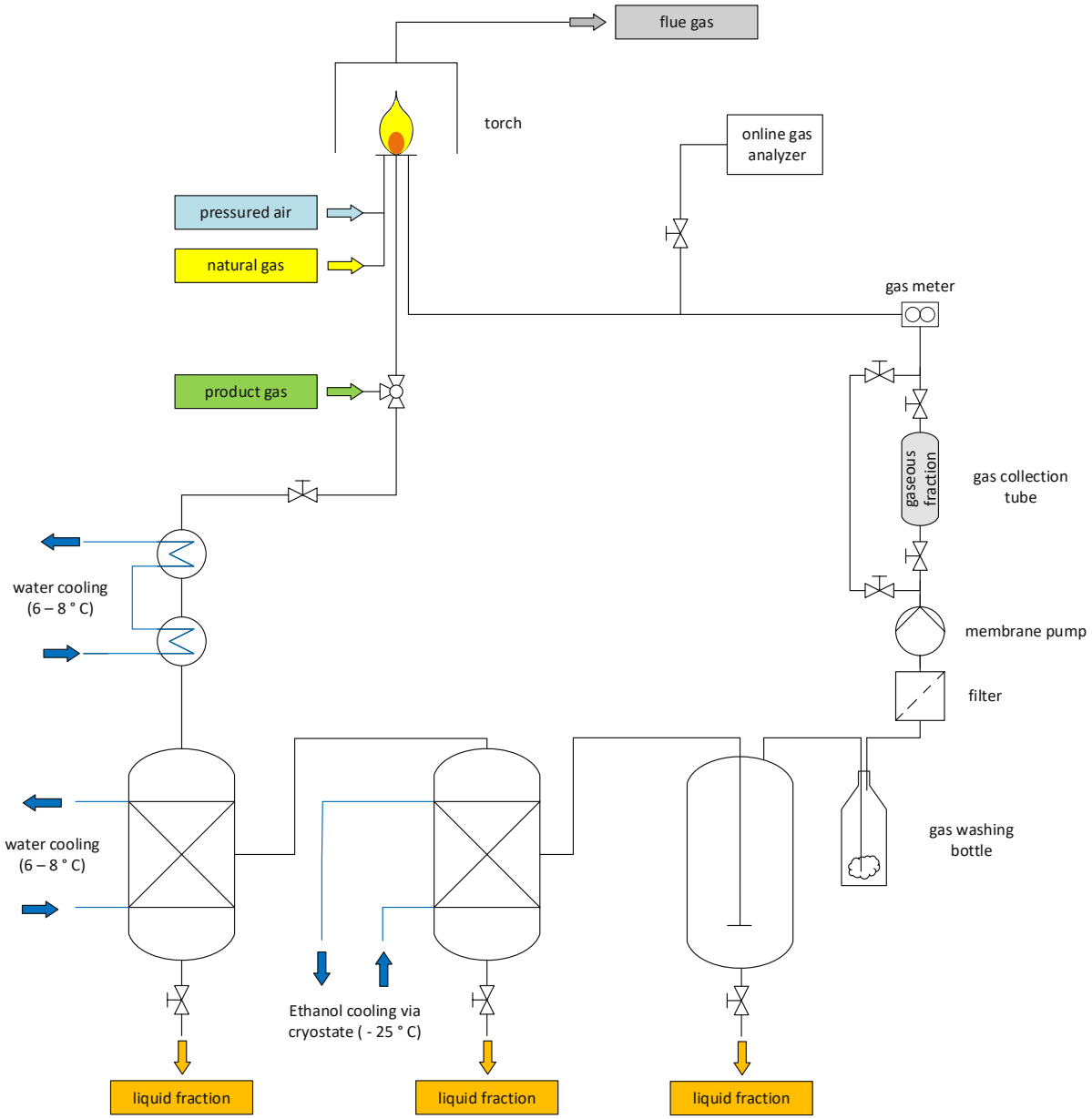

figure 23: probe collection of FCC product gas (adapted from [143])

3.6 Process parameters

To run the experiments at the desired configurations, parameters must be adequately defined. One such parameter is the riser temperature at which the cracking reactions occur. As was mentioned before, cracking reactions are endothermic which leads to falling temperatures from bottom to top of the riser reactor. To account for this the mean riser temperature was chosen as the defining parameter. In total 3 thermal sensors measure the temperature in the riser of the pilot plant (2 at the entrance where the feed evaporates and 1 at the exit shortly before the catalyst and feed vapors are separated). The riser temperature is thereby defined in equation (17):

$$\bar{T}_{Riser} = \frac{\frac{T_{Riser,in\,1} + T_{Riser,in\,2}}{2} + T_{Riser,out}}{2} \tag{17}$$

The mass flow of catalyst into the riser (also called circulation rate) is measured via a method developed by Reichhold [133]. In stationary operation the pressure drop in the regenerator is constant. However, when measuring the circulation rate the syphon fluidization is temporarily shut off (90 seconds) which stops spent catalyst from entering the regenerator and accumulating in the return flow tube. The fluidization of other plant sections is independent from this temporary change which leads to a still continuous flow of regenerated catalyst into the riser. As a consequence, the catalyst bed height in the regenerator declines which can be measured by a sinking pressure drop in the regenerator (see figure 24). The pressure drop declines hereby linearly which proportionally corresponds to the circulation rate. Therefore, by measuring the pressure drop and using regression an approximation of the circulation rate is possible. After turning on again the syphon fluidization the catalyst in the return flow tube is transported again into the regenerator and a new stationary state is generated. This measuring method works well for hot and cold settings as well as in not accessible plant sections and is only limited by the amount of time the syphon can be turned off. This limitation exists due to the necessary energy needed for cracking reactions provided by burning of coke from the catalyst and the height of the catalyst bed in the regenerator.

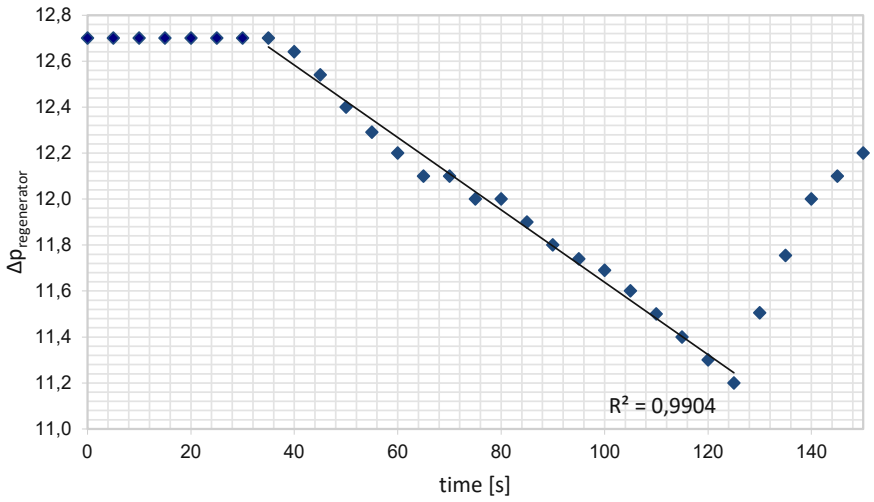

figure 24: pressure drop in regenerator during circulation rate measurement

The derivation of this method based on fluidized bed technology is mentioned by Weinert [137] in more detail. The final calculation of the catalyst mass flow rate can be described as follows:

$$\dot{m}_{catalyst} \approx \frac{A_{Regenerator}}{g} \cdot \frac{\Delta(\Delta p_{Regenerator})}{\Delta t_U} \tag{18}$$

Utilizing the catalyst mass flow and the feed rate the catalyst to oil (C/O) ratio can be calculated (see equation (19)):

$$\frac{C}{O}\,ratio = \frac{\dot{m}_{catalyst}}{\dot{m}_{feed}} \tag{19}$$

In the pilot plant the catalyst flow rate and therefore, the C/O-ratio can be influenced by the plug valve that is installed at the bottom of the riser which changes the cross sectional area. Berchtold [136] tested different plug valves to see their effect on the circulation rate and the one deemed most suitable was also used during the work on this thesis. Additionally, the amount of nitrogen used for riser fluidization affects the C/O ratio as well as the feed rate. Also, the type of feed and the cracking temperatures have an influence.

3.7 Comparability with industrial plants

Representability of the results with industrial-sized FCC units is a main reason why a continuously operated pilot plant was chosen rather than just conducting micro activity tests (MATs). To accomplish maximum comparability equilibrium catalysts that were deactivated in the corresponding industrial FCC unit were used for the experiments. By using these, differences in catalyst activity which influence severity were avoided. As a second parameter the riser-temperature was chosen according to the one in the industrial FCC unit.

In order to test said comparability data from a project partners FCC unit was obtained (see figure 25). The exact location of this industrial FCC unit cannot be disclosed due to confidentiality reasons. The lumps that were used for the comparison differ slightly regarding the liquid fraction since the refinery operator uses different cutting points and further distinguishes between light and heavy gasoline, kerosene etc. Therefore, only a summarized fuel lump was used.

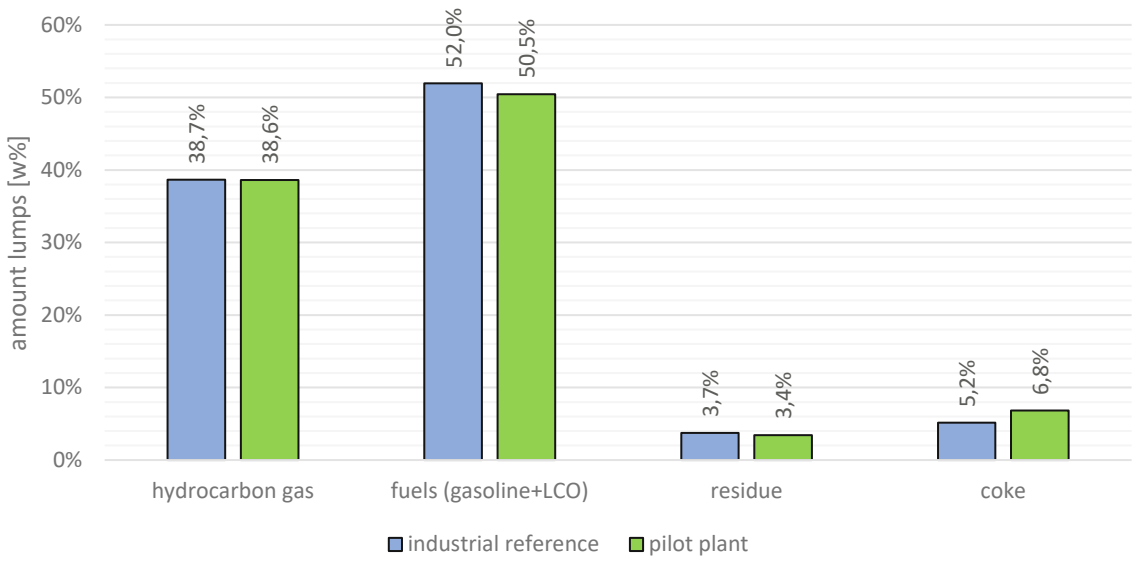

figure 25: main lump comparison between the utilized pilot plant and an industrial reference plant

The comparison illustrates that the hydrocarbon gas sum and the residue (or slurry) match well with deviations less than 0.5 w%. The fuel and coke yields differ slightly more in the range of 1.5-2 w%. It is estimated that these differences originate in an incomplete stripping of product from the catalyst pores which result in higher catalyst circulation coke that is carried over from the riser to the regenerator. Higher amounts of fluidization gas in the syphon could be a cheap and easy mitigation strategy for this issue.

One parameter that does differ quite greatly between the pilot plant and industrial-sized plants is the catalyst to oil ratio. C/O-ratios of 8-10 which are normally employed in industrial-sized FCC units cannot always be implanted in the pilot plant using the installed plug valve. This is especially true for experiments using gas boosting catalysts at higher temperatures where the increased production of gases amplifies circulation rate. However, even though the C/O-ratios are higher in the pilot plant the results are nonetheless comparable (as was demonstrated in figure 25). It is believed this is due to lower residence times in the riser which counteract most effects of the higher C/O-ratios. To further research the C/O-ratios effect in the pilot plant an experimental campaign has been conducted as part of this thesis.

3.8 Lump model

In the refinery sector processes often generate a vast variety of products that necessitates the grouping of them in so called lumps. In this work a 7 lump model was chosen for product analysis which is depicted in figure 26. There, it can be seen that the products are distinguished into solids, liquids and gases. The gaseous fraction consists of the carbon oxide lump and the hydrocarbon gas lump. The liquid fraction is made up of an organic part (gasoline, light cycle oil and residue) and water. The solid fraction consists only of coke. The products are grouped according to their molecular structure and their distillation temperature. Note that no water lump is generated when feedstocks that don't contain water or oxygen are fed.

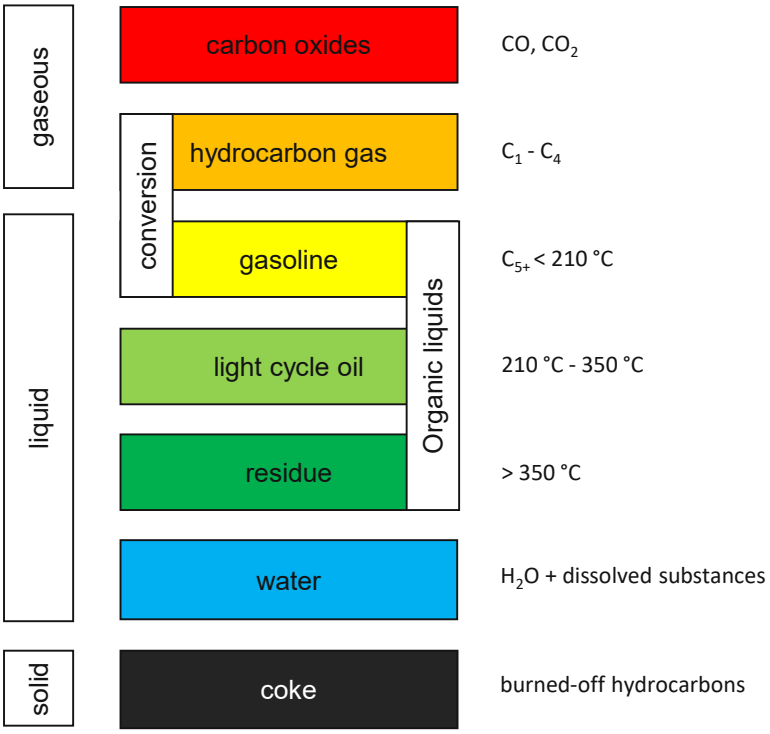

figure 26: lump model chosen for the analysis of the product groups

The gasoline lumps upper distillation boundary was defined to be 210 °C, which is the final boiling point stated in the norm EN 228:2017 for gasoline [144]. In the norms EN 590:2013+A1:2017 for diesel fuel [145] and DIN 51603-1 for extra-light heating oil [146] it is stated that at 350 °C a minimum of 85 v% of fuel must be evaporated. For diesel fuel it is additionally stated that 95 v% of fuel must be evaporated at 360 °C. So to fulfill this requirements the final distillation point for light cycle oil in this work was chosen to be 350 °C since it generally can be used as a blending component for diesel fuel and heating oil [52]. However, due to its high aromatics content and low cetane number LCO is often fed back into the plant, hence its name light cycle oil [147]. Therefore, in the definition for the conversion LCO is not included since the focus in this thesis mainly is on gasoline and olefins. The conversion (also called total fuel yield = TFY) is made up of the valuable products hydrocarbon gas and gasoline in comparison to the feed that is fed into the plant (see equation (20))

$$Conversion = \frac{\dot{m}_{hydrocarbon\ gas} + \dot{m}_{gasoline}}{\dot{m}_{feed}} \tag{20}$$

3.9 Analytics

The analytical pathway of the generated products is depicted in figure 27. The product gas is sent through a condensation apparatus and the liquid products are separated from the gaseous fraction (see figure 23). The gas products are then collected in a gas collection tube and the liquid products are gathered in simple flasks.

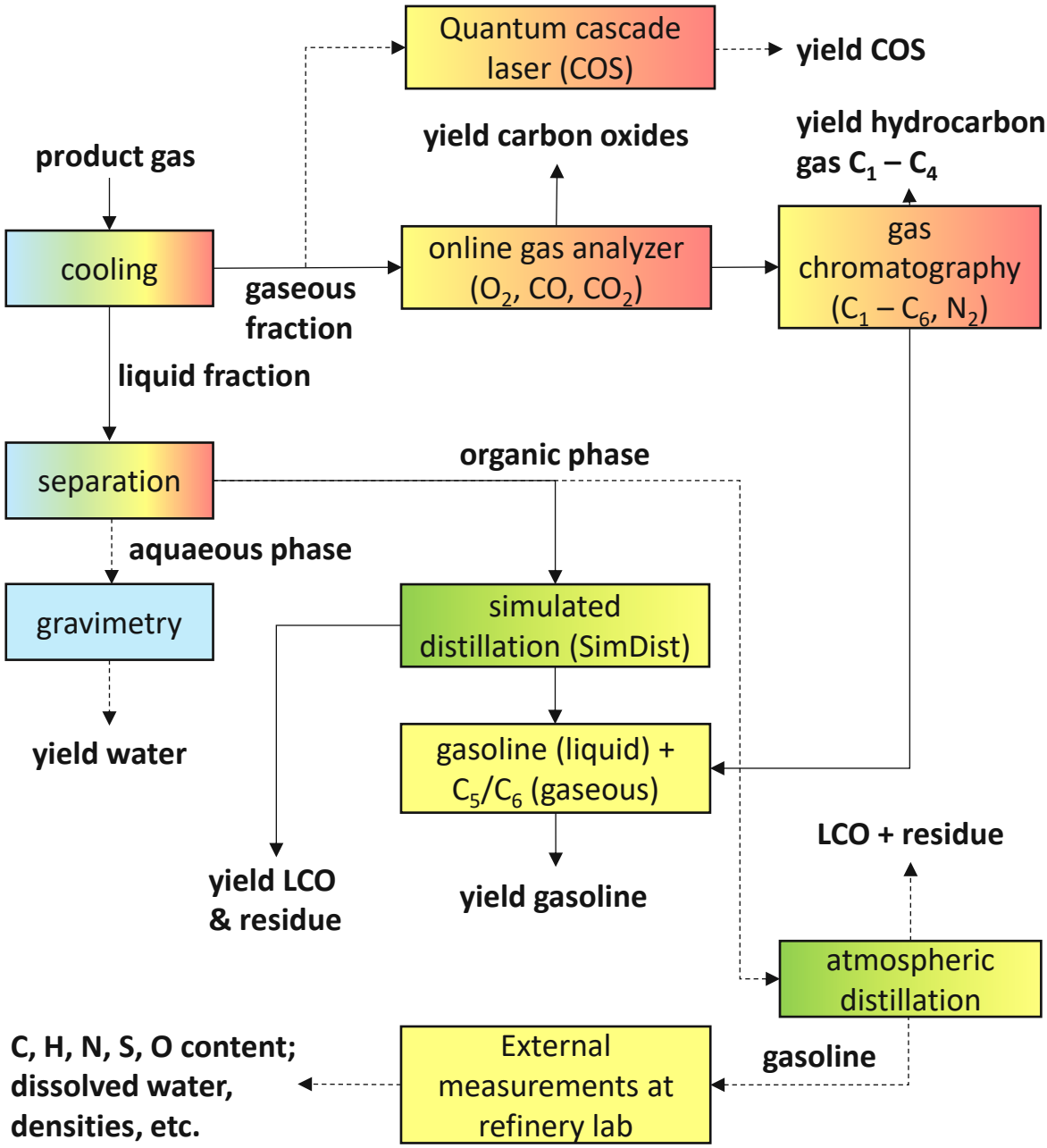

figure 27: analytical path of the gaseous and liquid products

3.9.1 Gas analytics

CO and CO_2 concentrations of the gaseous fraction are measured online via a Rosemount NGA2000 MLT3 gas analyzer. Additional information regarding the gas analyzer is summarized in table 8. Further analysis of the gaseous fraction is performed using a Shimadzu GC-17A gas chromatograph (details see table 9). It is important to note that the gas samples have a limited shelf life. This is due to rests of C_5 and C_6 molecules in the probe that condensate over time. These molecules can be detected when still in gaseous phase in the gas chromatograph and are grouped together in the gasoline mass balance. Another reason for the limited shelf lives are leakages through the septum especially after it has already been perforated at least once. When the probe then further cools down to ambient temperature a under pressure in the vessel is created which sucks in air over time. Therefore, the measurements of the gas fraction have to be conducted on the same day as the experiments.

table 8: online gas analyzer basic principles

manufacturer	emerson process management
type	Rosemount NGA 2000 MLT3
measurements	CO, CO_2, O_2
analysis methods	CO_x: NDIR O_2: paramagnetic

The sample is taken from the gas collection tube via a Hamilton syringe and a defined volume of 50 µl is transferred into the injector. There the components are measured via 2 separate sections. The first line measures the hydrocarbons (C_1 to C_6) via a flame ionization detector. The second line measures the nitrogen via a thermal conductivity detector. To get more data and increased accuracy each sample was measured mostly 2 times. Higher numbers of measurements were often not possible due to the above mentioned limited shelf life.

table 9: gas chromatography setup for gas measurements

type	Shimadzu GC-17A
injector	splitless 50 µl @ 200 °C
carrier gas	helium 1.46 ml/min constant flow
temperature program	50 °C to 200 °C; dwell time 30 min
Number of sections	2 (I & II)
columns	I: Varian CP-Al_2O_3/Na_2SO_4 II: CP CarboPLOT P7
dimensions	I: 50 m length x 0.25 mm inner diameter x 4 µm film thickness II: 25 m length x 0.53 mm inner diameter x 25 µm film thickness
detectors	I: flame ionization detector (FID) @ 200 °C II: thermal conductivity detector (TCD) @ 125 °C

In the experimental campaign using vacuum gas oil A and atmospheric residues as feedstock an additional gas measurement method was conducted that was not done for the other campaigns. In these runs carbonyl sulfide (COS) was measured in ppb ranges using a quantum cascade laser-based gas sensor prototype located at the institute of chemical technologies and analytics at TU Wien. These samples were collected separately in gas collection bags instead of gas collection tubes after the standard sample collection was finished. For further information regarding this measuring principle and device refer to [148]. The method is calibrated according to norm DIN 32645.[149].

3.9.2 Liquid analytics

The liquid fraction consists of an organic and an aqueous phase when feedstocks containing water or oxygen are fed. For fossil feedstocks the water phase mostly does not occur. The amount of liquid product is measured gravimetrically and then the organic and water phase are separated via a separation funnel. The water then is again measured gravimetrically. It is made up of water and dissolved hydrocarbons. The organic phase is filtered to remove any remaining solid particles (coke and catalyst).

The organic liquid sample is then also inserted in a Shimadzu GC 17-A gas chromatography by injection via a syringe (1.5 µl volume). This gas chromatograph conducts a simulated distillation in which the compounds of the probe are separated by their boiling point. The grouping of said compounds was done according to the lump model described in figure 26. The GC configuration for the simulated distillation are listed in table 10.

table 10: configuration of GC for simulated distillation

type	Shimadzu GC-17A
injector	split 30:1 1.5 µl @ 350 °C
carrier gas	hydrogen 1.68 ml/min constant flow
temperature program	35 °C to 350 °C; dwell-time 22 min
column	Zebron ZB-1
dimension	30 m length x 0.32 mm inner diameter x 0.25 µm film thickness
detector	flame ionization detector (FID) @ 350 °C

The organic samples of some experimental campaigns were manually distilled in an atmospheric distillation column to get the gasoline fraction for further analysis. As an upper boundary for gasoline a boiling temperature of 210 °C was chosen to comply with the aforementioned lump model. This gasoline fraction was then sent to the technical laboratory of the OMV Refining and Marketing GmbH. There various analysis were conducted such as density at 15 °C, elemental analysis (CHNSO), dissolved water content, inorganic contaminants (ICP-MS & Chlorides) and PIONA (paraffin, isomer, olefin, naphthene and aromatic content). Due to confidentiality the OMV laboratory does not want to publicize the exact measurement procedures and the corresponding norms.

3.9.3 Solid analytics

The coke as the sole component of the solid fraction is determined indirectly since it is burnt off in the regenerator. The so produced flue gas is constantly measured (again via an NGA 2000 MLT3 gas analyzer), which gives the values of CO, CO_2 and O_2. Via combustion calculation the amount of coke can then be determined. It must be noted that residual product gas can remain in the catalyst pores after the stripper. This residual product gas is also burned in the regenerator. Thus, creating a slight overestimation of the coke lump.

3.9.4 Ash content – ash residue

The ash content of the different feedstocks were measured using the norm DIN EN ISO 6245 [150]. There a weighted amount of feed was placed in a crucible and put in a muffle furnace. The sample was heated up over 4 hours from room temperature to 775 °C. Then this temperature was kept for 4 hours to make sure that all organic compounds were burned off. Then the oven was turned off and the probes cooled down. As soon as the temperatures were low enough the samples were transferred into an exicator for further cooling to prevent any moisture of potentially falsifying the weighing. The mass of the ash was lastly determined when the probes in the crucibles were at room temperature.

3.9.5 Coke tendencies – Conradsen carbon residue

A feedstock's carbon residue can be described as the amount of residue that is left over after the feedstock's thermal decomposition. This leftover is of carbonaceous solid nature. In FCC units the tendency of a feedstock to form coke determines the thermal balance of the autothermal operation mode. Higher coke formation can lead to lower maximum feed throughput since the regenerator's capacity to burn coke is limited. These tendencies can be measured using standardized tests like the conradson carbon residue (CCR) or the microcarbon residue (MCR) tests [151].

For this work the CCR method has been chosen due to its simplicity and popularity in the refinery sector. The CCR test is defined in the norm ASTM D189 [152]. Downsides of the method are its low reproducibility and its labor intensity. Another point of critique is that it measures thermal coke formation rather than catalytic formation [151]. However, for our comparison of feedstocks the accuracy of the CCR test was good enough. The CCR results of all feedstocks that were used in this thesis and a more detailed description of the measurements were first published by Weber [153].

3.10 Catalysts

All three catalyst samples that were used to run the experiments are commercially available equilibrium catalysts (E-cats) that were taken directly out of an industrial scale refinery. This was done to provide maximum comparability and to ensure that the activity and thus the results correspond to real life results in industrial scale plants. The three catalyst samples consist of a propene boosting catalyst, a heavy residue catalyst with focus on gasoline production and a mixture of two different catalysts. These two catalysts were the propene boosting one and a catalyst with focus on LPG production and are henceforth referred to LPG boosting catalyst mix. In table 11 some parameters of the three utilized catalysts are listed.

table 11: selected parameters of the three utilized catalysts

parameter	propene boosting cat.	heavy residue cat.	LPG boosting cat. mix	unit
total surface area	179	119	173	m^2/g
unit cell size	24.26	-	24.29	Å
average bulk density	0.83	0.93	0.84	g/cm^3
pore volume	0.39	-	0.39	cm^3/g
nickel	54	3912	609	ppm
vanadium	106	2162	105	ppm
sodium	0.25	0.35	0.22	w%
iron	0.23	0.94	0.3	w%
rare earth oxides (RE_2O_3)	1.30	1.55	1.75	w%
cerium oxide (CeO_2)	-	0.02	-	w%
lanthanum oxide (La_2O_3)	-	1.52	-	w%
aluminium oxide (Al_2O_3)	50.30	39.00	47.70	w%
phosphor pentoxide (P_2O_5)	2.00	-	2.52	w%
silicon oxide (SiO_2)	-	48.70	-	w%
titanium	-	0.91	-	w%

These parameters show significant differences in elemental composition of the three utilized catalysts depending on their purposes. Indeed, the heavy residue catalyst contains significantly higher amounts of heavy metals, namely nickel, vanadium but also iron, which originates from the heavy feedstock it is used for. All three catalysts, however, also show similarity.

They all are zeolite-based with the bulk of the catalyst being comprised of aluminium oxide and silicon oxide. Additionally, all are doped with rare-earths (lanthanum and cerium oxide), even though only for the heavy residue catalyst more exact values were provided for the rare earth elements. In figure 28 and figure 29 the particle density and particle sum distribution of the catalysts are illustrated. The measurements for these diagrams were conducted at TU Wien using a Mastersizer 2000 laser diffraction measurement device by malvern panalytical.

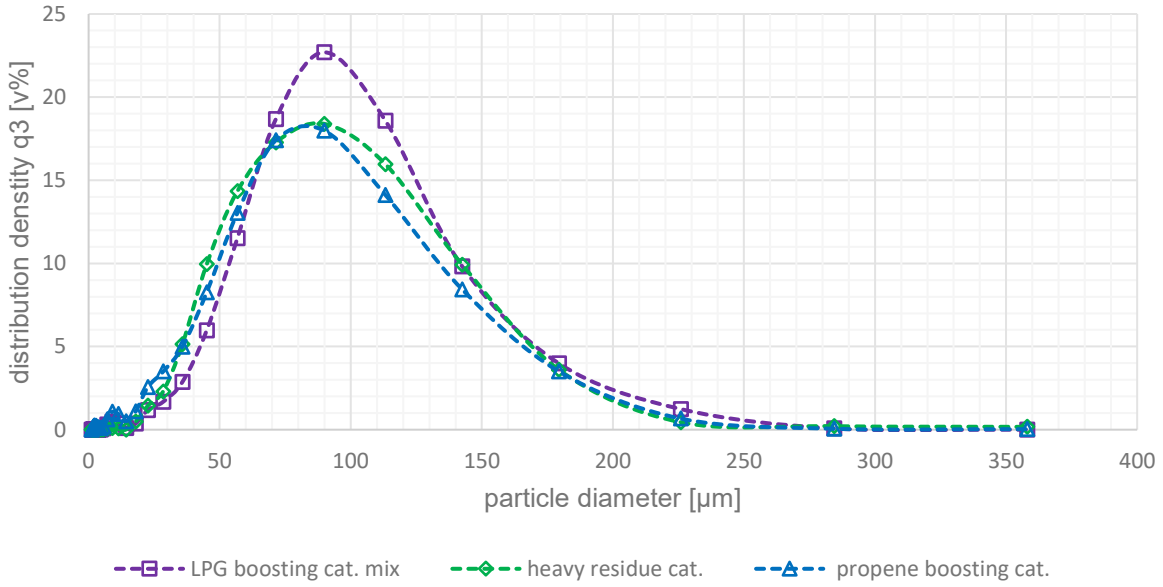

figure 28: particle size distribution of the three utilized catalysts

The sauter mean diameter of the three catalysts are listed in table 12. The main fractions of the catalysts are in the particle range from around 28 to 139 µm.

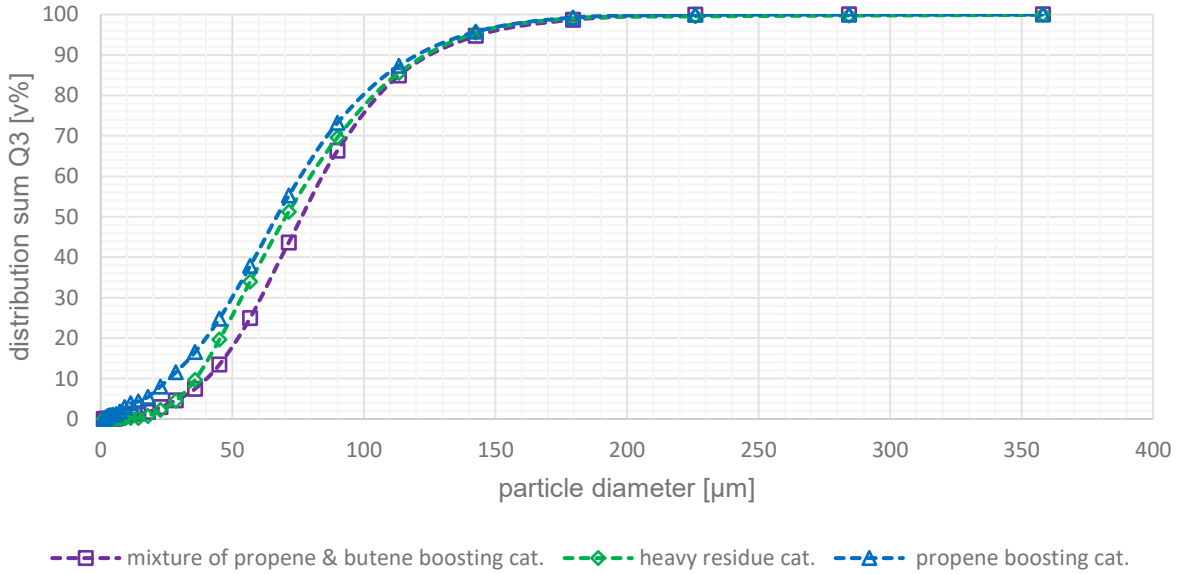

figure 29: particle sum distribution of the three utilized catalysts

table 12: Sauter mean diameter of the catalysts

	propene boosting cat.	heavy residue cat.	LPG boosting cat. mix	unit
d_{SV}	43.41	66.41	67.49	µm

3.11 Feedstocks

3.11.1 Vacuum gas oil (VGO) A, B & C

Vacuum gas oil is one of the standard feedstocks in fluid catalytic cracking units. It is the top product of the vacuum distillation and can either be hydrogenated or unhydrogenated [53] [25]. For the experiments described in this thesis three different batches of VGO were used. VGO A und VGO C are hydrogenated and are taken from an industry partner in Central Europe which employs an FCC unit that focuses on petrochemical base chemicals beside gasoline production. VGO B is unhydrogenated and significantly heavier than the other two batches. It was provided by another industry partner from Central Europe whose focus is on heavy residue processing and gasoline yield maximation. To comply with non-disclosure agreements the names of the suppliers will not be mentioned here.

In table 13 some selected parameters of these three batches are listed. The heavier nature of VGO B is represented by the higher viscosity at 100 °C (20.4 compared to 6.25 and 5.58 mm²/s) and the significantly higher Conradson carbon residue (CCR) of 5.39 w% which is in stark contrast to the values of VGO A and C at 0.16 and 0.20 w%, respectively. The hydrogenation of VGO A and B also constitutes significantly lower amounts of sulfur and nitrogen (see table 13) with the values of VGO B being more than ten times higher for sulfur and more than 6 times higher for nitrogen compared to the other batches. VGO B also contains higher amounts of nickel and vanadium which also corresponds to the batch's heavier nature.

table 13: parameters of three different VGO batches used in this thesis

parameter	VGO A	VGO B (heavy)	VGO C	unit
density at 15 °C	0.89	0.9136	0.8848	g/cm³
viscosity at 100 °C	6.25	20.4	5.58	mm²/s
sulfur	214	3500	290	mg/kg
nitrogen	143	1865	275	mg/kg
vanadium	2	6	2	mg/kg
nickel	2	9	2	mg/kg
total aromatics	32.6	16.6	23.8	w%
ash content	below LOD	0.0094	below LOD	w%
CCR	0.16	5.39	0.20	w%

In figure 30 the boiling curves of the VGO batches are illustrated. While all three batches roughly have the same initial boiling points around 260 to 310 °C their final boiling points differ quite significantly. For VGO A and C these are almost the same at around 550 °C while VGO B constitutes of compounds of which 40 w% have a higher boiling point. The final boiling point of VGO B is even above 750 °C. This difference in boiling curves is in accordance to the higher values for CCR and viscosity of VGO B.

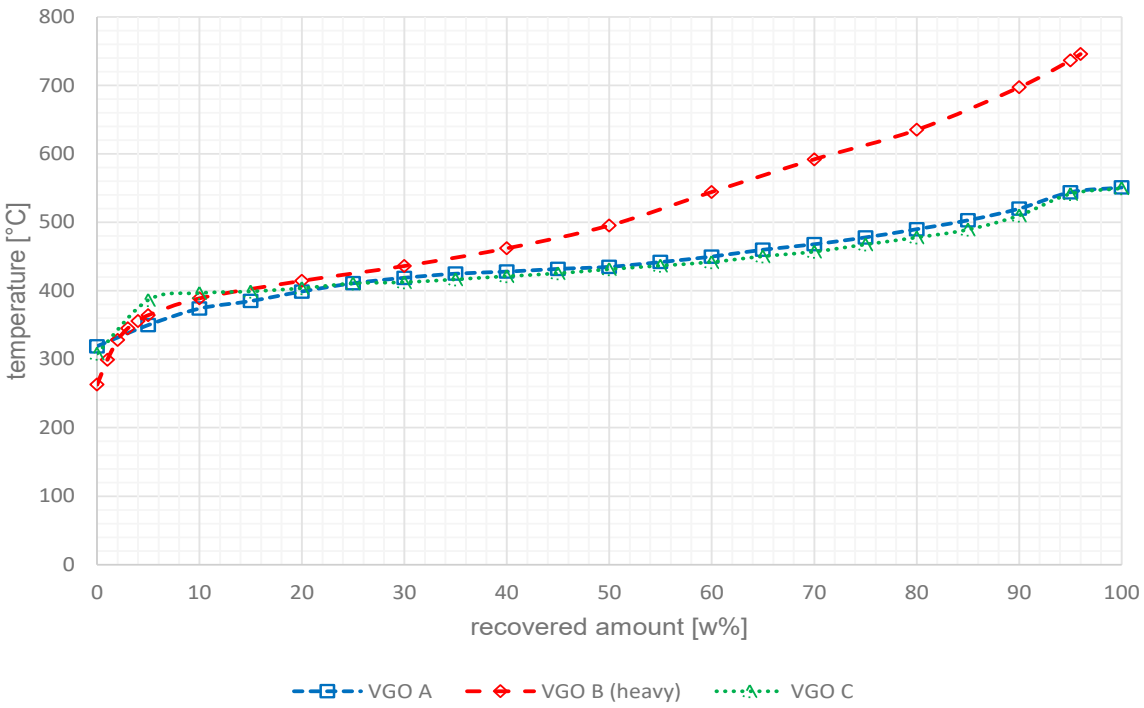

figure 30: boiling curves of the three different VGO batches used in this thesis

3.11.2 Atmospheric residue

Atmospheric residue is the bottom product of the atmospheric distillation column. To foster the conversion of the highest boiling constituents of crude oil refinery operators have started to blend atmospheric residue to their gas oil and vacuum gas oil feedstocks for fluid catalytic cracking. This blending is in the range of only a low proportion up to a complete substitution of feedstock. Depending on the co-processing ratios minor adaptions or a revamp of the plants are necessary [39].

The atmospheric residue batch used in this thesis was provided by a Central European refinery operator which cannot be disclosed due to confidentiality reasons. It was generated under ambient pressure via a three tray flash distillation with a top temperature of 360 °C. Some selected properties are listed in table 14. The provided batch was not hydrogenated which reflects on its comparably high sulfur and nitrogen content (when comparing to VGO A and VGO C for example). Furthermore, it has a relatively high density at 0.97 g/cm³ and a kinematic viscosity of 64.7 mm²/s which originates from its residual nature. The CCR is also quite high at 8.3 w%.

table 14: selected parameters of atmospheric residue batch

parameter	value	unit
density at 15 °C	0.97	g/cm³
viscosity at 100 °C	64.74	mm²/s
acid number	1.45	mg KOH/g
sulfur	0.356	w%
nitrogen	1258	mg/kg
vanadium	1	mg/kg
nickel	10	mg/kg
ash content	Below LOD	w%
CCR	8.320	w%

figure 31 presents the residues boiling curve. The initial boiling point of the batch is hereby at around 330 °C and the final boiling point is at 740 °C. About 40 w% of the atmospheric residue batch consists of compounds with a boiling temperature of more than 550 °C which is the final boiling point for many feedstocks for fluid catalytic cracking [53].

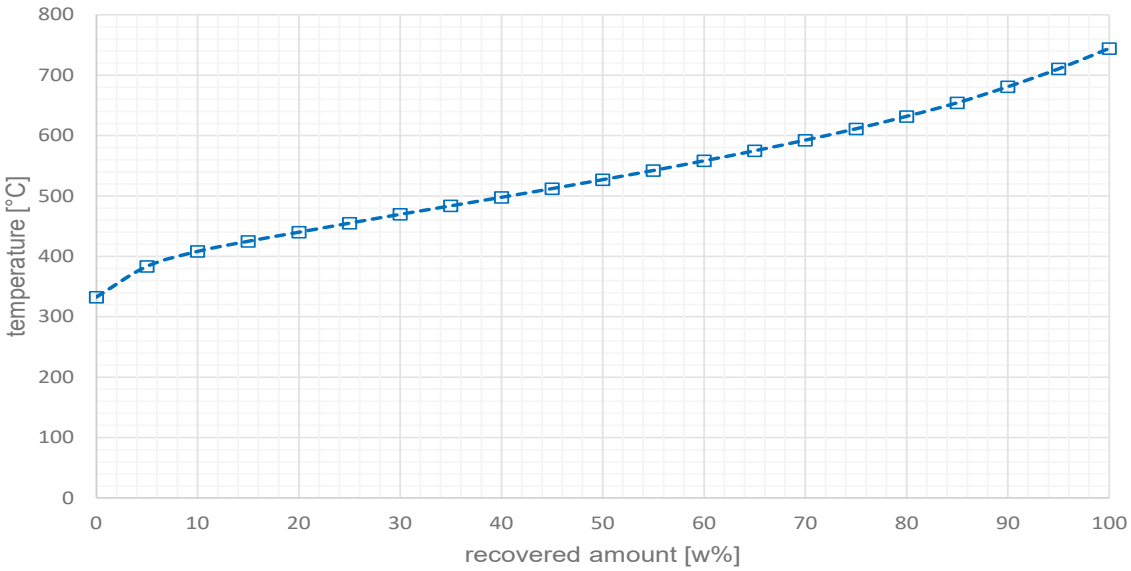

figure 31: boiling curve of atmospheric residue batch

3.11.3 Deasphalted oil

Deasphalted oil (DAO) is a feedstock derived from solvent deasphalting in which a solvent (mostly a short-chain paraffin) is used to deasphalte vacuum residue. The obtained lighter fraction (the DAO) is then separated from the solvent in a second process step. Impurities like metals and sulfur are hereby concentrated in the heavier asphalt-like insoluble phase [154]. For more details on this process refer to chapter 2.9.

The batch of deasphalted oil utilized in this thesis was provided by a southern European refinery operator. Due to a non-disclosure agreement no information about this operator can be shared at this point. Some parameters of this batch (which were provided by said operator) are listed in table 15. Ash cotent and CCR were measured Rests of asphaltenes can still be found in the DAO (1.14 w%) which stems from its origin as part of the vacuum bottom residue. Also, the relatively high viscosity (34.8 mm²/s), sulfur and nitrogen content (1.92 w% and 2845 mg/kg) and CCR (4.636 w%) are typical for residual feedstocks.

table 15: selected parameters of deasphalted oil batch

parameter	value	unit
density at 15 °C	0.9527	g/cm³
viscosity at 100 °C	34.8	mm²/s
sulfur	1.92	w%
nitrogen	2845	mg/kg
vanadium	2.3	mg/kg
nickel	2	mg/kg
asphaltenes	1.14	w%
ash content	below LOD	w%
CCR	4.636	w%

In figure 32 the boiling curve of the deasphalted oil is illustrated. The evaporation of feed starts at around 266 °C and ends at 730 °C. Around 50 w% of the DAO is made of compounds with a boiling point higher than 550 °C, therefore, it is significantly heavier than many standard (vacuum) gas oil feedstocks.

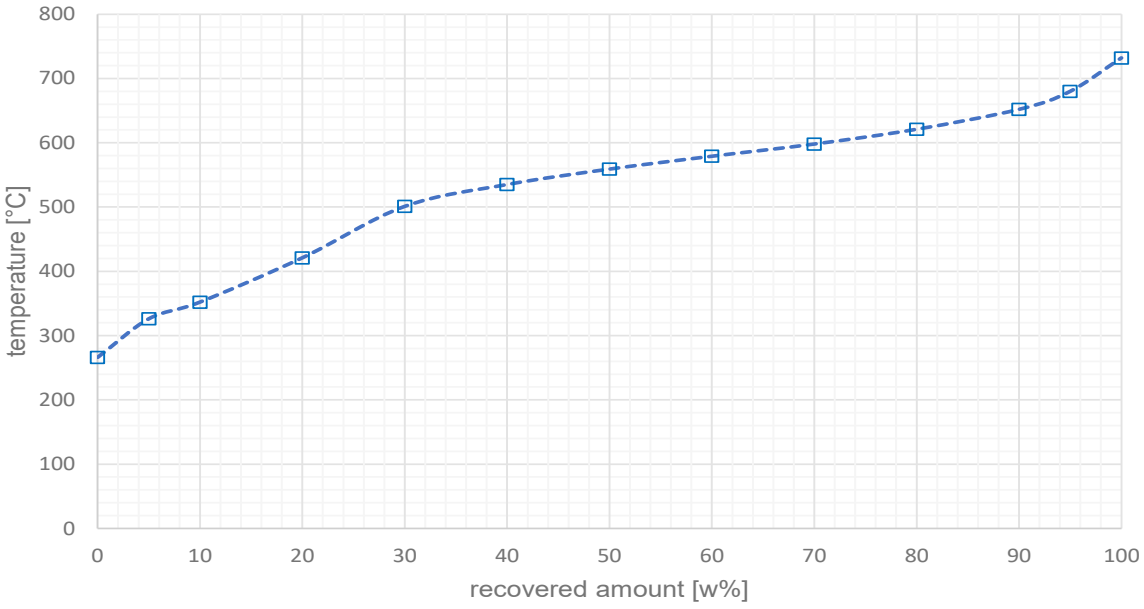

figure 32: boiling curve of deasphalted oil (DAO) batch

3.11.4 Plastic waste derived pyrolysis oil

The plastic waste-derived pyrolysis oil (henceforth simply called plastic PO) was provided by a Central European startup company which will not be disclosed due to confidentiality reasons. The plastic types, which were used for the generation of the plastic PO and their proportions are described in table 16. The proportions were hereby chosen to reflect typical compositions of mixed plastic wastes as they appear in municipal waste sorting plants.

table 16: composition of plastic waste utilized for the production of the plastic derived pyrolysis oil batch

plastic type	amount
LD-PE	30 w%
HD-PE	15 w%
PP	15 w%
PS	10 w%
ABS	10 w%
PVC	10 w%
PET	10 w%

The plastic pyrolysis oil was produced using a screw reactor at 500 °C with integrated hot gas filtriation and at ambient pressure. This intermediate pyrolysis process was develop at the Institute for Technical chemistry at the Karlsruhe Institute of Technology (KIT). The average residence time of plastic waste in the reactor was around 30 minutes. The pyrolysis vapors leave the screw reactor via ceramic filter candles and conveyed to the condensation apparatus. The cake which deposits on the outside of the filters is removed via over pressure and leaves the plant together with the char via a solid outlet. For further information please refer to complementary literature by Tomasi Morgano et al. [108] [155].

In table 17 some selected parameters that were provided by the feedstock producer are listed. The density of the plastic PO (0.875 g/cm³) is in the range of vacuum gas oils. Unlike fossil feeds the plastic PO has a measurable oxygen content of 4.5 w% which originates most probably from different plastic wastes like PET. Also, chlorine is found in significant amounts of 310 mg/kg which enters the oil probably via PVC. The sulfur content is below 100 mg/kg and therefore lower than in residual oils. The low ash content and CCR value indicate no problems regarding pipe clogging.

table 17: selected parameters of plastic derived pyrolysis oil batch

parameter	value	unit
density at 15 °C	0.875	g/cm³
viscosity at 40 °C	10 - 15	mm²/s
carbon	82.3	w%
hydrogen	10.7	w%
oxygen	4.5	w%
sulfur	<100	mg/kg
nitrogen	<1	w%
chlorine	310	mg/kg
water	0.5	w%
olefins	15.7	w%
paraffins	28.3	w%
cyclo-paraffins	5.1	w%
cyclo-olefins	3.3	w%
aromatics	34.9	w%
ash content	0.0052	w%
CCR	0.868	w%

In figure 33 the boiling curve of the plastic PO is illustrated. The boiling points of its components stretch from around 110 to 560 °C and therefore does not exceed that of vacuum gas oils. The plastic PO constitutes mainly of light components with boiling temperatures below 200 °C (up to 65 w%) and is therefore significantly lighter than standard FCC feedstocks.

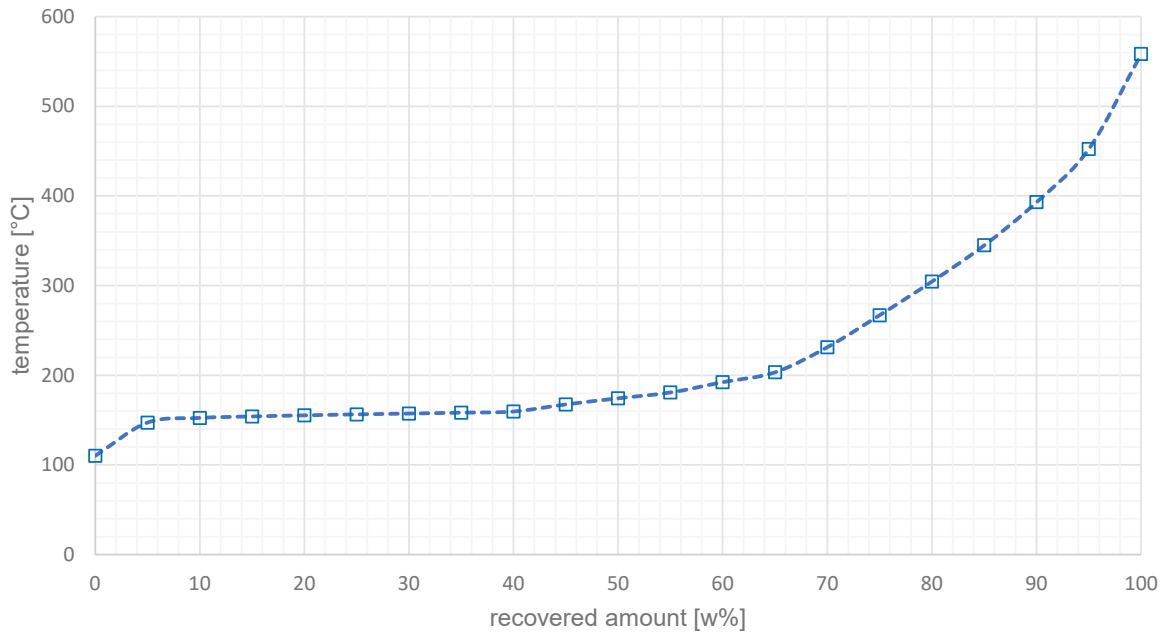

figure 33: boiling curve of plastic derived pyrolysis oil batch

3.11.5 Clean wood derived pyrolysis oil

The clean wood-derived pyrolysis oil batches were provided by BTG (Biomass Technology Group) E.V. in Enschede, the Netherlands. The untreated pyrolysis oil (henceforth only called PO) was produced in the EMPYRO plant that is located in Hengelo, the Netherlands. Empyro employs the rotating cone technology and feeds up to 5 t/h of biogenic feedstocks into the process. For the PO production saw dust from a Swedish saw mill was used. For more information regarding Empyro and the rotating cone process refer to BTG and chapter 2.9 [156].

Such pyrolysis liquids can then be hydrogenated to increase their thermal stability and reduce their tendency for undesired polymerization [91]. In a first hydrogenation step leading to so called stabilized pyrolysis oil (SPO) around 10 kg of liquid were generated (of which roughly 6 liters were supplied by BTG). The reactor system for hydrogenation consists of four separate reactors which were filled with packed beds of 30-35 g Picula™ catalysts each. Before the SPO generation the catalyst was activated under hydrogen atmosphere at temperatures of 600 °C and under ambient pressure.

Part of that SPO was further hydrogenated in a single-step process to create stabilized and deoxygenated pyrolysis oil (SDPO). The same plant as for SPO generation was used. The four reactors were filled with 25 g of a commercially available NiMo catalyst which was also activated beforehand. This activation was conducted with hydrogen and diesel with traces of dimethyl disulfide (DMDS) at 350 °C and under a pressure of 200 bar. The process conditions and flow rates for SPO/SDPO generation are described in table 18. For further information regarding the production of SPO and SDPO as it was applied in this thesis please refer to Wang et al [128].

table 18: process conditions for hydrogenation to generate SPO/SDPO

	Temperature [°C]				Pressure [bar]	Average liquid flow [g/h]	Average hydrogen flow [Nl/h]
	Reactor 1	Reactor 2	Reactor 3	Reactor 4			
SPO	75	100	140	200	200	80	30
SDPO	200	250	300	350	200	100	60

In table 19 some parameters of untreated and hydrogenated pyrolysis oils are listed. The influence of the hydrogenation can be observed via the alterations in carbon, hydrogen and oxygen contents. The carbon and hydrogen contents both increase with higher hydrogenation severity just as the oxygen content decreases. Furthermore, the lower polarity of hydrogenated oils lead to significantly lower water contents (PO 20.5 w%, SPO 8.88 w% and SDPO 0.54 w%). As a consequence of this compositional changes the lower heating values increase from 17.0 to 23.4 and 38.2 MJ/kg for PO, SPO and SDPO respectively. The Conradson carbon residue was also significantly reduced at higher hydrogenation severity. Raw PO has a relatively high CCR of more than 20 w% which can be reduced to 10.78 w% for SPO and eventually to 1.97 w% for SDPO. These high CCR values give an indication of a strong coking tendency for wood derived unhydrotreated pyrolysis liquids. No significant ash contents were measured for the different pyrolysis liquid batches. Due to their thermal instability and tendency to form coke under elevated temperatures the generation of boiling curves via simulated distillation is not possible [80]. Therefore, no boiling curves can be provided as was done for other feedstocks.

table 19: selected parameters of pyrolysis oil (PO), stabilized pyrolysis oil (SPO) and stabilized and deoxygenated pyrolysis oil (SDPO) batch

feedstocks	PO	SPO	SDPO	
parameter		value		unit
carbon	43.9	54.2	83.5	w%
hydrogen	7.9	9.3	10.4	w%
oxygen by difference	48.2	36.5	6.1	w%
LHV, calculated after Boie	17.0	23.4	38.2	MJ/kg
water	20.5	8.88	0.54	w%
ash content	<0.01	0	0	w%
acid number	-	35.2	7	w%
pH	2.5 - 3.5	5.3	3.8	mg KOH/g
carbonyl content	-	1.82	1.15	mg BuO/g
CCR	20.459	10.780	1.973	w%
chlorine	<10	-	-	mg/kg
nickel	<1	-	-	mg/kg
vanadium	<1	-	-	mg/kg

4. Experimental work at the pilot plant

The experimental section of this work is divided into three main sections:

- Experimental campaigns that research the influences of different plant settings and catalysts
- Heavy residue tests including deasphalted oil and atmospheric residue co-feeding
- Co-feeding of pyrolysis liquids that are derived from mixed plastic wastes and clean pinewood wastes

4.1 Catalyst testing

4.1.1 Background

The European Commission sets new intermediate targets to reach net-zero CO_2 emissions by 2050 in its newly proposed "Fit for 55" – legislature package. In this package a significant reduction by 2030 in the transportation sector is planned with a cutback of car emissions of 55%. New cars are expected to generate zero emissions starting from the year 2035 [157].

These targets will inevitably affect the desired product spectra of FCC units since gasoline will not be needed in the same amounts in the future. Therefore, a product shift towards hydrocarbon gases could ensure profitable operation. These shifts require substantial changes in FCC settings and equipment which are commonly conducted in plant revamps during planned shutdowns.

Pilot plant experiments are a relatively quick and risk minimizing way for refinery operators to test out new potential catalysts. To give an overview about the influences of the catalysts that were used in different projects test runs were conducted where the catalyst was the varying parameter. The results of this catalyst testing campaign were presented online at the Minisymposium Verfahrenstechnik 2020 by Büchele [158].

For the catalyst comparison experiments with three different catalysts at two different temperatures were conducted (see table 20). As feedstock VGO A was used. The other experimental settings like feed inlet-temperature, amount of riser fluidization gas and feedrate were kept constant for all experiments.

table 20: experimental setting for catalyst testing campaign

catalyst	feedrate [kg/h]	T_{riser} [°C]	$T_{feeding}$ [°C]	riser fluidization [Nl/min]
propene boosting cat.	2.49	549	322	0.1
propene boosting cat.	2.52	532	322	0.1
heavy residue cat.	2.45	552	328	0.1
heavy residue cat.	2.48	527	328	0.1
LPG boosting cat. mix	2.44	550	318	0.1
LPG boosting cat. mix	2.49	530	318	0.1

4.1.2 Results

The product yields according to the lump model depending on catalyst are illustrated in figure 34 and figure 35 for 550 °C and 530 °C riser temperature, respectively. In figure 34 the biggest differences in the hydrocarbon gas yields were observed between the gas boosting and the heavy residue catalysts. The LPG boosting catalyst mix generated 39.7 w% and the propylene boosting cat. 40.4 w% whereas the heavy residue catalyst only converted 26.8 w% of feed into hydrocarbon gases, an astonishing difference. The difference between the gas promoting catalysts was negligible. Regarding gasoline production the results are contrary to the hydrocarbon gases. The heavy residue catalyst generates 55.4 w% of gasoline yield. The usage of gas promoting catalysts lead to 42.8 and 43.8 w% with no statistically significant difference between them. Adding up these values in the total fuel yield no relevant differences can be made out. All catalyst show TFYs of just above or below 83 w%. The LCO lump varies between 7.6 and 8.4 w% with a significant difference only occurring when comparing the LPG boosting catalyst and the heavy residue catalyst. For the residual yields no significant differences can be observed (low yields of 2.8 to 3.4 w%). The highest coke yield is obtained for the mix of LPG boosting catalyst at 5.7 w%. For the heavy residue and propylene boosting catalysts the values are 5.4 and 4.7 w%, respectively.

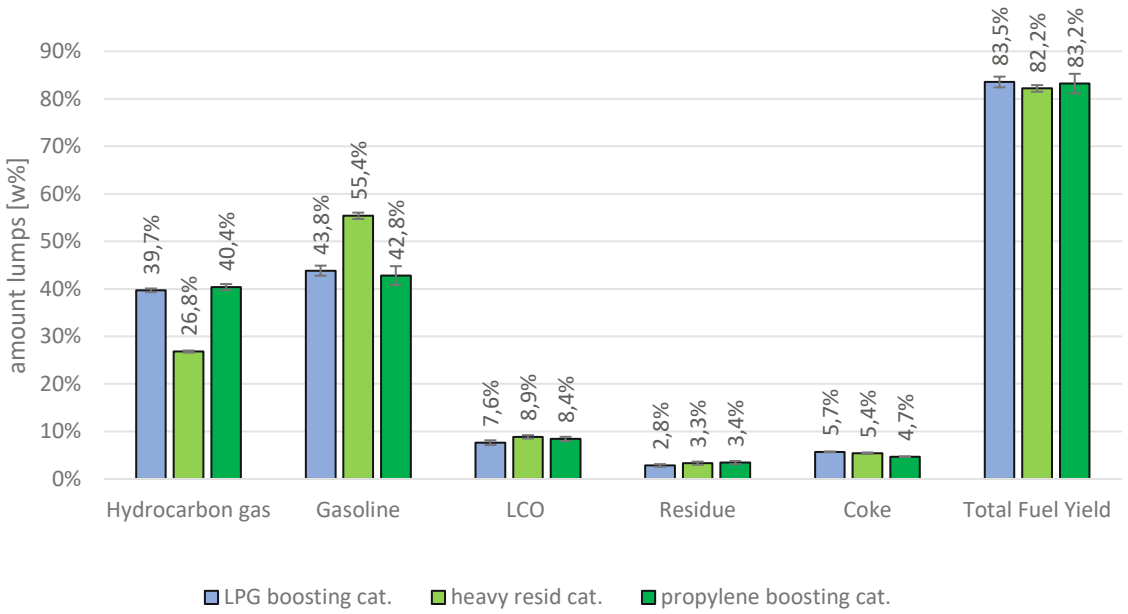

figure 34: Lump distribution of all three catalysts at 550 °C riser temperature

In figure 35 the same yields as for 550 °C are displayed for 530 °C riser temperature. The overall picture when comparing the three catalysts was hereby the same as for the 550 °C catalyst comparison. The use of heavy residue catalyst results in the lowest hydrocarbon gas yields (22.7 w%) and the highest gasoline yields (58.1 w%). The yields of gasoline for both gas boosting catalysts were not significantly different. Also, LCO and residue formation are promoted when using the gasoline boosting catalyst (10.2 and 4.2 w%, respectively). The highest coke formation is observed for the propylene boosting catalyst (5.2 w%) followed in order by the heavy residue catalyst (4.6 w%) and the LPG boosting catalyst mix (4.4 w%). The obtained values for hydrocarbon gases, coke and total fuel yield were lower than at 550 °C (see figure 34). The liquid product fractions (gasoline, LCO and residue), however, all showed higher results for lower temperatures.

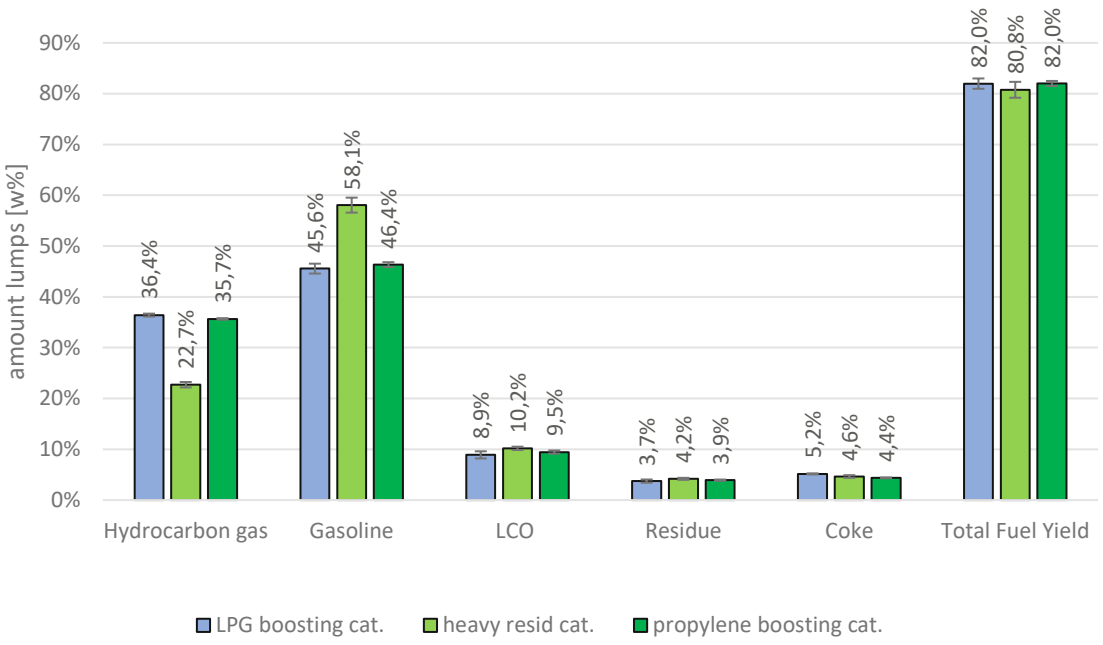

figure 35: Lump distribution of all three catalysts at 530 °C riser temperature

The olefinic gases are displayed in detail in figure 36 for all riser temperature and catalyst variations. The butenes (1-butene, isobutene, cis-2-butene, trans-2-butene) and alkanes (methane, ethane, propane, isobutane, n-butane) are grouped together. The highest propylene yields are generated when the propylene boosting catalyst is used. The highest amount is obtained at 550 °C at 14.8 w%. The lowest yield was measured for the heavy residue catalyst at 7.2 w% at 530 °C. Using the LPG boosting catalyst mix the yields for propylene are 13.8 and 12.6 w% for 550 and 530 °C, respectively. The same trend is also observed for ethylene. The highest yields are again obtained at 550 °C riser temperature at 3.7 w% for the propylene boosting catalyst and the lowest yield at 1.0 w% for the heavy residue catalyst at 530 °C. The same pattern depending on riser temperature and catalyst as for ethylene and propylene is also obtained for butenes. The yields for butenes are in the range from 5.7 to 9.1 w%. The highest alkane yield was obtained for the LPG boosting catalyst mix at 550 °C at 14.4 w%. The lowest was for the heavy residue catalyst at 9.0 w%. For all three catalysts higher olefinic and alkane yields are generated at higher temperatures. The differences between temperatures were up to almost 2 w%.

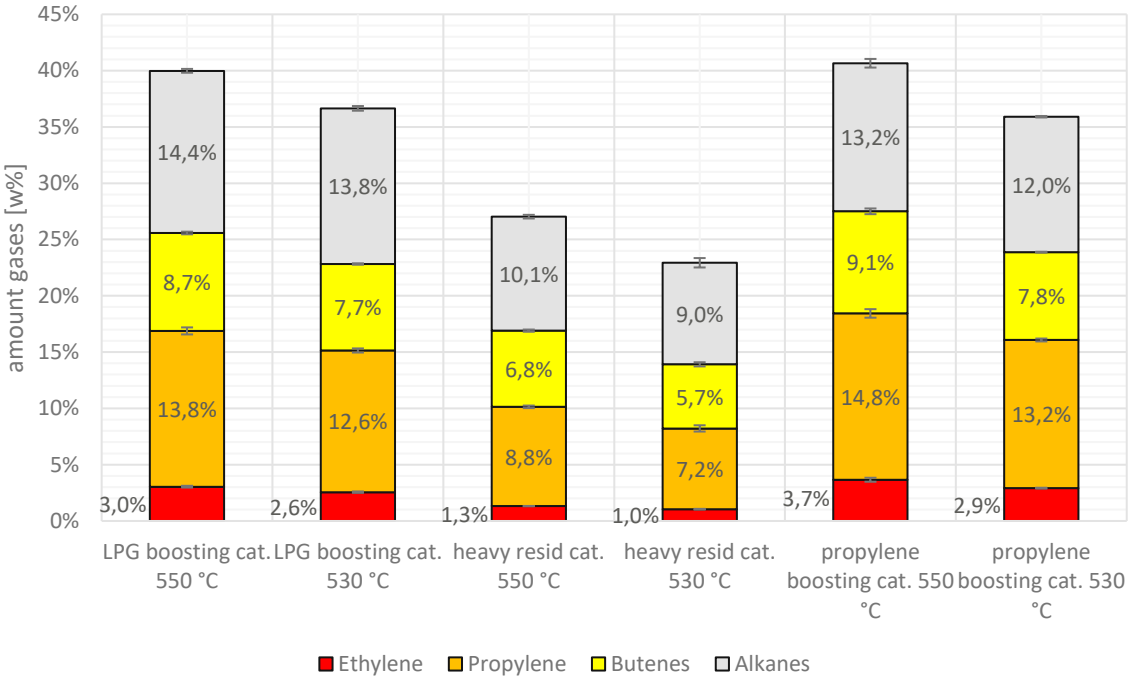

figure 36: olefin and alkane amounts depending on catalyst and riser temperature

The previous results for the olefinic gases and the alkanes are set in relation to the overall hydrocarbon gas lump in figure 37. The relative amounts of olefinic gases decreased for all three catalysts at lower temperatures which correspondingly results in an increase in alkanes of up to 2 w%. The highest yields for ethylene and propylene are obtainable with the propene boosting catalyst for 550 °C at 9.0 and 36.3 w%, respectively. The lowest yields are again observed with the heavy residue catalyst at 530 °C. The highest amounts of butenes are generated using the heavy residue catalyst. No difference is found depending on the riser temperature with values of 25.0 and 24.8 w%. The highest shares of alkanes are also generated with the heavy residue catalyst. The single highest yield is at 530 °C riser temperature with 39.3 w% and the lowest for the propylene boosting catalyst at 550 °C at 32.3 w%.

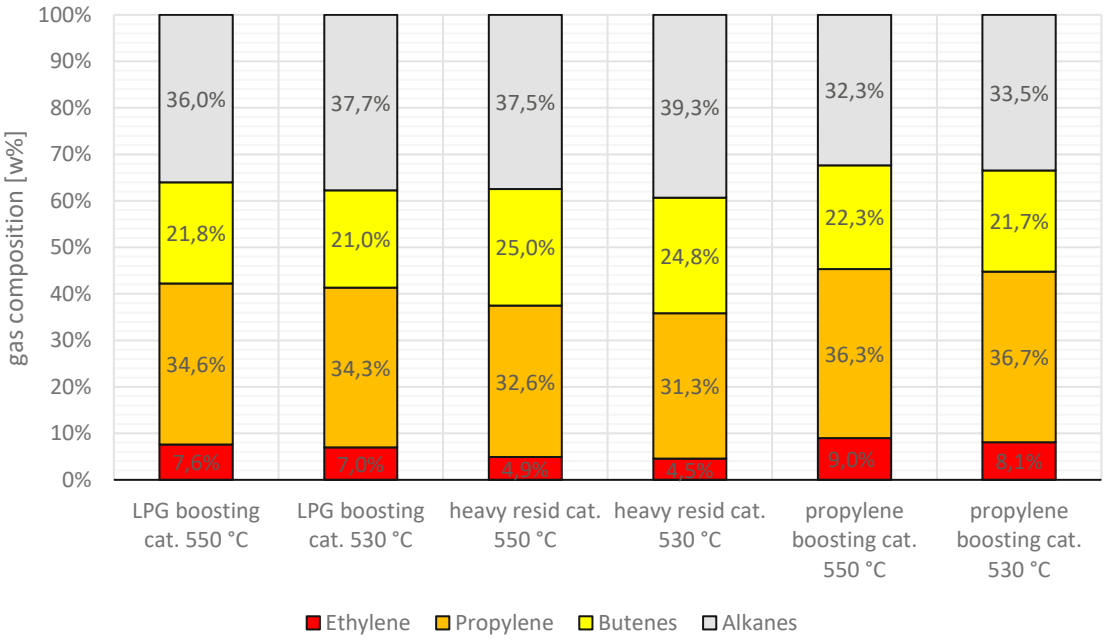

figure 37: gas composition in respect to olefins and alkanes depending on catalyst and riser temperature

The yields of butenes are disaggregated and displayed in figure 38 according to the utilized catalyst and the riser temperature. Between the LPG and propene boosting catalyst no clear differences can be observed for 1-butene and cis-2-butene. Only for the heavy residue catalyst significantly lower measurements of 1.2 w% for 1-butene at 530 °C for example are obtained. The lowest value for cis-2-butene is measured at the same temperature at 1.1 w%. The highest butene yields are for isobutene (3.3 – 1.9 w%) where the usage of the heavy residue catalyst again leads to the lowest amounts (2.2 and 1.9 w% for 550 and 530 °C, respectively). The same picture can be drawn for trans-2-butene. There, no differences between the gas boosting catalysts can be made out. Only the residue catalyst leads to lower yields. In general, all butenes decrease when a lower riser temperature is chosen.

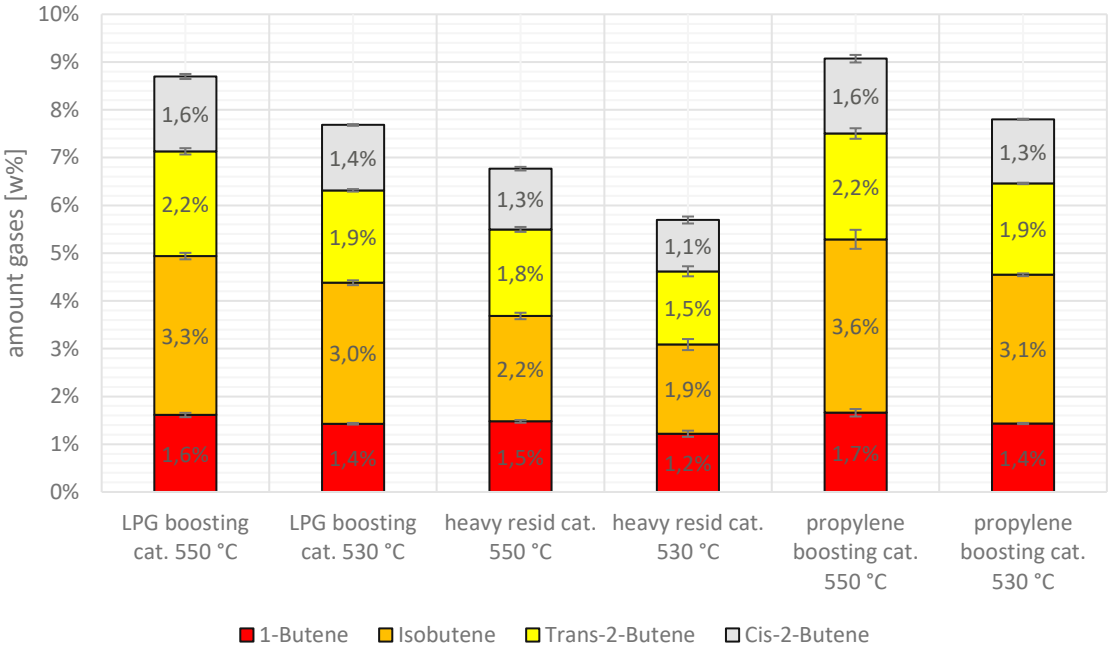

figure 38: butenes distribution depending on catalyst and riser temperature

The alkanes and their amount are depicted in figure 39. Unlike for other gases the heavy residue catalyst promotes the formation of methane with 1.4 and 1.1 w% for 550 and 530 °C, respectively. For the gas boosting catalysts, the yields are at 1.0 w% and below. For ethane no significant difference can be concluded between the three catalysts with yields between 0.7 and 0.4 w%. For the other three alkanes (propane, n-butane and isobutane) usage of the heavy residue catalyst leads to the lowest yields of all three catalysts. The LPG boosting catalyst facilitates isobutane with yields of 8.2 and 8.4 w%. No significant difference can be made out between the two riser temperatures. The values for the propene boosting catalyst are slightly lower at 7.2 and 7.0 w% with no relevant difference between them. For propane and n-butane clear differences between the gas promoting catalysts can hardly be observed. In general, for most catalysts and alkanes the reduction of riser temperature corresponds to a reduction in yield.

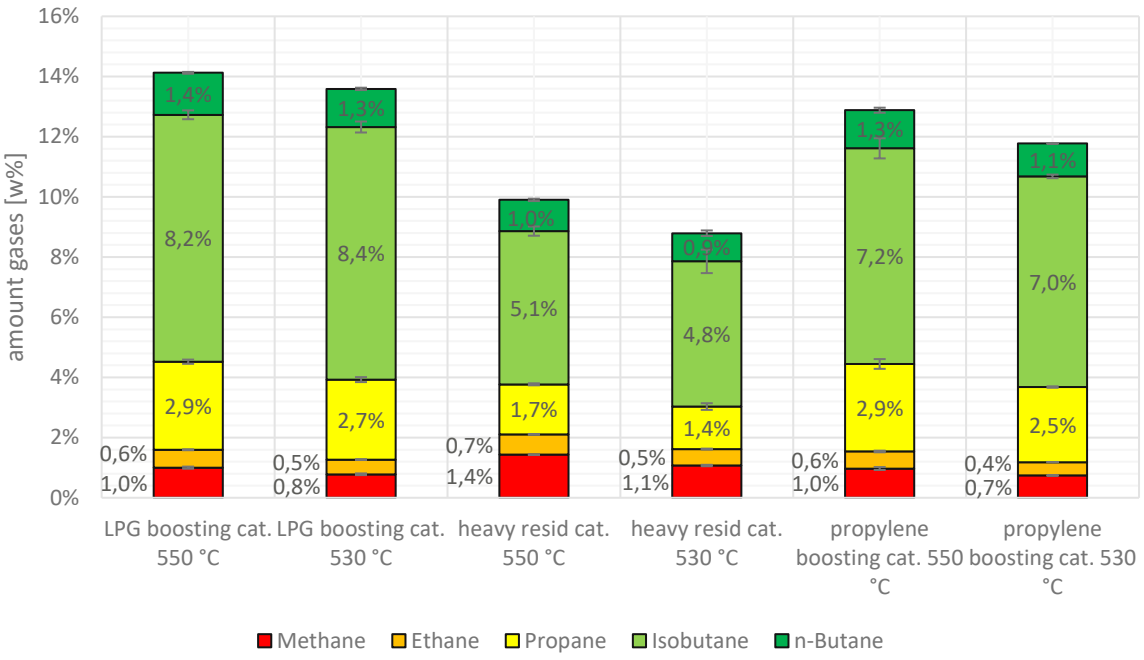

figure 39: alkane distributions depending on catalyst and riser temperature

4.1.3 Discussion

The comparison of product groups depending on the catalysts displayed different product yields. All catalysts promoted the product fractions which they were designed for with the highest yields of gasoline being obtained for the gasoline boosting heavy residue catalyst. Usage of the gas boosting catalysts thereby created significantly lower gasoline yields for both riser temperatures. Correspondingly, the hydrocarbon gas lumps were increase for said catalysts. Therefore, all catalysts behaved according to manufacturer descriptions in the fluid catalytic cracking pilot plant without any changes to the test rig. This proves that the pilot plant is suitable for catalyst testing.

Differences between the propylene and the mixture of propylene and butane boosting catalysts were not statistically significant for the hydrocarbon gas lump and the gasoline lump. However, when analyzing the olefins it can be seen that pure propylene boosting catalysts lead to the highest propene yields whereas the mixture or propylene and butane boosting catalyst created higher yields of butanes, especially isobutane. Again, the product yields matched the manufacturer descriptions.

Beside the catalyst variation an additional temperature variation was added to the experimental campaign to further investigate if the pilot plant behaves according to literature for different catalysts. Judging from the results for both 550 °C and 530 °C this question has been answered satisfactorily. For all three catalysts higher riser temperatures lead to an increased formation of hydrocarbon gases which was expected since higher temperatures promote cracking reactions. Consequently, lower temperatures result in lower cracking severity which corresponds to higher yields of heavy fractions. This again was observed for all catalysts where increased amounts at 530 °C were generated for all liquid products (gasoline, LCO and residue).

The coke yield was lower at 530 °C for all three catalysts compared to the yields at 550 °C. This is probably also due to the fewer cracking reactions which generate coke in secondary reactions. Therefore, it can be concluded that the majority of coke generated when using high quality feedstock like vacuum gas oil is so called catalytic coke.

4.2 Influence of nitrogen boost fluidization in feed inlet on product spectra

4.2.1 Background

Testing a variety of different feedstocks in a pilot plant can prove challenging, especially for residual and other unconventional feedstocks like pyrolysis oils since in industrial-sized FCC plants units are often adapted to the exact corresponding feedstock. These specific design adaptations are not directly possible in the utilized pilot plant and it would also not prove feasible to revamp the plant for each project.

One operational problem that occurs quite often is coking especially when residual and lignin-based liquids are fed. To counteract the coking and ease the feeding into the plant the amount of fluidization gas into the riser can be increased. By doing that the residence time of feed in the tubular oven is reduced (which diminishes coking there) and feed atomization at the feed inlet nozzle in the riser is boosted. Increasing gas lift capacity is a method which is also applied in residual FCC units [159].

Applying this method, however, has side effects on the pressure balance of the pilot plant and circulation rates increase since more catalyst particles are sucked into the riser entry. As a countermeasure the plug valve which controls catalyst flow could be closed further but this is not manageable with the current system since further closing the valve hinders catalyst flow all-together. As a consequence, circulation rate inevitably increases at higher amounts of fluidization gases into the riser which then has an effect on catalyst to oil ratio.

Industrial sized FCC plants utilize C/O-ratios in the range of 7 – 15 [40] which is slightly lower than the values obtained at the pilot plant for minimum fluidization gas into the riser (whose values are around 20 and between 10-15 for 550 and 530 °C riser temperature, respectively). By employing the above mentioned adaptation, it is believed that C/O-ratios would rise further away from industry specifications. This could have implications on product spectra and plant comparability. To prove this hypothesis an experimental campaign was conducted in which different amounts of riser fluidization gas were used when feeding standard VGO at 550 °C riser temperature. As a catalyst the mixture of propylene and butene boosting catalysts was chosen. In total four experiments were performed that are listed in table 21.

table 21: experimental setting for amount of riser fluidization gas variation testing campaign

feedstock	feedrate [kg/h]	T_{riser} [°C]	riser fluidization gas supply [Nl/min]	C/O-ratio [-]
pure VGO A	2.02	550	0.1	20.5
pure VGO A	2.00	550	1	32.3
pure VGO A	1.97	550	2.5	45.3
pure VGO A	1.97	550	5	57.7

4.2.2 Results

The changes of the hydrocarbon gas and gasoline lumps as well as the total fuel yield depending on the catalyst to oil ratio are illustrated in figure 40. There, the hydrocarbon gas yields shows a strict rising trend from 43.3 to 55.0 w% from the lowest to the highest observed C/O-ratio. Counterbalancing these rises in hydrocarbon gases the gasoline yields decline significantly from 41.6 to 32.8 w%. The changes in hydrocarbon gases and gasoline yields between the two lowest C/O-ratios, however, were not statistically significant due to overlapping error margins. This significance was only met at higher ratios. The differences in the aforementioned yields results in varying total fuel yields. From 20 to around 45 C/O-ratio the total fuel yield stays almost constant between 84.1 and 84.8 w% whereas at around 58 C/O-ratio a rise in TFY to approximately 87.7 w% is observed.

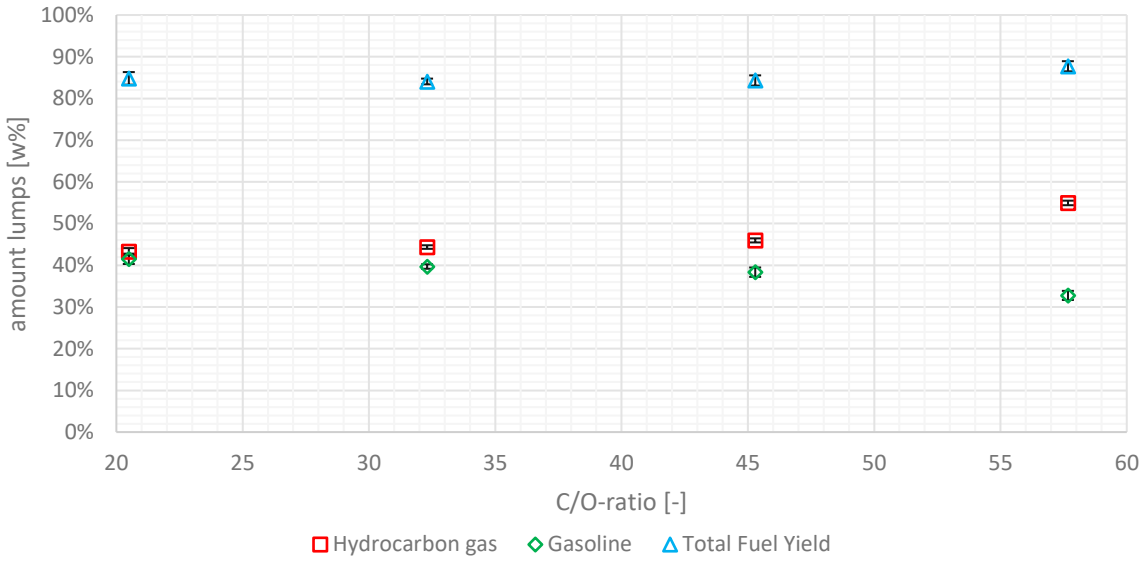

figure 40: hydrocarbon gas, gasoline and TFY distribution depending on C/O-ratio

The light cycle oil lump, which is depicted in figure 41, shows a falling trend with rising C/O-ratios. These drops are, however, not significant between 20 and 45 C/O-ratio due to high error margins. Only at the highest amount of riser fluidization a significant fall from 7.0 to 4.7 w% is detected. The same pattern is also observed for the residual lump. Again, the only significant drop is for the highest C/O-ratio to around 1.9 w%. For the other experiments the parameter insignificantly declines from 3.0 to 2.5 w%. The coke lump does not show any clear trend regarding its dependence on catalyst to oil ratio. While a rise from 4.7 to 6.0 w% is first observed, a decline follows to 5.5 w%.

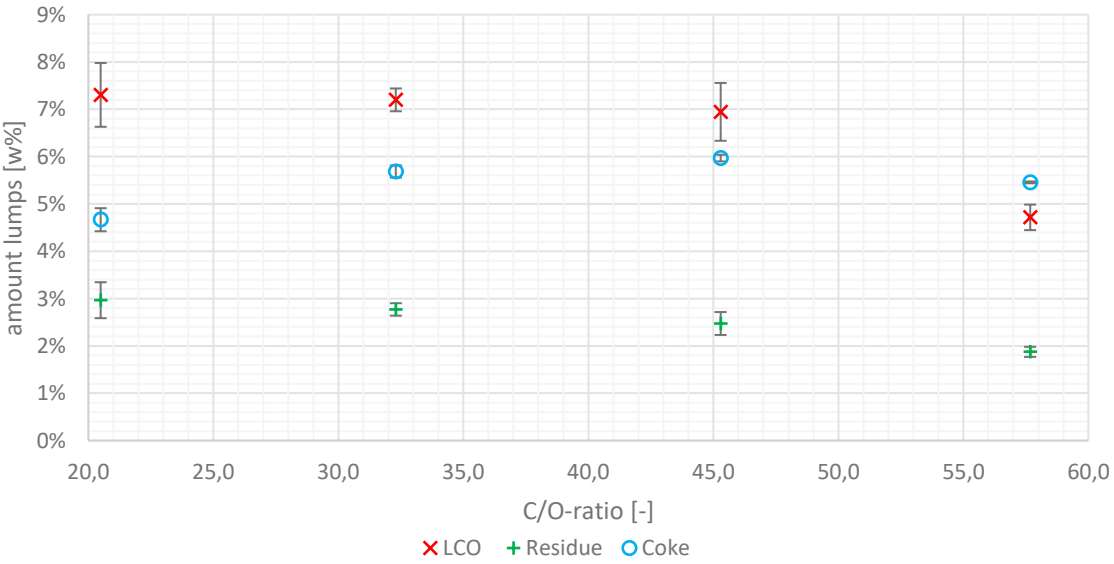

figure 41: LCO, residue & coke distribution depending on C/O-ratio

The yields of olefinic gases and alkanes are found in in figure 42. The ethylene amounts showed a rising trend for higher C/O-ratios with the highest yield being 4.1 w%, the lowest was 3.5 w%. The propylene numbers skyrocketed from around 14.2 to just over 20 w% when comparing the highest and lowest C/O-ratios. Just like the other olefins the butenes also increased significantly from 9.1 to 14.7 w%. The alkanes, however, follow a different trend. They first decline from around 17 w% to 15.3 w% and then rise again to 15.8 w% for the highest observed C/O-ratio. This rise is however inside overlapping error margins and therefore not statistically relevant.

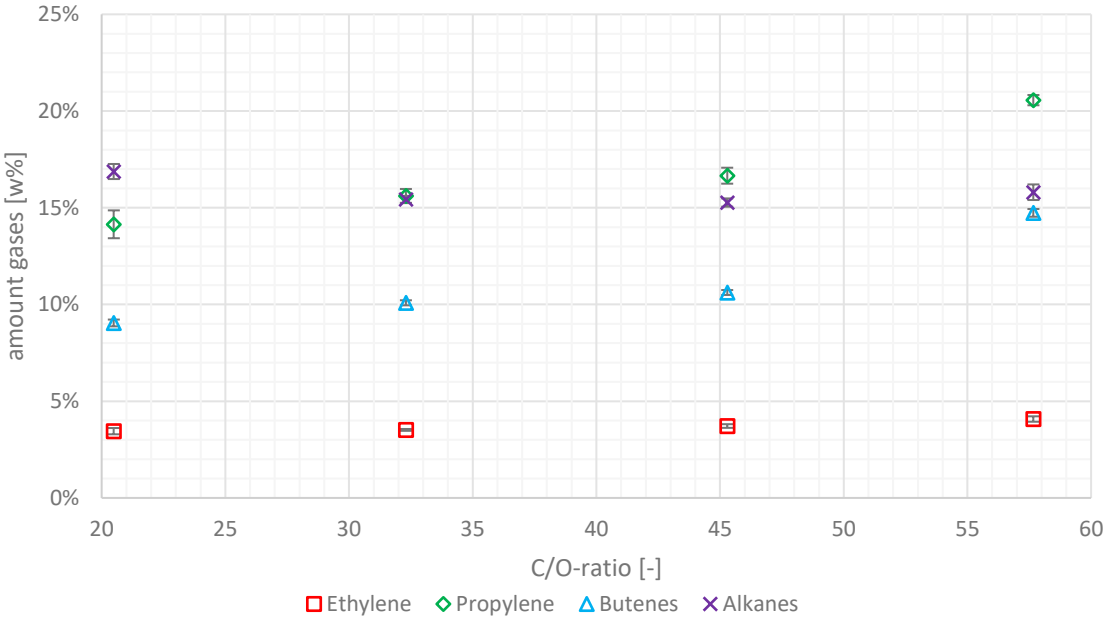

figure 42: olefins and alkanes distribution depending on C/O-ratio

The values from figure 42 were set in comparison to the overall gas lump from figure 42 to evaluate the changes in gas quality (figure 43). When comparing gas quality the ethylene yields do not show a clear trend with stable values around 7.9-8.0 w% which drops to 7.4 w% at the highest C/O-ratio. The propylene amounts in the product strictly increase from lowest to highest C/O-ratios (from 32.5 to 37.3 w%). The same trend was also observed for butenes with a rise from 20.8 to 26.7 w%. The alkanes trend goes into the opposite direction with a decline from 38.8 to 28.6 w%.

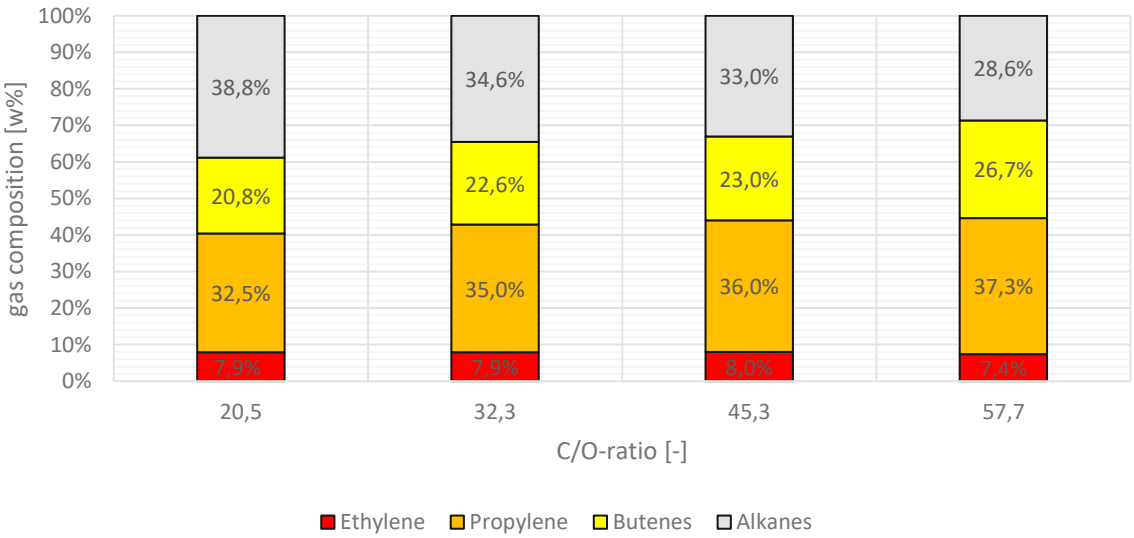

figure 43: gas composition in respect to olefins and alkanes depending on C/O-ratio

The results of the butenes lumps is analyzed in detail in figure 44. 1-butene follows hereby the trend of the butene sums by increasing at higher C/O-ratios. Starting from 1.6 w% a slight increase is observed at first which later accelerated up to 2.7 w%. The exact same trend was observed for all other butene yields. Isobutene rises from 3.5 to 5.5 w% and trans-2-butene and cis-2-butene from 2.3 to 3.8 w% and from 1.6 to 2.8 w%, respectively.

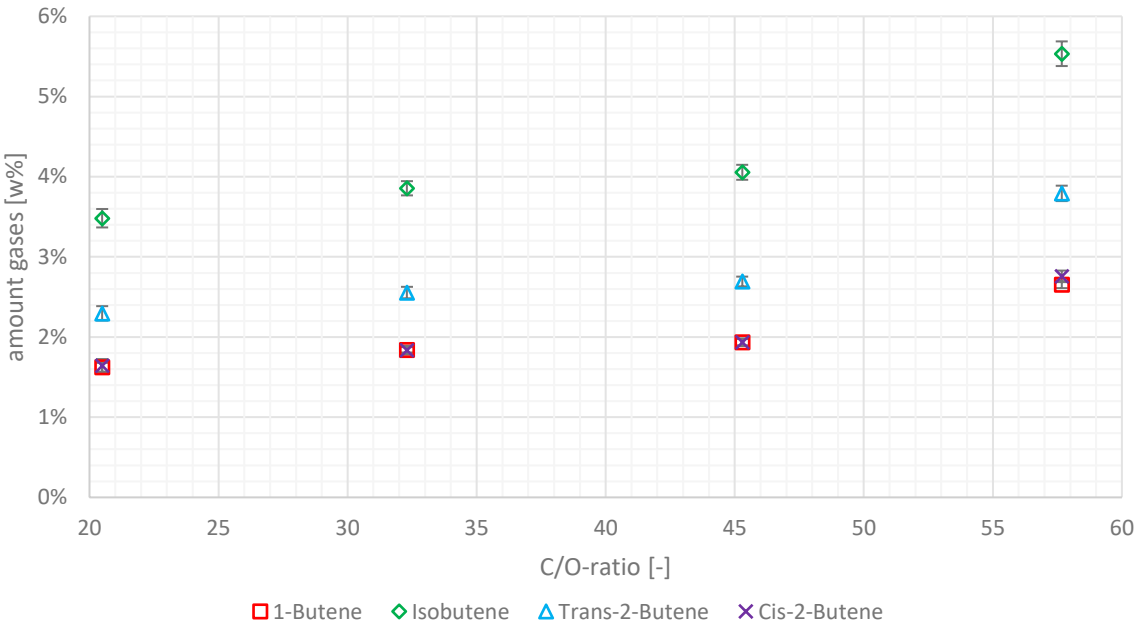

figure 44: butenes distribution depending on C/O-ratio

Similar to the butenes the alkanes are disaggregated as well in figure 45. Methane and ethane showed declining numbers with rising C/O-ratios. They were measured in the ranges of 1.2 to 1.0 w% and 0.7 to 0.6 w% for methane and ethane, respectively. For propane the same dependencies were detected with a decline from 3.5 to 2.9 w%. The isobutane and n-butane yields behaved in the same way with an exception at the highest C/O-ratio (57.7 w%) where a rise was detected. The butane yields varied hereby from 9.6 to 8.7 w% and from 1.7 to 1.5 w% for isobutane and n-butane, respectively.

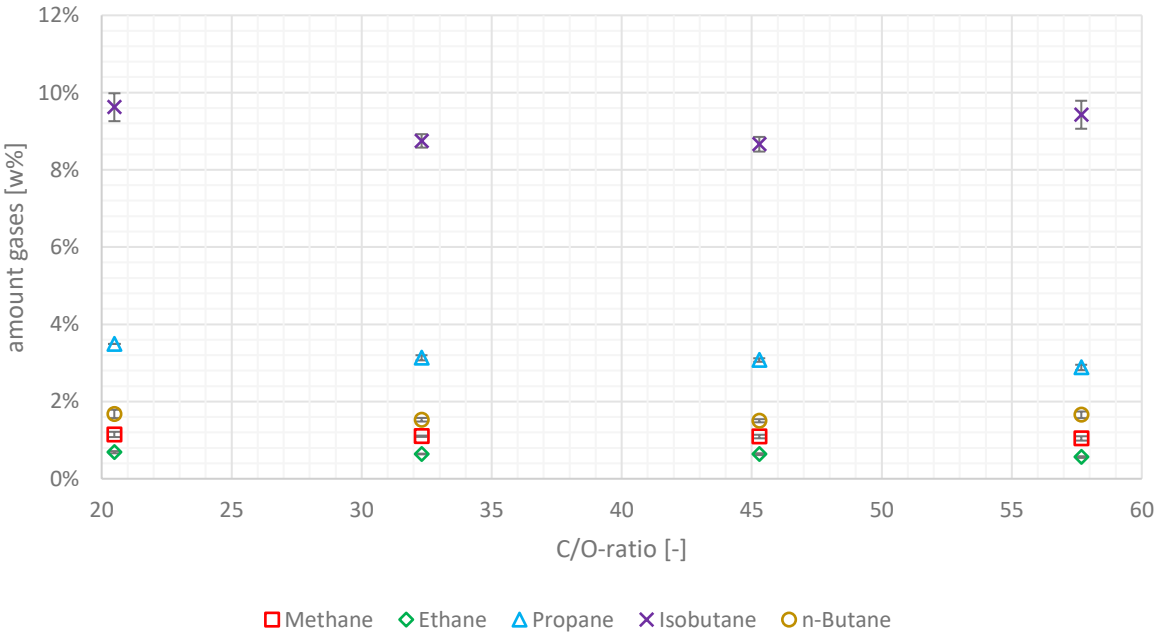

figure 45: alkanes distribution depending on C/O-ratio

4.2.3 Discussion

Adding nitrogen into the riser section to boost feed atomization and hinder pipe clogging through coking led to a surge in catalyst to oil ration from around 20 to around 58 at the highest possible amount of fluidization gas. It was expected that this abundance of active sites on the catalyst at constant feeding rates would inevitably lead to higher cracking severity.

These expectations were fulfilled with a rise in the hydrocarbon gases. The gasoline yield showed a severe drop which is a significant downside since it is a desired product. Overall, however, the drop in gasoline was overcompensated with the rise in hydrocarbon gases manifesting in an increasing conversion rate. Therefore, no significant downsides regarding the production of valuable products were observed. However, when focus is on gasoline production lower catalyst to oil ratios are recommended. Heavier product fractions like residue and LCO decreased which is also a result of the higher catalyst to oil ratio and therefore an increased cracking of the feedstock.

Interestingly, while changes in product yields follow more or less a linear trend for 20 to 45 C/O-ratio, the highest C/O-ratio at around 58 lead to significant deviations from that pattern. Therefore, additional experiments with varying amounts of fluidization gases are recommended to further determine product trends. Especially, data points in between the ones run in this campaign should be researched to determine if and where there is a transition between a linear and an exponential trend.

In-depth analysis of the hydrocarbon gas lump leads to the conclusion that certain gases decrease even though a stark increase is observed for the sum of all C_1 to C_4 gases. These decreases occur for short chain alkanes like methane, ethane and propane. Indeed, butanes do not show such a strict declining trend. Reason for this observation is probably the boosting effect of the catalyst on butane formation which counteracts the decline in alkane formation.

Olefin generation is significantly boosted at higher C/O-ratios with the highest yields being obtained for the highest C/O-ratio. These changes are measured for propene (which in itself is already favored by the utilized catalyst) and also for ethylene and the butene group. These increases originate most probably from the catalytic cracking mechanism where the generation of olefins is a result of β-scission (see chapter 2.7.2). Therefore, higher catalyst to oil ratios not only promote hydrocarbon gas formation but especially olefin generation which is economically favorable.

The key takeaway of this experimental campaign is that the variation of riser fluidization gas flow rates leads to significantly different catalyst to oil ratios and consequently to different product yields. Therefore, when conducting for example a co-processing test series, it is of utmost importance to conduct the reference experiments with vacuum gas oil under the exact same fluidization settings as the co-processing experiments. Even though vacuum gas oil can be fed without hardly any additional riser fluidization gas. By doing so it is guaranteed that any eventual changes in the product spectrum originate only from the feedstock variation which is important for result interpretation and evaluation of the suitability of a potential FCC feedstock.

4.3 Utilization of heavy residues: atmospheric residue

4.3.1 Background

A refinery operator planned to switch its overall strategy towards more petrochemical products and less fuel production to generate higher profit margins and enable a less CO_2-intensive operation. To achieve these goals the corresponding oil and gas company wanted to co-feed comparably low-value atmospheric residue together with hydrogenated vacuum gas oil into their FCC plant. In the past said unhydrogenated atmospheric residue was used for fuel oil production. By co-feeding the residue the product portfolio would henceforth be altered towards high-octane gasoline and gaseous products (especially LPG). The maximum planned co-feeding amounts would be only up to 5 w% according to the refinery operator.

Co-feeding of atmospheric residue is an already well-known and tested operation mode in FCC plants and especially for small admixtures of only up to 5 w% no major modifications for the plant should be necessary [39]. The higher sulfur content in the unhydrogenated residue (3560 ppm) compared to the hydrogenated vacuum gas oil (214 ppm), however, could lead to problems in product quality. One such sulfur compound is carbonyl sulfide (COS), which is not found in crude oil fractions and is mainly generated in conversion processes out of sulfur contained in the feedstock [160]. This compound then further accumulates in the C_2 and C_3 gas fractions due to overlapping boiling points. About 90% of the COS enriches in the C_3 where it acts as a contaminant for petrochemical production processes downstream [161]. Its role as a catalyst poison is hereby significant in the polymer industry and especially in polypropylene production [161] [162]. The refinery operator, therefore, contracted the research group to investigate the change in product spectra and the formation of carbonyl sulfide using pilot plant experiments.

In total 4 different experiments were conducted in the atmospheric residue campaign which are described in table 22. As a reference point pure VGO A was chosen. The other mixtures included low percentages of atmospheric residue which were prepared in advance and fed via one pump (due to the feedstocks high miscibility). As catalyst the propylene enhancing catalyst was chosen. Both admixture rates, riser-temperature and catalyst choice were instructed by the industrial partner. Since only small amounts of residue were administered to the vacuum gas oil low amounts of riser fluidization gas were chosen. The selected feed rate is an average of former experimental campaigns. Parts of the results of this experimental campaign were published by Büchele et al in 2019 [163].

table 22: experimental settings for atmospheric residue campaign

feedstock	feedrate [kg/h]	T_{riser} [°C]	riser fluidization [Nl/min]
100% VGO A	2.5	551	0.1
97.5% VGO A + 2.5% atmospheric residue	2.4	552	0.1
95% VGO A + 5% atmospheric residue	2.5	550	0.1
90% VGO A + 10% atmospheric residue	2.5	552	0.1

4.3.2 Results

The hydrocarbon gas lump tends to sink at higher admixture rates of atmospheric residue (figure 46). At pure VGO and at 2.5 w% atmospheric residue values around 39 w% were obtained (with no statistically significant differences) while at 5 and 10 w% atmospheric residue the yield was around 36 to 37 w%. Accordingly, the gasoline yield increased from 43-44 w% to 45 – 46 w% for pure VGO A to 5 and 10 w% admixtures of atmospheric residue. The total fuel yield stayed stable around 83 w% and only dropped for the highest admixture rate to around 81 w%.

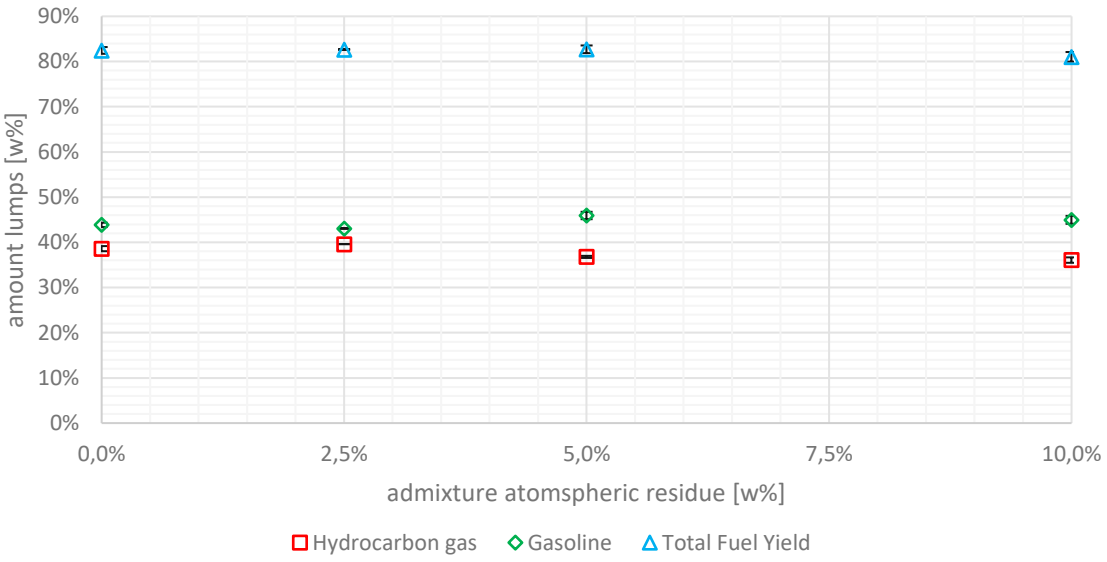

figure 46: hydrocarbon gas, gasoline and TFY distribution depending on admixture of atmospheric residue

Regarding the residue and coke lumps no clear trends can be observed since all measurements scatter inside the standard deviation. The coke and residue lump vary between 6.4 and 7.1 w% and 3.0 and 3.4 w%, respectively. However, an increase in LCO is observed in figure 47 with rising atmospheric residue content in the feedstock. The highest yield was hereby obtained with 8.2 w% at an admixture rate of 10 w% atmospheric residue. For the admixture of 2.5 w% no standard deviation could be calculated since part of the measurements were flawed.

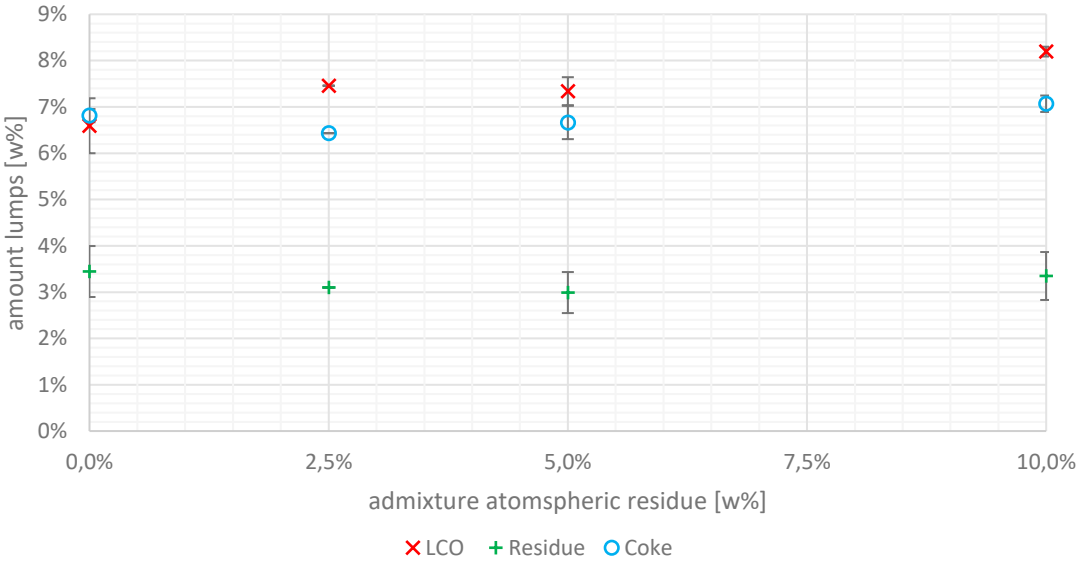

figure 47: LCO, residue and coke distribution depending on admixture of atmospheric residue

The olefinic high-value products are illustrated in figure 48 together with the alkanes. The ethylene yield slightly fell from 2.9 to 2.6 w% (just outside the error margin) for higher admixture rates of atmospheric residue to pure VGO A. Yields of propylene, however, indicated no clear trend with scattering numbers around 13.4 to 14 w%. Butenes and alkanes were again in accordance with the trend of ethylene and showed falling tendencies even though just in comparably small quantities.

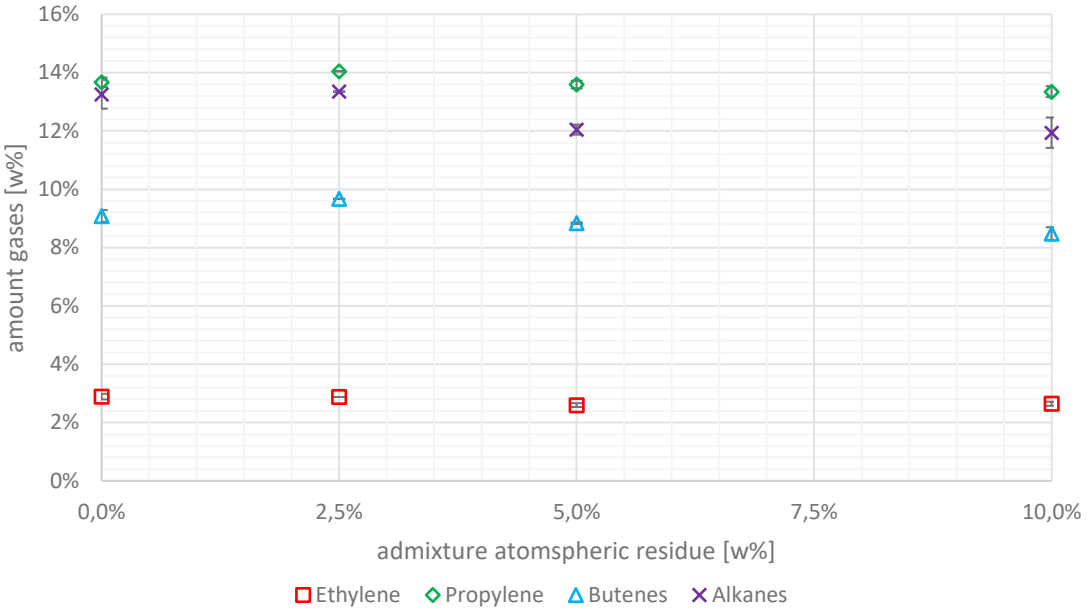

figure 48: olefins and alkanes distribution depending on admixture of atmospheric residue

To determine the influence of atmospheric residue content in feed on gas quality the gas-based numbers of the olefinic gases have been calculated and illustrated in figure 49. There, the olefinic gases do not show any significant variation depending on the feedstock. Ethylene, propylene and butenes fluctuate around 7-7.4 w%, 35.1 to 36.7w% and 23.4 to 24.2 w%, respectively. The alkanes show a declining trend for higher admixture rates of atmospheric residue compared to pure VGO A.

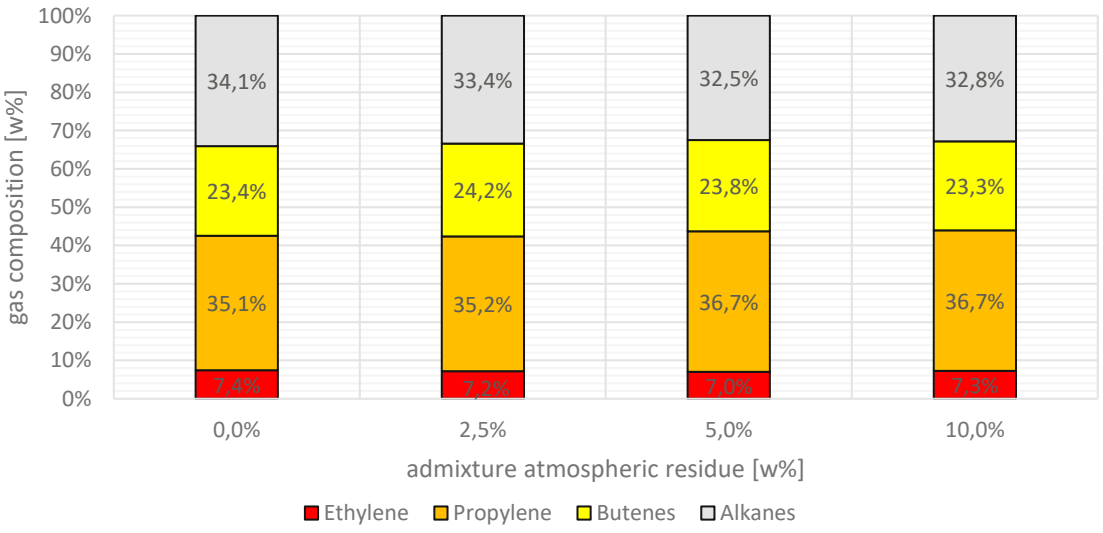

figure 49: gas composition in respect to olefins and alkanes depending on admixture of atmospheric residue

A detailed illustration of the butenes (1-Butene, isobutene, trans-2-butene, cis-2-butene) is found in figure 50. The highest values of butenes were obtained at an admixture rate of 2.5 w% but again due to faulty data no error margins could be calculated so it is assumed that these changes were not significant in comparison with pure VGO A. The yields of 1-butene showed an unclear trend with varying values around 1.7 to 1.52 w%. The yields of isobutene, trans-2-butene and cis-2-butene indicate a falling tendency at higher atmospheric residue contents, however, still not outside standard deviation ranges.

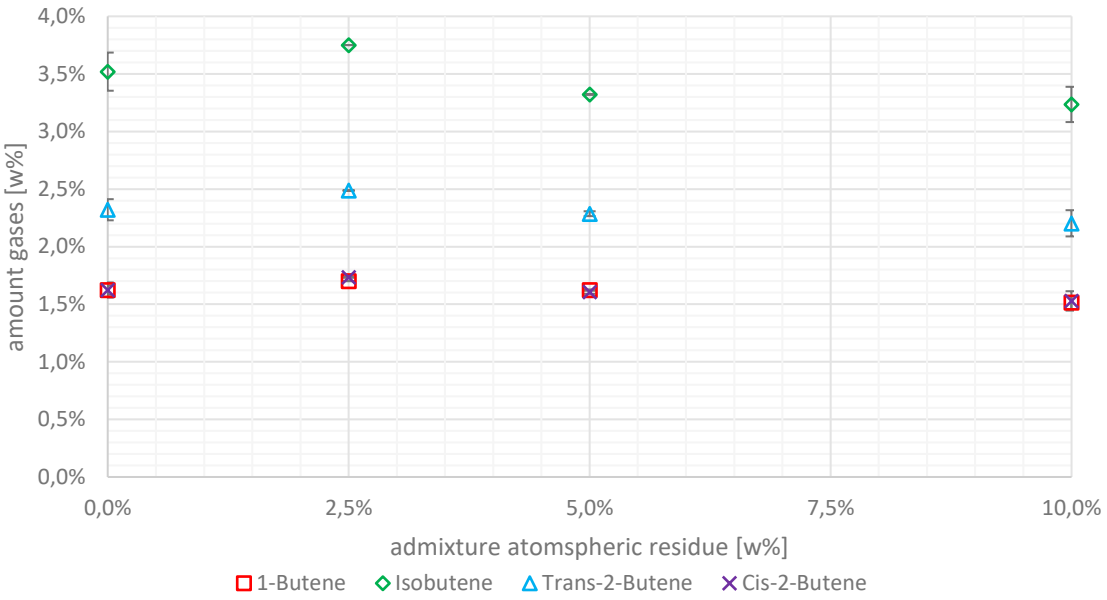

figure 50: butenes distribution depending on admixture of atmospheric residue

The alkane yields (methane, ethane, propane, isobutane and n-butane) are illustrated in figure 51. An influence of feedstock for methane and ethane was not observable with yields around 1 w% and 0.6 w%, respectively. For propane the results show higher values of around 2.8 to 2.7 w% for pure VGO A and low admixtures of atmospheric residue and higher values around 2.4 to 3.5 w% for higher admixtures. For isobutane and n-butane a small drop was observed which was just outside the error margins.

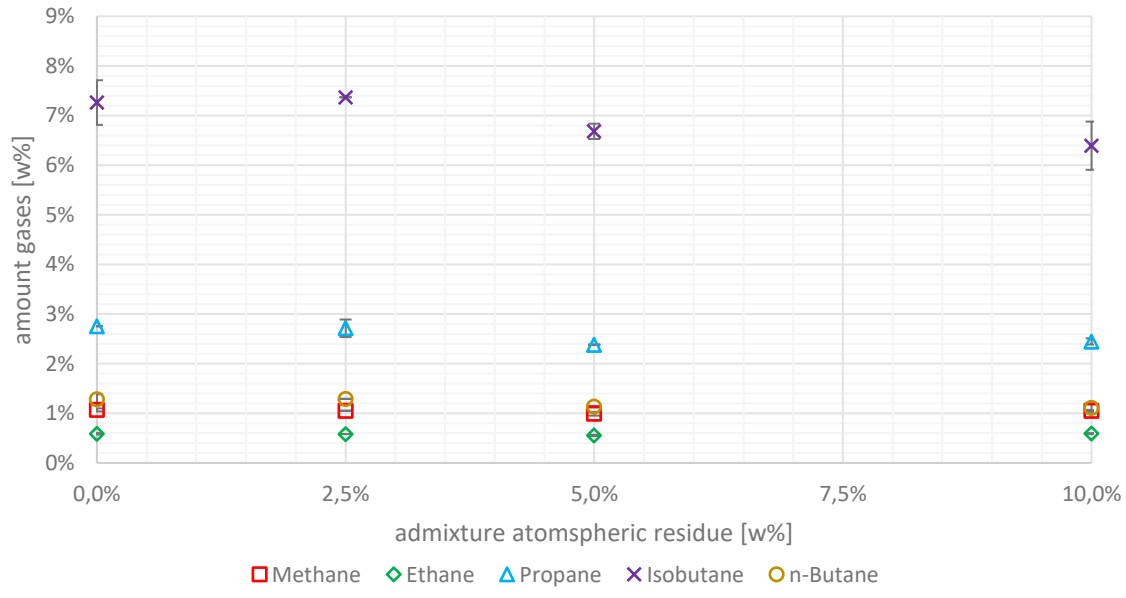

figure 51: alkanes distribution depending on admixture of atmospheric residue

The yields of carbonyl sulfide (COS) were determined and illustrated in figure 52 to research if the higher sulfur content in the atmospheric residue (compared to VGO A) has any significant influence on its generation in fluid catalytic cracking. The values were in comparably low ranges of 179 to 278 ppb which necessitated high-sensitivity measurements conducted via quantum cascade lasers. The measurements showed that admixtures of up to 5 w% atmospheric residue did not have any statistically relevant influence on COS generation (179 to 187 ppb). At 10 w% admixture rate a value of 278 ppb was obtained which was significantly different to lower admixture rates. No illustration of carbon oxide levels was found necessary due to their inconsistent behavior and fluctuation around 0.1 w% (CO) and 0.2 w% (CO_2) which was expected since both feedstocks do not contain any substantial amount of oxygen.

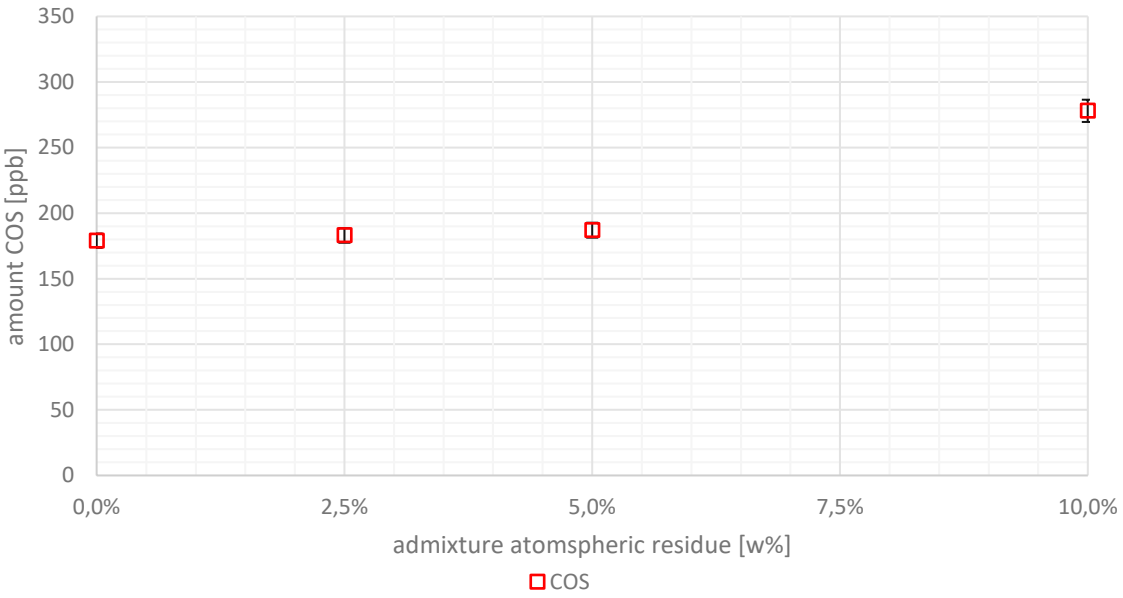

figure 52: COS amount depending on admixture of atmospheric residue

4.3.3 Discussion

The co-feeding of up to 10 w% of unhydrogenated atmospheric residue to hydrogenated vacuum gas oil was possible without any significant operational changes. The slight decrease of hydrocarbon gases of around 3 percentage points when comparing pure VGO A and the 10 w% residue admixtures can be attributed to the composition of atmospheric residue which contains more components with higher boiling temperatures up to 700 °C. In comparison VGO A has a final boiling point of around 550 °C. Balancing the loss in gases the gasoline and LCO lumps increase which also originates in the heavier nature of residue compared to VGO. Naturally, the decline in overall hydrocarbon gases lead to a drop in olefinic gas yields as well. However, in regard to adding value the admixing rate of up to 10 w% atmospheric residue did not show alarming drops in quality. The gas composition even shifted slightly towards olefins and less alkanes. The change in butene and alkane yields were overall neglectable even though a decreasing trend was observed. To obtain statistically relevant results regarding the influence of atmospheric residue content on butenes and alkanes generation experiments at higher admixture rates are recommended. The carbonyl sulfide yields did not show a significant change up to 5 w% admixture of atmospheric residue (from 179 to 187 ppb) due to overlapping standard deviations. As a result co-feeding of up to 5 w% of atmospheric residue should pose no problems downstream in the gas cleaning system and the propylene's further use in polymer production. Therefore, the plan of the refinery operator to shift its product portfolio is supported by the experiments. For higher admixtures operational changes are probably necessary. Either via more sophisticated gas cleaning systems after FCC unit or by hydrogenating the atmospheric residue. As a suggestion, the residue could already be co-fed into the hydrodesulfurization unit at the desired admixture rate and then directly be fed into the FCC unit.

4.4 Utilization of heavy residues: deasphalted oil

4.4.1 Background

A Central European refinery operator employs two different FCC units which are set to maximize liquid fuel production. These units are fed with comparably heavy vacuum gas oil (VGO B) and therefore use heavy residue catalysts which are less prone to catalyst poisoning and boost gasoline generation. In the near future it is believed that large quantities of heavy feedstocks with lower quality become available and the average quality of crude oil deteriorates as these heavier feedstocks are sent to refineries [164]. Reasons for this are amongst others the shift away from burning fuel oil for power generation and the elimination of using high sulfur bunker fuel [13].

To tackle these challenges and to diversify its feedstocks the refinery plans as a first step to feed deasphalted oil into their FCC unit which was provided by a Southern European oil and gas company. Deashpalted oil is a heavy feedstock generated in solvent deasphalting and is a fraction of the vacuum residue. Tests in the pilot plant at TU Wien were to be conducted to evaluate the plants different behavior when feeding heavy vacuum gas oil and deasphalted oil and to diminish any operational risks which for example any residual asphaltenes in the DAO could elicit.

The settings for the deasphalted oil campaign are listed in table 23. The riser temperature as well as the feedstock composition were instructed by the industrial partner. As catalyst the heavy residue catalyst for enhanced gasoline production was chosen. The feedrates were chosen at the lower spectrum of what can be fed into the pilot plant due to the feedstocks heavy residual nature. Accordingly, a higher amount of fluidization into the riser was chosen to promote feed atomization and ease evaporation. This approach is supported by literature where for industrial application a steam rate for atomization of at least 5 w% of the feed rate is recommended [159]. Furthermore, the preheating temperature was increased so that a higher feeding temperature ($T_{feeding}$) was chosen with the restriction that no or only minor thermal cracking was to occur in the tubular oven.

table 23: experimental settings for deasphalted oil campaign

feedstock	feedrate [kg/h]	T_{riser} [°C]	$T_{feeding}$ [°C]	riser fluidization [Nl/min]
100% VGO B	1.47	532	367	5
50% VGO B + 50% DAO	1.45	532	365	5
100% DAO	1.51	531	367	5

4.4.2 Results

The hydrocarbon gas and gasoline lumps as well as the TFY depending on the amount of DAO are depicted in figure 53. The hydrocarbon gas lump declines from 36.8 to 32.7 w% when VGO B is fed compared to DAO. Furthermore, a decline in gasoline is observed from 42.1 to 34.6 w%. As a consequence, the TFY also sinks from 78.9 to 67.3 w% marking a drop in the number of valuable products generated. The values for the 50/50-mixture of VGO B and DAO correspond well since they are positioned in between the values of pure VGO B and pure DAO so a linear trend can be assumed. All changes are significant and outside standard deviation.

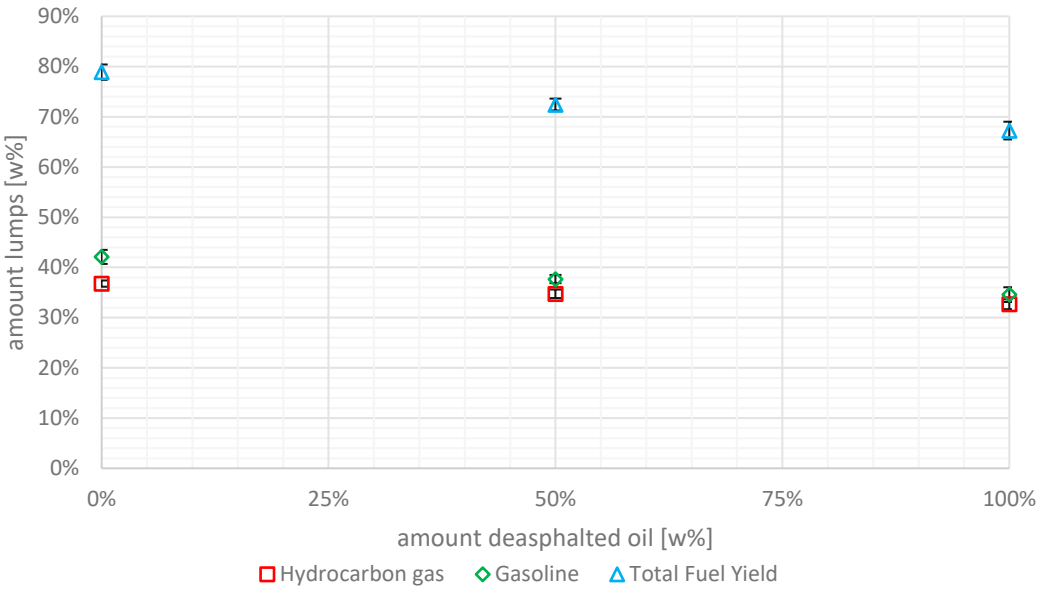

figure 53: hydrocarbon gas, gasoline and TFY distribution depending on amount of DAO

Counter-balancing the falling trends in figure 53 the values of LCO and residue show an increasing trend in figure 54. Light cycle oil and residue rise from 6.2 to 12.6 w% and from 2.6 to 7.3 w%, respectively. Again, the values for the 50/50 mixture are positioned in between the values for pure VGO B and pure DAO. The coke yield follows no clear trend with values varying from 11.8 w% for pure VGO B and at 12 w% for the 50/50 mixture.

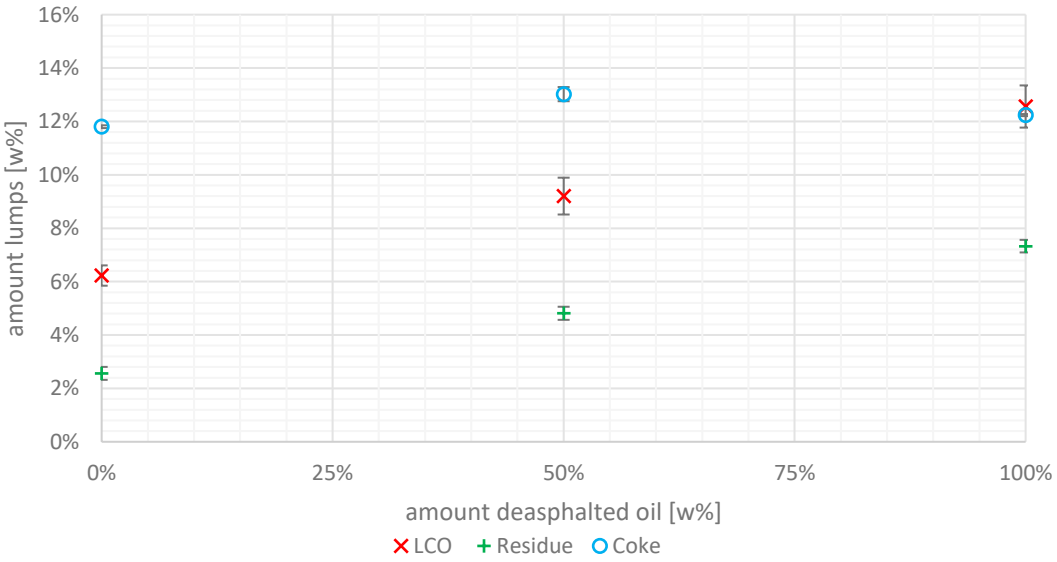

figure 54: LCO, residue and coke distribution depending on amount of DAO

The olefinic gases (ethylene, propylene, butenes) and the sum of alkanes are illustrated in figure 55. Ethylene increases from 1.5 to 1.8 w% when comparing pure VGO B and DAO. On the contrary propylene is reduced from 11.2 to 10.0 w%. These changes are miniscule but just outside of the error margins, therefore, still significant. The values of the 50/50 mixture are in between those for the pure substances leading to the conclusion that a falling and rising linear trend can be assumed for ethylene and propylene, respectively. For the butenes only insignificant alterations were observed with values between 11.1 and 11.7 w%. The group of alkanes, however, follow a significant reduction from 12.9 to 10.3 w%.

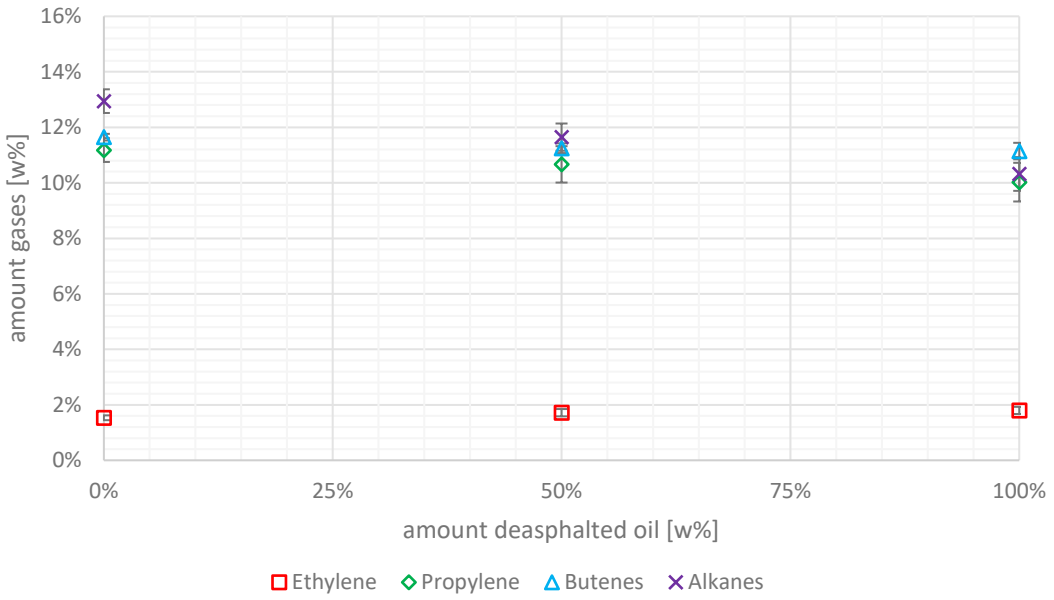

figure 55: olefins and alkanes distribution depending on amount of DAO

To determine the gas composition and quality the numbers of olefinic gases and alkanes are set in comparison to the overall hydrocarbon gas lump (gas-based numbers) in figure 56. These gas-based numbers show a relative increase in the hydrocarbon gas lump of olefinic gases. Ethylene hereby increases from 4.1 to 5.4 w% and butenes increase from 31.2 to 33.5 w%. Propylene does not show any significant change staying around 30 w%. Alkanes, on the other hand, decrease when DAO is compared to VGO B from 34.7 to 31 w%.

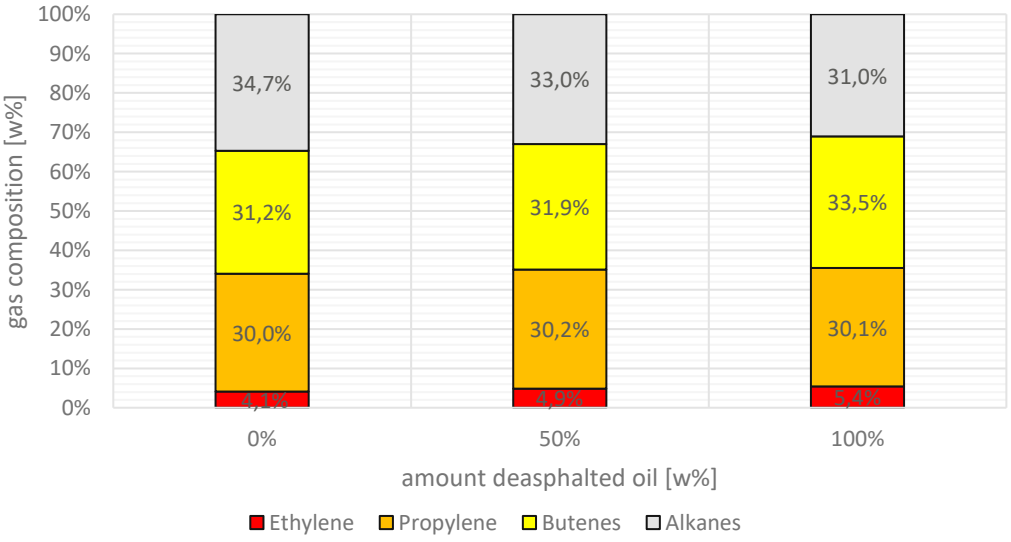

figure 56: gas composition in respect to olefins and alkanes depending on amount of DAO

For detail analysis the butenes (1-butene, isobutene, trans-2-butene and cis-2-butene) are disaggregated in figure 57. 1-butene drops in a linear trend from 2.3 to 2.2 w% comparing pure VGO B to DAO (just outside the error margin). The same falling trend is observed for cis-2-butene (2.3 to 2.2 w%), but with no statistical significance. Isobutene and trans-2-butene also show no statistically relevant changes with values around 3.8 w% and between 3.2 and 3.0 w%, respectively.

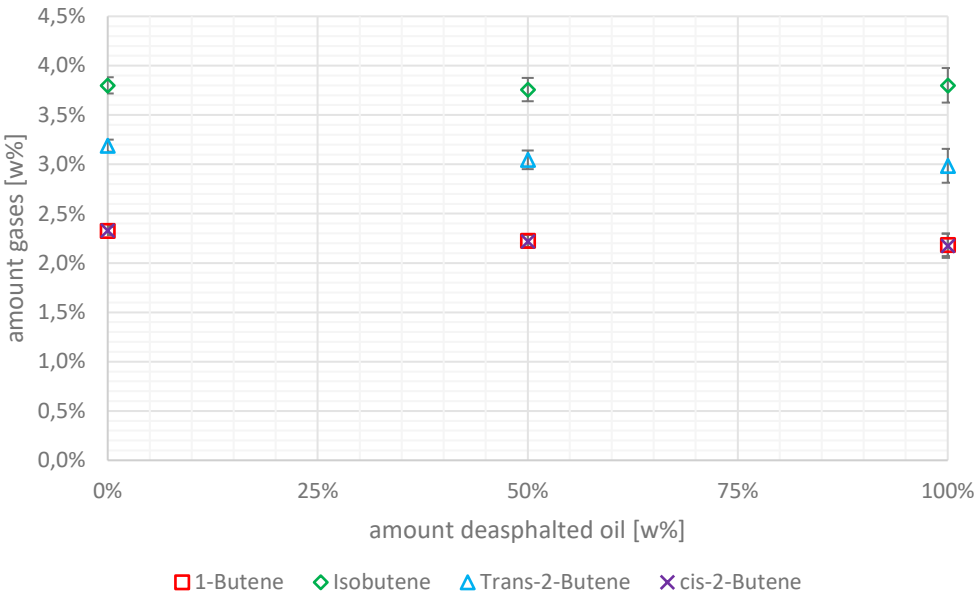

figure 57: butenes distribution depending on amount of DAO

Similar to butenes the alkanes (methane, ethane, propane, isobutane and n-butane) are disaggregated in figure 58. Here, counter-intuitive trends are illustrated considering the heavier nature of DAO compared to VGO B namely a rise in methane and ethane from 1.7 to 2.3 w% and from 0.7 to 1.1 w%, respectively.. For the other alkanes significant falling trends occur with the biggest drop for isobutane from 6.9 to 4.2 w%. A depiction of carbon oxides was left out for this experimental campaign since no changes in their generation was observed and due to their low values of around 0.2 and 0.3 w% for CO and CO_2, respectively.

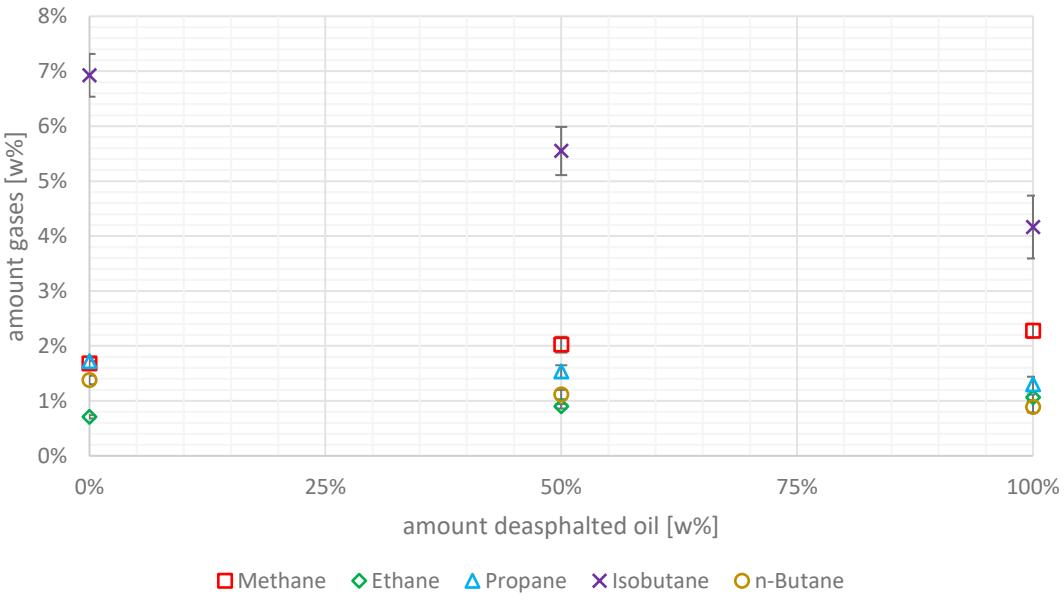

figure 58: alkanes distribution depending on amount of DAO

4.4.3 Discussion

Feeding DAO into the pilot plant led to significant declines in hydrocarbon gas and gasoline production when comparing to heavy VGO (VGO B). These shifts are most probably explainable by the DAO's composition. The used deasphalted oil batch is around 70 w% comprised of compounds with a boiling temperature greater than 500 °C. VGO B, on the other, is only comprised of such compounds to an extent of 50 w%. Counterbalancing the loss in valuable products, the generation of light cycle oil and residual oil is enhanced when feeding DAO. This probably originates from the rests of asphaltenes and aromatics in the DAO which are not crackable in the FCC process (note a comparably low aromatics content of only around 16-17 w% in the VGO B batch). However, due to a lack of data this is only speculation. All coke yields are relatively high which is caused by the high number of compounds in the feedstocks with high boiling temperature. Additionally, rests of asphaltenes (1.14 w%) in the DAO also promote coke formation. Furthermore, the CCR numbers for DAO (4.64 w%) and VGO B (5,39 w%) indicate a tendency of coke promotion. The shrinking of most gaseous compounds could also be attributed to higher amounts of aromatics in the DAO as well as lower amounts of alkanes and naphthenes but again this is only speculation. The rise in gaseous C_1 and C_2 fraction when DAO is fed contradicts the results for the other gaseous compounds. It is concluded that these changes could occur due to cracking of rests of solvents still found in the deasphalted oil from its production process (solvent deasphaltation). These solvents are low molecular alkanes and therefore convertible in the FCC process. Summarized, the feeding of DAO into an FCC unit at high fractions should be possible if said unit is already adapted to handle other heavy feedstocks. Comparing to heavy VGO B feeding DAO leads to significant losses in valuable product yields and therefore, a plummeting TFY from 78.9 to 67.3 w%. These losses would need to be handled somehow.

4.5 Utilization of pyrolysis oils: pyrolysis oil derived from waste plastic

4.5.1 Background

In 2020 around 367 million tons of plastic were produced with Europe having a share of around 55 million tons [165]. In the future even higher worldwide production volumes are expected with an increase to almost 600 million tons in 2050 (for thermoplastics) [166]. Naturally, this led and will lead to shear amounts of plastic waste and up to date the potential for recycling plastic waste still is mostly unexploited in the EU [167]. This is partly due to the past common procedure of exporting plastic waste from high-income countries to countries like China, which was abruptly stopped after the Chinese import ban on plastic waste in 2018 [168]. As a result, plastic waste is planned to be handled more domestically, especially after other countries in South-East Asia have started restricting imports as well [169]. However in 2020, the majority of post-consumer waste was still not recycled in the European Union but either incinerated or landfilled. To tackle this issue the EU has set up a strategy for plastics in a circular economy to reduce plastic waste and greenhouse gases [167].

One still rather uncharted pathway for plastic wastes recycling is chemical recycling with subsequent co-processing in refinery units such as FCC. Together with one Central European refinery operator and a start-up company which currently commercializes a waste plastic pyrolysis process a project was started to research this promising process chain. The vacuum gas oil (VGO B) and the catalyst (heavy residue catalyst) were supplied by the refinery operator through one of their FCC units. The pyrolysis company provided the batch of plastic based pyrolysis oil.

An experimental campaign was conducted in which first a base case was run as reference point. Then three different co-feeding rates up to 40 w% were tried out and compared to the reference point. Due to the high boiling range of VGO B a high amount of riser fluidization gas was used to boost feedstock atomization and enable a more constant plant operation. The riser temperature was chosen to be around 530 °C to boost gasoline production and was predetermined by the project partners. In table 24 the experiments and some of their parameters are summarized.

table 24: experimental settings for plastic waste-derived PO campaign

feedstock	feedrate [kg/h]	T_{riser} [°C]	$T_{feeding}$ [°C]	riser fluidization [Nl/min]
100% VGO B	1.47	532	367	5
90% VGO B + 10% plastic waste derived PO	1.44	530	370	5
80% VGO B + 20% plastic waste derived PO	1.52	531	369	5
60% VGO B + 40% plastic waste derived PO	1.51	531	365	5

4.5.2 Results

The valuable product lumps hydrocarbon gas, gasoline as well as the total fuel yield depending on the amount of co-fed waste plastic-derived pyrolysis oil are displayed in figure 59. Pure VGO B and the admixture of 10 w% of plastic-derived PO showed here significantly higher values for hydrocarbon gases with values around 36.3 – 36.8 w%. Higher admixtures, on the other hand, led to values around 30.6-31.1 w%. The gasoline fraction followed an exact contrary direction with increasing yields at higher admixtures. The values rose hereby from around 42 w% to more than 50 w%. These two parameters add up to the total fuel yield which increased for higher admixtures of waste plastic PO. The error margins were, however, comparably high so that these changes cannot be considered significant.

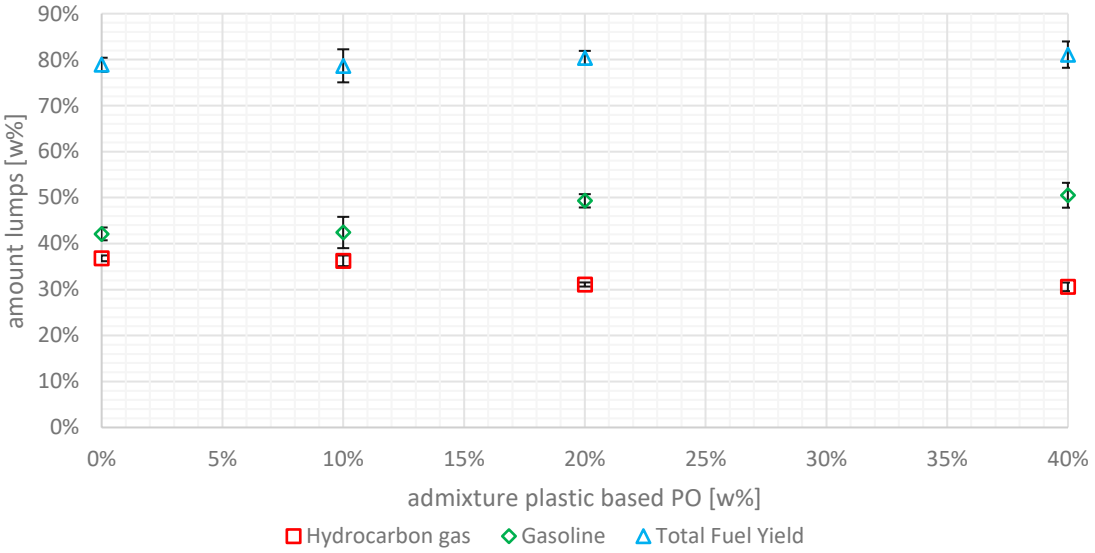

figure 59: hydrocarbon gas, gasoline and TFY distribution depending on admixture of plastic based PO

The heavier liquid fractions of LCO and residue do not follow a clear trend depending on the plastic PO admixture rate (see figure 60). The LCO values fluctuate around 6.2 to 7.4 w% with a high overlap of the error margins. A similar conclusion is drawn from the residue results which vary around 2.5 and 1.9 w%. Again no significant differences can be observed due to overlapping error margins. The coke yield, however, follows a strict falling trend and is also presented in figure 60. The highest coke yield was obtained at pure VGO B at 11.8 w% and the lowest at a 40 w% admixture rate of plastic PO at 9.6 w%. The other admixtures led to yields in between the two.

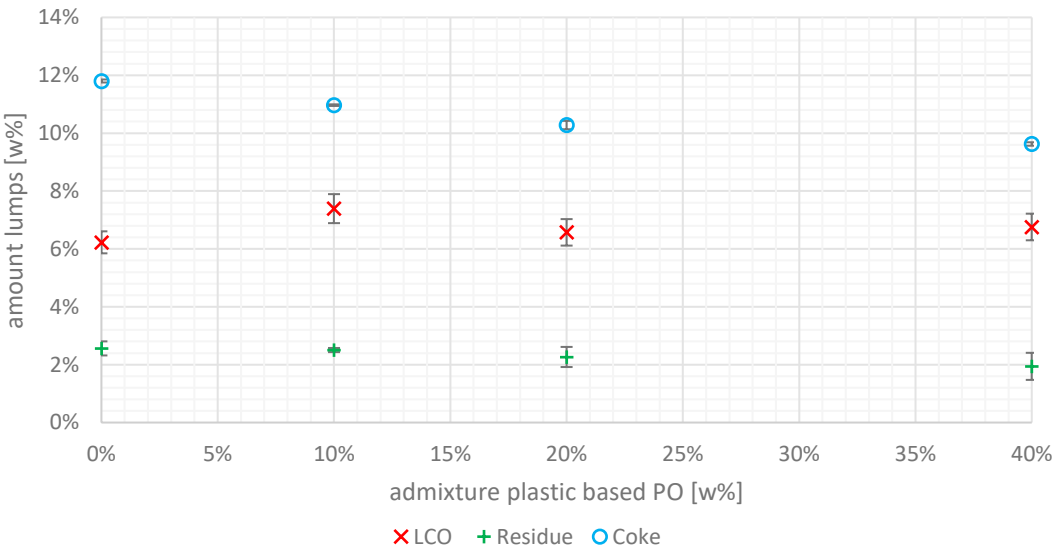

figure 60: LCO, residue and coke distribution depending on admixture of plastic based PO

The yields of olefinic gases and the alkanes are illustrated in figure 61. Ethylene showed a linear falling trend for plastic base PO admixtures. It decreased from 1.5 to 1.3 w% when comparing pure VGO B and higher admixture rates of plastic PO. Propylene, butenes and alkanes are represented in considerable higher amounts in the hydrocarbon product gas lump. Propylene declined from 11.2 to 10 w% following a strict falling trend. This also applies to the butenes which also sink from 11.7 to 10 w%. However, at 40 w% plastic PO admixture rate higher error margins were calculated which nullified any significant differences between 20 and 40 w% plastic PO admixture rate. Lastly, alkanes showed the biggest drop of 3.1 percentage points from 12.9 to 9.8 w%.

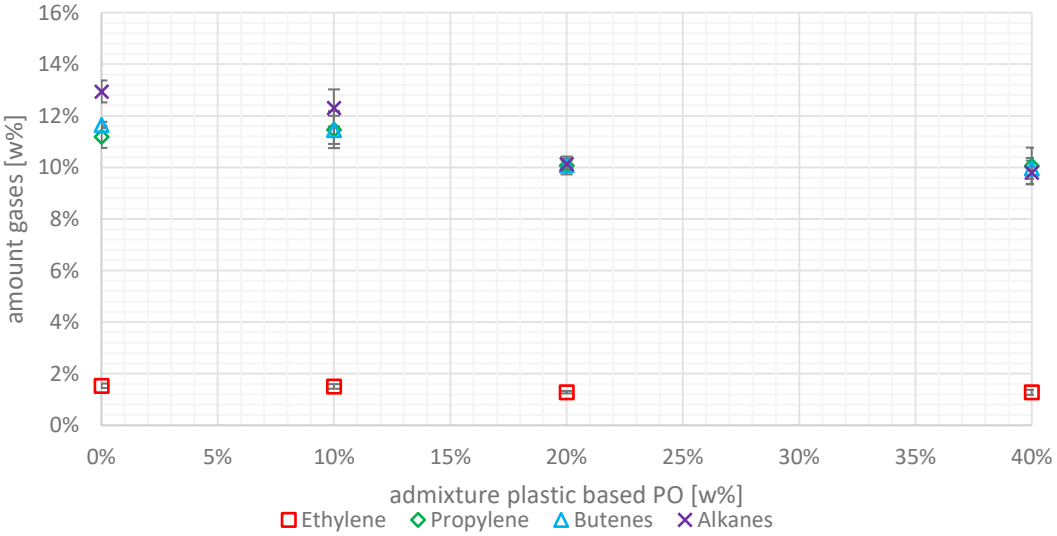

figure 61: olefins and alkanes distribution depending on admixture of plastic based PO

The high value gaseous components (olefins) were illustrated in figure 62 as gas-based numbers to give insight into a change in gas quality (rather than just quantity). The gas-based values do not show any change for the ethylene yield in the product gas. Propylene, however, strictly increases from 30.0 to 32.4 w% with the lowest amount being obtained for pure VGO B and the highest for an admixture rate of 40 w% of plastic PO. Also, the butenes slightly increase from 31.2 to 32.0 w% when comparing low and high admixture rates. Alkanes is the only fraction which decreases from 34.7 to 31.5 w%. The falling trend is hereby strictly linear.

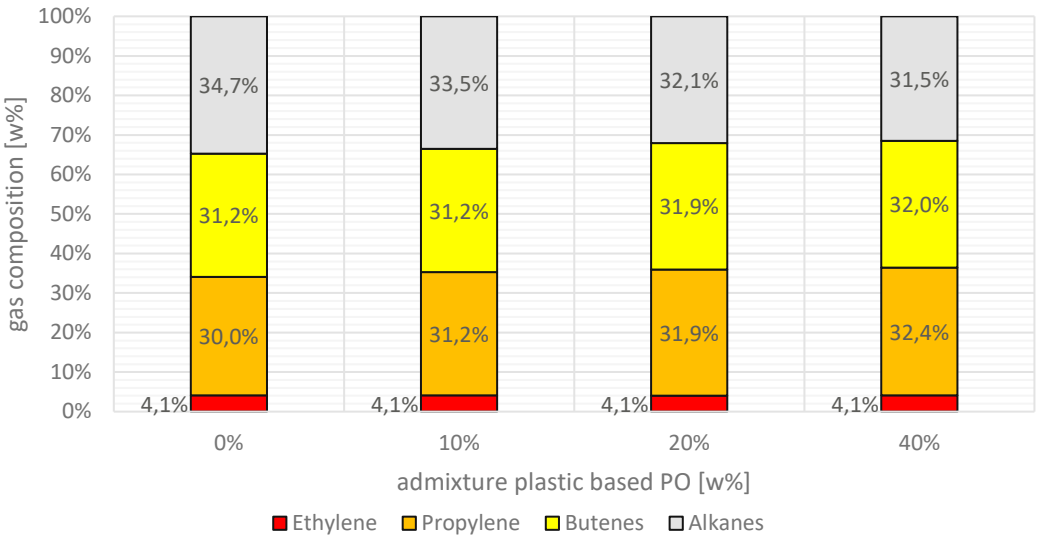

figure 62: gas composition in respect to olefins and alkanes depending on admixture of plastic based PO

The butenes are described in detail in figure 63 to give insight into their individual changes during the experimental campaign. 1-butene and cis-2-butene show the same trend depending on plastic PO admixture rate. Both decrease from 2.3 to 2 and 1.9 w%, respectively. The differences are hereby significant between lower or no and higher admixture rates. Trans-2 butene and isobutene show the same behavior as well. They both drop slightly around 0.5 w%. Again, the differences between high and no/low admixture rates are significant.

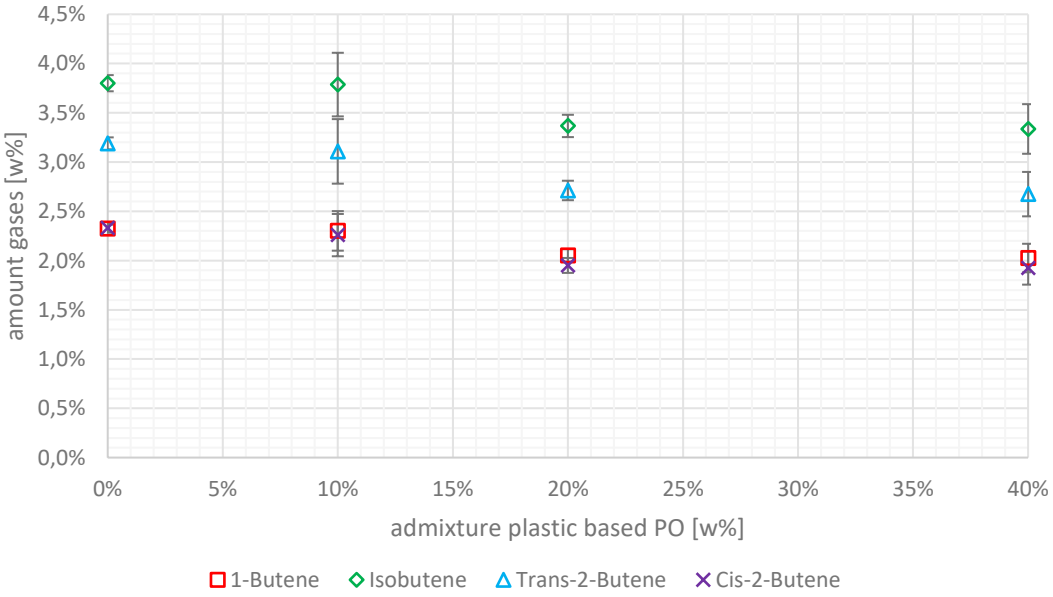

figure 63: butenes distribution depending on admixtures of plastic based PO

The disaggregated values for the alkanes are illustrated in figure 64. Methane and ethane both sink from an already low reference value of 1.7 and 0.7 w% for pure VGO B to 1.4 and 0.6 w% for the 40 w% admixture rate of plastic PO. Both trends are significant and outside error margins. The same trends are also observable for n-butane and propane at slightly higher levels. The biggest change was for isobutane with a significant drop of 1.7 percentage points.

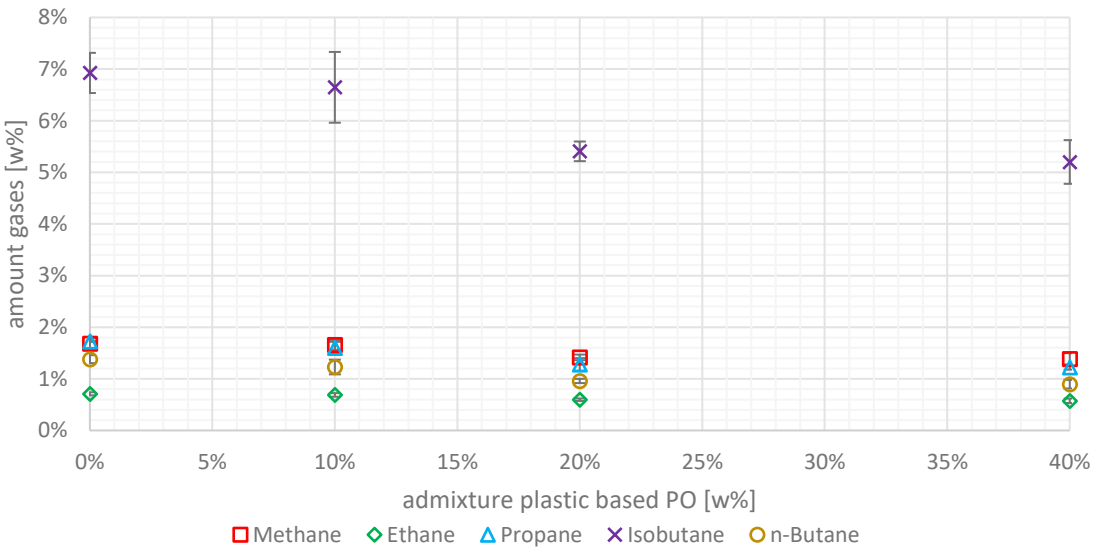

figure 64: alkanes distribution depending on admixtures of plastic based PO

The carbon oxide levels in the product gas do not show any clear trends depending on the admixture rate of waste plastic-derived PO (see figure 65). CO and CO_2 yields fluctuate around 0.2 and 0.3 w% independent of the admixture rate with relatively high error margins. The sum of the carbon oxides consequently varies around 0.5 w%.

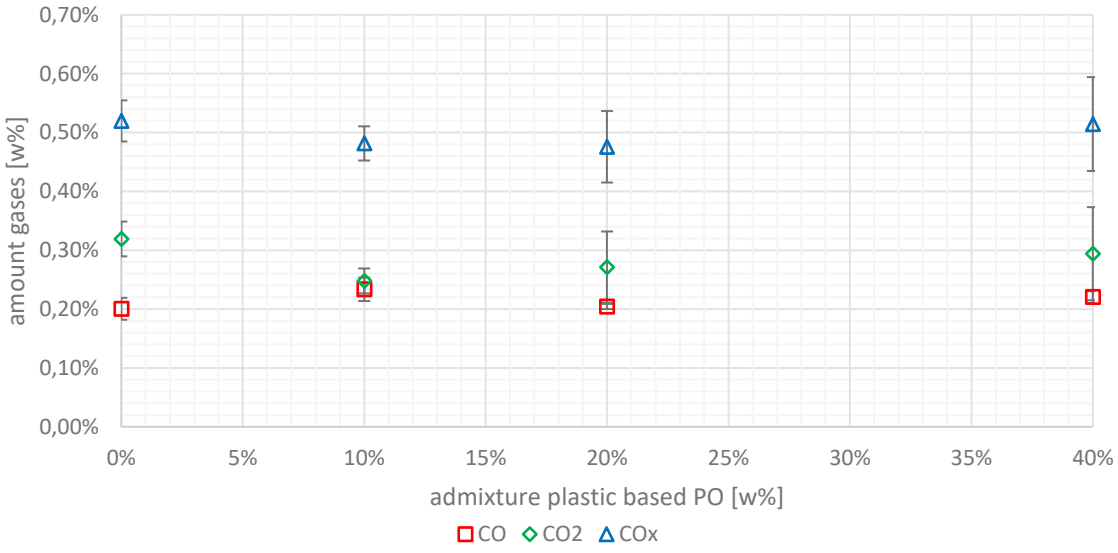

figure 65: carbon oxides distribution depending on admixtures of plastic based PO

4.5.3 Discussion

The product distributions for the co-processing of plastic derived pyrolysis oil and vacuum gas oil clearly indicate decreasing hydrocarbon gas and increasing gasoline yields and form strictly linear trends. This finding was at first surprising since the distillation curve of plastic crude shows that it contains significantly more constituents at lower boiling temperatures than VGO B does. These changes in products, however, probably originate probably from the higher aromatics content of plastic crude (34.9 w%) compared to VGO B (16.6 w%) whereas the aromatics enrich in the liquid fraction since they are not crackable under FCC conditions. Therefore, feeding plastic pyrolysis oil seems to be a better feedstock for sustainable fuel production rather than production of petrochemical base stocks. The increase in liquids, however, was not observed for residual oil and LCO which was indicated by the lower boiling curve of plastic crude compared to VGO.

Even though, the gas yields decreased a stable or slightly rising gas quality was observed. When analyzing the gas composition the amounts of ethylene stayed stable while propylene and butenes slightly increased for higher admixtures of plastic crude. This is probably due to the high percentages of polypropylene and polyethylene which made up 60 w% of the mixed plastic wastes which acted as a source for pyrolysis oil production. These long change paraffinic structures greatly react to olefins via the ionic reaction mechanisms of FCC. However, in absolute numbers the olefinic yields decrease notably.

The pyrolysis crude contains a miniscule amount of water which should have been found in the liquid product fraction which was not the case. It is believed that this is solely due the inability of the condensation apparatus to adequately capture such low amounts of water since water is inert in the FCC process. Nonetheless, due to the low amount of water no significant influence was expected anyway.

Furthermore, no increasing amounts of carbon oxides where measured for the plastic crude admixtures since the changes in yields all were within error margins. This result is interesting since the batch of plastic derived pyrolysis liquid contains around 4.5 w% oxygen probably originating from PET and/or contaminants like paper. It is speculated that the oxygen of the plastic crude might form oxygenates which could end up in the liquid fraction. Therefore, further analysis of the liquid products are recommended. The low percentages of carbon oxides which were detected stem from the regenerator since the syphon does not act as a perfect barrier from flue gas.

4.6 Utilization of pyrolysis oils: pyrolysis oil derived from clean wood waste (wood chips)

4.6.1 Background

The following experimental campaign was conducted in the “WASTE2ROAD – Biofuels from Waste to Road transport” project funded by the Eureopean Framework Programme for Research and Innovation Horizon 2020. In this project the goal is to develop second generation biofuels out of waste streams. To accomplish this the project partner aim to generate dedicated value chains from the collection of low-cost residual and waste streams to conversion processes up to engine tests of these novel biofuels. To ensure implementation and reduce costs usage of already existing refinery technology shall be achieved [170].

The value chain relevant in this work is the co-feeding of clean wood-derived pyrolysis oils supplied by BTG in an FCC pilot plant. The pyrolysis liquids were hydrogenated beforehand to ensure processability. SPO was hydrogenated once under milder conditions (max. 200 °C) whereas SDPO was hydrogenated twice, in a mild (max. 250 °C) and more severe (350 °C) processing step. Co-feeding was then conducted with VGO C using the LPG boosting catalyst mixture. The cracking temperatures (530 °C & 550 °C) were chosen to gain data for gasoline boosting (530 °C) and hydrocarbon gas boosting (550 °C) conditions. Parts of the SPO/SDPO co-feeding campaign were published by Büchele et al [171] at Open Research. A Summary of the experimental settings can be found in table 25.

table 25: settings for SPO & SDPO experimental campaign

feedstock	feedrate [kg/h]	T_{riser} [°C]	$T_{feeding}$ [°C]	riser fluidization [Nl/min]
100% VGO C	2.02	549	324	0.1
100% VGO C	2.01	531	324	0.1
95% VGO C + 5%SPO	2.01	550	310	0.1
95% VGO C + 5%SPO	1.92	530	319	0.1
90% VGO C + 10% SPO	1.96	550	313	0.1
90% VGO C + 10% SPO	1.87	529	315	0.1
95% VGO C + 5% SDPO	1.97	550	323	0.1
95% VGO C + 5% SDPO	2.04	532	323	0.1
90% VGO C + 10% SDPO	2.05	549	323	0.1
90% VGO C + 10% SDPO	2.02	530	323	0.1

4.6.2 Results

4.6.2.1 SPO – admixtures at 550 °C

The diagrams figure 66 - figure 72 display the change of product yields depending on the amount of SPO admixture at 550 °C riser temperature. In figure 66 the hydrocarbon gas and gasoline yields as well as the total fuel yield are depicted. The hydrocarbon gases increase when SPO is co-fed from 44.0 to 46.3 w%. This trend was observed to be strictly linear. To the contrary, the gasoline yield falls from 40.5 to 36.8 w% for the same admixtures. The changes from pure VGO C and 10 w% admixture of SPO are hereby outside the error margins. Even though the hydrocarbon gases increase, the total fuel yield still declined slightly from 84.5 to 83.1 w%. However, the standard deviations overlap, therefore, the decrease is not considered significant.

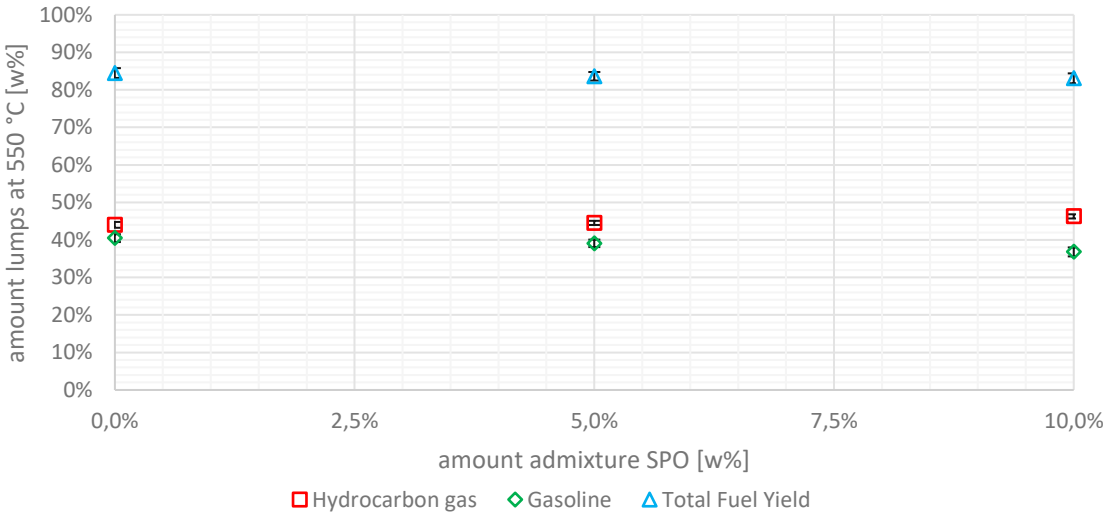

figure 66: hydrocarbon gas, gasoline and TFY distribution depending on admixture of wood based SPO at 550 °C

The trends of the non-valuable lumps (LCO, residue, coke and water) for a 550 °C riser temperature are illustrated in figure 67. The LCO and residue yields followed the trend for gasoline decreasing at higher admixture rates of SPO. These trends can be considered significant for LCO (7.3 to 6.3 w%) but not for the residue (3.1 to 2.6 w%). Coke increased linearly from 4.8 to 6.1 w%. The water yield, which is not generated with pure VGO C rises linearly to 1.1 w%.

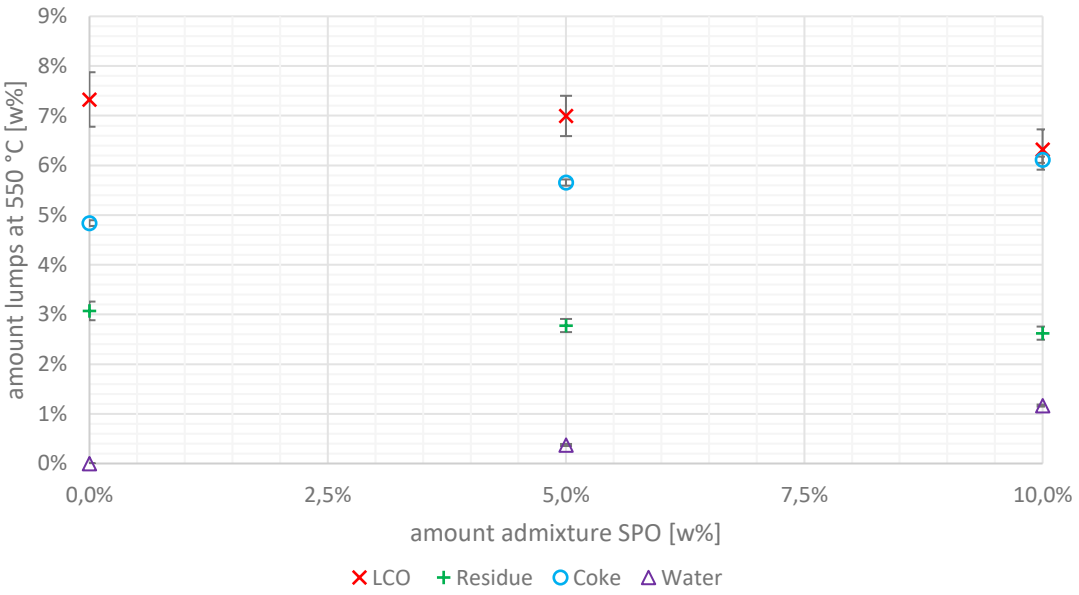

figure 67: LCO, residue and coke distribution depending on admixture of wood based SPO at 550 °C

The trends of olefinic gases and alkanes in figure 68 show different behaviors of the compounds. While ethylene and propylene increase at higher admixtures of SPO from 3.4 to 4.0 w% and from 14.2 to 16.5 w%, respectively, the alkanes change contrarily. They fall first from 17.4 to 16.1 w% and then rise again to 16.6 w%. However, the latter rise occurs inside error margins. The Butene follows again the olefinic trend of rising at higher admixture rate (from 9.4 to 9.9 w%).

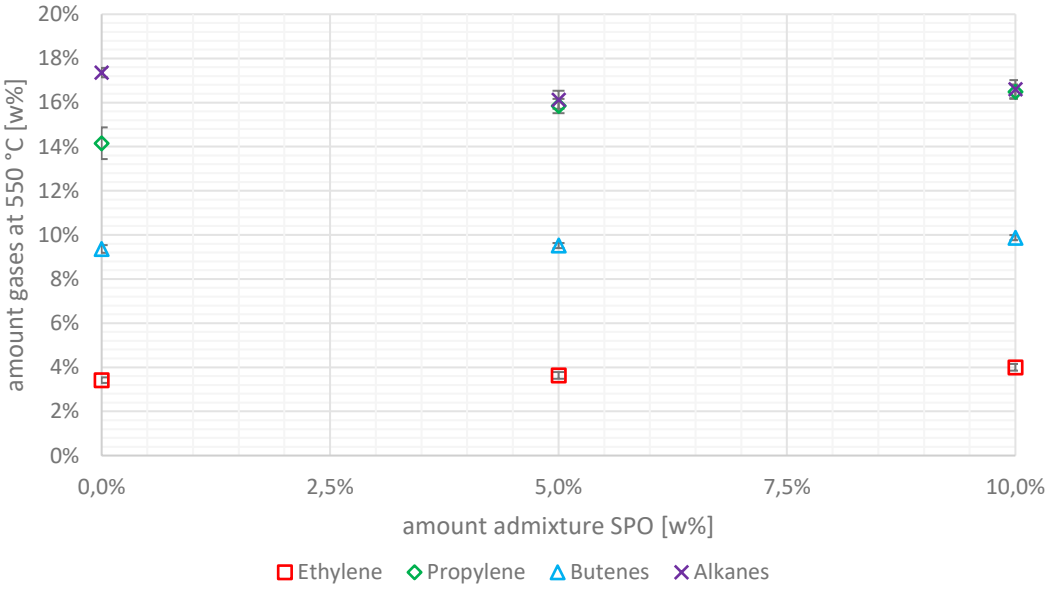

figure 68: olefins and alkanes distribution depending on admixture of wood based SPO at 550 °C

The gas yields of figure 68 are set in relation to the gas lump itself to determine the changes in gas composition (see figure 69). There, ethylene rises linearly from 7.7 to 8.5 w%. Also propylene rises when SPO is co-fed to 35.1 w% independent of the co-feeding rate. The butenes remain roughly the same around 21 w% while the alkanes decrease significantly from 39.2 to 35.7 – 35.4 w%. Overall, the changes in gas composition were greater between pure VGO C and admixtures of SPO than between the admixture.

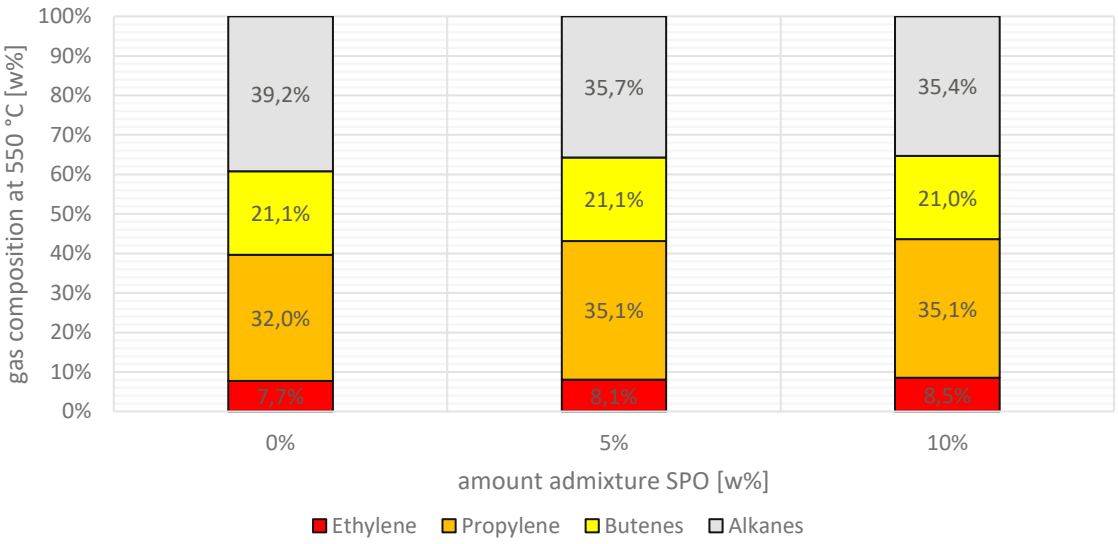

figure 69: gas composition in respect to olefins and alkanes depending on admixture of wood based SPO at 550 °C

A detailed analysis of the butenes is illustrated in figure 70. Cis-2-butene and 1-butene both show a minimal rising trend when SPO is cofed. However, the change for cis-2-butene is not significant so a stable value around 1.7 – 1.8 w% is assumed. Cis-2-butene rises from 1.7 to 1.9 w% for pure VGO C and an admixture of 10 w% SPO, respectively. Trans-2-butene's change is also not significant and inside error margins with values from 2.4 to 2.5 w%. Isobutene is the dominant compound in the product gas with numbers from 3.6 to 3.7 w%. Again, no statistical significance was determined.

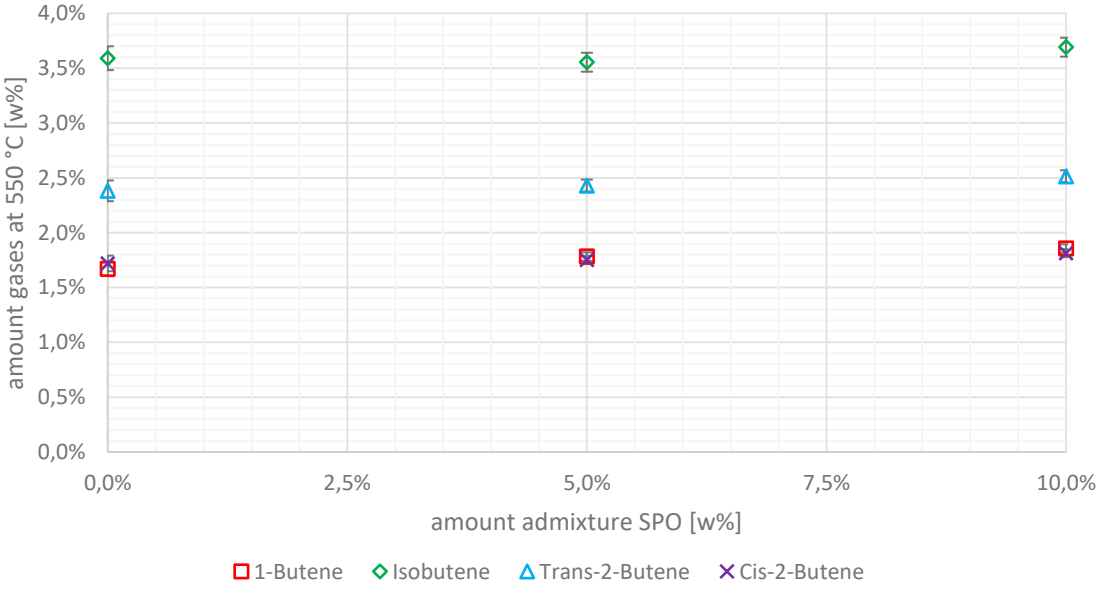

figure 70: butenes distribution depending on admixtures of wood based SPO at 550 °C

The alkanes are separately depicted in figure 71. Methane and ethane rise linearly when SPO is admixed with measurements from 1.1 to 1.3 w% and 0.7 to 0.8 w%, respectively. These values are just outside error margins. Propane has an indifferent behavior. First it sinks from 3.6 to 3.2 w% and then rises again to 3.3 w% with the latter change not being statistically relevant. N-butane sinks from 1.8 to 1.5 w% when comparing pure VGO C and the admixture of 5 w% SPO. For the 10 w% admixture it remains stable. The biggest change is observable for isobutane with a decrease from 9.9 to 9.0 w%. Again, the change between 5 and 10 w% admixture rate of SPO is inside error margins.

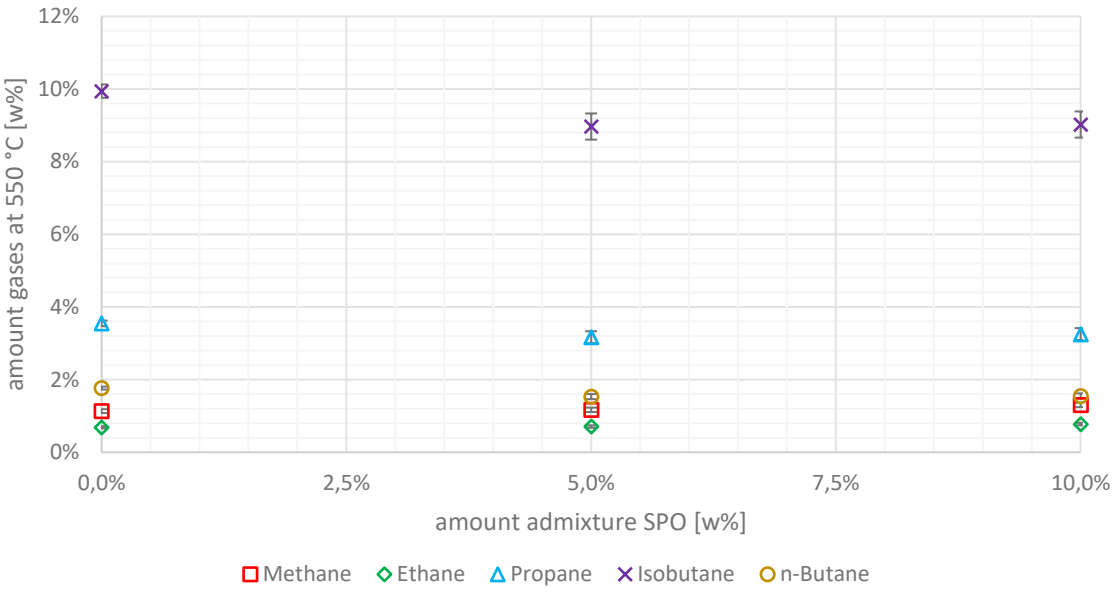

figure 71: alkanes distribution depending on admixtures of wood based SPO at 550 °C

The carbon oxide yields in the product gas depending on the SPO admixture are illustrated in figure 72. Carbon dioxide does not show any significant increase depending on the feedstock with a rather constant value between 0.2 – 0.3 w% and overlapping standard deviations. Carbon monoxide and the sum of both carbon oxides, however, both show a significant increase. CO rises from 0.1 to around 0.4 w% and CO_x from 0.3 to 0.7 w%.

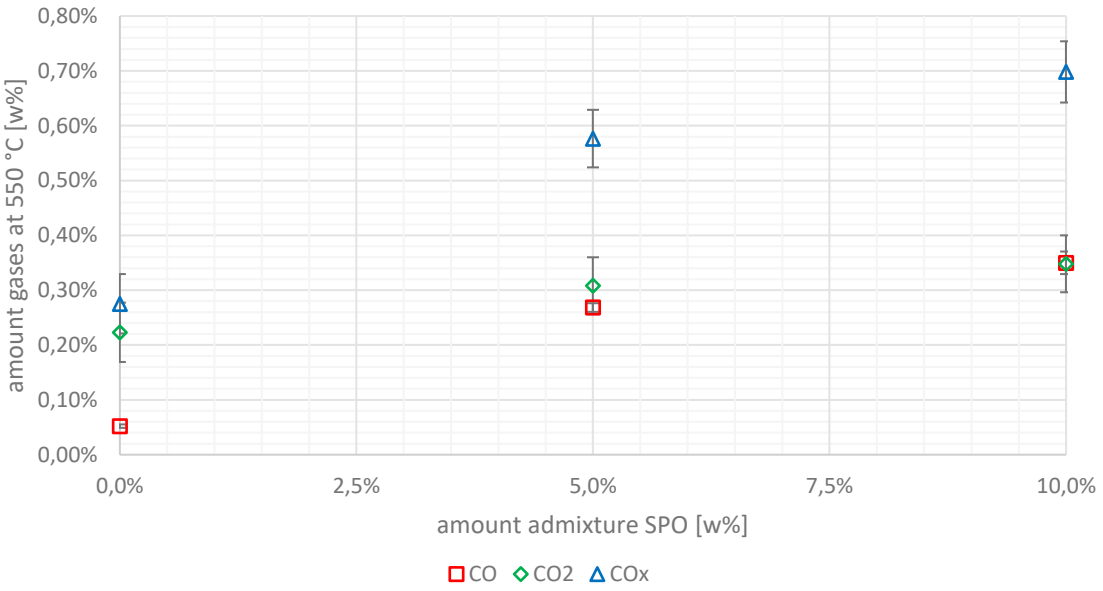

figure 72: carbon oxides distribution depending on admixtures of wood based SPO at 550 °C

4.6.2.2 SPO – admixtures at 530 °C

The same measurements and yields at 550 °C riser-temperature where also conducted and depicted for 530 °C riser temperature (figure 73 – figure 79). Again, the amount of SPO admixture is the variable. The hydrocarbon gases increase from 39 to 41.3 w% but due to the relatively high error margins these changes are not considered significant (see figure 73). The gasoline lump decreases from 44.7 to 39.9 w% comparing VGO C and 10 w% SPO admixture. The total fuel yield declines from 84.5 to 83.1 w%. These changes have, however, overlapping standard deviations.

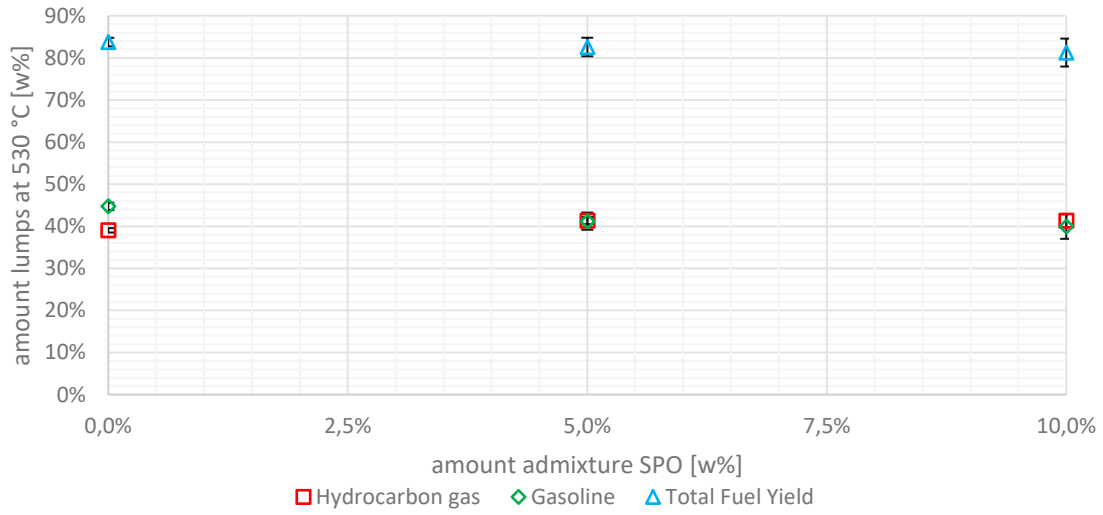

figure 73: hydrocarbon gas, gasoline and TFY distribution depending on admixture of wood based SPO at 530 °C

The changes of the heavier liquid products LCO and residue are shown in figure 74. The changes of LCO are not considered significant because of high error margins. A sinking trend, however, can be suspected. Residue does not show a coherent trend with varying numbers ranging from 2.8 to 3.2 w%. The coke yields strictly increases with rising SPO admixing rates from 4.7 w% for pure VGO C to 5.1 and consequently to 5.9 w%. Feeding pure VGO does not create any water. When admixing SPO this lump becomes, however, measurable with values ranging up to 1.8 w%.

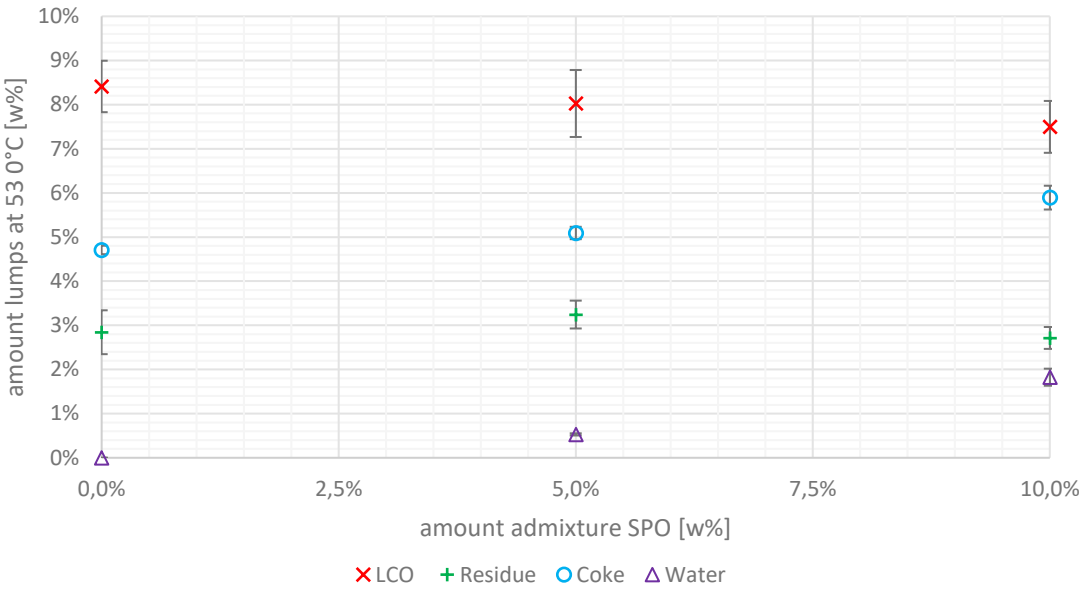

figure 74: LCO, residue and coke distribution depending on admixture of wood based SPO at 530 °C

The changes in olefinic gases and the group of alkanes are found in figure 75. The valuable gases ethylene and propylene show an increase when SPO is co-fed. Ethylene rises hereby from 2.8 to 3.3 w% and propylene grows from 12.2 to 14.5 w% but the increase from 5 to 10 w% SPO is not statistically significant. The butenes also increase while the alkanes show a slight drop from 16.3 to 15.8 w% remaining inside standard deviations.

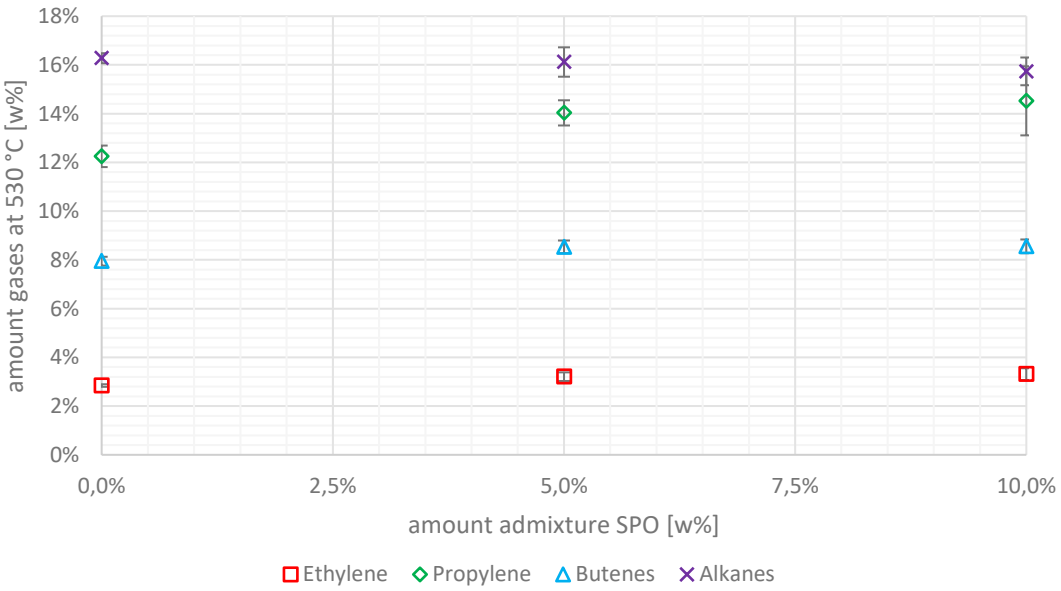

figure 75: olefins and alkanes distribution depending on admixture of wood based SPO at 530 °C

The gas-based numbers of said olefins and alkanes are examined in figure 76. Ethylene and propylene show a relative growth in the gaseous fraction (0.7 and 3.3 percentage points, respectively) while butenes remained stable just above 20 w%. The relative amount of alkanes significantly decreased from 41.4 to 37.3 w%.

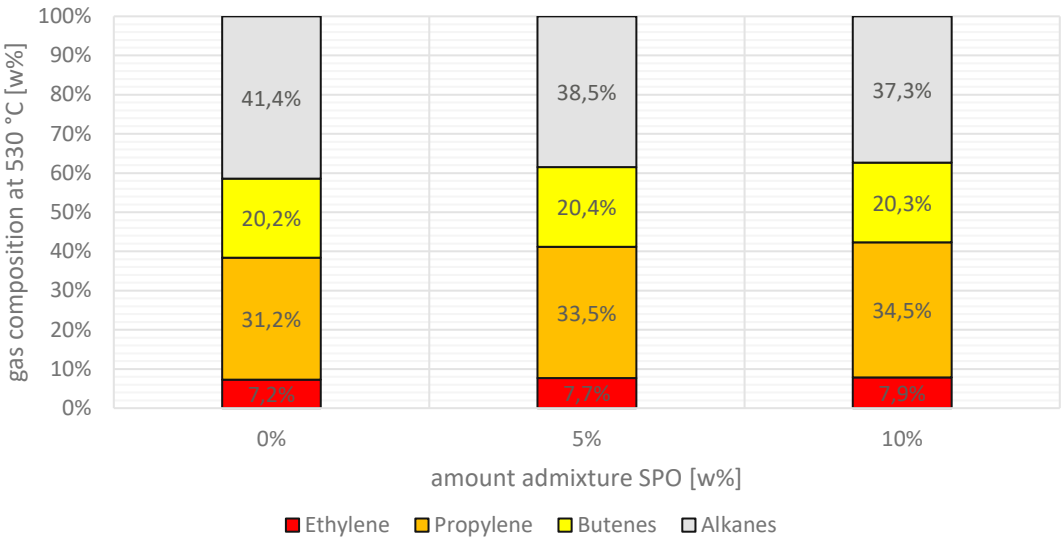

figure 76: gas composition in respect to olefins and alkanes depending on admixture of wood based SPO at 530 °C

The trends of the butenes are illustrated in figure 77. The lowest yields were hereby obtained for 1-butene and cis-2-butene. Cis-2-butene does not show any significant changes (1.7-1.8 w%) whereas 1-butene slightly increases from 1.7 to 1.9 w% for SPO admixtures. Both for trans-2-butene and isobutene no statistically relevant changes were observed with fluctuating values of around 2.0-2.2 w% and 3.1-3.3 w%, respectively.

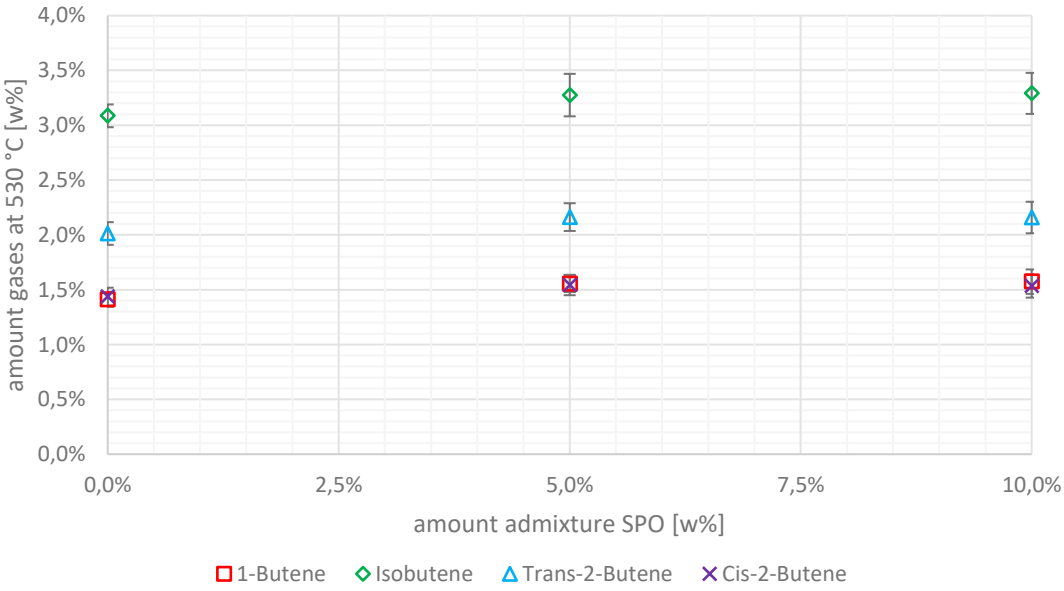

figure 77: butenes distribution depending on admixtures of wood based SPO at 530 °C

The alkane lump is disaggregated in figure 78 to show the different trends for each alkane. Methane and ethane show a slight increase from 0.9 to 1.1 w%and from 0.6 to 0.8 w% with rising SPO content in feed. Contrary to that, n-butane and isobutane decrease at higher SPO admixtures from 1.6 to 1.4 w% and from 9.8 to 8.8 w%, respectively. Both changes are just outside error margins. Propane is not influenced by SPO content in feed in a statistically relevant way.

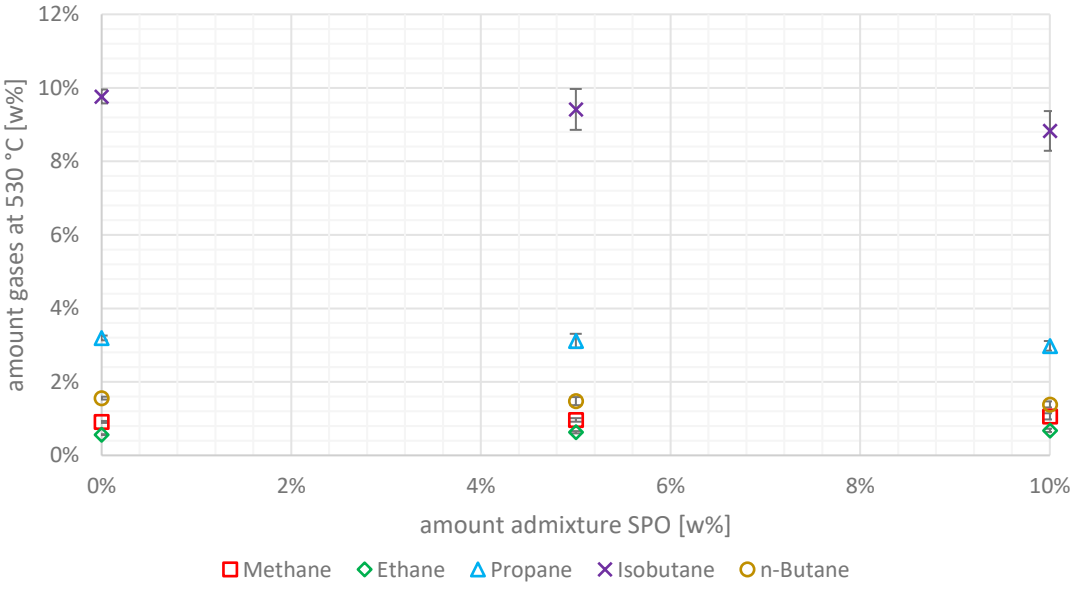

figure 78: alkanes distribution depending on admixtures of wood based SPO at 530 °C

Just like at 550 °C the experiments at 530 °C led to an increase in carbon oxide formation for higher SPO admixture rates (see figure 79). The rise in CO levels were hereby more significant than for CO_2 with an increase of 0.3 percentage points to 0.4 w%. The CO_x levels rose linearly from 0.3 to 0.8 w%.

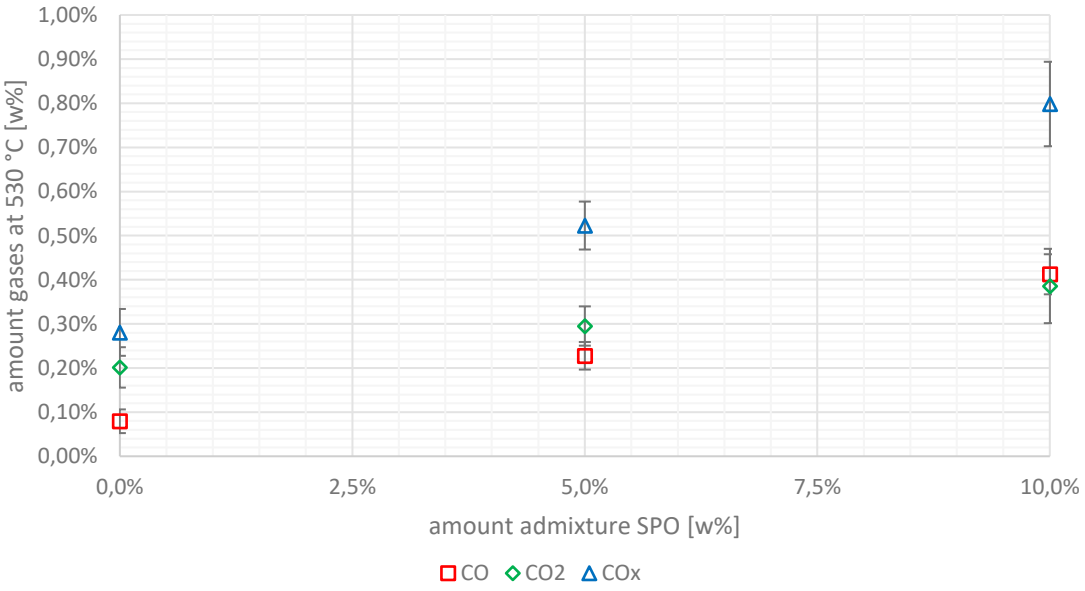

figure 79: carbon oxides distribution depending on admixtures of wood based SPO at 530 °C

4.6.2.3 SDPO – admixtures at 550 °C

The experimental campaign of pure VGO C and varying SDPO admixture rates at 550 °C riser temperature are portrayed in figure 80-figure 86. In figure 80 the hydrocarbon gas lump, the gasoline lump and the total fuel yield are illustrated depending on feed composition. The hydrocarbon gases decrease from 44.0 to 40.4 w% when comparing pure VGO C and 10 w% admixture rate of SDPO and the gasoline yield rises from 40.5 to 42.8 w%. Both trends are statistically significant. The total fuel yield shows a slight declining trend from 84.5 to just above 83 w%. However, due to overlapping standard deviations these are not significant.

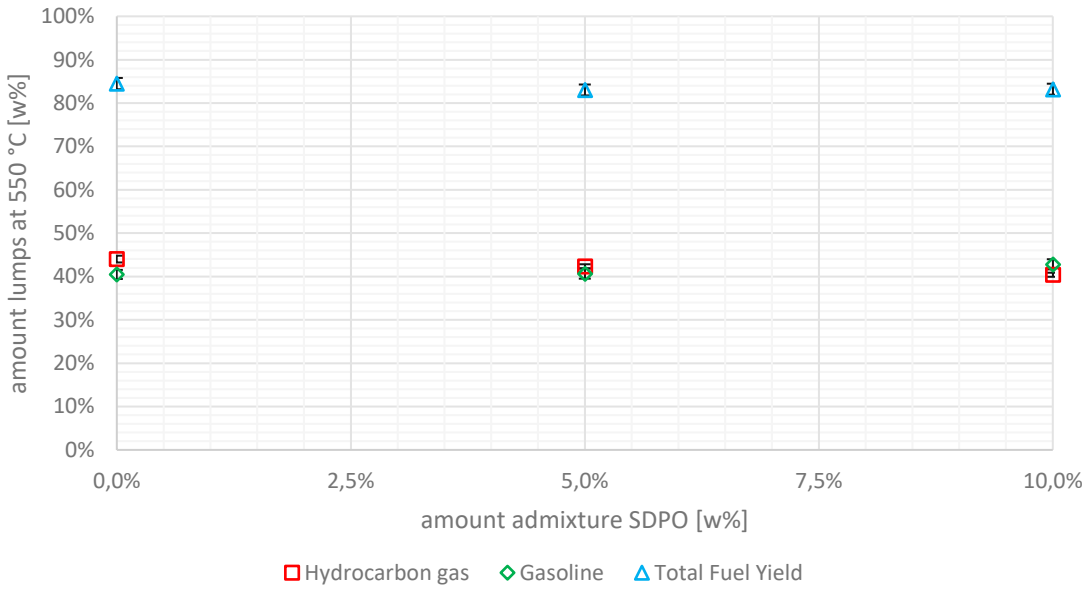

figure 80: hydrocarbon gas, gasoline and TFY distribution depending on admixture of wood based SDPO at 550 °C

The non-valuable products LCO, residue and coke show indifferent trends. LCO increases (7.3 to 8.4 w%) when SDPO is co-fed but with overlapping standard deviations (see figure 81). Residue declines from 3.1 to 2.7 w% but again the changes are inside the error margins. The coke yields starts at 4.8 w% and increases to 5.6 w% for the results of 5 w% of SDPO in feed where it remains for higher admixtures.

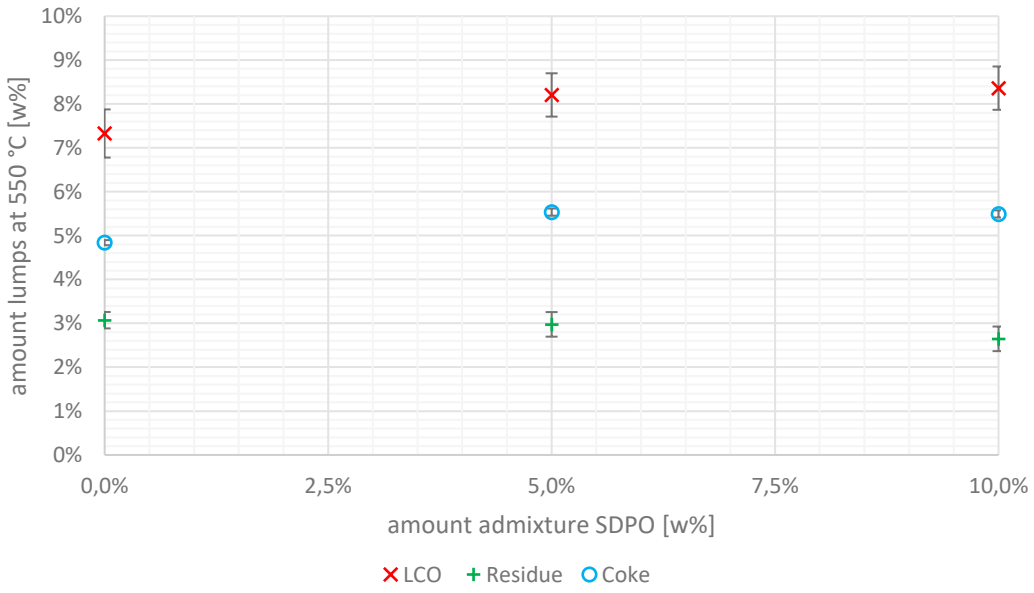

figure 81: LCO, residue and coke distribution depending on admixture of wood based SDPO at 550 °C

The trends of the olefinic gases and the sum of alkanes are found in figure 82. Ethylene slightly falls from 3.4 to 3.1 w% and propylene increases from 14.2 to 14.3 w% with the latter not being statistically relevant. The butenes decline linearly from 9.4 to 8.1 w% when comparing pure VGO C and 10 w% SDPO in feed. The aggregated alkanes fall from 17.4 to 15.2 w%.

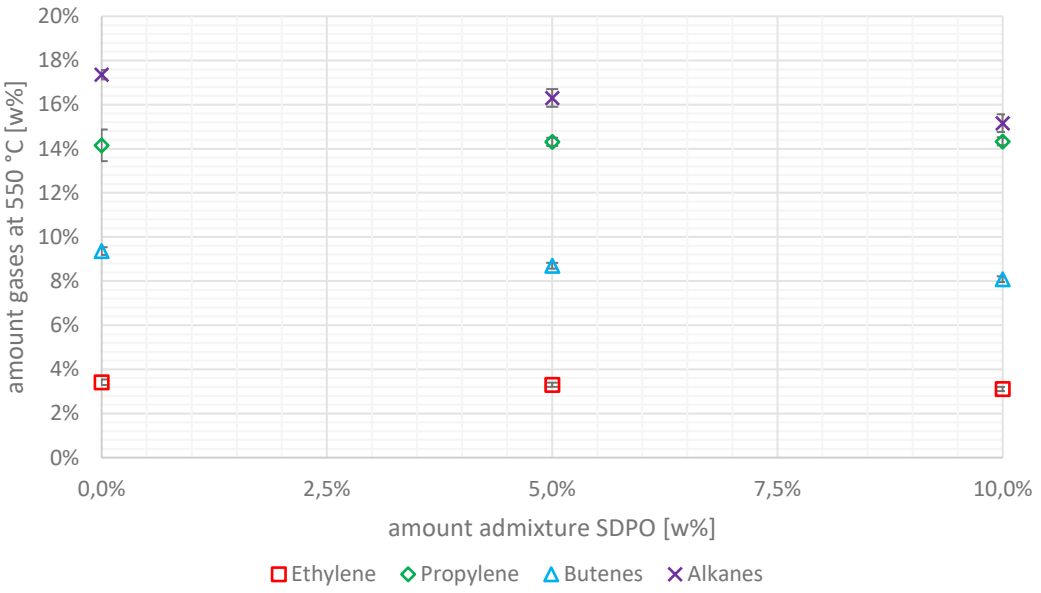

figure 82: olefins and alkanes distribution depending on admixture of wood based SDPO at 550 °C

The components described in figure 82 are set in relation to the hydrocarbon gas lump in figure 83 to reflect the gas composition. Ethylene remains stable around 7.6 – 7.8 w% whereas propylene increases from 32.0 to 35.2 w% with rising SDPO admixture rates. Butenes and alkanes both decrease for SDPO co-feeding around 1-2 w%.

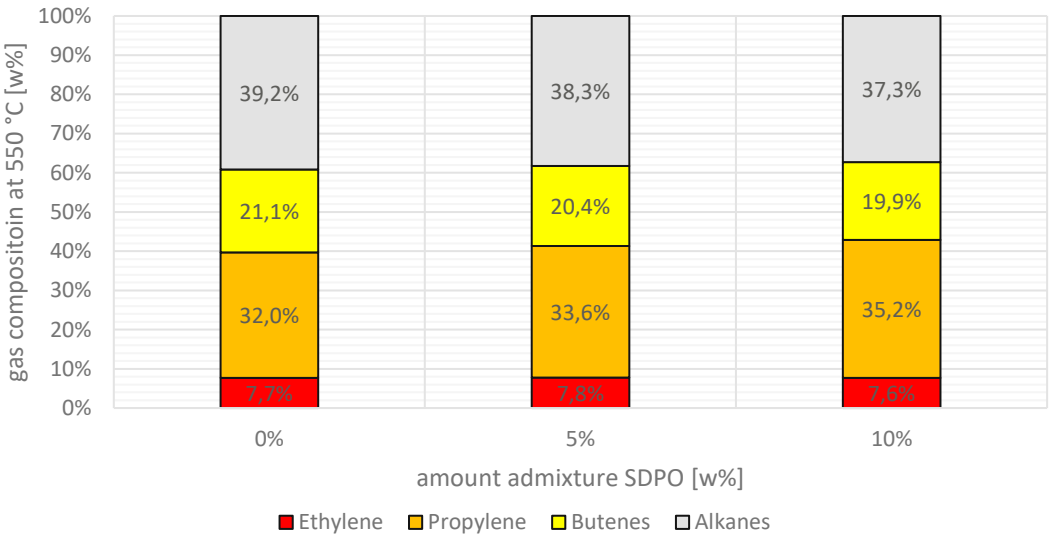

figure 83: gas composition in respect to olefins and alkanes depending on admixture of wood based SDPO at 550 °C

The sum of butenes is broken down into its components and illustrated in figure 84. 1-butene and cis-2-butene both slightly decline when SDPO is co-fed. The same falling trend can also be observed for isobutene and trans-2-butene. The isobutene yields were hereby the highest of all butenes with a decrease from 3.6 to 2.9 w%. The declines for the other butenes were lower in the ranges of 0.3 to 0.1 percentage points. All trends were statistically significant.

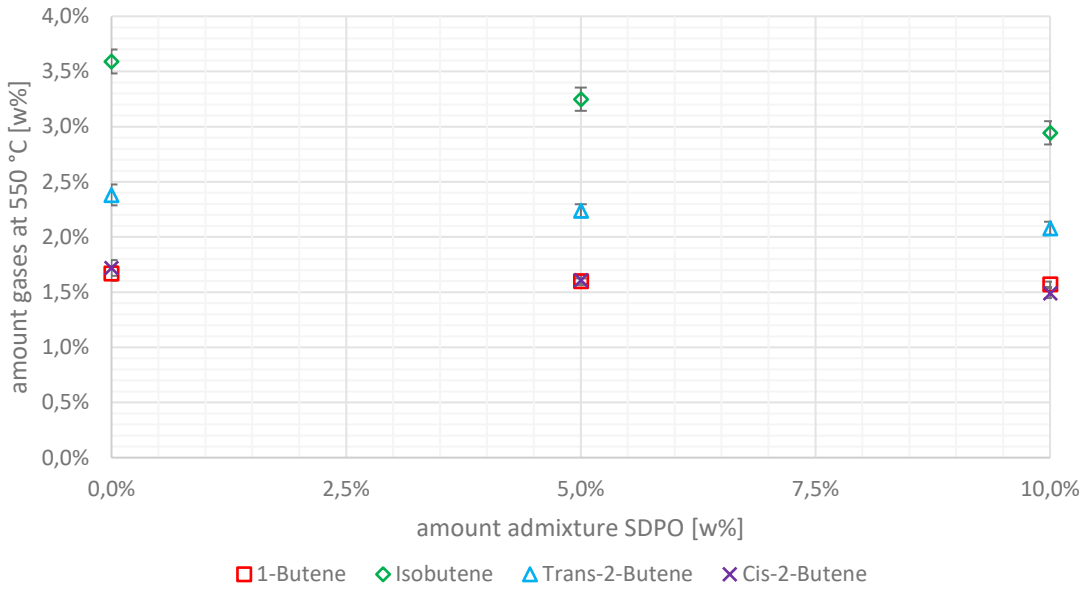

figure 84: butenes distribution depending on admixtures of wood based SDPO at 550 °C

The results for each alkane are found in figure 85. Methane and ethane do not change when SDPO is co-fed and remain stable at 1.1 and 0.7 w%, respectively. The other three alkanes (n-butane, isobutane and propane) decrease proportionally when SDPO rates are increased in the feedstock. The biggest drop is hereby observed for isobutane from 9.9 to 8.6 w%.

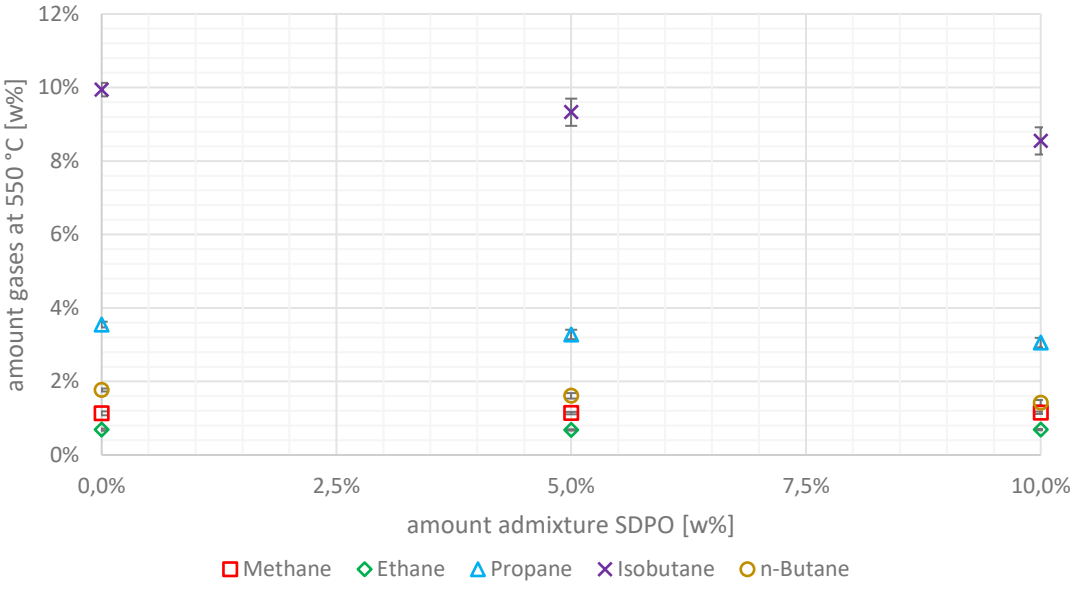

figure 85: alkanes distribution depending on admixtures of wood based SDPO at 550 °C

The carbon oxide yields are portrayed in figure 86. The results for both CO, CO_2 as well as CO_x do not show any measurable influence of the feedstock composition since most changes are inside error margins and do not show any clear trend. The lowest value was obtained for CO at 0.5 w% for pure VGO C and the highest value was measured at around 0.2 w% for CO_2 at 10 w% admixture rate of SDPO and pure VGO.

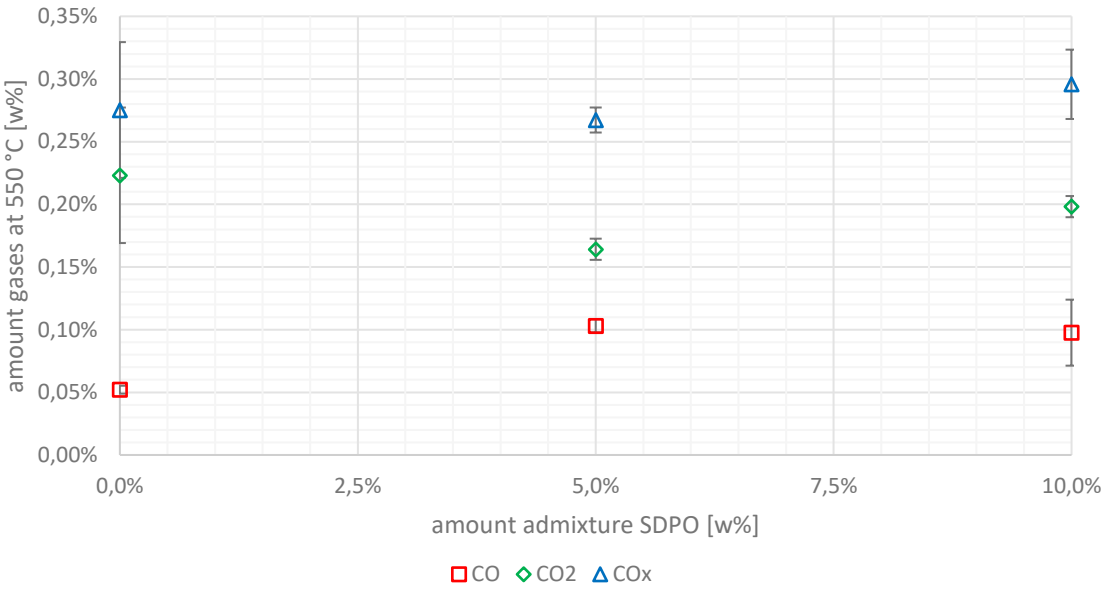

figure 86: carbon oxides distribution depending on admixtures of wood based SDPO at 550 °C

4.6.2.4 SDPO admixtures at 530 °C

Analogue to the SPO co-feeding experiments an analysis of the results of the SDPO admixtures at 530 °C riser-temperature are shown in figure 87 - figure 93. In figure 87 the yields of hydrocarbon gases, gasoline and the total fuel yield are portrayed. Herein hydrocarbon gas decreases when SDPO is co-fed from 39 to 37.3 w%. As a contrast, gasoline remains stable just above 44 w% resulting in a decline in total fuel yield from 83.8 to 81.8 w%.

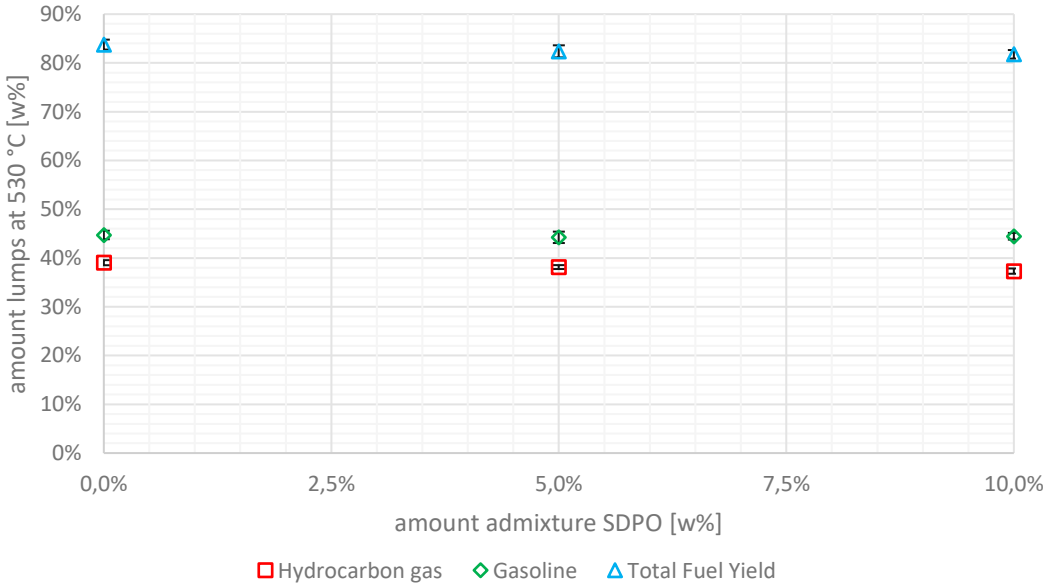

figure 87: hydrocarbon gas, gasoline and TFY distribution depending on admixture of wood based SDPO at 530 °C

The trends of the other main lumps: LCO, residue and coke are found in figure 88. LCO shows a rise from 8.4 to 9.6 w% which is not statistically relevant due to overlapping standard deviations. Residue follows an indifferent pattern with varying numbers between 2.8 and 3.6 w%. The coke lump remains stable up to 5 w% SDPO admixture and rises then slightly to 5 w%.

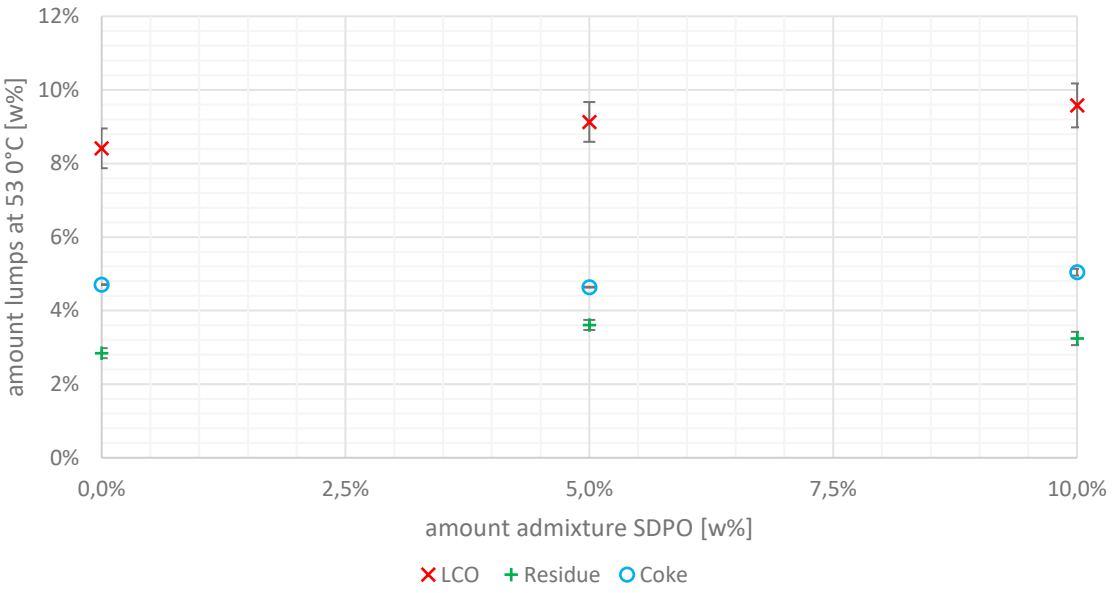

figure 88: LCO, residue and coke distribution depending on admixture of wood based SDPO at 530 °C

The olefinic gases and the alkanes distribution are illustrated in figure 89. Ethylene sank slightly from 2.8 to 2.6 w% whereas propylene stayed the same around 12.3-12.5 w%. The butenes did not show any significant changes with varying values between 8.0 – 7.5 w%. Only the alkanes displayed a significant decline from more than 16 w% to just above 15 w%.

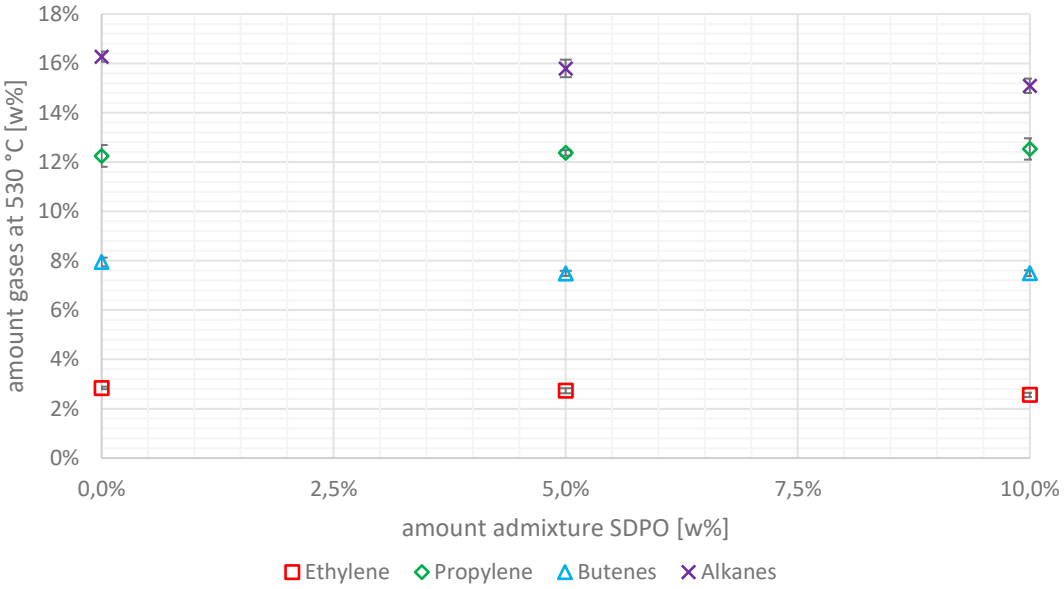

figure 89: olefins and alkanes distribution depending on admixture of wood based SDPO at 530 °C

The measurements from figure 89 are set in relation to the hydrocarbon gas lump to display the gas composition (see figure 90). There it is shown that ethylene and alkanes decrease when SDPO is cofed. Propylene however shows a relative increase from 31.2 to 33.3 w%. The sum of butenes provide no conclusive trends and seems to vary.

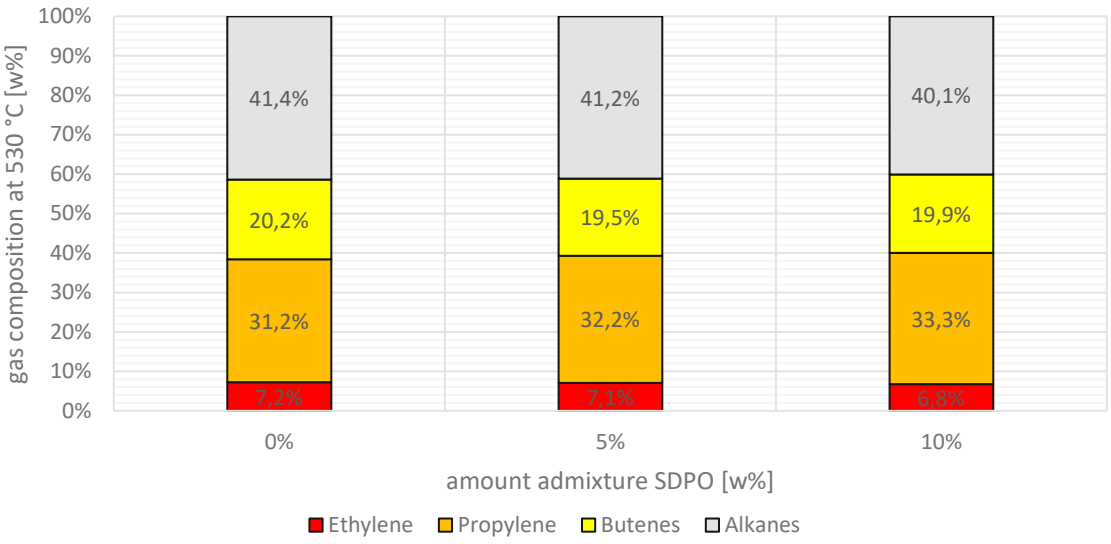

figure 90: gas composition in respect to olefins and alkanes depending on admixture of wood based SDPO at 530 °C

The disaggregated measurements of the butenes are shown in figure 91. The amounts of 1-butene and cis-2-butene generated are just below 2 w% and do not show any trends when co-feeding SDPO. The same also applies to trans-2-butene. Only isobutene decreases in a statistically relevant amount from 3.1 to 2.7 w%.

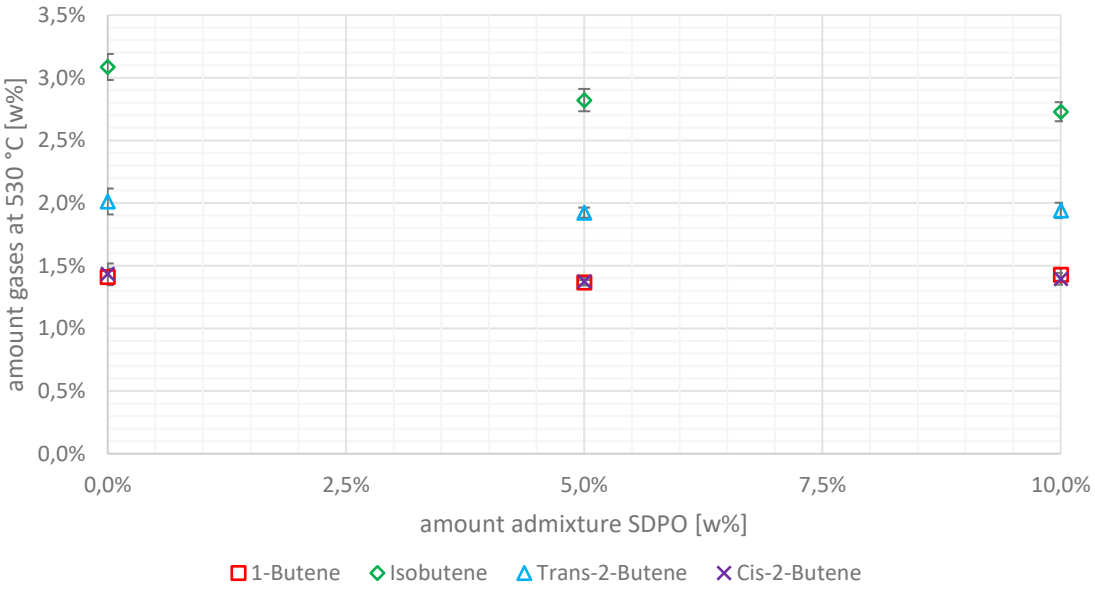

figure 91: butenes distribution depending on admixtures of wood based SDPO at 530 °C

figure 92 shows the distribution of the different alkanes depending on feedstock composition. Methane, ethane and n-butane account for less than 2 w% each. For methane and ethane no relevant changes are observed but with n-butane a small decrease from 1.6 to 1.4 w% was measured which was greater than the measurement error margins. Propane and isobutene seem to sink linearly with the proportion of SDPO in the feed. Isobutane for example decreases from 9.8 to 9.5 and 9.0 w% for pure VGO C, 5 w% SDPO and 10 w% SDPO, respectively.

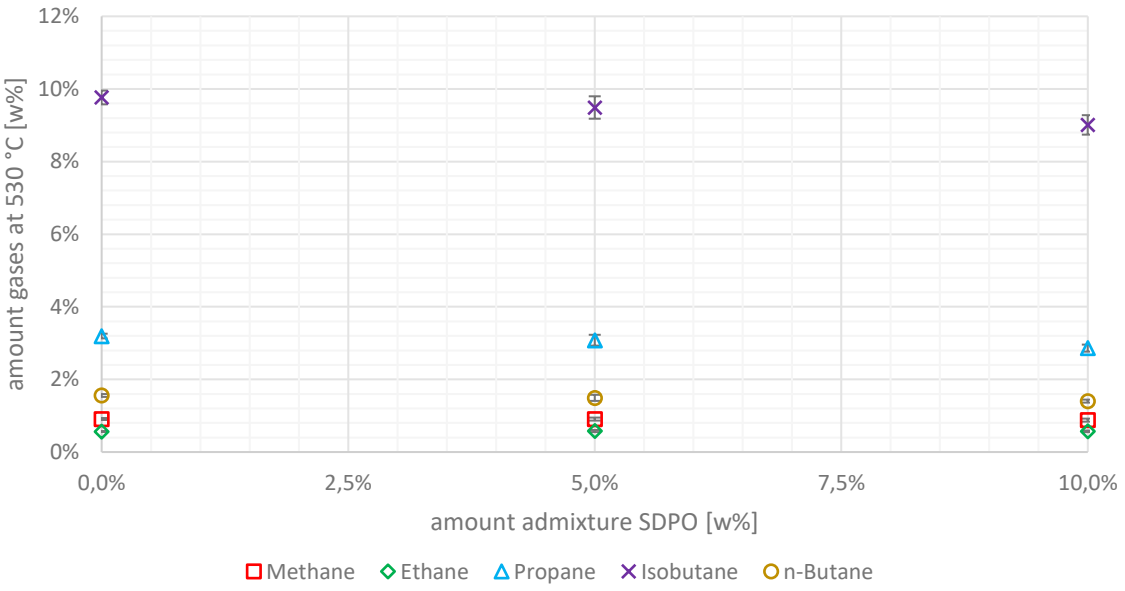

figure 92: alkanes distribution depending on admixtures of wood based SDPO at 530 °C

The carbon oxides in the product gas are depicted in figure 93. Neither for CO, CO_2 nor for CO_x any statistically relevant changes were observed due to overlapping error margins. All measured values are below 0.4 w%.

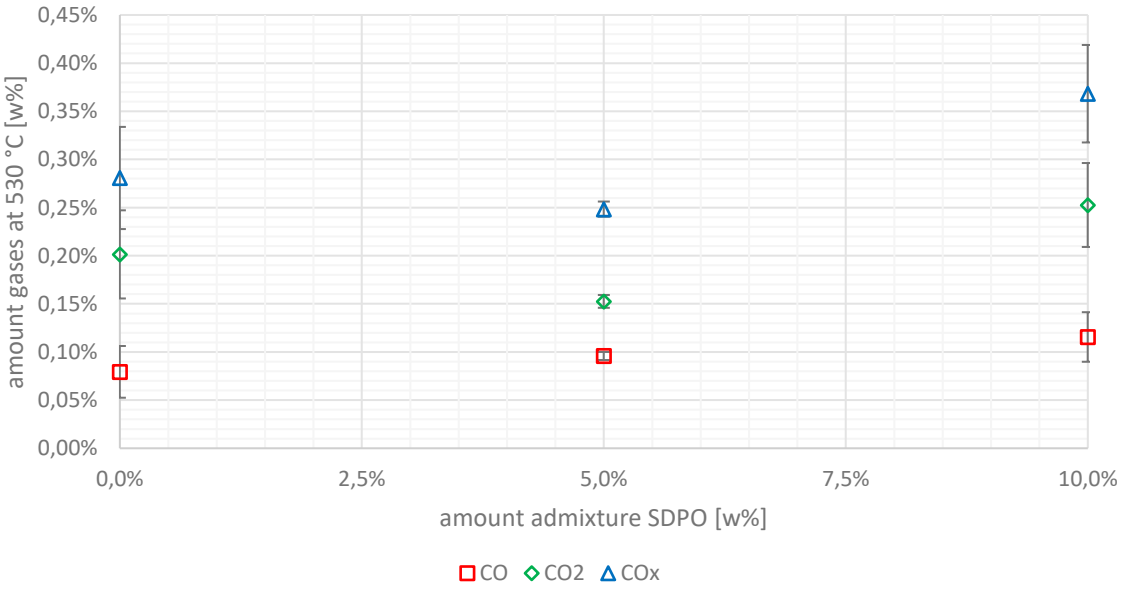

figure 93: carbon oxides distribution depending on admixtures of wood based SDPO at 530 °C

4.6.2.5 Gasoline fraction

The liquid fraction of the SPO & SDPO admixing campaign were distilled to obtain gasoline which was investigated in an external laboratory. No error margins can be displayed since all measurements were conducted only once. The exact norms and equipment that were utilized for the gasoline analysis cannot be disclosed due to confidentiality.

In figure 94 the densities at 15 °C of the gasoline depending on the SPO/SDPO admixture rate and the riser temperature are illustrated. The highest density is obtained for pure VGO C at 550 °C at around 808 kg/m³. Adding SDPO and SPO to the feedstock leads then to a decline in densities. The lowest amounts are measured at 10 w% admixture rates at 801 and 790 kg/m³ at 550 and 530 °C, respectively. The densities at 530 °C do not show any clear trend for neither SPO nor SDPO. Most values vary between 790 and 792 w% with an exception of the 5 w% SDPO admixture at 530 °C which leads to around 798 kg/m³.

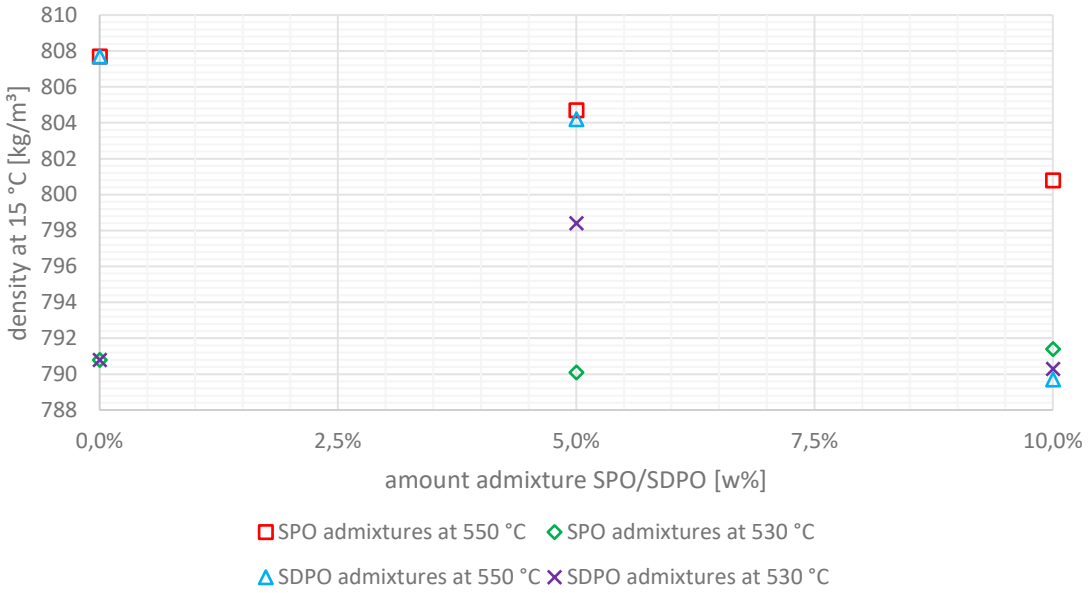

figure 94: densities at 15 °C of gasoline depending on SPO/SDPO admixtures and riser temperature

For all gasoline samples no amount of free water is measurable. The dissolved water content, however, shows significant differences depending on admixture rate (see figure 95). For pure VGO C the dissolved water content is for both temperatures roughly the same around 100 – 112 mg/kg. Adding SDPO to the feedstock leads from this reference point onwards to no significant increase. For the 10 w% admixture rates results around 117 to 126 mg/kg are obtained. Contrary to that the admixing of SPO leads to a clear rise in dissolved water content which is most significant for the 10 w% admixture. The highest water amount is generated at 550 °C riser temperature and 10 w% SPO at 350 mg/kg. For 530 °C a drastically lower value of 181 mg/kg is measured.

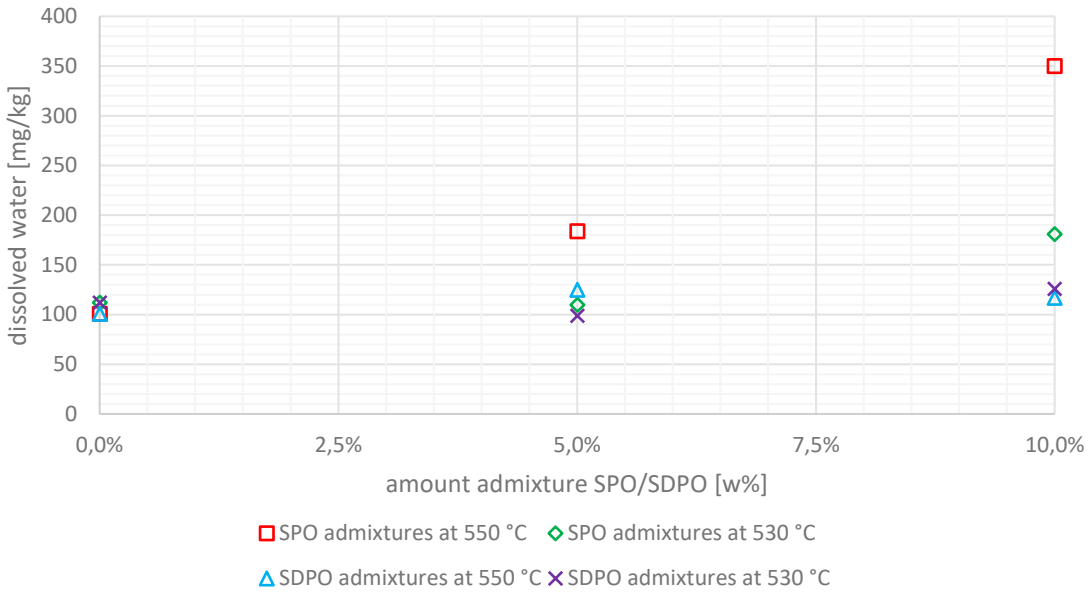

figure 95: dissolved water in gasoline depending on SPO/SDPO admixtures and riser temperature

The nitrogen content depending on pyrolysis oil amount in the feedstock and riser temperature is found in figure 96. For pure VGO C miniscule amounts of nitrogen are determined with values between 2 – 3 mg/kg. For all admixtures of SPO and SDPO a strict rising trend is observed. The nitrogen in gasoline hereby rises continuously the more pyrolysis oil is cofed. 10 w% SPO admixtures result in the highest values of more than 16 mg/kg independent of riser temperature. The admixtures of SDPO lead to overall lower nitrogen content, however, still a significant increase is observed.

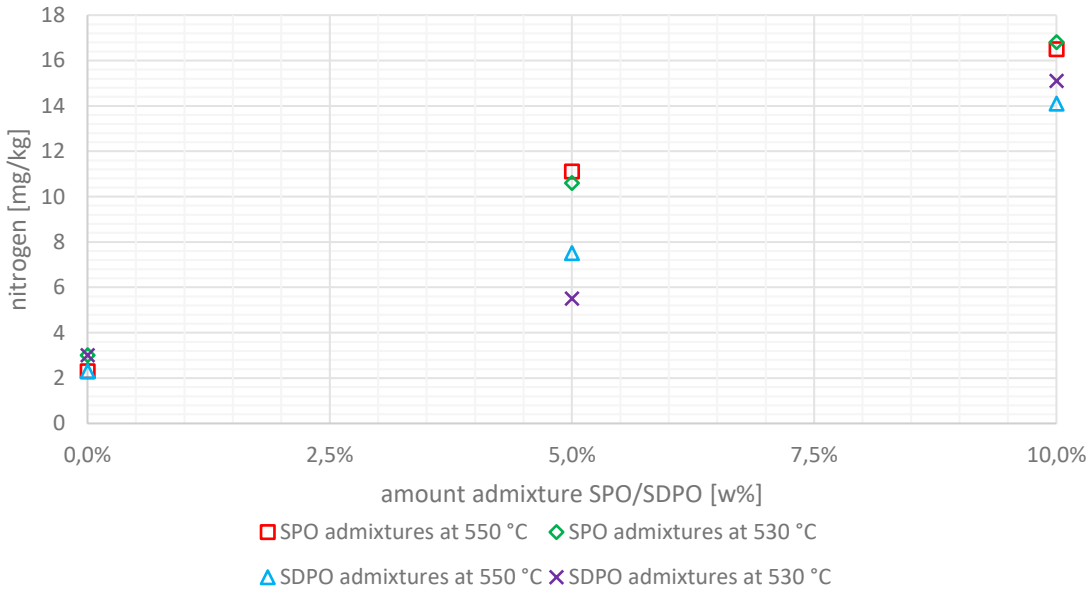

figure 96: nitrogen content of gasoline depending on SPO/SDPO admixtures and riser temperature

Like nitrogen the sulfur content in the gasoline samples were measured and are depicted in figure 97. There is no clear dependance of sulfur content and riser temperature or admixture rate of SDPO and SPO observable. All results vary between 10 – 18 mg/kg with the lowest value being obtained for pure VGO C at 530 °C and the highest value for 5 w% SDPO admixture rates at 550 °C. For pure VGO C and 5 w% SPO/SDPO admixture rate the results for 530°C are lower than for 550 °C.

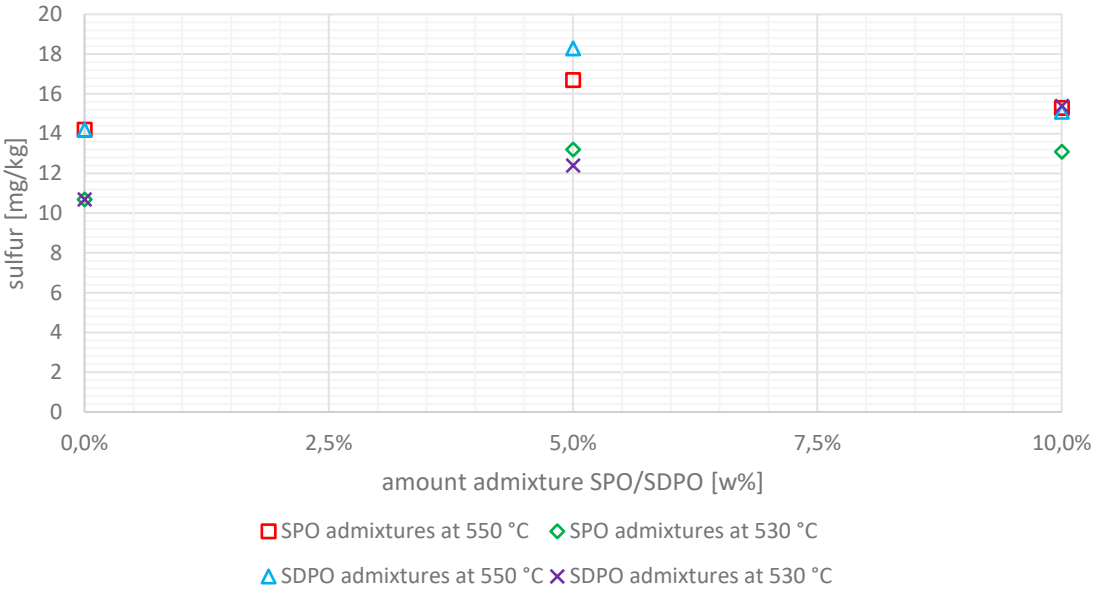

figure 97: sulfur content of gasoline depending on SPO/SDPO admixtures and riser temperature

The main elements of gasoline beside nitrogen and sulfur are listed in table 26 (carbon, hydrogen, oxygen). For those elements no significant differences were measurable. For all gasoline samples the oxygen amount is below the limit of 0.1 w%. Accordingly, the lower heating value does not show any significant change depending on riser temperature or feedstock composition. The calculation was done by using the Boie formula [172]. No inorganic impurities were measurable for any gasoline sample (see table 29 in Appendix)

table 26: basic parameters of gasoline depending on SPO/SDPO admixtures and riser temperature

plant settings	550 °C					530 °C				
	-	5% SPO	10% SPO	5% SDPO	10% SDPO	-	5% SPO	10% SPO	5% SDPO	10% SDPO
C [w%]	87.3	87.2	87.1	87.1	86.9	86.8	86.8	86.9	86.9	86.8
H [w%]	11.8	11.8	11.9	11.9	12.1	12.3	12.3	12.2	12.1	12.3
O [w%]	<0.1	<0.1	<0.1	<0.1	<0.1	<0.1	<0.1	<0.1	<0.1	<0.1
lower heating value [MJ/kg]	41.5	41.4	41.5	41.5	41.6	41.8	41.8	41.7	41.6	41.8

The paraffin content depending on riser temperature and wood derived pyrolysis oils is illustrated in figure 98. The paraffin content is hereby defined as the sum of n-paraffins and i-paraffins. The paraffin content is found to be between 19 and 25 w%. For most feedstocks at 530 °C the paraffin content is significantly lower than at 550 °C with one exception at 10 w% SDPO admixture rate. For those the paraffin contents all vary between 19-20 w%.

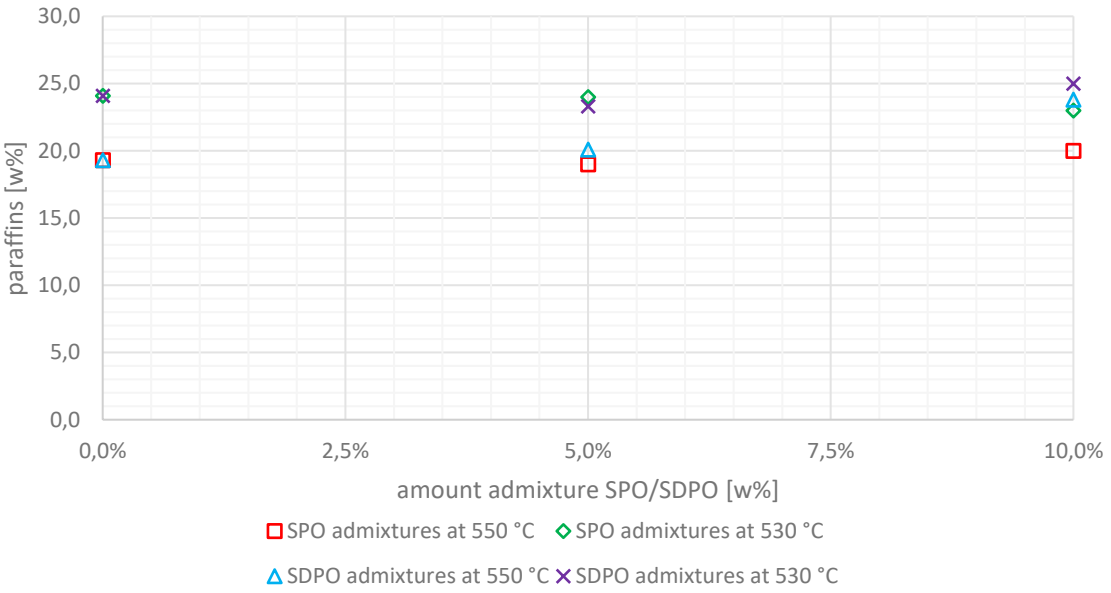

figure 98: paraffin content in gasoline depending on admixture rate and riser temperature

The olefin content of the gasoline samples are portrayed in figure 99 analogue to the paraffin contents. The olefins are hereby the summarized values of n-olefins, i-olefins and olefinic naphthenes. The results range from 9.2 to 12 w%. No clear trends are observed regarding temperature and feedstock influence.

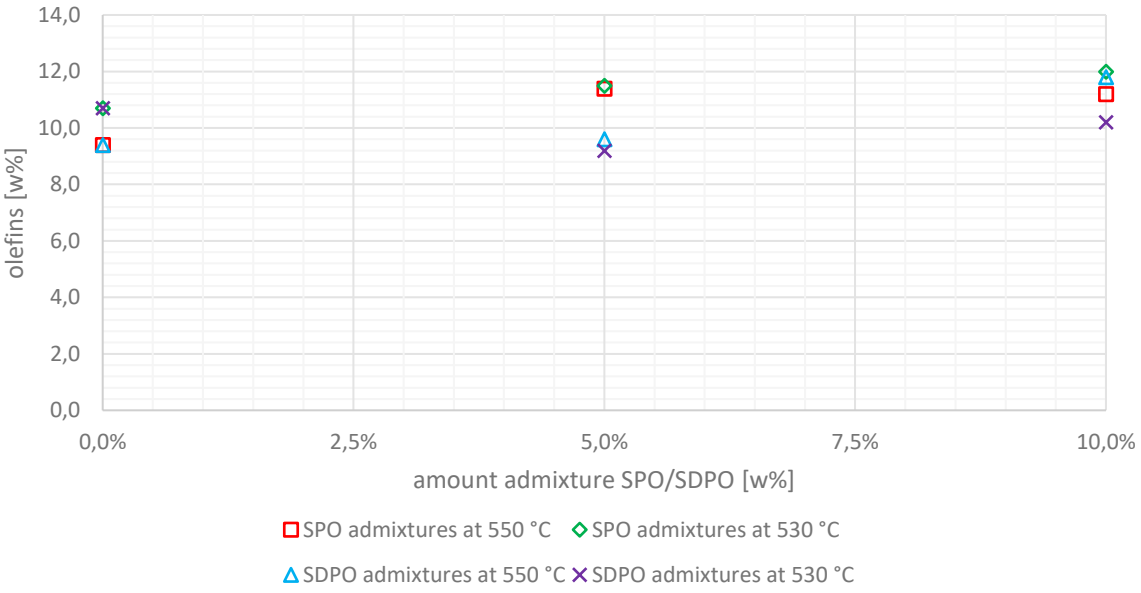

figure 99: olefin content in gasoline depending on admixture rate and riser temperature

The naphthenes (or cycloalkanes) are illustrated in figure 100 similarly as olefins and paraffins. Among the hydrocarbon molecules the naphthenes constitute the lowest share of only 7.1 to 10.2 w%. Again, no clear tendencies for all feedstock variations are found. However, for SDPO admixtures at 550 °C a slight increase could be observed. More importantly the riser temperature influences the naphthene formation in gasoline so that the naphthene contents at 550 °C are between 7.1 and 8.8 w% and therefore, significantly lower than the ones at 530 °C.

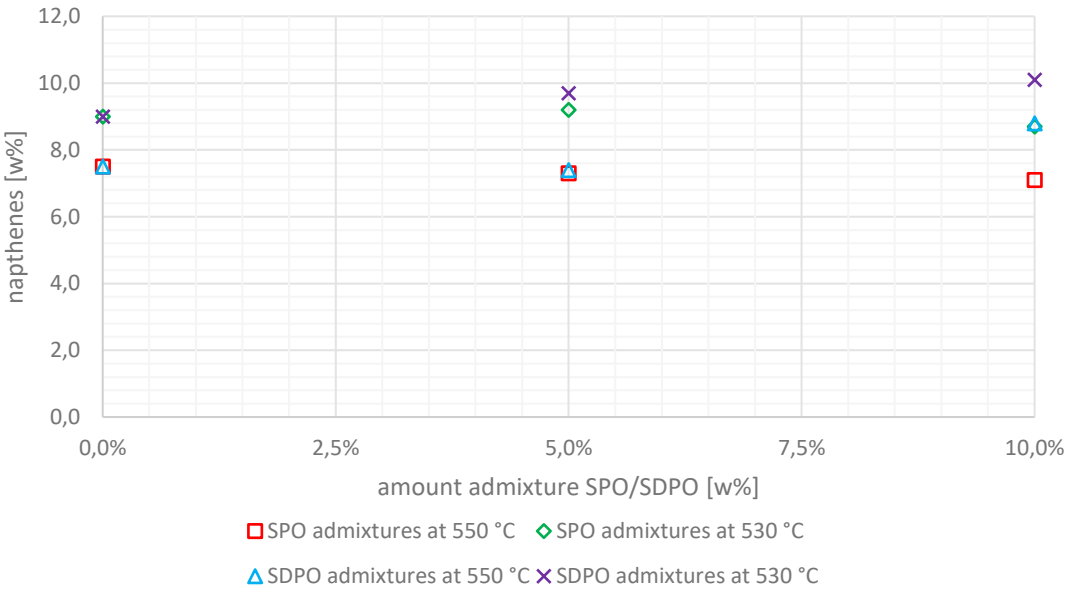

figure 100: naphthene content in gasoline depending on admixture rate and riser temperature

The aromatics content of the gasoline fractions is found in figure 101. The aromatics form the highest share of hydrocarbons in the gasoline with the lowest amount being at 54.6 w% and the highest at 63.8 w%. For the experiments at 550 °C a strict decrease is observed when SDPO and SPO is cofed with the lowest amounts being obtained at the 10 w% admixture (61,7 and 55.6 w% for 550 and 530 °C, respectively). The aromatics for the 530 °C experiments do not show a clear trend regarding their influence on feedstock composition. However, they are substantially lower than most results at 550 °C with fluctuating values between 54.6 and 57.8 w%.

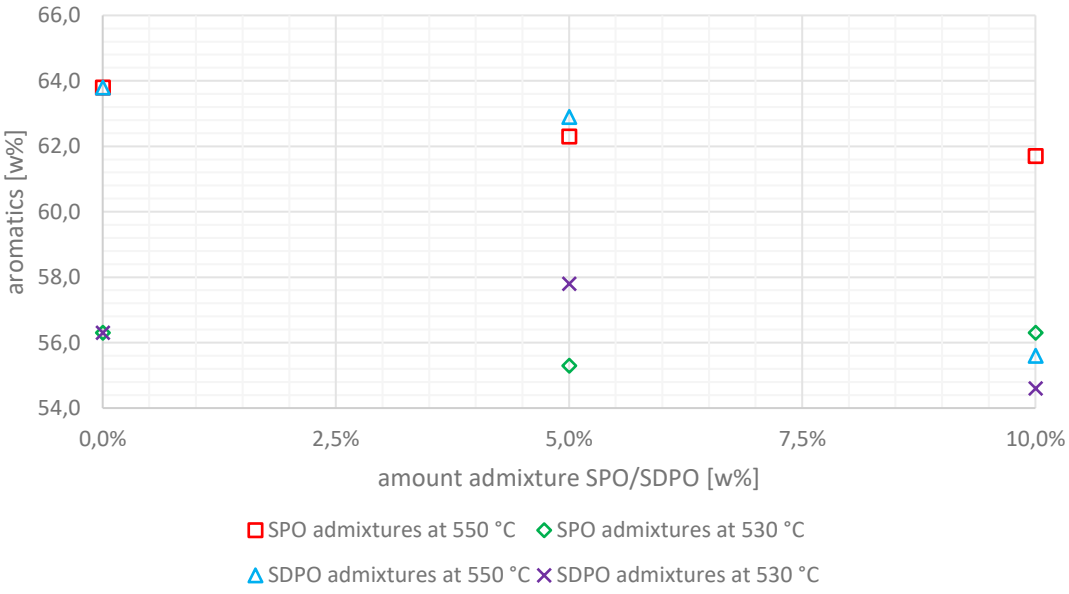

figure 101: aromatics content in gasoline depending on admixture rate and riser temperature

4.6.3 Discussion

The experimental runs with stabilized pyrolysis oils showed a stable plant operation for admixtures of 5 w%. For 10 w% plant instabilities were observed due to fouling and clogging in the tubular oven and the feed inlet pipes. This originated from polymerizing and coking of the stabilized pyrolysis oil so the chosen approach of diluting SPO with VGO before it was heated in the tubular oven was not deemed satisfactory. It is recommended that a second feeding line is established so that SPO and VGO do not get in contact before entering the riser so that said clogging is prevented. It is assumed that with this adaptation higher SPO mixtures could be feedable.

The experiments at 550 °C yielded higher amounts of hydrocarbon gases and coke than the ones at 530 °C for all SPO admixtures. This is due to the lower amount of cracking reactions at lower temperatures which was expected. As a result the gasoline yields increased at lower temperatures. The yields of LCO followed the same pattern because of the same reason. The oxygen in the SPO (36.5 w%) led to measurable amounts of water in the liquid fraction which increased at higher admixtures rates of SPO. The increases in carbon oxides when co-feeding SPO also originate from the oxygen content in SPO. These changes are, however, marginal but nonetheless statistically significant. When analyzing the hydrocarbon gases in detail it is observed that ethylene and propylene increase not only relatively compared to other gases but also in regard to the feeding rate which undermines the SPOs potential to boost the generation of valuable base chemicals for plastic polymer production.

As next steps experiments with adapted feed nozzles are recommended to compare them with the already obtained results as a mean to research potential influences of feed cracking in the feed inlet pipes on the product spectra. Furthermore, higher admixture rates of around 20 w% should be tested if the pipe clogging incidents can be solved with the previous mentioned plant adaptations. The product spectra of the runs with clean wood derived SPO should be considered as benchmarks for other biogenic waste-derived SPO later in the Waste2Road project.

The second hydrogenation step when generating SDPO showed significant effects on the product spectra. SDPO co-feeding led to a decreasing trend in hydrocarbon gas generation for both riser temperatures but an increase in gasoline for 550 °C. The highest gasoline yield was obtained at 530 °C with a constant trend around 44 – 45 w%. Other liquid fractions like LCO also increased when co-feeding SDPO. Therefore, co-feeding SDPO at lower riser temperatures seems to be the ideal combination when maximizing the generation of second generation biofuels which is the goal of the waste2road project.

Unlike when co-feeding SPO the SDPO experiments did not lead to measurable amounts of water that were separable from the liquid product fraction. However, SDPO still contains miniscule amounts of water (around 0.5 w%) which should be measurable in the product since water is inert under FCC reaction conditions. It is believed that these rather low amounts of water are trapped inside the condensation apparatus and lost during sampling. Furthermore, the significant decrease in oxygen content also did not lead to any measurable changes in carbon oxide generation.

Since SDPO was fully mixable with vacuum gas oil due to its low oxygen content and low polarity a feeding via a joined inlet pipe was chosen. This setting worked as expected and no clogging or fouling incidents were observed. Thus, no separate feeding line seems necessary when utilizing SDPO which is a significant advantage compared to SPO since it safes plant adaptations. For the next steps higher admixtures of SDPO are recommended even though SDPO availability is so far limited to determine its maximum co-feeding rate and estimate its potential. Judging from the results so far even pure SDPO feeding could be achievable if product distribution shifts can be handled in downstream units.

The gasoline samples of both SPO and SDPO experimental runs were analyzed in a technical lab of a refinery operator. The results regarding elemental composition illustrate that no relevant changes in carbon or hydrogen content can be determined depending on pyrolysis oil admixture rates. Additionally, even though SPO and to a lesser extent SDPO contain significant amounts of oxygen compared to VGO all oxygen levels in the gasoline samples were below 0.1 w% and therefore below the LOD of the used measurement method. This finding is positive as it signifies rather steady quality of gasoline and provides a stable energy content around 41 – 42 MJ/kg independent from feedstock composition.

Gasoline needs to fulfill strict thresholds for sulfur (10 ppm [144]) so a rise of sulfur levels in FCC gasoline fractions might be problematic for blending. For the admixture of SPO and SDPO with VGO C no clear tendencies were observable. This is probably due to the fact that all utilized feedstocks were previously hydrogenated and hydrodesulfurization is a standard method for sulfur reduction. But higher admixture rates of SPO/SDPO could lead to significant increase so further experiments are recommended. Moreover, feeding crude wood-derived pyrolysis oils could lead to rises in sulfur levels since crude PO is not a hydrogenated feedstock. Unlike sulfur, nitrogen was continuously rising at higher admixtures of SPO as well as SDPO which is an impairment of gasoline quality. Since these levels were still comparably low with a maximum value around 17 ppm it remains unclear when and if problems could occur in regard to nitro oxide emissions via combustion.

The amounts of dissolved water in the gasoline did not change for the SDPO experimental campaign, however, for SPO a rather linear rise in water amounts were measured. These findings can again be explained by the higher water and oxygen content of SPO compared to SDPO. It remains unclear if any significant impairment of gasoline quality results from these elevated dissolved water levels since they are still in the ppm range.

It was found out that inorganics did not enrich in the gasoline fraction as there were no measurable amounts independent from riser temperature and feedstock. However, these first co-FCC experiments for the Waste2Road project were conducted with clean wood derived pyrolysis oils. Later in the project more contaminated source material (contaminated wood or sunflower husks) will be used for pyrolysis crude generation which could then lead up to inorganics in the product fraction which must be strictly monitored.

Summarized, hydrogenated pyrolysis oils from clean wood waste proved to be a viable feedstock for FCC co-feeding as no major drawbacks in quality were observed. SDPO was especially easy to use since it was fully mixable with fossil feedstock and did not show any fouling or plugging tendencies. But the necessary second hydrogenation step to generate SDPO makes it comparatively more expensive. If adaptations regarding feeding are implanted such as a second cooled or isolated feeding line SPO should also not pose any major downsides as product yields were promising. Ideally, with feeding crude wood-based PO, hydrogenation and therefore a process step could be saved which would be favorable economically. Thus, experiments with crude wood PO should be conducted if feeding proves possible.

5. Synopsis and outlook

This thesis describes the Fluid catalytic cracking process, one of the state-of-.the-art refinery conversion processes and the possible usage of its high versatility. Based on current technology trends this work revolves around experiments conducted at a pilot plant located at TU Wien. Utilizing said plant heavy residues and new alternative feedstocks like pyrolysis oils are processed and their suitability and quality for conversion in FCC units are assessed. Furthermore, experiments were conducted to determine the pilot plants ability to act as an FCC catalyst test rig. Lastly, the influence of fluidization rates corresponding to different catalyst to oil rations on product spectra were researched.

The catalyst testing campaign was conducted to establish comparison data between all three catalysts that were utilized in the various projects accumulating in this work. The goal was to assess the pilot plant's ability to act as a catalyst test rig for future projects as well as to determine the exact influence of the propylene boosting, the heavy residue gasoline boosting and the LPG boosting catalyst. For increased comparison all runs used the same batch of vacuum gas oil so that only the catalyst was a varying parameter. The LPG and propylene boosting catalyst favoured hydrocarbon gas production with yields of 39.7 and 40.4 w%, respectively whereas the residue catalyst encouraged gasoline formation over proportionally (55.4 w%). Reducing cracking temperature increased gasoline formation for all three catalysts, consequently, by counterbalancing this via decreasing hydrocarbon yields. Highest propylene yields where obtained using the propene boosting catalyst (14.8 w% at 550 °C). The LPG boosting catalyst mix still gave satisfying propene yields but also elevating butenes and especially isobutane (8.2 – 8.4 w%) yields. The pilot plant proved to be a formidable test rig to compare the catalyst's influence on product spectra in industry-near operation mode unlike simple batch operated Micro-activity-tests. All catalysts proved to act according to manufacturer information. Using the pilot pant for catalyst testing, therefore, was proven to be a risk-minimizing way for refinery operators to help choosing their possible next FCC catalysts in their industrial scale unit.

To prepare for the next section comprising of heavy residual feedstock testing an experimental campaign was conducted to evaluate differences in riser fluidization gas rates on product spectra. This was conducted because residual FCC units often use higher amounts of steam for enhanced feed atomization and transport. Therefore, experiments were launched at different riser fluidization rates that led to differences in catalyst to oil ratio since higher rates of fluidization gas increased catalyst circulation at steady feed rates. The results proved that the changes in catalyst to oil (C/O) ratio had tremendous influence on product spectra. The reference case using only a minor fluidization rate that is standard for experiments at the pilot plant. The catalyst to oil ratio was for the reference case 20 and increased in correlation to the rising fluidization gas rates to around 58 at the highest rate. The results corresponded well to literature with a rise in hydrocarbon gas yields at higher fluidization gas rates as more active catalyst sites where available for cracking. The hydrocarbon gases hereby increased from around 43 to 55 w%. Accordingly, the liquid fractions decreased with the highest drop observed for the gasoline yield (41.6 to 32.8 w%). These findings show the importance of running all experiments in a campaign using the same fluidization settings as otherwise a clear attribution of e.g. the effect of feedstock change cannot be clearly determined. Furthermore, direct comparability with industrial plants is decreased at higher fluidization settings since commercial plants run at significantly lower C/O-ratios. Thus, it is recommended to modify the used plug valve for heavy residual cracking in the future to lower circulation rate and increase comparability with industrial sized plants.

The second objective of the thesis was the assessment of heavy residual oil fractions that could increase the generation of high-value products of a refinery since the production of low-value fuels like heating oil, bunker oil etc. already declines and is expected to further decline in the future due to environmental regulations and technological changes.

In this setting a refinery operator planned on changing product streams in the refinery by co-feeding small percentages (up to 10 w%) of atmospheric reside together with vacuum gas oil in an FCC unit. This procedure is state-of-the-at, however, its effects on the product stream, especially on the hydrocarbon gas lump is not yet completely researched in literature. Previously, the unhydrogenated residue was used as blending feedstock for fuel oil production. But declining sales of said product necessitate alternative scenarios for usage. Since the standard feedstock VGO was hydrogenated consequences on product quality were feared when unhydrogenated feedstock would be co-feed. Focus was laid here on carbonyl sulfide (COS) which enriches in the propylene stream due to close boiling temperatures and would diminish its quality. Downstream usage of said propene in the polymer industry was endangered since COS acts as a strong catalyst poison.

Therefore, an experimental campaign was conducted to generally research possible product shifts with emphasis on the propylene production on COS contamination. Key results of this campaign are listed in table 27. This findings show a decline in hydrocarbon gases and an increase in gasoline yields starting from 5 w% admixture rate of residue and higher. Using the propylene boosting catalyst only a minor decrease of propene yield was observed. Additionally, COS levels remained inside error margins up to 5 w% atmospheric residue admixture. At 10 w% the increase was significant. This led to the conclusion that residue can be cofed under current circumstances up to 5 w% without significant product impairment. For higher percentages hydrogenation of atmospheric residue is probably required to ensure constant product quality.

table 27: essential findings of atmospheric residue co-feeding campaign

feedstock	Hydrocarbon gas [w%]	Gasoline [w%]	Propylene [w%]	COS [ppb]
100% VGO	38.6	43.9	13.7	179
97.5% VGO & 2.5% AR	39.6	43.1	14.1	183
95% VGO & 5% AR	36.8	45.9	13.6	187
90% VGO & 10% AR	36.1	45.0	13.4	278

The second heavy residue employed in this work was deasphalted oil (DAO). A feedstock that is harvested out of vacuum residue via solvent deasphalting. Using this feedstock a refinery operator that currently utilizes a heavy VGO wanted to diversify its possible FCC feedstocks and choose comparably cheap DAO. The refineries emphasis was on gasoline generation so that mean cracking temperatures were set at only 532 °C. Using DAO in FCC units is a well-established process but concrete numbers on product shifts compared to already heavy VGO batches are not easily available.

In total three experiments were conducted with pure VGO, pure DAO and a 50/50 mixture of it. Some key results of this campaign are summarized in figure 102. Pure VGO proved hereby to be despite its heavy nature a more promising feedstock than DAO. Feeding it led to lower yields of high value products both for hydrocarbon gases and gasoline. Therefore, total fuel yields declined significantly with the lowest being achieved for pure DAO. Overall, using DAO will lead to lower plant profitability which could only be compensated if DAO prices were significantly below the heavy VGO batch. On a positive note, DAO co-feeding only led to minor increases in coke yield so that residual FCC units should be able to process it.

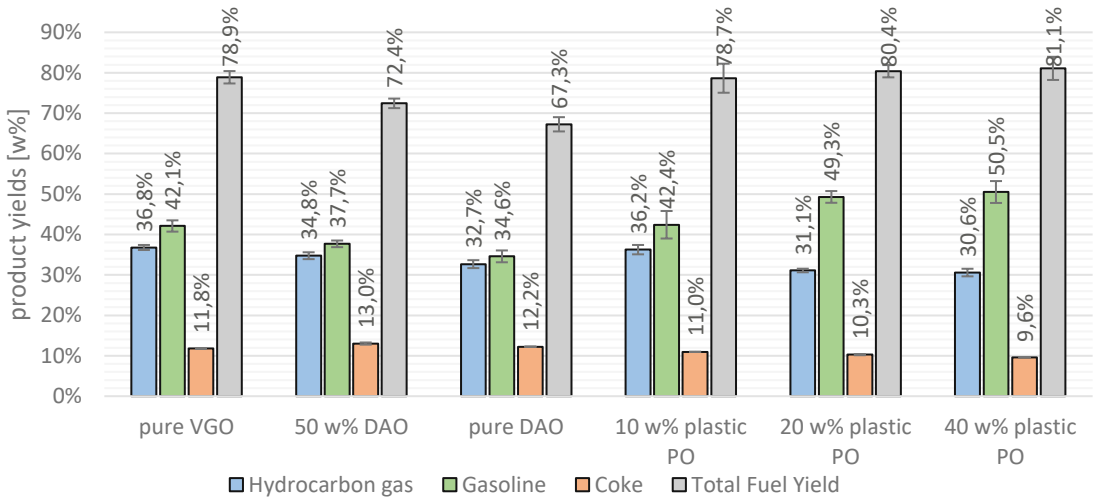

figure 102: selected product lumps of heavy VGO co-feeding with DAO and plastic PO

The third section of this work encompasses the utilization of still unconventional/alternative feedstocks that were generating using pyrolysis processes. (Fast) pyrolysis is an ideal process to generate liquids that can then enter downstream a conventional refinery and be used to valorize the fast pyrolysis feedstock into competitive products. A big advantage, hereby, is the pyrolysis process' ability to convert solid low-value wastes from biogenic sources like wood or fossil sources like mixed plastic wastes. The last object of this thesis was then to co-feed this sustainable feedstocks in the pilot FCC unit and to generate research data for quantifying and evaluating their potential as a feedstock. Currently only few data thereof is publicly available and if then mostly of batch reactors (MATs).

The refinery operator testing the DAO that was described in the previous section also planned on introducing new alternative recycling based feedstocks into its refinery to reduce its dependency on crude oil fractions. The plastic PO batch that was provided for pilot plant tests originated from a startup company that currently commercializes a pilot scale process from the laboratory in a demonstration plant. The plastic PO was created out of mixed plastic wastes that corresponded well to fractions that are found in household wastes. The obtained plastic PO was to be tested regarding its suitability as a refinery feedstock. Since focus was on gasoline production the cracking temperature was kept at 532 °C and a heavy residue catalyst was utilized since heavy VGO was used as a reference case.

The results from the campaign (10 to 40 w% admixture rate) showed promising results (see figure 102). The total fuel yields stayed constant compared to the reference case. Decreasing hydrocarbon gas lumps were balanced with equally increasing gasoline yields. It was determined that plastic PO was to be predominantly used for fuel production. However, to create a more circular economy olefin yields would need to be increased when feeding plastic PO. Therefore, further experiments are recommended using olefin boosting catalysts and at higher riser temperatures. Nonetheless, plastic PO proved to be a valuable feedstock for co-refining encouraging the employment of chemical recycling of mixed plastic wastes via pyrolysis.

In the European Union funded Horizon 2020 project Waste2Road new pathways for the generation of advanced biofuels were investigated. One such pathway was the conversion of clean pinewood wastes into biocrudes via fast pyrolysis. The project partner BTG with its fully commercialized pyrolysis process produced said biocrude. Due to high oxygen and water content as well as low thermal stability which leads to fouling and pipe clogging additional treatment was necessary. Via hydrogenation 2 different grades of pyrolysis liquids were synthesized out of crude liquid. The first, stabilized pyrolysis oil (SPO) underwent one mild hydrotreatment step in contrary to the stabilized and deoxygenated pyrolysis oil (SDPO) which underwent two steps. These differences in treatment resulted in different quality grades. Where SDPO had lower water and oxygen content and lower coke tendency but would also cost more in production because of higher hydrogen consumption and lower overall yields.

The next processing step for the hydrogenated pyrolysis liquids was FCC co-processing where the feedstocks processability and feedability were to be assessed. Furthermore, possible shifts in product spectra were to be discovered. The hydrogenation of the wood pyrolysis oils proved to have significant influence on the coke build up and therefore on the pumpability of the feedstocks since no clogging was observed for the twice hydrogenated SDPO but for the once hydrogenated SPO. As a result plant operation for SDPO was much smoother than for SPO which led to higher error margins in the results for the SPO yields. Nonetheless, general feedability was observed for admixture rates up to 10 w% and it is expected that in industrial plants less clogging problems will occur due to higher pipe diameters.

In figure 103 focus is laid on the hydrocarbon gases and gasoline yields, which are the processes main high-value product groups, and are of most interest for the proposed value chains to be established in the Waste2Road project. Generally, higher cracking temperatures led to higher gas and lower gasoline yields which was expected due to higher cracking activity and therefore severity. SPO was found to lead to increasing hydrocarbon gas yields compared to the other feedstocks with a maximum at 46.3 w% for 10 w% SPO admixture and a riser temperature of 550 °C. SDPO feeding, on the other hand, resulted in higher gasoline yields compared to SPO. The highest yields were obtained at 530 °C where no significant differences were observed for pure VGO or admixtures of SDPO up to 10 w%. Regarding the goal of Waste2Road which is the generation of advanced biofuels the admixture rate of 10w% at 530 °C is deemed the most suitable.

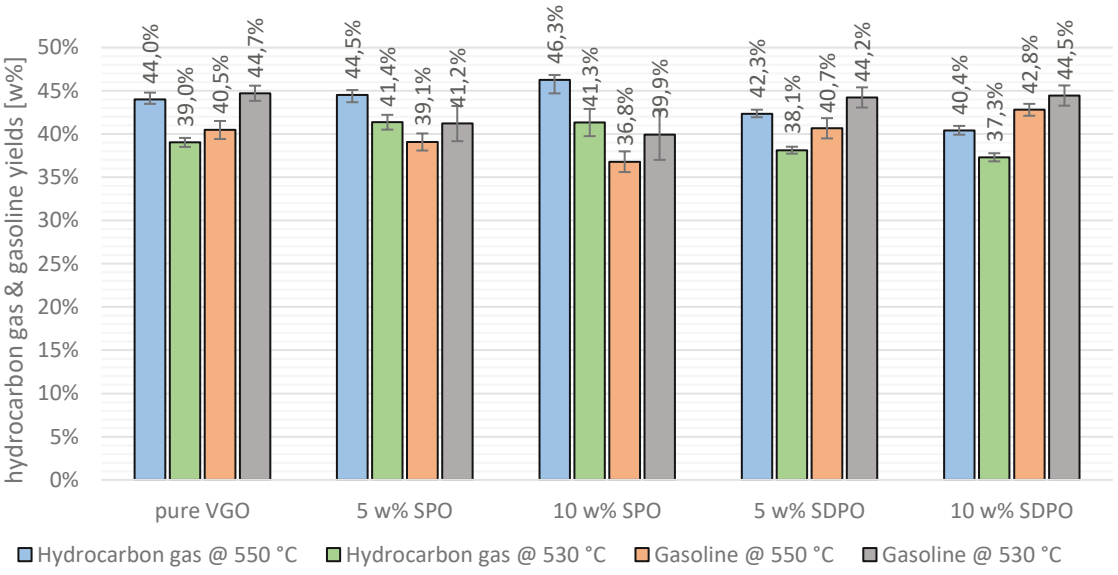

figure 103: hydrocarbon gas and gasoline lumps depending on temperature and co-feeding of SPO/SDPO

The obtained liquid samples were then manually distilled to obtain around 150 ml per experimental run of gasoline. As a cut-off temperature 210 °C were chosen in accordance to European norms [144]. These gasoline samples were then analysed in a technical laboratory of a refinery partner to obtain some basic parameters to assess gasoline quality.

The elemental analysis did not reveal any significant changes in carbon or hydrogen content. For oxygen quantification was not possible since all samples were below the detection limit of 0.1 w%. This finding was considered positive, since pyrolysis liquids contain substantial higher amounts of oxygen which ultimately did not enrich in the gasoline cut. Sulfur is a major contaminant were extremely low limits (10 ppm [144]) need to be kept so increases in sulfur levels due to co-feeding would be considered harmful for gasoline quality. The analysis showed that all gasoline samples (also from pure VGO) did not comply with regulations and were above the mentioned threshold value since FCC gasoline is the blending component with the highest sulfur content. This, however, was not considered problematic, since it is standard procedure to even this out at blending. Furthermore, the numbers showed that no direct influence of co-feeding on sulfur levels. was observed. This is probably due to the hydrogenation of the pyrolysis liquids since hydrodesulfurization is a standard sulfur reduction method in the refinery sector. However, it was concluded that cracking temperature did have an influence on sulfur concentrations since values obtained at 530 °C riser cracking where mostly lower than the ones at 550 °C. Unlike sulfur, nitrogen levels increased for SPO and SDPO co-feeding strictly linearly with no clear difference between those two. The second hydrogenation step for SDPO generation, therefore, does not have much influence on nitrogen levels. It is uncertain if these elevated nitrogen levels could lead to problems later when combusting the gasoline. Fortunately, the obtained values were low with maximums between 16 – 17 ppm.

A parameter where biogenic and fossil feedstocks often differ from each other is the water content. SPO and SDPO consist of comparably large amounts of water with 8.9 and 0.5 w%, respectively. Therefore, an increase in water content was expected when co-feeding SPO/SDPO but only for SPO measurable amounts were obtained that were separable from the organic phase. Additionally, the gasoline fraction was then analyzed regarding any dissolved water and remaining free water that was not obtainable via separation funnel. For all samples no free water was detectable. Dissolved water, however, was detectable for all samples in ranges from 100 to 350 ppm. Hereby, SPO co-feeding seemed to correlate with increased dissolved water traces whereas for SDPO this phenomena was not discovered. Nonetheless, the measured water contents can be considered miniscule so that no impairment of gasoline quality emerged. The lower heating value was then calculated according to Boie using the above mentioned results leading to no substantial differences between the gasoline samples. Further, no inorganics were measurable for any sample.

The wood derived hydrogenated pyrolysis liquids (SPO/SDPO) proved overall to be excellent co-feeding feedstocks for fluid catalytic cracking which deserve further in-depth research. Depending on desired product spectra either SPO or SDPO might be the better choice. The only downside was partial pipe clogging of SPO in the feeding pipe which should be a lesser problem for industrial plants. Summarized, satisfying reference cases were obtained for comparison of future waste-derived pyrolysis feedstocks produced in the course of the Waste2Road project.

5.1 Outlook

Discussing the results in this thesis led to the conclusion that the following topics should be further investigated in future research:

- Fluidization rate variation experimental campaign with narrower datapoints for trend specification
- Research on contamination distribution throughout product spectra when waste-derived and therefore, contaminated feedstock is utilized
- Maximum admixture rates of wood derived pyrolysis oil types for FCC co-feeding depending on hydrogenation
- Implementation of second feeding line to pilot plant to enable a wider variety of feedstock utilization
- Methods for successful co-feeding experiments with crude wood-derived pyrolysis oils
- In-depth quality analysis of gasoline derived from pyrolysis liquid co-feeding via engine tests
- Co-feeding experiments with two different feedstocks as admixtures to counteract possible feedstock supply shortages and enable greater plant flexibility
- Pilot plant tests with different biogenic waste-derived pyrolysis oils to diversify feedstock supply and determine additional suitable feedstock sources beside clean wood waste
- Implementation of a recognized biocarbon tracking method to quantify possible carbon oxide emission savings
- Determination of ecological and economic benefits of co-feeding sustainable feedstocks by e.g. using life cycle costing methods

6. Literature

[1] P. D. United Nations, Department of Economic and Social Affairs, “World Population Prospects 2019: Highlights,” 2019.

[2] U.S. Energy Information Administration, “International Energy Outlook 2021,” 2021. [Online]. Available: https://www.eia.gov/outlooks/ieo/.

[3] IEA, “Total primary energy supply by fuel, 1971 and 2019,” 2021. [Online]. Available: https://www.iea.org/data-and-statistics/charts/total-primary-energy-supply-by-fuel-1971-and-2019.

[4] UNFCCC, “Report of the Conference of the Parties on its twenty-first session, held in Paris from 30 November to 13 December 2015 Addendum Contents Part two: Action taken by the Conference of the Parties at its twenty-first session,” *Decis. 1/CP.21 Adopt. Paris Agreem.*, vol. 01192, no. January, pp. 1–36, 2015.

[5] European Commission, “A Clean Planet for all. A European long-term strategic vision for a prosperous, modern, competitive and climate neutral economy,” 2018.

[6] European Commission, “European Green Deal: Commission proposes transformation of EU economy and society to meet climate ambitions,” 2021. [Online]. Available: https://ec.europa.eu/commission/presscorner/detail/en/ip_21_3541.

[7] R. Smith, “The Refinery of the Future: A dynamic investment outlook as multi-billion-dollar green capex spend looms,” *Energy & Natural Resources Research & Analysis*, 2021. [Online]. Available: https://ihsmarkit.com/research-analysis/the-refinery-of-the-future.html.

[8] M. A. Alabdullah *et al.*, “A Viewpoint on the Refinery of the Future: Catalyst and Process Challenges,” *ACS Catal.*, vol. 10, no. 15, pp. 8131–8140, Aug. 2020, doi: 10.1021/acscatal.0c02209.

[9] OPEC, “World Oil Outlook 2021,” Vienna, 2021.

[10] A. J. Kamphuis, F. Picchioni, and P. P. Pescarmona, “CO 2 -fixation into cyclic and polymeric carbonates: principles and applications,” *Green Chem.*, vol. 21, no. 3, pp. 406–448, 2019, doi: 10.1039/C8GC03086C.

[11] A. Corma *et al.*, “Crude oil to chemicals: light olefins from crude oil,” *Catal. Sci. Technol.*, vol. 7, no. 1, pp. 12–46, 2017, doi: 10.1039/C6CY01886F.

[12] E. T. C. Vogt and B. M. Weckhuysen, “Fluid catalytic cracking: recent developments on the grand old lady of zeolite catalysis,” *Chem. Soc. Rev.*, vol. 44, no. 20, pp. 7342–7370, 2015, doi: 10.1039/C5CS00376H.

[13] J. GUGEL, “Executive Viewpoint: Introducing the refinery of the future,” *Hydrocarb. Process.*, vol. March, pp. 29–30, 2019.

[14] W. M. Burton, “Medal Address. Chemistry in the Petroleum Industry,” *J. Ind. Eng. Chem.*, vol. 10, no. 6, pp. 484–486, Jun. 1918, doi: 10.1021/ie50102a030.

[15] W. M. Burton, “Address of Acceptance,” *J. Ind. Eng. Chem.*, vol. 14, no. 2, pp. 162–163, Feb. 1922, doi: 10.1021/ie50146a035.

[16] R. Fletcher, “The History of Fluidized Catalytic Cracking: A History of Innovation: 1942-2008,” in *ACS Symposium Series*, vol. 1000, 2008, pp. 189–249.

[17] American Chemical Society, *National Historic Chemical Landmarks. The Houdry Process for Catalytic Cracking for the catalytic conversion of crude petroleum to high-octane gasoline*. Washington D.C.: National Historic Chemical Landmarks program of the American Chemical

Society, 1996.

[18] A. M. Mcafee, “The manufacture of gasoline as a by-product from high boiling petroleum oil, and the Manufacture of Gasoline as a By-product There from, by the Action of Aluminum Chloride.,” *Ind. Eng. Chem.*, vol. 7, no. 10, pp. 737–741, 1915, doi: 10.1021/ie50082a046.

[19] A. M. Mcafee, “The Manufacture of Commercial Anhydrous Aluminum Chloride,” *J. Chem. Educ.*, vol. 7, no. 21, pp. 670–673, 1929, doi: 10.1021/ed007p2376.

[20] E. J. Houdry, “Catalysis. [silicious bed],” US Patent 2161677, 1939.

[21] A. M. Squires, “THE STORY OF FLUID CATALYTIC CRACKING: THE FIRST ‘CIRCULATING FLUID BED,’” in *Circulating Fluidized Bed Technology*, P. Basu, Ed. Oxford: Elsevier, 1986, pp. 1–19.

[22] E. Houdry, W. F. Burt, J. A . E. Pew, and J. W. A . Peters, “The Houdry Process,” *Oil Gas J.*, vol. 37, no. 20, pp. 40–45, 1938.

[23] J. G. Speight, “Catalytic Cracking Processes,” in *Heavy Oil Recovery and Upgrading*, J. G. Speight, Ed. Elsevier, 2019, pp. 357–421.

[24] A. D. Reichle, “Fluid catalytic cracking hits 50 year mark on the run,” *Oil Gas J.*, vol. 90, no. 20, pp. 41–48, 1992.

[25] R. Sadeghbeigi, “Fluid catalytic cracking process description—converter section,” in *Fluid Catalytic Cracking Handbook*, Fourth., Butterworth-Heinemann, 2020, pp. 1–22.

[26] American Chemical Society, *National Historic Landmark. The fluid bed reactor*. National Historic Chemical Landmarks program of the American Chemical Society, 1998.

[27] A. A. Avidan, “Fluid catalytic cracking,” in *Circulating Fluidized Beds*, J. R. Grace, A. A. Avidan, and T. M. Knowlton, Eds. Dordrecht: Springer Netherlands, 1997, pp. 466–488.

[28] A. A. Murcia, “Numerous changes mark FCC technology advance,” *Oil Gas J.*, vol. 90, no. 20, pp. 68–71, 1992.

[29] J. M. Matsen, “Design and scale-up of CFB catalytic reactors,” in *Circulating Fluidized Beds*, J. R. Grace, A. A. Avidan, and T. M. Knowlton, Eds. Dordrecht: Springer Netherlands, 1997, pp. 489–503.

[30] J. R. Murphy, “Evolutionary design changes mark FCC process,” *Oil Gas J.*, vol. 90, no. 20, pp. 49–56, 58, 1992.

[31] W. Letzsch, “Fluid Catalytic Cracking (FCC) in Petroleum Refining,” in *Handbook of Petroleum Processing*, vol. 1, S. A. Treese, P. R. Pujadó, and D. S. J. Jones, Eds. Cham: Springer International Publishing, 2015, pp. 261–316.

[32] A. A. Avidan, “Chapter 1 Origin, Development and Scope of Fcc Catalysis,” in *Fluid Catalytic Cracking: Science and Technology*, vol. 76, J. S. Magee and M. M. Mitchell, Eds. Elsevier, 1993, pp. 1–39.

[33] J. E. Otterstedt, S. B. Gevert, S. G. Jääs, and P. G. Menon, “Fluid catalytic cracking of heavy (residual) oil fractions: a review,” *Appl. Catal.*, vol. 22, no. 2, pp. 159–179, Apr. 1986, doi: 10.1016/S0166-9834(00)82626-3.

[34] R. J. Argauer and G. R. Landolt, “Crystalline zeolite ZSM-5 and method of preparing the same,” US Patent 3,702,886, 14-Nov-1972.

[35] A. Akah and M. Al-Ghrami, “Maximizing propylene production via FCC technology,” *Appl. Petrochemical Res.*, vol. 5, no. 4, pp. 377–392, 2015, doi: 10.1007/s13203-015-0104-3.

[36] T. F. Degnan, G. K. Chitnis, and P. H. Schipper, “History of ZSM-5 fluid catalytic cracking additive development at Mobil,” *Microporous Mesoporous Mater.*, vol. 35–36, pp. 245–252, 2000, doi: https://doi.org/10.1016/S1387-1811(99)00225-5.

[37] A. Aitani, T. Yoshikawa, and T. Ino, “Maximization of FCC light olefins by high severity operation and ZSM-5 addition,” *Catal. Today*, vol. 60, no. 1, pp. 111–117, 2000, doi: https://doi.org/10.1016/S0920-5861(00)00322-9.

[38] Y. Fujiyama *et al.*, “Development of High Severity FCC Process for Maximizing Propylene Production —Catalyst Development and Optimization of Reaction Conditions—,” *J. Japan Pet. Inst.*, vol. 53, no. 6, pp. 336–341, 2010, doi: 10.1627/jpi.53.336.

[39] J. G. Speight, “Catalytic Cracking Processes,” in *Handbook of Petroleum Refining*, CRC Press, 2016.

[40] M. J. Kaiser, A. de Klerk, J. H. Gary, and G. E. Hwerk, “Fluid Catalytic Cracking,” in *Petroleum Refining Technology, Economics and Markets*, CRC Press, 2019, pp. 481–506.

[41] J. H. Gary, J. H. Handwerk, M. J. Kaiser, and D. Geddes, “Fluid Catalytic Cracking,” in *Petroleum Refining - Technology and Economics*, CRC Press, 2007, pp. 121–160.

[42] A. K. Coker, “Catalytic Cracking,” *Petroleum Refining Design and Applications Handbook*. pp. 259–304, 20-Aug-2018, doi: https://doi.org/10.1002/9781119257110.ch8.

[43] E. T. Habib Jr, H. Owen, P. W. Snyder, C. W. Streed, and P. B. Venuto, “Artificially metals-poisoned fluid catalysts. Performance in pilot plant cracking of hydrotreated resid,” *Ind. Eng. Chem. Prod. Res. Dev.*, vol. 16, no. 4, pp. 291–296, 1977.

[44] S. Parkash, “Gasoline Manufacturing Processes,” in *Refining Processes Handbook*, S. Parkash, Ed. Burlington: Gulf Professional Publishing, 2003, pp. 109–152.

[45] R. Sadeghbeigi, “Catalyst and feed additives,” in *Fluid Catalytic Cracking Handbook*, Fourth., R. Sadeghbeigi, Ed. Elsevier, 2020, pp. 111–117.

[46] M. M. Mitchell, J. F. Hoffman, and H. F. Moore, “Chapter 9 Residual Feed Cracking Catalysts,” in *Fluid Catalytic Cracking: Science and Technology*, vol. 76, J. S. Magee and M. M. Mitchell, Eds. Elsevier, 1993, pp. 293–338.

[47] J. G. Speight, “Introduction to Refining Processes,” in *Handbook of Petroleum Refining*, no. 59970, 2016, pp. 181–219.

[48] A. K. Coker, “Process Descriptions of Refinery Processes,” in *Petroleum Refining Design and Applications Handbook*, vol. 1, Hoboken, NJ, USA: John Wiley & Sons, Inc., 2018, pp. 111–148.

[49] M. A. Fahim, T. A. Alsahhaf, and A. Elkilani, “Introduction,” in *Fundamentals of Petroleum Refining*, Elsevier, 2010, pp. 1–9.

[50] J. H. Gary, J. H. Handwerk, M. J. Kaiser, and D. Geddes, “Crude Distillation,” in *Petroleum Refining: Technology and Economics*, Fifth Edit., CRC Press, 2007, pp. 71–96.

[51] U. Navarro, M. Ni, and D. Orlicki, “FCC 101: How to estimate product yields cost-effectively and improve operations,” *Hydrocarb. Process.*, vol. 94, no. 2, pp. 41–49, Feb. 2015.

[52] R. Sadeghbeigi, “Products and economics,” in *Fluid Catalytic Cracking Handbook*, Fourth., Elsevier, 2020, pp. 163–182.

[53] M. A. Fahim, T. A. Alsahhaf, and A. Elkilani, “Chapter 8 - Fluidised Catalytic Cracking,” in *Fundamentals of Petroleum Refining*, M. A. Fahim, T. A. Alsahhaf, and A. Elkilani, Eds. Amsterdam: Elsevier, 2010, pp. 199–235.

[54] R. Sadeghbeigi, “Unit monitoring and control,” in *Fluid Catalytic Cracking Handbook*, 4th ed.,

Elsevier, 2020, pp. 129–161.

[55] T. M. John and B. W. Wojciechowski, “On identifying the primary and secondary products of the catalytic cracking of neutral distillates,” *J. Catal.*, vol. 37, no. 2, pp. 240–250, 1975, doi: https://doi.org/10.1016/0021-9517(75)90158-X.

[56] R. Sadeghbeigi, “Chemistry of FCC reactions,” in *Fluid Catalytic Cracking Handbook*, Elsevier, 2020, pp. 119–128.

[57] B. C. Gates, J. R. Katzer, and G. C. A. Schuit, *Chemistry of catalytic processes*. New York: Mcgraw-Hill College, 1979.

[58] H. J. Bernstein, “Bond energies in hydrocarbons,” *Trans. Faraday Soc.*, vol. 58, p. 2285, 1962, doi: 10.1039/tf9625802285.

[59] T. M. John and B. W. Wojciechowski, “On identifying the primary and secondary products of the catalytic cracking of neutral distillates,” *J. Catal.*, vol. 37, no. 2, pp. 240–250, 1975, doi: https://doi.org/10.1016/0021-9517(75)90158-X.

[60] P. B. Venuto and E. T. Habib, *Fluid catalytic cracking with zeolite catalysts*. New York, NY [u.a.]: Dekker, 1979.

[61] W. G. Appleby, J. W. Gibson, and G. M. Good, “Coke Formation in Catalytic Cracking,” *Ind. Eng. Chem. Process Des. Dev.*, vol. 1, no. 2, pp. 102–110, Apr. 1962, doi: 10.1021/i260002a006.

[62] B. S. Greensfelder, H. H. Voge, and G. M. Good, “Catalytic and Thermal Cracking of Pure Hydrocarbons: Mechanisms of Reaction,” *Ind. Eng. Chem.*, vol. 41, no. 11, pp. 2573–2584, Nov. 1949, doi: 10.1021/ie50479a043.

[63] B. S. Greensfelder, H. H. Voge, and G. M. Good, “Catalytic and Thermal Cracking of Pure Hydrocarbons: Mechanisms of Reaction,” *Ind. Eng. Chem.*, vol. 41, no. 11, pp. 2573–2584, Nov. 1949, doi: 10.1021/ie50479a043.

[64] R. Sadeghbeigi, “FCC catalysts,” in *Fluid Catalytic Cracking Handbook*, Fourth., Elsevier, 2020, pp. 83–110.

[65] A. Humphries and J. R. Wilcox, “Zeolite components and matrix composition determine FCC catalyst performance,” *Oil Gas J.*, vol. 87, no. 6, pp. 45–51, 1989.

[66] C. M. Hayward and W. S. Winkler, “FCC: matrix/zeolite interactions,” *Hydrocarb. Process.*, vol. 69, no. 2, pp. 55–56, 1990.

[67] H. W. Beck, J. D. Carruthers, E. B. Cornelius, R. A. Kmecak, S. M. Kovach, and W. P. Hettinger, “High performance catalysts for carbometallic oil conversion and their manufacturing and use,” US Patent 4,480,047, 1984.

[68] J. M. Maselli and A. W. Peters, “Preparation and Properties of Fluid Cracking Catalysts for Residual Oil Conversion,” *Catal. Rev.*, vol. 26, no. 3–4, pp. 525–554, Aug. 1984, doi: 10.1080/01614948408064725.

[69] G. T. Kokotailo, S. L. Lawton, D. H. Olson, and W. M. Meier, “Structure of synthetic zeolite ZSM-5,” *Nature*, vol. 272, no. 5652, pp. 437–438, 1978, doi: 10.1038/272437a0.

[70] C. Liu, Y. Deng, Y. Pan, Y. Gu, B. Qiao, and X. Gao, “Effect of ZSM-5 on the aromatization performance in cracking catalyst,” *J. Mol. Catal. A Chem.*, vol. 215, pp. 195–199, Jun. 2004, doi: 10.1016/j.molcata.2004.02.001.

[71] J. B. McLean, B. W. Hoffer, G. M. Smith, D. M. Stockwell, and A. S. Shackleford, “Multi-stage reaction catalysts: A breakthrough innovation in FCC technology,” *NPRA Annu. Meet. Tech. Pap.*, pp. 1–19, Jan. 2011.

[72] Kelkar Iselin, “New developments in FCC catalysis,” in *Catalysis – Innovative Applications in Petrochemistry and Refining*, 2011, pp. 115–126.

[73] J. G. Speight, “Solvent Processes,” in *Heavy and Extra-heavy Oil Upgrading Technologies*, Elsevier, 2013, pp. 129–147.

[74] E. C. Oden and E. L. Foret, “Deasphalting Crude Residuum for Catalytic Cracker,” *Ind. Eng. Chem. Res.*, vol. 42, no. 10, pp. 2088–2095, 1950.

[75] M. S. Rana, V. Sámano, J. Ancheyta, and J. A. I. Diaz, “A review of recent advances on process technologies for upgrading of heavy oils and residua,” *Fuel*, vol. 86, no. 9 SPEC. ISS., pp. 1216–1231, 2007, doi: 10.1016/j.fuel.2006.08.004.

[76] J. G. Speight, “Deasphalting and dewaxing,” in *The Refinery of the Future*, Elsevier, 2020, pp. 227–255.

[77] J. M. Lee *et al.*, “Separation of solvent and deasphalted oil for solvent deasphalting process,” *Fuel Process. Technol.*, vol. 119, pp. 204–210, 2014, doi: 10.1016/j.fuproc.2013.11.014.

[78] A. V. Bridgwater and G. V. C. Peacocke, “Fast pyrolysis processes for biomass,” *Renew. Sustain. energy Rev.*, vol. 4, no. 1, pp. 1–73, 2000, doi: 10.1016/S1364-0321(99)00007-6.

[79] S. V. Pisupati and A. H. Tchapda, *Thermochemical processing of biomass*. 2015.

[80] R. H. Venderbosch and W. Prins, “Fast Pyrolysis,” in *Thermochemical Processing of Biomass*, Chichester, UK: John Wiley & Sons, Ltd, 2011, pp. 124–156.

[81] R. H. Venderbosch, “Fast Pyrolysis,” *Thermochemical Processing of Biomass*. pp. 175–206, 06-May-2019, doi: https://doi.org/10.1002/9781119417637.ch6.

[82] F. Shafizadeh, “Pyrolytic Reactions and Products of Biomass,” in *Fundamentals of Thermochemical Biomass Conversion*, R. P. Overend, T. A. Milne, and L. K. Mudge, Eds. Dordrecht: Springer Netherlands, 1985, pp. 183–217.

[83] S. R. A. Kersten, X. Wang, W. Prins, and W. P. M. van Swaaij, “Biomass Pyrolysis in a Fluidized Bed Reactor. Part 1: Literature Review and Model Simulations,” *Ind. Eng. Chem. Res.*, vol. 44, no. 23, pp. 8773–8785, Nov. 2005, doi: 10.1021/ie0504856.

[84] X. Wang, S. R. A. Kersten, W. Prins, and W. P. M. van Swaaij, “Biomass Pyrolysis in a Fluidized Bed Reactor. Part 2: Experimental Validation of Model Results,” *Ind. Eng. Chem. Res.*, vol. 44, no. 23, pp. 8786–8795, Nov. 2005, doi: 10.1021/ie050486y.

[85] P. McKendry, “Energy production from biomass (part 1): overview of biomass,” *Bioresour. Technol.*, vol. 83, no. 1, pp. 37–46, 2002, doi: https://doi.org/10.1016/S0960-8524(01)00118-3.

[86] H. Yang, R. Yan, T. Chin, D. T. Liang, H. Chen, and C. Zheng, “Thermogravimetric Analysis−Fourier Transform Infrared Analysis of Palm Oil Waste Pyrolysis,” *Energy & Fuels*, vol. 18, no. 6, pp. 1814–1821, Nov. 2004, doi: 10.1021/ef030193m.

[87] A. K. Gupta and D. G. Lilley, “Thermal Destruction of Wastes and Plastics,” *Plastics and the Environment*. pp. 629–696, 28-Jan-2005, doi: https://doi.org/10.1002/0471721557.ch15.

[88] H. Yang, R. Yan, H. Chen, D. H. Lee, and C. Zheng, “Characteristics of hemicellulose, cellulose and lignin pyrolysis,” *Fuel*, vol. 86, no. 12, pp. 1781–1788, 2007, doi: https://doi.org/10.1016/j.fuel.2006.12.013.

[89] A. Oasmaa, D. C. Elliott, and J. Korhonen, “Acidity of Biomass Fast Pyrolysis Bio-oils,” *Energy & Fuels*, vol. 24, no. 12, pp. 6548–6554, Dec. 2010, doi: 10.1021/ef100935r.

[90] L. Moens, S. K. Black, M. D. Myers, and S. Czernik, “Study of the Neutralization and Stabilization of a Mixed Hardwood Bio-Oil,” *Energy & Fuels*, vol. 23, no. 5, pp. 2695–2699, May 2009, doi:

10.1021/ef8009266.

[91] D. C. Elliott, “Historical Developments in Hydroprocessing Bio-oils,” *Energy & Fuels*, vol. 21, no. 3, pp. 1792–1815, May 2007, doi: 10.1021/ef070044u.

[92] A. V Bridgwater, “Review of fast pyrolysis of biomass and product upgrading,” *Biomass and Bioenergy*, vol. 38, pp. 68–94, 2012, doi: https://doi.org/10.1016/j.biombioe.2011.01.048.

[93] D. S. Scott and J. Piskorz, “The flash pyrolysis of aspen-poplar wood,” *Can. J. Chem. Eng.*, vol. 60, no. 5, pp. 666–674, Oct. 1982, doi: https://doi.org/10.1002/cjce.5450600514.

[94] J. Piskorz, D. S. A. G. Radlein, D. S. Scott, and S. Czernik, “Liquid Products from the Fast Pyrolysis of Wood and Cellulose,” in *Research in Thermochemical Biomass Conversion*, A. V Bridgwater and J. L. Kuester, Eds. Dordrecht: Springer Netherlands, 1988, pp. 557–571.

[95] R. G. Graham, B. A. Freel, D. R. Huffman, and M. A. Bergougnou, “Applications of Rapid Thermal Processing of Biomass,” in *Advances in Thermochemical Biomass Conversion*, A. V Bridgwater, Ed. Dordrecht: Springer Netherlands, 1993, pp. 1275–1288.

[96] Ensyn, “A Long History of Innovation and Commercial Deployment.” [Online]. Available: http://www.ensyn.com/history.html. [Accessed: 17-Jan-2022].

[97] K. Sipilä, Y. Solantausta, P. Jokela, and M. Raiko, “Method for carrying out pyrolysis,” *WO Pat.*, vol. 2009047387, p. A1, 2008.

[98] A. Oasmaa, J. Lehto, Y. Solantausta, and S. Kallio, “Historical Review on VTT Fast Pyrolysis Bio-oil Production and Upgrading,” *Energy & Fuels*, vol. 35, no. 7, pp. 5683–5695, Apr. 2021, doi: 10.1021/acs.energyfuels.1c00177.

[99] BTG-BTL, “A true trailblazer.” [Online]. Available: https://www.btg-bioliquids.com/plant/green-fuel-nordic-lieksa-finland/. [Accessed: 22-Feb-2022].

[100] BTG-BTL, “From sawdust to tank.” [Online]. Available: https://www.btg-bioliquids.com/plant/pyrocell-gavle-sweden/. [Accessed: 22-Feb-2022].

[101] S. D. Anuar Sharuddin, F. Abnisa, W. M. A. Wan Daud, and M. K. Aroua, “A review on pyrolysis of plastic wastes,” *Energy Convers. Manag.*, vol. 115, pp. 308–326, 2016, doi: https://doi.org/10.1016/j.enconman.2016.02.037.

[102] K. Ragaert, L. Delva, and K. Van Geem, “Mechanical and chemical recycling of solid plastic waste,” *Waste Manag.*, vol. 69, pp. 24–58, 2017, doi: https://doi.org/10.1016/j.wasman.2017.07.044.

[103] S. M. Al-Salem, A. Antelava, A. Constantinou, G. Manos, and A. Dutta, “A review on thermal and catalytic pyrolysis of plastic solid waste (PSW),” *J. Environ. Manage.*, vol. 197, no. 1408, pp. 177–198, 2017, doi: 10.1016/j.jenvman.2017.03.084.

[104] F. Abnisa and W. M. A. Wan Daud, “A review on co-pyrolysis of biomass: An optional technique to obtain a high-grade pyrolysis oil,” *Energy Convers. Manag.*, vol. 87, pp. 71–85, 2014, doi: https://doi.org/10.1016/j.enconman.2014.07.007.

[105] M. N. Islam, M. H. M. Ali, and M. Haziq, “Fixed bed pyrolysis of biomass solid waste for bio-oil,” in *AIP Conference Proceedings*, 2017, vol. 1875, p. 020015, doi: 10.1063/1.4998369.

[106] M. Lopez, G., Amutio, M., Elordiz, G., Artetxe, M., Altzibary, H., Olazarz, “A conical spouted bed reactor for the valorisation of waste tires,” in *13th International Conference on Fluidization - New Paradigm in Fluidization Engineering.*, 2021.

[107] K. Murata, K. Sato, and Y. Sakata, “Effect of pressure on thermal degradation of polyethylene,” *J. Anal. Appl. Pyrolysis*, vol. 71, no. 2, pp. 569–589, 2004, doi: https://doi.org/10.1016/j.jaap.2003.08.010.

[108] M. Tomasi Morgano, H. Leibold, F. Richter, and H. Seifert, “Screw pyrolysis with integrated sequential hot gas filtration,” *J. Anal. Appl. Pyrolysis*, vol. 113, pp. 216–224, May 2015, doi: 10.1016/j.jaap.2014.12.019.

[109] M. Zeller, N. Netsch, F. Richter, H. Leibold, and D. Stapf, “Chemical Recycling of Mixed Plastic Wastes by Pyrolysis – Pilot Scale Investigations,” *Chemie Ing. Tech.*, vol. 93, no. 11, pp. 1763–1770, Nov. 2021, doi: 10.1002/cite.202100102.

[110] Arcus Greencycling GmbH, “Patented in the name of nature,” 2018. [Online]. Available: https://www.arcus-greencycling.com/en-index#en-solution. [Accessed: 20-Jan-2022].

[111] Karlsruhe Intitute of Technology, “Making chemical plastics recycling respectable,” 2021. [Online]. Available: https://www.kit-technology.de/en/blog/making-chemical-plastics-recycling-respectable. [Accessed: 25-Jan-2022].

[112] M. Lehner, M. Bauer, and W. Hofer, “Prozesskette zum stofflichen Recycling von Kunststoffabfällen,” *BHM Berg- und Hüttenmännische Monatshefte*, vol. 161, no. 6, pp. 246–251, Jun. 2016, doi: 10.1007/s00501-016-0482-6.

[113] M. Fraubaum, “Plastic2Plastic: ReOil completes the circle in plastics recycling,” 2021. [Online]. Available: https://www.omv.com/en/blog/plastic2plastic-reoil-completes-the-circle-in-plastics-recycling. [Accessed: 12-Feb-2022].

[114] OMV Public Relations, “OMV scales up innovative ReOil® recycling technology at Schwechat refinery,” 2021. [Online]. Available: https://www.omv.com/en/news/221220-omv-scales-up-innovative-reoil-recycling-technology-at-schwechat-refinery. [Accessed: 15-Feb-2022].

[115] E. Butler, G. Devlin, and K. McDonnell, “Waste Polyolefins to Liquid Fuels via Pyrolysis: Review of Commercial State-of-the-Art and Recent Laboratory Research,” *Waste and Biomass Valorization*, vol. 2, no. 3, pp. 227–255, Aug. 2011, doi: 10.1007/s12649-011-9067-5.

[116] M. S. Qureshi *et al.*, “Pyrolysis of plastic waste: Opportunities and challenges,” *J. Anal. Appl. Pyrolysis*, vol. 152, p. 104804, Nov. 2020, doi: 10.1016/j.jaap.2020.104804.

[117] D. Castello and L. Rosendahl, “Coprocessing of pyrolysis oil in refineries,” in *Direct Thermochemical Liquefaction for Energy Applications*, L. Rosendahl, Ed. Elsevier, 2018, pp. 293–317.

[118] J. D. Adjaye and N. N. Bakhshi, “Production of hydrocarbons by catalytic upgrading of a fast pyrolysis bio-oil. Part I: Conversion over various catalysts,” *Fuel Process. Technol.*, vol. 45, no. 3, pp. 161–183, 1995, doi: https://doi.org/10.1016/0378-3820(95)00034-5.

[119] S. Vitolo, M. Seggiani, P. Frediani, G. Ambrosini, and L. Politi, “Catalytic upgrading of pyrolytic oils to fuel over different zeolites,” *Fuel*, vol. 78, no. 10, pp. 1147–1159, 1999, doi: https://doi.org/10.1016/S0016-2361(99)00045-9.

[120] N. Y. Chen, D. E. Walsh, and L. R. Koenig, “Fluidized-Bed Upgrading of Wood Pyrolysis Liquids and Related Compounds,” in *Pyrolysis Oils from Biomass*, vol. 376, American Chemical Society, 1988, pp. 24–277.

[121] D. V Naik *et al.*, “Catalytic cracking of jatropha-derived fast pyrolysis oils with VGO and their NMR characterization,” *RSC Adv.*, vol. 5, no. 1, pp. 398–409, 2015, doi: 10.1039/C4RA08128E.

[122] T. Lammens, G. Talebi, and E. Gbordzoe, “Co-Processing Fast Pyrolysis Bio-Oil in FCC Units: Principle and FAQ,” 2019.

[123] T. Lammens, “Personal communication.” 2021.

[124] Preem AB, “Pyrocell commences production,” *Preem Press Department*, 20-Sep-2021.

[125] A. de R. Pinho, M. B. B. de Almeida, F. L. Mendes, V. L. Ximenes, and L. C. Casavechia, “Co-

processing raw bio-oil and gasoil in an FCC Unit," *Fuel Process. Technol.*, vol. 131, pp. 159–166, Mar. 2015, doi: 10.1016/j.fuproc.2014.11.008.

[126] C. Lindfors, V. Paasikallio, E. Kuoppala, M. Reinikainen, A. Oasmaa, and Y. Solantausta, "Co-processing of Dry Bio-oil, Catalytic Pyrolysis Oil, and Hydrotreated Bio-oil in a Micro Activity Test Unit," *Energy & Fuels*, vol. 29, no. 6, pp. 3707–3714, Jun. 2015, doi: 10.1021/acs.energyfuels.5b00339.

[127] A. de R. Pinho *et al.*, "Fast pyrolysis oil from pinewood chips co-processing with vacuum gas oil in an FCC unit for second generation fuel production," *Fuel*, vol. 188, pp. 462–473, 2017, doi: https://doi.org/10.1016/j.fuel.2016.10.032.

[128] C. Wang, R. Venderbosch, and Y. Fang, "Co-processing of crude and hydrotreated pyrolysis liquids and VGO in a pilot scale FCC riser setup," *Fuel Process. Technol.*, vol. 181, no. July, pp. 157–165, 2018, doi: 10.1016/j.fuproc.2018.09.023.

[129] E. Rodríguez *et al.*, "Coke deposition and product distribution in the co-cracking of waste polyolefin derived streams and vacuum gas oil under FCC unit conditions," *Fuel Process. Technol.*, vol. 192, pp. 130–139, 2019, doi: https://doi.org/10.1016/j.fuproc.2019.04.012.

[130] E. Rodríguez, R. Palos, A. Gutiérrez, D. Trueba, J. M. Arandes, and J. Bilbao, "Towards waste refinery: Co-feeding HDPE pyrolysis waxes with VGO into the catalytic cracking unit," *Energy Convers. Manag.*, vol. 207, p. 112554, 2020, doi: https://doi.org/10.1016/j.enconman.2020.112554.

[131] F. Knaus, A. Reichhold, W. Tesch, A. Pazos Costa, H. Lutz, and M. Büchele, "Plastic to petrochemicals - Recycling of pyrolyzed municipal plastic waste by FCC Co-Processing," in *DGMK Tagungsbericht*, 2021, vol. 2021-Octob, pp. 68–79.

[132] G. Fogassy, N. Thegarid, G. Toussaint, A. C. van Veen, Y. Schuurman, and C. Mirodatos, "Biomass derived feedstock co-processing with vacuum gas oil for second-generation fuel production in FCC units," *Appl. Catal. B Environ.*, vol. 96, no. 3, pp. 476–485, 2010, doi: https://doi.org/10.1016/j.apcatb.2010.03.008.

[133] A. Reichhold, "Entwicklung von Reaktions/Regenerationssystemen für Adsorptions/Desorptionsprozesse und für katalytisches Cracken auf Basis von intern zirkulierenden Wirbelschichten," TU Wien, 1996.

[134] P. Bielansky, "Alternative Feedstocks in Fluid Catalytic Cracking," TU Wien, 2012.

[135] J. Fimberger, "Optimization of FCC process for production of middle destillates," TU Wien, 2017.

[136] M. Berchtold, "Optimization of process characteristics of an FCC-pilot plant for catalytic conversion of heavy feeds," TU Wien, 2016.

[137] A. Weinert, "Durchführung von Crackversuchen an einer Technikumsanlage im Rahmen der Entwicklung eines FCC-Konzepts mit Aspekten der Nachhaltigkeit," 2013.

[138] M. Büchele, "Einsatz von Glycerin-Rapsöl-Mischungen in einer intern zirkulierenden FCC-Pilotanlage," TU Wien, 2017.

[139] C. Y. Wen and Y. H. Yu, "A generalized method for predicting the minimum fluidization velocity," *AIChE J.*, vol. 12, no. 3, pp. 610–612, May 1966, doi: 10.1002/aic.690120343.

[140] W. R. A. Goossens, "Review of the empirical correlations for the drag coefficient of rigid spheres," *Powder Technol.*, vol. 352, pp. 350–359, 2019, doi: https://doi.org/10.1016/j.powtec.2019.04.075.

[141] H. Kalman and D. Portnikov, "Analyzing bulk density and void fraction: A. the effect of archimedes number," *Powder Technol.*, vol. 381, pp. 477–487, 2021, doi: https://doi.org/10.1016/j.powtec.2020.12.014.

[142] J. Sauter, *Die Grössenbestimmung der in Gemischnebeln von Verbrennungskraftmaschinen vorhandenen Brennstoffteilchen*. Berlin: VDI-Verlag, 1926.

[143] A. Buchner, “Bildung und Entfernung von Carbonylsulfid aus dem C3-Schnitt im FCC-Prozess,” TU Wien, 2018.

[144] DIN Deutsches Institut für Normung, “Kraftstoffe – Unverbleite Ottokraftstoffe – Anforderungen und Prüfverfahren; Deutsche Fassung EN 228:2012+A1:2017,” Berlin, 2017.

[145] DIN Deutsches Institut für Normung, “Kraftstoffe – Dieselkraftstoff – Anforderungen und Prüfverfahren; Deutsche Fassung EN 590:2013+A1:2017,” Berlin, 2017.

[146] DIN Deutsches Institut für Normung, “Flüssige Brennstoffe – Heizöle – Teil 1: Heizöl EL, Mindestanforderungen; DIN 51603-1,” Berlin, 2020.

[147] A. Corma, V. González-Alfaro, and A. V. Orchillés, “Decalin and tetralin as probe molecules for cracking and hydrotreating the light cycle oil,” *J. Catal.*, vol. 200, no. 1, pp. 34–44, 2001, doi: 10.1006/jcat.2001.3181.

[148] H. Moser, W. Pölz, J. P. Waclawek, J. Ofner, and B. Lendl, “Implementation of a quantum cascade laser-based gas sensor prototype for sub-ppmv H2S measurements in a petrochemical process gas stream,” *Anal. Bioanal. Chem.*, vol. 409, no. 3, pp. 729–739, 2017, doi: 10.1007/s00216-016-9923-z.

[149] DIN Deutsches Institut für Normung, “Chemische Analytik – Nachweis-, Erfassungs- und Bestimmungsgrenze unter Wiederholbedingungen – Begriffe, Verfahren, Auswertung, DIN 32645,” 2008.

[150] DIN Deutsches Institut für Normung, “Mineralölerzeugnisse Bestimmung der Asche; EN ISO 6245,” 2003.

[151] R. Sadeghbeigi, “FCC feed characterization,” in *Fluid Catalytic Cracking Handbook*, Fourth., Elsevier Inc., 2020, pp. 47–81.

[152] American Society for Testing and Materials, “Standard Test Method for Conradson Carbon Residue of Petroleum Products; ASTM D189,” 2006.

[153] B. Weber, “Einsatz von Pyrolyseöl unterschiedlicher hydrierender Behandlungsstufen in einer FCC-Pilotanlage zur Evaluierung der Auswirkungen auf das Produktspektrum,” TU Wien, 2021.

[154] J. G. Speight, “Upgrading by Solvent Treatment,” in *Heavy Oil Recovery and Upgrading*, J. G. Speight, Ed. Elsevier, 2019, pp. 529–558.

[155] M. Tomasi Morgano, H. Leibold, F. Richter, D. Stapf, and H. Seifert, “Screw pyrolysis technology for sewage sludge treatment,” *Waste Manag.*, vol. 73, pp. 487–495, 2018, doi: 10.1016/j.wasman.2017.05.049.

[156] BTG-Bioliquids, “Technology to convert biomass residues into a bio-oil,” 2020. [Online]. Available: https://www.btg-bioliquids.com/our-technology/#section--1. [Accessed: 17-Jan-2022].

[157] European Commission, “Delivering the European Green Deal,” 2021. [Online]. Available: https://ec.europa.eu/info/strategy/priorities-2019-2024/european-green-deal/delivering-european-green-deal_en#making-transport-sustainable-for-all. [Accessed: 14-Dec-2021].

[158] M. Büchele, H. Lutz, F. Knaus, and A. Reichhold, “Catalyst Testing in a Continuously Operated Fluid Catalytic Cracking Pilot Plant,” in *Proceedings of the 16th Minisymposium Verfahrenstechnik and 7th Partikelforum (TU Wien, Sept. 21/22, 2020)*, 2020, pp. MoP3-(10) 1-5, doi: 10.34726/561.

[159] R. Sadeghbeigi, Ed., “Residue and deep hydrotreated feedstock processing,” in *Fluid Catalytic Cracking Handbook*, Elsevier, 2020, pp. 297–308.

[160] R. J. Ferm, “The Chemistry Of Carbonyl Sulfide,” *Chem. Rev.*, vol. 57, no. 4, pp. 621–640, Aug. 1957, doi: 10.1021/cr50016a002.

[161] P. D. N. Svoronos and T. J. Bruno, “Carbonyl Sulfide: A Review of Its Chemistry and Properties,” *Ind. Eng. Chem. Res.*, vol. 41, no. 22, pp. 5321–5336, Oct. 2002, doi: 10.1021/ie020365n.

[162] H. Wise, “Mechanisms of Catalyst Poisoning by Sulfur Species,” in *Catalyst Deactivation*, vol. 68, C. H. Bartholomew and J. B. Butt, Eds. Elsevier, 1991, pp. 497–504.

[163] M. Büchele, M. Swoboda, A. Reichhold, and H. Moser, “Co-Processing of Atmospheric Residue With Vacuum Gas Oil in a Fluid Catalytic Cracking Pilot Plant - Effects on Product Spectra and Carbonyl Sulfide Formation,” *Erdoel Erdgas Kohle*, vol. 135, no. 4, pp. 151–156, 2019, doi: 10.19225/190402.

[164] J. G. Speight, “Heavy Feedstock Refining—The Future,” in *Heavy and Extra-heavy Oil Upgrading Technologies*, J. G. Speight, Ed. Boston: Elsevier, 2013, pp. 149–162.

[165] Plastics Europe, “Plastics - the facts 2021,” *Plastic - the fasts 2021 - An analysis of European plastics production, demand and waste data*, 2021. [Online]. Available: https://plasticseurope.org/knowledge-hub/plastics-the-facts-2021/. [Accessed: 19-Dec-2021].

[166] IEA, “Production of key thermoplastics, 1980-2050,” 2020. [Online]. Available: https://www.iea.org/data-and-statistics/charts/production-of-key-thermoplastics-1980-2050. [Accessed: 05-Nov-2021].

[167] European Commission, “A European Strategy for Plastics,” 2018.

[168] B. A. L., W. Shunli, and J. J. R., “The Chinese import ban and its impact on global plastic waste trade,” *Sci. Adv.*, vol. 4, no. 6, p. eaat0131, Jan. 2022, doi: 10.1126/sciadv.aat0131.

[169] W. Wang *et al.*, “Current influence of China’s ban on plastic waste imports,” *Waste Dispos. Sustain. Energy*, vol. 1, no. 1, pp. 67–78, May 2019, doi: 10.1007/s42768-019-00005-z.

[170] D. Akporiaye, “WASTE2ROAD - Biofuels from WASTE TO ROAD transport,” 2020. [Online]. Available: https://www.sintef.no/projectweb/waste2road/. [Accessed: 14-Dec-2020].

[171] M. Buechele, H. Lutz, F. Knaus, A. Reichhold, R. Venderbosch, and W. Vollnhofer, “Co-feeding of vacuum gas oil and pinewood-derived hydrogenated pyrolysis oils in a fluid catalytic cracking pilot plant to generate olefins and gasoline [version 1; peer review: 2 approved],” *Open Res. Eur.*, vol. 1, p. 143, Nov. 2021, doi: 10.12688/openreseurope.14198.1.

[172] W. Boie, “Beiträge zum feuerungstechnischen Rechnen,” *Wissenschaftliche Zeitschrift der Tech. Hochschule Dresden*, vol. 2, p. 53, 1952.

7. Appendix

table 28: hydrocarbon types in gasoline fraction of SPO/SDPO co-feeding campaign

plant settings	550 °C					530 °C				
	-	5% SPO	10% SPO	5% SDPO	10% SDPO	-	5% SPO	10% SPO	5% SDPO	10% SDPO
sum total paraffins [w%]	19.3	19	20	20.1	23.8	24.1	24	23	23.3	25
sum n-paraffins [w%]	2.4	2.4	2.5	2.5	2.9	2.6	2.6	2.5	2.6	2.7
sum i-paraffins [w%]	16.9	16.6	17.5	17.6	20.9	21.5	21.4	20.5	20.7	22.3
sum total olefins [w%]	6.7	8.2	8.3	7.2	9.1	7.9	8.5	9	6.7	7.7
sum n-olefins [w%]	1.6	2	2.3	1.8	2.4	1.9	2.1	2.3	1.6	1.9
sum i-olefins [w%]	5.1	6.2	6	5.4	6.7	6	6.4	6.7	5.1	5.8
sum olef. Naphthenes [w%]	2.7	3.2	2.9	2.4	2.7	2.8	3	3	2.5	2.5
sum naphthenes [w%]	7.5	7.3	7.1	7.4	8.8	9	9.2	8.7	9.7	10.1
sum aromatics [w%]	63.8	62.3	61.7	62.9	55.6	56.3	55.3	56.3	57.8	54.6

table 29: inorganics in the gasoline fraction in the SPO/SDPO co-feeding campaign

plant settings	550 °C					530 °C				
	-	5% SPO	10% SPO	5% SDPO	10% SDPO	-	5% SPO	10% SPO	5% SDPO	10% SDPO
Al [mg/kg]	<1,00	<1,00	<1,00	<1,00	<1,00	<1,00	<1,00	<1,00	<1,00	<1,00
Ca [mg/kg]	<1,00	<1,00	<1,00	<1,00	<1,00	<1,00	<1,00	<1,00	<1,00	<1,00
Cr [mg/kg]	<1,00	<1,00	<1,00	<1,00	<1,00	<1,00	<1,00	<1,00	<1,00	<1,00
Fe [mg/kg]	<1,00	<1,00	<1,00	<1,00	<1,00	<1,00	<1,00	<1,00	<1,00	<1,00
K [mg/kg]	<1,00	<1,00	<1,00	<1,00	<0,00	<1,00	<1,00	<1,00	<1,00	<1,00
Mn [mg/kg]	<1,00	<1,00	<1,00	<1,00	<1,00	<1,00	<1,00	<1,00	<1,00	<1,00
Mo [mg/kg]	<1,00	<1,00	<1,00	<1,00	<1,00	<1,00	<1,00	<1,00	<1,00	<1,00
Na [mg/kg]	<1,00	<1,00	<1,00	<1,00	<1,00	<1,00	<1,00	<1,00	<1,00	<1,00
Ni [mg/kg]	<1,00	<1,00	<1,00	<1,00	<1,00	<1,00	<1,00	<1,00	<1,00	<1,00
Pb [mg/kg]	<1,00	<1,00	<1,00	<1,00	<1,00	<1,00	<1,00	<1,00	<1,00	<1,00
Si [mg/kg]	<1,00	<1,00	<1,00	<1,00	<1,00	<1,00	<1,00	<1,00	<1,00	<1,00
V [mg/kg]	<1,00	<1,00	<1,00	<1,00	<1,00	<1,00	<1,00	<1,00	<1,00	<1,00
Zn [mg/kg]	<1,00	<1,00	<1,00	<1,00	<1,00	<1,00	<1,00	<1,00	<1,00	<1,00
halogens [mg/kg]	<1	<1	<1	<1	<1	<1	<1	<1	<1	<1
Ag [mg/kg]	<1,00	<1,00	<1,00	<1,00	<1,00	<1,00	<1,00	<1,00	<1,00	<1,00
Cd [mg/kg]	<1,00	<1,00	<1,00	<1,00	<1,00	<1,00	<1,00	<1,00	<1,00	<1,00
Cu [mg/kg]	<1,00	<1,00	<1,00	<1,00	<1,00	<1,00	<1,00	<1,00	<1,00	<1,00
Mg [mg/kg]	<1,00	<1,00	<1,00	<1,00	<1,00	<1,00	<1,00	<1,00	<1,00	<1,00
Sn [mg/kg]	<1,00	<1,00	<1,00	<1,00	<1,00	<1,00	<1,00	<1,00	<1,00	<1,00

8. Publications

8.1 Publications as corresponding author

- Marco Büchele, Matthias Swoboda, Alexander Reichhold, Wolfgang Hofer, Canola oil/glycerol mixtures in a continously operated FCC pilot plant and comparison with vacuum gas oil/glycerol mixtures, Chemical Engineering and Processing - Process Intensification, Volume 142, 2019, https://doi.org/10.1016/j.cep.2019.107553.

- Marco Büchele, Matthias Swoboda, Alexander Reichhold, Harald Moser, Co-Processing of Atmospheric Residue With Vacuum Gas Oil in a Fluid Catalytic Cracking Pilot Plant - Effects on Product Spectra and Carbonyl Sulfide Formation, Erdoel Erdgas Kohle/EKEP, Volume 135, Issue 4, p. 151 – 156, 2019, https://doi.org/10.19225/190402

- Marco Büchele, Helene Lutz, Florian Knaus, Alexander Reichhold, Catalyst Testing in a Continuously Operated Fluid Catalytic Cracking Pilot Plant, Conference: 16th Minisymposium Verfahrenstechnik and 7th Partikelforum, September 2020, https://doi.org/10.34726/561

- Marco Büchele, Helene Lutz, Florian Knaus. Alexander Reichhold, Robbie Venderbosch, Wolfgang Vollnhofer, Co-feeding of vacuum gas oil and pinewood-derived hydrogenated pyrolysis oils in a fluid catalytic cracking pilot plant to generate olefins and gasoline [version 1; peer review: 2 approved]. Open Research Europe 2021, 1:143 https://doi.org/10.12688/openreseurope.14198.1

8.2 Publications as co-author

- Matthias Swoboda, Marco Büchele, Hannes Gruber, Alexander Reichhold, Wolfgang Hofer, *Catalytic Cracking of Glycerol - VGO Mixtures in a Continuously Operated FCC Pilot Plant*; Oil Gas European Magazine, Volume 45, Issue 3; p. 136 – 143, 2019,

- Matthias Swoboda, Marco Büchele, Alexander Reichhold, Wolfgang Hofer, *Catalytic Conversion of Pyrolysis Oils Derived From Plastics in a Continuously Operated FCC Pilot Plant*; Erdöl Erdgas Kohle/EKEP, Volume 135, Issue 5, p. 215 – 223, 2019

- Florian Knaus, Alexander Reichhold, Walter Tesch, Alexandre Pazos Costa, Helene Lutz, Marco Büchele, Plastic to Petrochemicals – Recycling of Pyrolyzed Municipal Plastic Waste by FCC Co-Processing, Conference: Chemical Recycling – Beyond Thermal Use of Plastic and other Waste, October 2021, Volume: ISSN 1433-9013 ISBN 978-3-947716-30-2

- Helene Lutz, Marco Büchele, Alexander Reichhold, Florian Knaus, Wood derived fast pyrolysis bio-liquids as co-feed in a fluid catalytic cracking pilot plant: effect of hydrotreatment on process performance and gasoline quality, Energy Fuels 2022, XXXX, XXX, XXX-XXX, Publication Date:August 10, 2022, https://doi.org/10.1021/acs.energyfuels.2c01736

- Florian Knaus, Helene Lutz, Marco Büchele, Alexander Reichhold, Alexandre Pazos Costa, A renewable way of plastic waste recycling and fuel production from biogenic and recycled feedstock, currently under preparation

Titles of publications under preparation might be subject to change.